K/UR-29
Part 5

ORGDP

OAK
RIDGE
GASEOUS
DIFFUSION
PLANT

UNION
CARBIDE

HYDROGEOCHEMICAL AND STREAM SEDIMENT DETAILED GEOCHEMICAL SURVEY FOR TRANS-PECOS, TEXAS

CHINATI MOUNTAINS PROJECT AREA

T. R. Butz, M. E. Wagner, J. G. Grimes,
C. S. Bard, R. N. Helgerson, and P. M. Pritz
Uranium Resource Evaluation Project

CAUTION
This is a time release report.
Do not release any part of this
publication before
_____, _____

October 31, 1980

OPERATED BY
UNION CARBIDE CORPORATION
FOR THE UNITED STATES
DEPARTMENT OF ENERGY

A computer readable magnetic tape containing measurement, analysis, and location data may be purchased from the GJOIS Project, UCC-ND Computer Applications Dept., 4500 North Building, Oak Ridge National Laboratory, P. O. Box X, Oak Ridge, Tennessee 37830.

Date of Issue: October 31, 1980

Report Number: K/UR-29
Part 5

Subject Category: UC-51, Nuclear Raw Materials

HYDROGEOCHEMICAL AND STREAM SEDIMENT DETAILED GEOCHEMICAL SURVEY FOR TRANS-PECOS, TEXAS

CHINATI MOUNTAINS PROJECT AREA

T. R. Butz, M. E. Wagner, J. G. Grimes, C. S. Bard, R. N. Helgerson, and P. M. Pritz

Uranium Resource Evaluation Project

Union Carbide Corporation, Nuclear Division
Oak Ridge Gaseous Diffusion Plant
Oak Ridge, Tennessee

Prepared for the U. S. Department of Energy
Assistant Secretary for Resource Applications
Grand Junction Office, Colorado
under U. S. Government Contract W-7405 eng 26

Uranium Resource Evaluation Project
J. W. Arendt, Project Manager
T. R. Butz, Assistant Project Manager

Geology and Geochemistry
T. R. Butz, Project Geologist/Geochemist
P. M. Pritz, Field Geology Program Director
M. E. Wagner, Field Geology Supervisor

J. H. French, S. A. Roberts, C. J. Stannard,
C. S. Lide, and D. J. Tieman, Field Geologists

Analytical Chemistry, Detailed Survey Geochemistry, and Report Preparation
J. D. Joyner, Data Management and Information Processing
R. N. Helgerson, Analytical Chemistry
J. G. Grimes and C. S. Bard, Detailed Geochemical Reporting

Uranium Resource Evaluation Project
Oak Ridge Gaseous Diffusion Plant
P. O. Box P, Mail Stop 246
Oak Ridge, Tennessee 37830
Telephone: (615) 574-8882
FTS 624-8882

CONTENTS

LIST OF TABLES

LIST OF FIGURES

LIST OF PLATES

(In Back Pocket)

ABSTRACT

Results of the Chinati Mountains project area of the detailed geochemical survey for Trans-Pecos, Texas are reported. Field and laboratory data are presented for 24 groundwater and 121 stream sediment samples. Statistical and areal distributions of uranium and possible uranium-related variables are given. A generalized geologic map of the project area is provided, and pertinent geologic factors which may be of significance in evaluating the potential for uranium mineralization are briefly discussed.

The five highest and five lowest uranium values for groundwater samples in the Chinati Mountains project area are described. Variables associated with these samples and their producing horizons are delineated. Results indicate that groundwater samples collected from the Chinati Mountains Group display lower uranium values than samples collected from other volcanic units.

Stream sediments containing significant amounts of soluble and total uranium occur in four areas: the Shely prospect, Woods Ranch, the Red Hill prospect, and Cienega Mountain. Elements associated with soluble and insoluble uranium are discussed for the four areas. Insoluble uranium is associated with the elements zirconium, yttrium, niobium, titanium, and cerium; while soluble uranium is associated with the elements iron, manganese, beryllium, lithium, phosphorus, and vanadium. The Allen Intrusive Complex, in the Shely prospect area, has been cited as a definite source for uranium, however source rocks cannot be determined for the other areas.

CHINATI MOUNTAINS PROJECT AREA

INTRODUCTION

The National Uranium Resource Evaluation (NURE) Program was established by the U. S. Atomic Energy Commission, now the U. S. Department of Energy (DOE), in the spring of 1973 to assess uranium resources and to identify favorable areas for detailed uranium exploration throughout the United States. The principal objectives of the NURE Program are: (1) to provide a comprehensive in-depth assessment of the nation's uranium resources for national energy planning, and (2) to identify areas favorable for uranium resources. A NURE Program report covering uranium resource assessment in 116 National Topographic Map Series (NTMS) 1° x 2° quadrangles, which contain 100% of the currently estimated uranium resources, is targeted for 1980. The complete resource assessment of the 272 highest-priority quadrangles is scheduled for completion in 1985, and the first comprehensive assessment report of the entire United States is scheduled for completion in 1988. This program, which is being administered by DOE, is expected to increase the activity of commercial exploration for uranium in the United States.

The NURE Program consists of five parts:

1. Hydrogeochemical and Stream Sediment Reconnaissance (HSSR) Program,
2. Aerial Radiometric and Magnetic Survey,
3. Surface Geologic Investigations,
4. Drilling for Geologic Information, and
5. Geophysical Technology Development.

The objective of the HSSR Program is to provide information to be used in accomplishing the overall NURE Program objectives. This is accomplished by a reconnaissance of surface water, groundwater, stream sediment, and lake sediment. The survey is being conducted by three Government-owned laboratories. Union Carbide Corporation, Nuclear Division (UCC-ND), under contract with DOE, is conducting its survey in 154 NTMS 1° x 2° quadrangles which cover approximately 2,500,000 km^2 (1,000,000 mi^2) of the central United States. This area includes most of the states of Texas, Oklahoma, Kansas, Nebraska, South Dakota, North Dakota, Minnesota, Wisconsin, Michigan, Indiana, Illinois, and Iowa, as well as parts of Arkansas, Missouri, New Mexico, and Ohio.

As a part of the HSSR Program, detailed geochemical surveys were initiated in the fall of 1978 to supply comprehensive detailed geochemical data from specific areas. These surveys are designed to characterize the hydrogeochemistry, stream sediment geochemistry, and/or radiometric patterns of known or potential uranium occurrences. The information can be used to interpret data from the 1° x 2° NTMS quadrangle basic data surveys.

This report on the Chinati Mountains project area represents the fifth volume of geochemical data which describe seven select areas in the Trans-Pecos region, Texas (see Figure 1 for the location and names of the last three of the seven project areas).

LOCATION AND PHYSIOGRAPHY

The Chinati Mountains project area of the Trans-Pecos detailed geochemical survey is located between lat. 29°30' to 30°15' N. and long. 104°00' to 104°45' W. The project area covers approximately 5,973 km^2 (2,307 mi^2), while the area of detailed sampling within the project area encompasses 986 km^2 (381 mi^2). The area described is outlined on the generalized geologic map of Texas (Figure 2) and lies within Presidio County in the Marfa and Presidio 1° x 2° NTMS Quadrangles. A generalized geologic map, with a stratigraphic column listing geologic codes used in this report, is presented in Figure 3 and Plate 7.

Physiographically, the Chinati Mountains project area borders the Rio Grande and is located south of the Rim Rock Country. The project area lies within the Mexican Highland section of the Basin and Range Province, which is characterized by Late Oligocene fault block mountain ranges and alluvium-filled basins. The highstanding, tilted mountain blocks are cut by arroyos and steep canyons with numerous alluvial fans splaying out onto the adjacent bolson areas along the Rio Grande. Chinati Peak is the highest point in the area, with an elevation of 2,356 m (7,730 ft) above sea level.

CLIMATE

The climate of the Trans-Pecos region of west Texas is classified as arid, subtropical. Western Trans-Pecos receives sunshine 80% of the time and maintains a normal average annual temperature of 18°C (64°F). Average potential evapotranspiration exceeds the annual average rainfall, which is about 29.5 cm/yr (11.6 in./yr). Rains tend to occur in the fall and spring with the greatest peak in September and a minor one in May. The more mountainous areas receive intense, short-lived, and sporadic afternoon thundershowers accounting for most of the annual precipitation (National Oceanic and Atmospheric Administration, 1974). The Chinati Mountains have been known to be snow-covered for short periods during the winter months.

RELATED STUDIES

In recent years, emphasis has been placed on resurgent caldera systems as favorable sites for uranium mineralization. Recent studies on uranium ore formation have focused on rhyolitic domes and plugs, intracaldera and extra-caldera ash-flows and ash falls, and volcanic derived sediments.

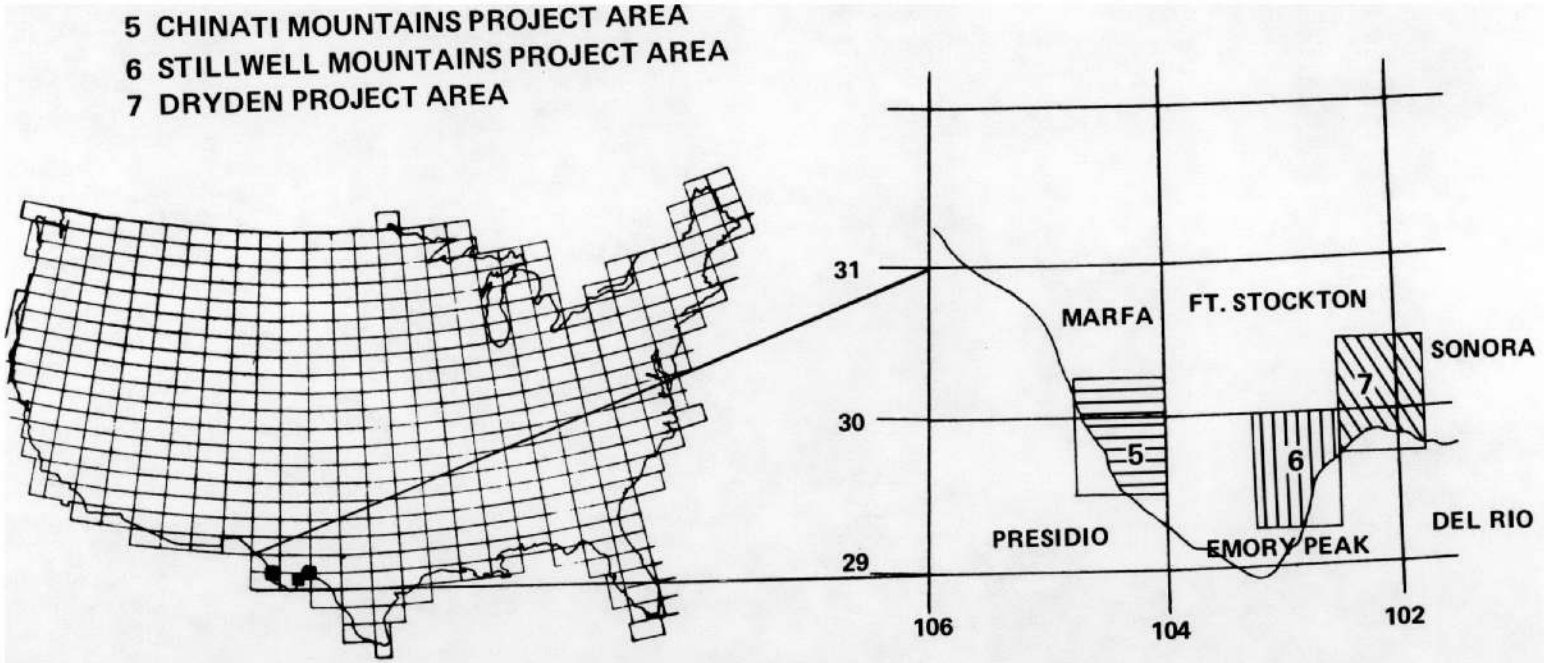

Figure 1

INDEX MAP SHOWING THE BOUNDARIES FOR THE CHINATI MOUNTAINS PROJECT AREA,(5)
TRANS-PECOS DETAILED GEOCHEMICAL SURVEY, TEXAS

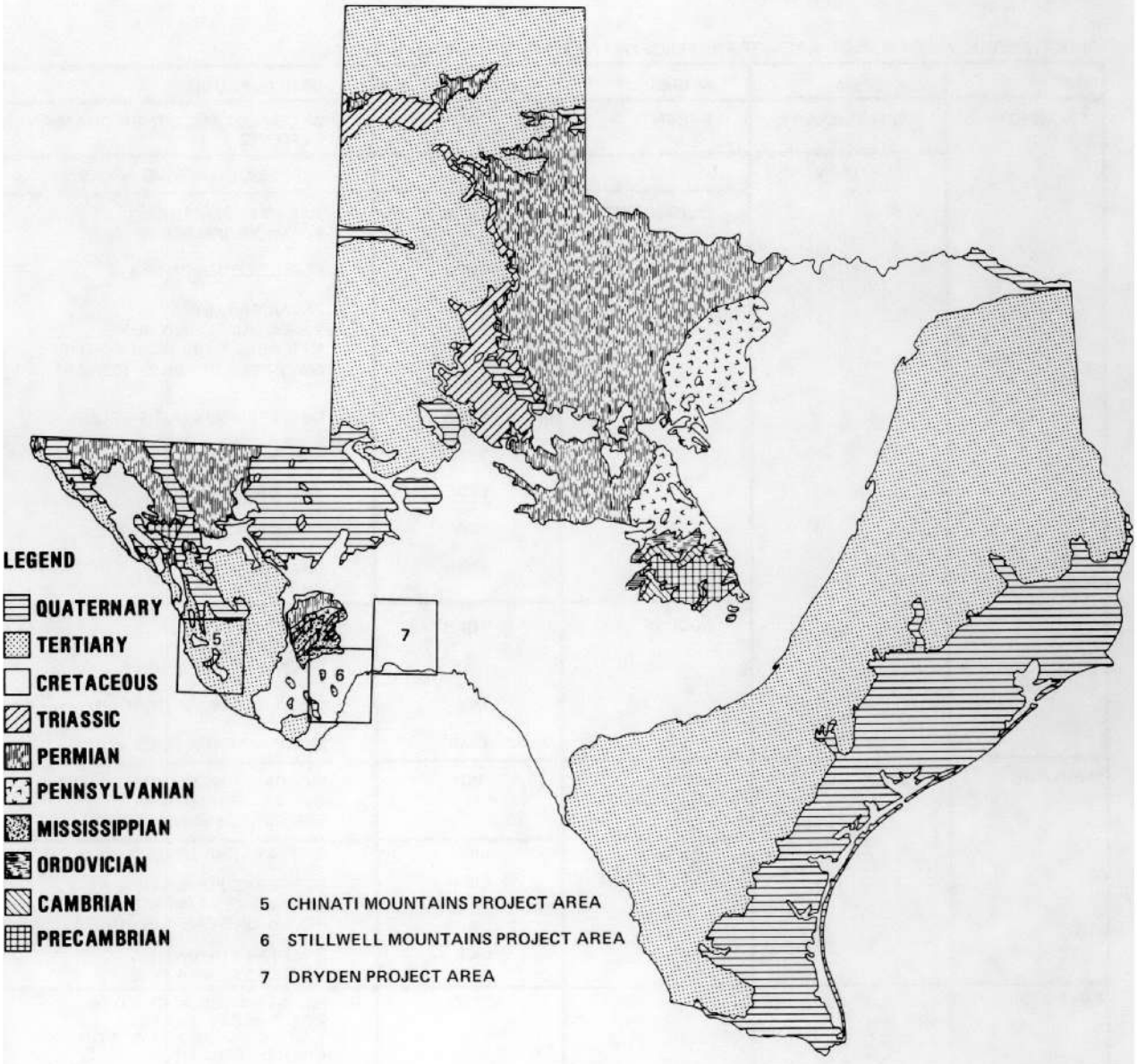

Figure 2

GENERALIZED GEOLOGIC MAP OF TEXAS WITH LOCATION
OF THE CHINATI MOUNTAINS PROJECT AREA,
TRANS-PECOS DETAILED GEOCHEMICAL SURVEY, TEXAS
(AFTER KING, ET AL, 1974)

CHINATI MOUNTAINS PROJECT AREA, TRANS-PECOS DETAILED GEOCHEMICAL SURVEY

ERA	SYSTEM	SERIES	MAP CODE	GEOLOGIC UNIT
CENOZOIC	QUATERNARY	RECENT	QD	ALLUVIUM AND OTHER QUATERNARY DEPOSITS
	TERTIARY		TI	INTRUSIVE IGNEOUS ROCKS
		OLIGOCENE	TERL	RAWLS FORMATION FRESNO FORMATION
			TEPC	PERDIZ CONGLOMERATE
			TETT	PETAN BASALT TASCOTAL FORMATION MITCHELL MESA WELDED TUFF DUFF-PRUETT FORMATIONS
			TECA	CHINATI MOUNTAINS GROUP
			TECI	SHELY GROUP
			TEDP	BRITE IGNIMBRITE
			TCA	CAPOTE MOUNTAIN TUFF
			TCBH	BRACHS RHYOLITE CHAMBERS TUFF
		EOCENE	TGCB	COLMENA TUFF GILL BRECCIA BUCKSHOT IGNIMBRITE
			TVJ	VIEJA GROUP (UNDIVIDED)
			TEMR	MORITA RANCH FORMATION
MESOZOIC	CRETACEOUS	UPPER CRETACEOUS	UKPO	PICACHO FORMATION OJINAGA FORMATION SAN CARLOS FORMATION
		LOWER CRETACEOUS	LKSE	SANTA ELENA LIMESTONE
			LKSP	SUE PEAKS FORMATION DEL CARMEN LIMESTONE TELEPHONE CANYON FORMATION
			LKT	SHAFTER FORMATION PRESIDIO FORMATION
PALEOZOIC			CPUD	MINA GRANDE FORMATION ROSS MINE FORMATION PINTO CANYON FORMATION CIBOLO FORMATION ALTA FORMATION

SOURCE OF GEOLOGY:

1. BARNES, V. E.; GEOLOGIC ATLAS OF TEXAS, EMORY PEAK-PRESIDIO SHEET (PRELIMINARY SHEET, 1977).
2. BARNES, V. E.; GEOLOGIC ATLAS OF TEXAS, MARFA SHEET (PRELIMINARY SHEET, 1978).
3. CEPEDA, J.C., "THE CHINATI MOUNTAINS CALDERA, PRESIDIO COUNTY, TEXAS," IN CENOZOIC GEOLOGY OF THE TRANS-PECOS VOLCANIC FIELD OF TEXAS, pp. 65-84 (1978).

LEGEND FOR FIGURE 3

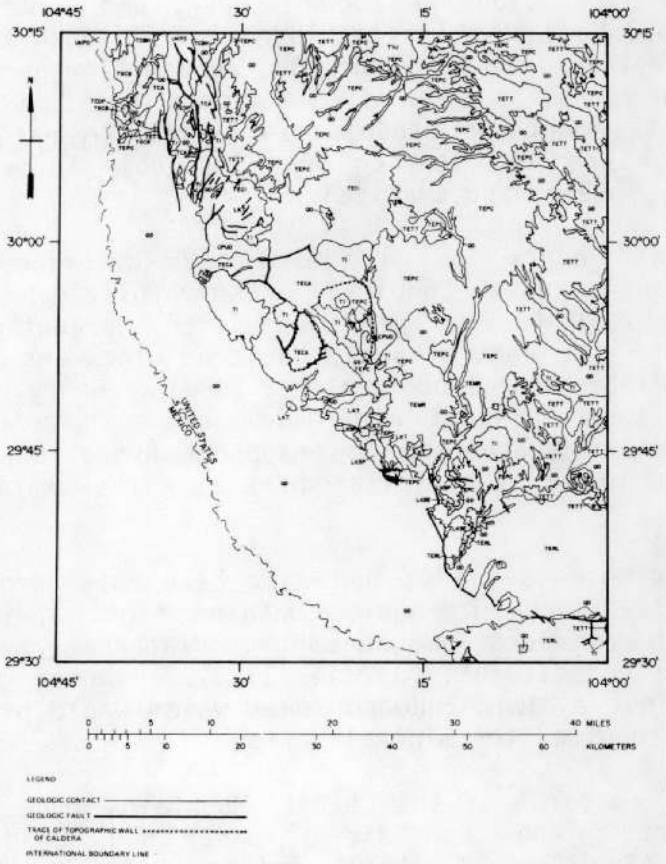

Figure 3

GENERALIZED GEOLOGIC MAP
OF THE CHINATI MOUNTAINS PROJECT AREA,
TRANS-PECOS DETAILED GEOCHEMICAL SURVEY, TEXAS

Henry and Tyner (1978), utilizing previous studies by Cepeda (1978), describe the alteration and release of uranium from formations within the Chinati Mountains Group (TECA) and its associated volcanic ash flows. The primary concentration of uranium is highest in the upper rhyolite of the Chinati Mountains Group. They calculate that approximately fifty percent of the unit's total uranium content was released during granophyric-like devitrification, either as volatiles in vapor phase or dispersed into adjacent wall rock. The remaining concentration of upper rhyolite uranium is insoluble, requiring total rock breakdown before uranium liberation can occur. Henry and Tyner also concluded that the Mitchell Mesa Rhyolite (included in TETT and referred to as the Mitchell Mesa Welded Tuff in Figure 3), an ash-flow genetically related to the Chinati Mountains caldera, is a poor uranium-source rock. As with the Chinati Mountains Group, devitrification has resulted in the release of most uranium, leaving only insoluble forms (i.e., uranium within zircons, sphene, and apatite).

Cofer (1980) and Henry, et al (1980) have described mineralization within the Allen Intrusive Complex. These rhyolitic porphyry domes are genetically related to the Shely Cauldron, predating the Chinati volcanic center. The central Shely Cauldron block was known previously as the Loma Plata Anticline (Cofer, 1980). Henry, et al, (1980) describes the known uranium mineralization as secondary in nature, caused by supergene weathering of amorphous hydroxides which released primary uranium to be reprecipitated as autunite, metatorbernite, and tyuyamunite.

The Perdiz Conglomerate (TEPC) had also been considered favorable for uranium mineralization. The unit contains highly permeable alluvial fans, evidenced by a large amount of groundwater movement and uranium-rich lithologic constituents (Jordan, 1978). However, the Perdiz Conglomerate does not exhibit reduced zones which would provide the trapping mechanism required for mineralization.

Additional NURE research of the Chinati Mountains project area includes the HSSR report on the Presidio 1° x 2° NTMS Quadrangle (Uranium Resource Evaluation Project, 1978) and the Union Carbide Trans-Pecos detailed geochemical survey report of the Sierra Vieja, Tascotal, and Solitario project areas (Butz, et al, 1979).

GEOLOGY

STRATIGRAPHY

Sedimentary units representing the Paleozoic and Cretaceous are limited in areal extent in the project area and are exposed only to the north and southeast of the Tertiary Chinati Mountains. The Paleozoic Pinto Canyon, Cibolo, and Alta Formations are visible in the deep stream canyons for which they are named and consist of "dirty" marine limestones with dolomite, chert, and bituminous laminations with calcareous

sandstone layers and lenses (Barnes, 1978). These units are combined with the Mina Grande and Ross Mine Formations and are shown as CPUD on the geologic map (Figure 3 and Plate 7).

The Lower Cretaceous Presidio and Shafter Formations are combined and are shown as LKT, and the Del Carmen Limestone and Telephone Canyon Formation are combined with the Sue Peaks Formation and shown as LKSP on Figure 3. These unconformably overlie the Paleozoic units. The Cretaceous (Trinitian), Presidio, and Shafter (Etholen-Cox; after Baker, 1929) Formations are exposed on the north side of Pinto Canyon and around the mining community of Shafter. These units are argillaceous limestones with interbedded sandy shales and conglomerates (Baker, 1929). Total thickness of the Paleozoic and Lower Cretaceous units is approximately 300 m (984 ft) in the Chinati Peak Northeast 7-1/2 Minute Quadrangle.

The Del Carmen Limestone and Telephone Canyon Formation are areally limited to the southern portion of the project area. These massive, nodular, gray limestone units are exposed near Shafter (lat. 29°49' N. and long. 104°18' W.) and attain a maximum thickness of 107 m (350 ft) (Barnes, 1977).

The units of Tertiary age are ash-flow and ash-fall tuffs, lavas, and intrusive igneous rocks. Minor outcrops of Tertiary sandstones and conglomerates also exist.

The Tertiary units within the area sampled are associated with three proposed calderas (Cepeda, 1978). The areal extent of each of the calderas are indicated by the outcrop pattern of their respective cauldron facies: the Morita Ranch Formation (TEMR), the Shely Group (TECI), and the Chinati Mountains Group (TECA). The Morita Ranch and Shely calderas are considered to be roughly contemporaneous (Cepeda, 1978), although the age of the cauldron facies is considered to be Eocene and Oligocene, respectively (Barnes, 1977 and 1978).

Filling the most southern of the three caulderas, the Morita Ranch Formation (TEMR), exposed west of the Cienega Mountains (lat. 29°46' N. and long. 104°17' W.), consists of interbedded flows, tuffs, and conglomerates. In contrast to the Shely and Chinati Mountains Groups, the Morita Ranch Formation is basaltic in composition. Rix (1953) divides this formation into four units consisting of an olivine basalt, a porphyritic ash-flow tuff, a basalt porphyry, and flow breccias (Maxwell, 1970).

Filling the northern most caldera, the Shely Group (TECI), exposed north of the Chinati Mountains, is made up of rhyolites, trachytes, ignimbrites, tuffs, and conglomerates (Maxwell, 1970). Amsbury (1958) divides the Shely Group into 8 units occurring in and around the Pinto Canyon area. Associated igneous intrusives include the Allen Intrusive Complex (lat. 30°00'25" N. and long. 104"18'58" W.) and the intrusive rocks in the Organ Pipe Hills (lat. 30°02' N. and long. 104°29' W.) (site of the Shely uranium prospect).

The Mitchell Mesa Welded Tuff (TETT) is a high-silica, low-aluminum ash-flow tuff. Phenocrysts within the glass matrix are composed of alkali feldspars, quartz, magnetite, and occasionally biotite. The formation ranges from a densely welded to a nonwelded tuff (Henry and Tyner, 1978). The Mitchell Mesa Welded Tuff is considered to have been erupted from the Chinati Mountains. Potassium-argon dates indicate that the tuff is older than the cauldron facies (31.5 and 31.2 mybp, respectively). Stratigraphic evidence suggests that the eruption of the tuff may have produced the Chinati Mountains caldera (Cepeda, 1978).

The Shely Group is separated from the Chinati Mountains Group (TECA) by a fault (the presumed Chinati Mountains caldera wall) with movement to the south, placing the younger Chinati Mountains Group against the older Shely Group. Cepeda (1978) has divided the Chinati Mountains Group into seven distinct units: a basal conglomerate composed of rocks of Lower Cretaceous (Comanchean) age, lower trachyte, middle trachyte, lower rhyolite, upper trachyte, upper rhyolite, and non-porphyritic domes and flows. Cepeda (1978), described these units as follows:

> The lower and middle trachytes located near the presumed caldera walls underlie the lower rhyolite facies. The trachytes are porphyritic with plagioclase and anorthoclase phenocrysts and a fine-grained groundmass of feldspar and clinopyroxene. Their total thickness measures approximately 20 m (65 ft).
>
> The lower rhyolite is the dominant facies of the volcanic series. The thickness varies from 20 m (65 ft) in the north to 390 m (1280 ft) in the Tinaja Prieta Canyon (lat. 29°52' N. and long. 104°26' W.). It forms the fairly flat areas to the east of the mountains, partially obscuring some of the non-porphyritic flows. The rhyolite is prophyritic with anorthoclase and quartz as phenocrysts.
>
> The upper trachyte is much like the middle trachyte facies except that it occupies a different stratigraphic position as it forms the highest peaks. It has two distinct textural layers consisting of a lower fine-grained and an upper phenocryst zone. Some basal vitrophyres exist with phenocrysts of plagioclase and anorthoclase. Thickness of the unit varies from 20 to 390 m (65 ft to 1,280 ft).
>
> The upper rhyolite is restricted to the central portion of the mountains. It is a grayish-green porphyritic tuff with anorthoclase and resorbed quartz phenocrysts and a clinopyroxene groundmass. Its thickness is approximately 175 m (575 ft). The upper rhyolite filled secondary collapse zones (shown on the generalized geologic map) produced by its own eruption.
>
> Four major domes of non-porphyritic texture are exposed south of the Wood Ranch headquarters (lat. 29°56' N. and long. 104°26' W.). These rhyolitic units follow an arcuate pattern suggesting development from a ring fracture zone. Blue flow-banded dikes and plugs intrude the upper trachyte north of the Wood Ranch headquarters.

The West Chinati Stock (TI) (lat. 29°55' N. and long. 104°30' W.) is a porphyritic hornblende granite. Phenocrysts are predominantly K-feldspar with a K-feldspar-hornblende-quartz groundmass. The stock itself is cut by dikes and plutons which are suggested as sources for uranium mineralization (McAnulty, 1975). Zinc, lead, and fluorite mineralization is present in shear zones within the stock (Cepeda, 1978).

The Perdiz Conglomerate (TEPC), consisting of erosional debris derived from the Chinati Mountains, has three main facies: proximal, mid, and distal fans (Jordan, 1978). The amount and size of sand, silt, and gravel differ with each facies.

Quaternary deposits of the Presidio Bolson are clay, silt, and gypsiferous sandstone deposits accumulating around the margin of the mountains and cut by the Rio Grande (Barnes, 1977). These units are combined with alluvium and other Quaternary deposits and are shown as QD (Figure 3 and Plate 7).

STRUCTURE

The Paleozoic structural framework of western Trans-Pecos is complicated due to orogenic events and thick Mesozoic sequences masking the underlying deformed basement rocks. During the Paleozoic, the Chinati Mountains project area existed within the northern limits of the Ouachita geosynclinal system, locally defined as the Marathon foldbelt. Deposition of limey, cherty clastic material along with carbonate shelf build-up characterized the Early Paleozoic geosynclinal environment. The Mississippian-Early Pennsylvanian age was marked by regional uplift of the area creating the Aldama Platform of Chihuahua, Mexico (lat. 29°00' N. and long. 106°15' W.) and restructured the southern margin of the Sierra Diablo Platform of the extreme western Trans-Pecos region (lat. 30°15' N. and long. 104°25' W.) (Greenwood, 1970). Differential subsidence and tectonic uplift created the Marfa Basin into which the Permian Cibolo, Alta, and Pinto Canyon Formations were deposited (McAnulty, 1975). The Diablo Platform shelf-margin at this time period existed just south of present-day Valentine, Texas (lat. 30°39' N. and long. 104°30' W.). An inter-basinal shelf existed at the south end of the present-day Chinati Mountains and extended south to Presidio, Texas (lat. 29°35' N. and long. 104°23' W.). Post Permian uplift and erosion has left Cretaceous units in direct contact with the Paleozoic basement. Transgression of Late Jurassic-Early Cretaceous seas moved the shelf margin to the west of the Chinati Mountains (lat. 29°50' N. and long 104°45' W.).

Two positive landmass projections into the Mexican geosynclinal sea (Chihuahua Trough and Sabinas Gulf) were the Coahuila and Tamaulipas Peninsulas (Smith, 1970). The Coahuila Peninsula junction with the Diablo Platform is the site of the Chinati Mountains (McAnulty, 1975). Sedimentation and trough subsidence continued in the Cretaceous with the

Diablo Platform remaining relatively stable. Sea transgression partially inundated the Coahuila Peninsula giving rise to the shallow shelf deposition of the Shafter and Presidio Formations (Muehlberger and Wiley, 1970).

The Late Cretaceous to Oligocene Laramide Orogeny caused folding and overthrusting of Mexican geosynclinal deposits against the stable Diablo Platform (Maxwell, 1970). Middle Tertiary volcanic activity occurred along the Chihuahua tectonic belt (lat. 30° N. and long. 105° W.), giving rise to an elevated volcanic plateau (McAnulty, 1975). The Shely Group, the shallow Allen Intrusive Complex, and the Morita Ranch Formation are presumed earlier members of this volcanic plateau (Henry and Tyner, 1978).

The Chinati cauldron (lat. 29°58' N. and long. 104°30' W.) is one of six known aligned volcanic centers present in the Chihuahua Tectonic Belt. This unstable zone trending N. 50° W. is approximately 325 km (202 mi) long and 30 km (19 mi) wide (McAnulty, 1976). The Chinati Mountains caldera exemplifies Smith and Bailey's (1968) criteria for a resurgent cauldron (McAnulty, 1976 and Files, 1978). The probable sequence of events in the Chinati Mountains from Oligocene to present is as follows:

1. Development of fracture zones in the unstable tectonic region acting as conduits for magma and subsequent ash-flow eruptions.
2. Caldera formation.
3. Magma resurgence with eruption of the lower and middle trachytes onto the Caldera floor (Amsbury, 1958 and Cepeda, 1978).
4. Emplacement of non-porphyritic domes and plugs, south of Wood Ranch headquarters on Osa Creek (lat. 29°55' N. and long. 104°24' W.), representing a ring fracture zone on the boundary of a secondary collapse zone (Cepeda, 1978).
5. Development of a secondary collapse zone and eruptive emplacement of the lower rhyolite near Cibolo Creek and Wood's Ranch access road (lat. 29°56' N. and long. 104°20' W.).
6. Trachytic volcanism of upper unit north of Wood Ranch headquarters (lat. 29°55' N. and long. 104°26' W.).
7. Eruptive emplacement of upper rhyolite flows in the collapse zone 1.9 km (1.2 mi) northeast of Cerro Orona (lat. 29°51' N. and long. 104°26' W.).
8. Caldera floor fracturing led to the intrusion of peralkaline dikes and plugs west of the Aguja Peak (lat. 29°57'30" N. and long. 104°23'30" W.).
9. Emplacement of major intrusives [West Chinati Stock of San Antonio Canyon (lat. 29°55' N. and long. 104°30' W.) and the South Chinati Laccolith (lat. 29°50' N. and long. 104°23' W.)] deformed Permian and Cretaceous units and caused doming of the overlying Chinati Mountains volcanics creating Tertiary synclines and anticlines (McAnulty, 1975). Late stage hydrothermal fluids moved through faults and fractures in the Permian and Cretaceous strata forming mineral deposits (McAnulty, 1975).

10. The end of volcanic activity led to erosion and the formation of Perdiz Conglomerate (TEPC) accumulations to the north and east of the cauldron system (Jordan, 1978).
11. Basin and Range-type faulting occurred in the Chinati Mountains between 18 and 23 mybp. South-southeast trending enechlon faults, reverse to the direction of geosynclinal overthrusting, broke up the volcanic series leaving Chinati Peak as an elevated structure. Some faults of this time period are visible in the upper Cibolo Creek area (lat. 29°57' N. and long. 104°20' W.) (Baker, 1929).
12. Bolson material derived from fault block erosion accumulated in areas to the west and south of the raised Chinati Mountain block, i.e., the Presidio Bolson.
13. The bolson material was then dissected when the Lower Rio Grande-Conchos River System merged with the Upper Rio Grande System in Late Pleistocene (Strain, 1970).

There have been arguments as to the sequence of emplacement of major intrusives and Basin and Range-type faulting. The Sierra Vieja Rim Rock Fault (lat. 30°07' N. and long. 104°35' W.) has been the central focus as it has been called both a Cenozoic block fault structure and an earlier Texas Lineament feature responsible for the West Chinati Stock (Twiss, 1970 and McAnulty, 1975). It has been proposed that the Rim Rock Fault (Texas Lineament ?) is a continental suggestion of the Pacific Murray Fracture Zone (Cebull, et al, 1976).

HYDROLOGY

A very limited amount of information is available on groundwater resources of the Chinati Mountains area. Well and spring samples collected were derived from three dominant rock types: (1) volcanics, (2) marine sediments, and (3) bolson deposits.

Run-off accumulations may exist beneath arroyo deposits cutting through volcanic regions.

URANIUM OCCURRENCES

Within the boundaries of the Chinati Mountains project area, the Shely Ranch prospect (lat. 29°58' N. and long. 104°31' W.) is the only known radioactive anomaly related to uranium mineralization. The mineralization occurs in the white rhyolite porphyry of the Allen Intrusive Complex. The Shely prospect is considered to be an authigenic uranium occurrence (Class 360 of Mathews, 1978). This deposit is formed ... "by post magmatic redistribution and concentration of uranium within the parent pluton. Uranium minerals occur in veins along shears, fractures, and microfractures adjacent to major shear zones" (Mathews, 1978).

Amsbury (1958) reports that the mineralized fracture zone was bulldozed and ore with an average grade of 0.34% U_3O_8 was stockpiled. Further studies showed that the mineralized zone did not extend beyond 27 m (90 ft) in depth. This abrupt termination is explained by Matthews (1978) as a function of the groundwater table location. Background radiometric readings over the volcanic rocks range from 900 to 1,300 cps (Reeves, et al, 1978). The uranium minerals identified include autunite, meta-torbernite, and tyuyamunite.

Numerous radioactive anomalies are incidental to locations of base and precious metal exploration. Within the Shafter Mining District (lat. 29°48' N. and long. 104°17' W.), thirteen anomalous sites are reported in fractures within limestones adjacent to igneous rocks of the Chinati Mountains caldera (Southern Interstate Nuclear Board, 1969). During the detailed sampling period of this project, renewed private exploration for uranium mineralization was on-going in the West Chinati Stock area (lat. 29°55' N. and long. 104°32' W.).

SAMPLE COLLECTION

CHRONOLOGY OF THE SURVEY

Sampling in the Chinati Mountains project area began in January 1980 and was completed in February 1980. Laboratory analysis and compilation and verification of all field and laboratory data were completed in May 1980. The final field and laboratory data base used to prepare the statistical and areal distribution of uranium and other related variables for this report was completed in June 1980.

FIELD PROCEDURES

A total of 24 groundwater and 121 stream sediment samples was collected during the detailed sampling of the Chinati Mountains project area. Spring water and well water samples are combined and reported as groundwater. Plates 1 and 4 show sample locations for groundwater and stream sediment sites, respectively. Radiometric sample locations are shown on Plate 8.

Sampling density for groundwater in the Chinati Mountains project area was less than optimal for several reasons. The scarcity of groundwater samples is a result of the lack of wells in the sparsely populated area. In addition, permission to sample was denied in several locations within the boundaries of the project area.

Detailed information regarding techniques in sample collection, recording site data, field equipment, and field measurements can be found in the following reports: "Hydrogeochemical and Stream Sediment Reconnaissance Procedures for the Uranium Resource Evaluation Project" (Arendt, et al, December 1979); "Procedures Manual for Groundwater Reconnaissance Sampling" (Uranium Resource Evaluation Project, March

1978); and "Procedures Manual for Stream Sediment Reconnaissance Sampling" (Uranium Resource Evaluation Project, May 1978). Field observations were recorded on the field form shown in Table C-2 and are included on microfiche in Appendix D.

Radiometric data were obtained using a GR-410 Exploranium Geometrics gamma-ray spectrometer and BGS-1SL Scintrex scintillator counters. The readings obtained were used in directing sampling towards geologic units with positive anomalous radioactivity.

CONTAMINATION

Precautions were taken to avoid the possibility of collecting contaminated samples. Wells which were affected by any chlorination, water-softening, or filtering devices were not sampled if a sample could not be taken before the water passed through such devices. Any well that had not been pumped recently was allowed to run as long as possible to flush the system. Any wells that the samplers considered might be contaminated were checked as such on the field forms.

Sediment samples were collected upstream from road crossings and railroad tracks, except where this was not feasible.

CHEMICAL ANALYSIS

All samples collected were returned to the URE Project laboratory in Oak Ridge, Tennessee for preparation and analysis. The elements determined and the analytical techniques used along with the appropriate detection limits are given in Table 1. These detection limits are considered the best average during normal operation; however, some variables have values reported below these limits. All water samples were received in 250-ml polyethylene bottles and were filtered through 0.45-μm cellulose acetate paper. Stream sediment samples were dried overnight at 85°C and sieved to collect the <150-μm fraction. Part of the sediment sample was dissolved in 10 ml of 1:1 nitric-hydrofluoric acid. The analytical procedures which were used have been described by Cagle (1977) and Arendt, et al (December 1979). All observed data from all samples are included on microfiche in Appendix D.

QUALITY CONTROL

MEASUREMENTS CONTROL

The procedures used to analyze URE Project samples require that calibration standards, check samples, and blanks be analyzed along with normal samples to ensure the validity of the reported results. A measurements control program provides information concerning precision

Table 1

DETECTION LIMITS OF VARIABLES DETERMINED IN WATER AND SEDIMENT SAMPLES

Variable	Method	Detection Limits Sediment (ppm)	Detection Limits Water (ppb)
U	Fluorometry	0.25	0.2
U-MS	Mass Spectrometry-Isotope Dilution	--	0.02
U-NT	Neutron Activation-Delayed Neutron Count	0.02	--
As	Atomic Absorption	0.1	0.5
Se	Atomic Absorption	0.1	0.2
Ag	Plasma Source Emission Spectrometry	2	2
Al	Plasma Source Emission Spectrometry	0.05(a)	10
B	Plasma Source Emission Spectrometry	10	4
Ba	Plasma Source Emission Spectrometry	2	2
Be	Plasma Source Emission Spectrometry	1	1
Ca	Plasma Source Emission Spectrometry	0.05(a)	0.1(b)
Ce	Plasma Source Emission Spectrometry	10	30
Co	Plasma Source Emission Spectrometry	4	2
Cr	Plasma Source Emission Spectrometry	1	4
Cu	Plasma Source Emission Spectrometry	2	2
Fe	Plasma Source Emission Spectrometry	0.05(a)	10
Hf	Plasma Source Emission Spectrometry	15	--
K	Plasma Source Emission Spectrometry	0.05(a)	0.1(b)
La	Plasma Source Emission Spectrometry	2	--
Li	Plasma Source Emission Spectrometry	1	2
Mg	Plasma Source Emission Spectrometry	0.05(a)	0.1(b)
Mn	Plasma Source Emission Spectrometry	4	2
Mo	Plasma Source Emission Spectrometry	4	4
Na	Plasma Source Emission Spectrometry	0.05(a)	0.1(b)
Nb	Plasma Source Emission Spectrometry	4	--
Ni	Plasma Source Emission Spectrometry	2	4
P	Plasma Source Emission Spectrometry	5	40
Pb	Plasma Source Emission Spectrometry	10	--
Sc	Plasma Source Emission Spectrometry	1	1
Si	Plasma Source Emission Spectrometry	--	0.1(b)
Sr	Plasma Source Emission Spectrometry	1	2
Th	Plasma Source Emission Spectrometry	2	--
Ti	Plasma Source Emission Spectrometry	10	2
V	Plasma Source Emission Spectrometry	2	4
Y	Plasma Source Emission Spectrometry	1	1
Zn	Plasma Source Emission Spectrometry	2	4
Zr	Plasma Source Emission Spectrometry	2	2
SO_4	Spectrophotometry	--	5(b)
Cl	Spectrophotometry	--	10(b)

(a)Detection limits expressed in percent.
(b)Detection limits expressed in ppm.

and reliability of these measurements. On a daily basis, control samples of two water batches and three sediment batches are submitted anonymously along with routine samples. Statistical summaries of results reported on control samples, which were analyzed along with the samples included in this survey, are given in Tables 2 and 3. Results of uranium analysis of water and sediment control samples obtained from the Ames Laboratory as part of the Multilaboratory Analytical Quality Control for the HSSR Program are reported by D'Silva, et al (1980).

PRINCIPAL COMPONENT ERROR ANALYSIS

A principal component analysis of data from groundwater and stream sediment samples was used to produce an ordered list of samples using the eigenvalue statistics as described by Kane, et al (1977), where the most extreme samples were listed first. Additional samples were identified if single-element measurements were outside a three standard deviation confidence interval around the mean. The laboratory and field data from the samples identified by this procedure were reviewed. Three groundwater samples (027319, 027331, and 029241) and three stream sediment samples (027420, 027433, and 029250) were submitted for reanalysis. The original results were compared to the results from reanalysis. Of the more than 175 individual analyses that were compared, the only results which were considered to be in error in the original analysis and thus require corrections were the multielement values for Groundwater Samples 027331 and 029241, and Sediment Samples 027420, 027433, and 029250. This low error rate for the samples indicates a high level of reliability for the laboratory measurements.

GEOCHEMICAL RESULTS

GEOCHEMICAL DISTRIBUTIONS IN GROUNDWATER

Sample locations for groundwater collected in the Chinati Mountains project area are shown on Plate 1. Areal distribution plots for uranium and specific conductance are presented on Plates 2 and 3, and Figures A-1b and A-2b, respectively. A map showing the units from which samples are produced is presented in Figure 4.

Groundwater data used to generate tables and figures in Appendix A include all groundwater samples collected within the project area. The number of groundwater samples collected from each of the stratigraphic units is given in Table 4.

Observed data for the variables uranium, specific conductance, the uranium:specific conductance ratio, boron, barium, calcium, lithium, magnesium, molybdenum, strontium, and sulfate are listed in Table A-3. The figures in Appendix A present log frequency, lognormal probability, percentile, and areal distribution plots for these same variables and the uranium:boron ratio, the uranium:sulfate ratio, silver, aluminum,

Table 2

SUMMARY OF THE MEASUREMENTS CONTROL RESULTS OBTAINED FROM GROUNDWATER SAMPLES FROM THE CHINATI MOUNTAINS PROJECT AREA, TRANS-PECOS DETAILED GEOCHEMICAL SURVEY, TEXAS

		Batch L-4				Batch H-4			
Element	Method	No. of Samples	Mean (ppb)	Standard Deviation (ppb)	Coefficient of Variation	No. of Samples	Mean (ppb)	Standard Deviation (ppb)	Coefficient of Variation
U	FL(a)	17	0.75	0.351	0.47	11	10.87	0.897	0.08
AS	AA(b)	20	3.3	1.11	0.33	17	0.6	0.31	0.55
SE	AA	20	1.2	0.31	0.26	17	0.8	0.24	0.29
AL	PS(c)	13	92.0	20.2	0.22	18	330.0	25.0	0.08
B	PS	13	1,570.0	62.2	0.04	19	69.0	4.6	0.07
BA	PS	12	140.0	3.3	0.02	19	31.0	1.4	0.05
CA	PS	14	10,000.0	850.0	0.08	18	91,400.0	6,190.0	0.07
CO	PS	14	20.0	4.1	0.20	17	90.0	2.9	0.03
CR	PS	14	93.0	5.6	0.06	18	18.0	1.8	0.10
CU	PS	8	45.0	1.8	0.04	18	202.0	23.3	0.11
FE	PS	13	103.0	7.2	0.07	18	960.0	50.7	0.05
K	PS	14	1,800.0	229.0	0.13	17	19,490.0	937.0	0.05
LI	PS	14	16.0	1.1	0.07	18	100.0	5.6	0.06
MG	PS	14	9,200.0	420.0	0.05	18	67,900.0	2,710.0	0.04
MN	PS	14	20.0	2.3	0.11	16	96.0	4.1	0.04
MO	PS	13	24.0	10.1	0.41	13	11.0	6.3	0.57
NA	PS	14	1,600.0	150.0	0.10	18	43,800.0	2,120.0	0.05
NI	PS	13	195.0	10.7	0.05	18	37.0	6.2	0.16
P	PS	13	90.0	23.8	0.26	17	4,498.0	134.3	0.03
SC	PS	13	63.0	2.8	0.04	17	11.0	0.5	0.05
SI	PS	14	870.0	164.0	0.19	18	7,940.0	371.0	0.05
SR	PS	14	56.29	2.644	0.05	18	5,012.55	170.85	0.03
TI	PS	13	118.0	8.2	0.07	18	38.0	4.4	0.11
V	PS	12	9.0	1.5	0.15	18	41.0	3.5	0.08
Y	PS	14	9.0	1.4	0.14	18	45.0	2.4	0.05
ZN	PS	14	498.0	42.7	0.09	18	45.0	24.3	0.54

(a)Fluorometric analysis.
(b)Atomic absorption.
(c)Plasma source emission spectroscopy.

Table 3

SUMMARY OF THE MEASUREMENTS CONTROL RESULTS OBTAINED WITH STREAM SEDIMENT SAMPLES FROM THE CHINATI MOUNTAINS PROJECT AREA, TRANS-PECOS DETAILED GEOCHEMICAL SURVEY, TEXAS

		Batch Q-1				Batch R-3				Batch S-3			
Element	Method	No. of Samples	Mean (ppm)	Standard Deviation (ppm)	Coefficient of Variation	No. of Samples	Mean (ppm)	Standard Deviation (ppm)	Coefficient of Variation	No. of Samples	Mean (ppm)	Standard Deviation (ppm)	Coefficient of Variation
U	FL[a]	40	0.79	0.268	0.34	37	4.26	0.469	0.11	38	28.52	2.674	0.09
U	NT[b]	39	0.67	0.160	0.24	50	4.91	0.102	0.02	35	26.25	0.797	0.03
AS	AA[c]	17	1.8	0.25	0.14	27	3.6	0.64	0.18	19	26.4	3.11	0.12
SE	AA	12	0.5	0.31	0.57	28	0.2	0.43	2.02	20	1.4	0.62	0.45
AL	PS[d]	36	9,700.0	490.0	0.05	39	34,100.0	2,730.0	0.08	30	48,700.0	3,430.0	0.07
B	PS	38	7.0	3.5	0.46	34	20.0	7.1	0.34	30	61.0	10.3	0.17
BA	PS	38	130.0	14.6	0.11	39	454.0	51.0	0.11	32	314.0	31.1	0.10
BE	PS	37	<1.0			40	<1.0			32	2.0	4.0	1.74
CA	PS	38	1,200.0	100.0	0.08	40	3,100.0	300.0	0.10	31	16,900.0	80.0	0.06
CE	PS	37	19.08	3.677	0.19	39	68.82	7.196	0.10	29	55.59	4.968	0.09
CO	PS	38	4.0	2.7	0.59	40	10.0	2.2	0.20	31	33.0	3.1	0.09
CR	PS	38	14.0	2.1	0.14	39	28.0	3.2	0.11	32	65.0	6.6	0.10
CU	PS	35	3.0	0.8	0.22	38	20.0	1.5	0.07	30	69.0	2.9	0.04
FE	PS	37	9,700.0	390.0	0.04	40	18,000.0	1,070.0	0.06	30	40,800.0	2,070.0	0.05
K	PS	37	1,900.0	190.0	0.10	38	9,900.0	930.0	0.09	31	17,200.0	2,000.0	0.12
LI	PS	37	9.0	0.8	0.08	39	23.0	1.8	0.08	32	35.0	3.6	0.10
MG	PS	38	1,100.0	50.0	0.05	39	2,200.0	110.0	0.05	32	5,600.0	260.0	0.05
MN	PS	37	317.0	9.9	0.03	40	1,909.0	87.8	0.05	30	404.0	15.9	0.04
MO	PS	1	<4.0			40	2.0	0.9	0.41	29	43.0	3.7	0.08
NA	PS	1	<500.0			40	1,600.0	190.0	0.13	31	1,600.0	220.0	0.14
NB	PS	37	2.0	0.7	0.32	41	8.0	4.3	0.49	33	2.0	1.6	0.58
NI	PS	37	6.0	1.0	0.16	41	20.0	3.1	0.15	30	108.0	6.3	0.06
P	PS	36	70.0	6.0	0.09	35	2,149.0	217.3	0.10	28	1,441.0	83.8	0.06
PB	PS	28	5.0	3.0	0.50	27	38.0	5.6	0.14	28	21.0	3.6	0.16
SC	PS	38	1.0	0.5	0.31	41	5.0	0.8	0.15	32	10.0	0.8	0.08
SR	PS	36	19.17	1.320	0.07	39	55.33	4.054	0.07	32	85.56	6.133	0.07
TH	PS	38	2.0	1.7	0.74	41	8.0	2.8	0.34	33	8.0	2.5	0.30
TI	PS	38	572.0	54.8	0.10	39	3,321.0	369.9	0.11	32	2,123.0	174.9	0.08
V	PS	35	20.0	0.9	0.04	38	55.0	4.4	0.08	30	166.0	6.7	0.04
Y	PS	37	4.0	0.3	0.08	39	20.0	1.7	0.08	30	33.0	1.6	0.05
ZN	PS	36	13.0	2.1	0.16	35	93.0	7.5	0.08	29	185.0	12.0	0.06
ZR	PS	38	30.0	2.9	0.10	38	136.0	10.9	0.08	31	83.0	6.0	0.07
HF	PS	27	2.11	1.577	0.75	27	3.83	2.685	0.70	28	1.95	1.455	0.75
LA	PS	28	20.89	3.023	0.14	27	78.00	15.056	0.19	28	90.61	4.787	0.05

(a)Fluorometric analysis.
(b)Neutron activation delayed neutron count.
(c)Atomic absorption.
(d)Plasma source emission spectroscopy.

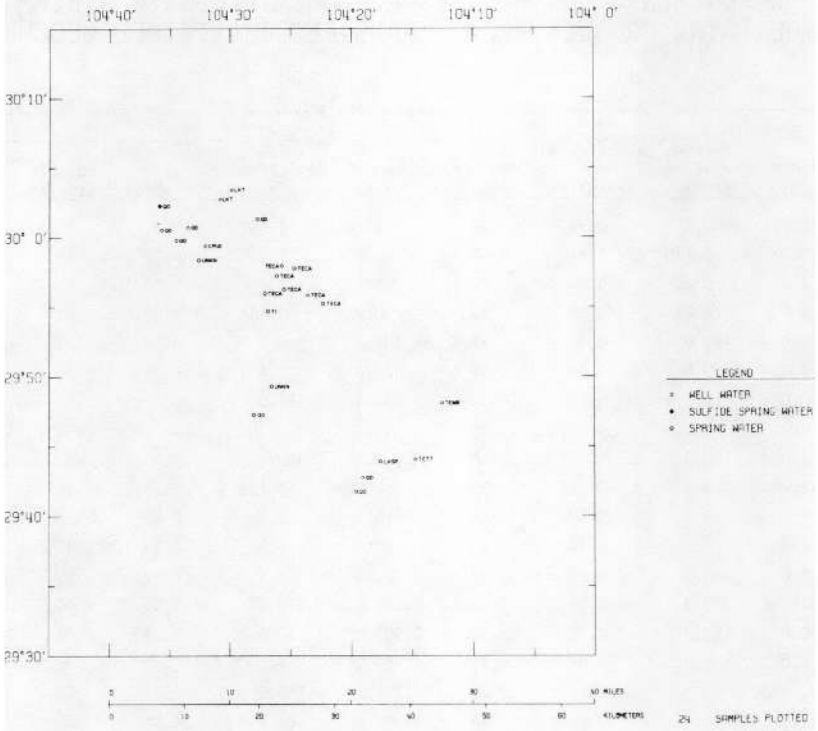

Figure 4

PRODUCING HORIZON MAP FOR GROUNDWATER
OF THE CHINATI MOUNTAINS PROJECT AREA,
TRANS-PECOS DETAILED GEOCHEMICAL SURVEY, TEXAS

Table 4

DISTRIBUTION OF SAMPLES BY GEOLOGIC UNIT CODE
FROM THE CHINATI MOUNTAINS PROJECT AREA,
TRANS-PECOS DETAILED GEOCHEMICAL SURVEY, TEXAS

Geologic Unit Code[a]	No. of Groundwater Samples	No. of Sediment Samples	No. of Radiometric Samples
QD	8	41	4
TI	1	9	21
TEPC	0	15	0
TECA	7	19	17
TECI	0	6	6
TEMR	1	11	8
TETT	1	0	5
LKSP	1	4	3
LKT	2	10	9
CPUD	1	6	4
UNKN	2	0	1
Total	24	121	78

[a]See Figure 3 for unit names.

arsenic, potassium, sodium, nickel, selenium, silicon, vanadium, chloride, pH, total alkalinity, and the sodium:chloride ratio.

The correlation matrix for groundwater geochemistry of the Chinati Mountains project area is presented in Table A-2. However, due to the limited number of groundwater samples, Table A-2 has not been used to interpret the hydrogeochemistry. Discussion of the groundwater geochemistry is given on a sample by sample basis, using the areal distribution plots as a guide to interpretation. The following discussion will be restricted to ten samples, five which display the highest uranium values and five which display the lowest values.

Groundwater samples with the highest uranium values are 029189, 027303, 027279, 027331, and 029241.

A spring, represented by Sample 029189 (lat. 29°54'43" N. and long. 104°26'53" W.), flowing from a Tertiary intrusive unit (TI) has a uranium concentration of 7.34 ppb and a specific conductance of 554 µmhos/cm. This sample also displays relatively high values for the following variables: the uranium:specific conductance ratio (Figure A-3b), the uranium:boron ratio (Figure A-4b), silver (Figure A-6b), magnesium (Figure A-14b), and molybdenum (Figure A-15b). Of all samples collected in the area, this sample displays the highest uranium:boron ratio (431.76) and molybdenum (100 ppb) value. The areal distribution plot for boron (Figure A-9b) indicates that concentrations of this element in this sample are relatively low. The elements silver and molybdenum are commonly found in nature as sulfides. The presence of sulfide mineralization together with high uranium:specific conductance and uranium:boron ratios may indicate a favorable environment for uranium mineralization.

Sample 027303 (lat. 29°59'24" N. and long. 104°32'06" W.) from Quaternary deposits (QD) has a uranium concentration of 8.42 ppb and a specific conductance of 1,421 µmhos/cm. This sample also displays relatively high values for the following variables: the uranium:boron ratio (Figure A-4b), silver (Figure A-6b), calcium (Figure A-11b), magnesium (Figure A-14b), strontium (Figure A-20b), total alkalinity (Figure A-25b), and sulfate (Figure A-24b). Of the samples observed, sulfate (412 ppm) and calcium (199.9 ppm) concentrations in this sample are the highest. The variables calcium, magnesium, strontium, and total alkalinity reflect a carbonate influence in the geochemical environment of the sample. Paleozoic carbonate sequences (CPUD) represent the major rock type within the area from which the sample was collected.

Sample 027279 (lat. 30°03'25" N. and long. 104°29'53" W.) from Lower Cretaceous (Trinitian) limestones (LKT) exhibits a uranium value of 8.52 ppb and a specific conductance of 1,279 µmhos/cm. This sample also displays relatively high values for the following variables: calcium (Figure A-11b), selenium (Figure A-18b), strontium (Figure A-20b), and sulfate (Figure A-24b). The variables calcium and strontium reflect a

carbonate influence in the geochemical environment. Of the samples observed, selenium (0.8 ppb) (Figure A-18b) and strontium (1,095 ppb) (Figure A-20b) concentrations were highest in this sample. High values for sulfate and selenium in this sample may indicate a sulfide occurrence favorable for uranium mineralization.

Sample 027331 (lat. 29°47'17" N. and long. 104°28'01" W.) from Quaternary deposits (QD) exhibits a uranium value of 9.64 ppb and a specific conductance of 2,123 µmhos/cm. This sample also displays relatively high values for the following variables: aluminum (Figure A-7b), boron (Figure A-9b), lithium (Figure A-13b), sodium (Figure A-16b), nickel (Figure A-17b), total alkalinity (Figure A-25b), and chloride (Figure A-22b). The variables boron, lithium, sodium, and chloride may reflect a saline-type influence on the geochemistry of the groundwater represented by this sample. Of the samples observed, aluminum (92 ppb), boron (758 ppb), lithium (225 ppb), sodium (332.2 ppm), total alkalinity (540 ppm), chloride (248 ppm), and specific conductance (2,123 µmhos/cm) concentrations were the highest in this sample. The areal distribution plots for calcium (Figure A-11b) and magnesium (Figure A-14b) indicate that concentrations of these elements are relatively low, suggesting that there is little or no carbonate influence upon the geochemistry of this sample. A white precipitate was observed surrounding the sampling site. The presence of this precipitate together with the relatively high concentrations of elements associated with saline environments suggests significant amounts of solids in solution. The high sulfate value (149 ppm) may indicate sulfide occurrences possibly favorable for uranium mineralization. This sample is located near the Red Hills prospect area where galena, malachite, and pyrite mineralization occur.

Sample 029241 (lat. 29°48'07" N. and long. 104°12'32" W.) from the Morita Ranch Formation (TEMR) displays the highest uranium value (18.34 ppb). The specific conductance is 1,061 µmhos/cm. This sample also displays relatively high values for the following variables: the uranium: specific conductance ratio (Figure A-3b), the uranium:sulfate ratio (Figure A-5b), sodium (Figure A-16b), and the sodium:chloride ratio (Figure A-26b). Of the samples observed, the uranium:specific conductance ratio (17.27) is the highest in this sample. The relatively high values for sodium and the sodium:chloride ratio are interpreted to be caused by the presence of feldspars and clays within the producing unit (TEMR).

The five lowest observed uranium concentrations are found in groundwater samples from the Chinati Mountains Group (TECA) (Samples 029283, 029257, 029246, 029190, and 029191). These samples also exhibit low values for sulfate (Figure A-24b).

Sample 029283 (lat. 29°57'47" N. and long. 204°24'43" W.) exhibits a uranium value of 0.75 ppb and a specific conductance of 459 µmhos/cm. This sample displays relatively high values for aluminum (Figure A-7b),

and the sodium:chloride ratio (Figure A-26b). These values are interpreted to be caused by the presence of feldspars and clays, major constituents of this volcanic group. The areal distribution plots for lithium (Figure A-13b), strontium (Figure A-20b), calcium (Figure A-11b), and total alkalinity (Figure A-25b) indicate that values for these variables are relatively low, signifying little or no carbonate influence on the geochemistry of this sample.

Sample 029257 (lat. 29°55'51" N. and long. 104°23'25" W.) has a uranium value of 0.98 ppb and a specific conductance of 619 µmhos/cm. This sample displays relatively high values for arsenic (Figure A-8b), selenium (Figure A-18b), silicon (Figure A-19b), vanadium (Figure A-21b), and the sodium: chloride ratio (Figure A-26b). The variables arsenic, selenium, and vanadium are considered pathfinder elements for uranium mineralization.

Sample 029246 (lat. 29°55'59" N. and long. 104°27'07" W.) has 1.01 ppb uranium and a specific conductance of 677 µmhos/cm. The areal distribution plots for potassium (Figure A-12b), sodium (Figure A-16b), strontium (Figure A-20b), boron (Figure A-9b), and calcium (Figure A-11b) indicate that values for these variables are relatively low for the sample.

Sample 029190 (lat. 29°56'17" N. and long. 104°25'33" W.) has 1.29 ppb uranium and a specific conductance of 818 µmhos/cm. This sample displays the highest value for silver (16 ppb) (Figure A-6b) and has high values for aluminum (Figure A-7b), molybdenum (Figure A-15b), and silicon (Figure A-19b). The areal distribution plots for strontium (Figure A-20b), barium (Figure A-10b), and sulfate (Figure A-24b) indicate that values for these variables are relatively low.

Sample 029191 (lat. 29°57'14" N. and long. 104°26'09" W.) has 1.83 ppb uranium and a specific conductance of 767 µmhos/cm. This sample displays relatively high values for aluminum (Figure A-7b), barium (Figure A-10b), and pH (Figure A-23b). The areal distribution plots for lithium (Figure A-13b), calcium (Figure A-11b), and silicon (Figure A-19b) indicate that the values for these elements in this sample are relatively low.

Summary of Groundwater Data

Samples collected from wells and springs within the Chinati Mountains Group (TECA) display lower uranium values than samples derived from other volcanic units (TEMR, TECI, and TI). This agrees with the data from the HSSR Presidio 1° x 2° NTMS Quadrangle (Uranium Resource Evaluation Project, 1978).

Samples which display the highest uranium values are from the Morita Ranch Formation (TEMR), Lower Cretaceous limestones (LKT), and Quaternary deposits (QD). Samples from the Presidio reconnaissance survey

from the Morita Ranch Formation (TEMR) have a similar range of concentrations as Sample 029241 from the Chinati Mountains project. Sample 027331, producing from QD, occurs within the vicinity of the Red Hills prospect area where sulfide mineralization occurs.

GEOCHEMICAL DISTRIBUTIONS IN STREAM SEDIMENTS

Sample locations from which stream sediment samples were collected in the Chinati Mountains project area are shown on Plate 4. Areal distribution maps for hot-acid-soluble uranium (U) as determined by fluorometric analysis and thorium are presented on Plates 5 and 6, and Figures B-1b and B-4b, respectively. Stream sediment data used to generate the tables and figures in Appendix B include all sediment samples collected from each of the geologic units in the project area and are presented in Table 4.

Observed data for hot-acid-soluble uranium determined by fluorometric analysis (U), total uranium determined by neutron activation (U-NT), thorium, the thorium:U-NT ratio, arsenic, lithium, molybdenum, nickel, phosphorus, titanium, and vanadium are given in Table B-3. The figures in Appendix B present log frequency, lognormal probability, percentile and areal distribution plots for these variables and U:U-NT ratio, boron, barium, beryllium, cerium, cobalt, chromium, iron, potassium, manganese, sodium, niobium, scandium, selenium, strontium, yttrium, and zirconium. All data for the sediment samples are included on microfiche in Appendix D.

Uranium

The areal distribution plot of soluble uranium values (Plate 5 and Figure B-1b) shows that the highest concentrations (≧2.70 ppm.) occur in the following areas: (1) western Cienega Mountain area (lat. 29°46' N. and long 104°12' W.) where the dominant geologic formations are the Perdiz Conglomerate (TEPC), Morita Ranch Formation (TEMR), Tertiary intrusives (TI), and Quaternary deposits (QD); (2) the Red Hill prospect area (lat. 29°45' N. and long. 104°28' W.) where bedrock is the Chinati Mountain Group (TECA), Tertiary intrusives (TI), Cretaceous limestones (LKT), and Paleozoic marine sediments (CPUD); (3) Wood's Ranch area (lat. 29°56' N. and long. 104°27' W.) where the units present are the Chinati Mountains Group (TECA) and Tertiary intrusives (TI); and (4) the Shely prospect area (lat. 30°00' N. and long. 104°29' W.) where bedrock is primarily the Shely Group (TECI), associated Tertiary intrusives (TI), Lower Cretaceous marine units (LKT), and Paleozoic marine sediments (CPUD).

The percentile plot in Figure B-1a indicates that the highest soluble uranium values are from sediments representing Tertiary intrusive rocks (TI) from all four of the anomalous areas. These intrusives are associated with the three calderas present in the project area.

The areal distribution plot for total uranium [analyzed by neutron activation (U-NT)] (Figure B-2b) illustrates that the high U-NT values are generally within the same areas as the high soluble uranium values. However, the Woods Ranch area has much higher total uranium than soluble uranium values, suggesting that uranium in the Woods Ranch area is predominantly in an insoluble (resistate) form. The percentile plot (Figure B-2a) indicates that the highest U-NT values are from sediments of predominantly Tertiary intrusive origin (TI).

The U:U-NT ratio indicates the percentage of total uranium in sediments which is present in hot-acid-soluble form. A sample with a high U:U-NT ratio and a high U-NT value may indicate anomalous accumulations of uranium in a hot-acid-soluble form. Low U:U-NT ratios in samples with high U-NT values indicate that the uranium present is probably within relatively insoluble (resistate) minerals [i.e., zircon, allanite, pyrochlore, monazite, and xenotime (Levinson, 1980)]. The areal distribution plot for the U:U-NT ratio (Figure B-3b) indicates that the majority of anomalously high uranium values for the Chinati Mountains project area are indicative of soluble (mobile) uranium. Those sediment samples with high U-NT values and low U:U-NT ratio values are derived from areas dominated by the Chinati Mountains Group (TECA) and the associated Tertiary intrusives (TI) (Woods Ranch area).

The correlation matrix, Table B-2, indicates a significant positive correlation ($\geq$0.24), for both Pearson and Spearman correlations, between the natural log of U and the natural logs of U-NT, lithium, thorium, zinc, manganese, the U:U-NT ratio (shown as LUTU), beryllium, niobium, potassium, cerium, and yttrium. Significant positive Pearson and Spearman correlations ($\geq$0.24) are indicated between the natural log of U-NT and the natural logs of U, lithium, zirconium, thorium, iron, titanium, zinc, manganese, phosphorus, beryllium, niobium, aluminum, sodium, potassium, cerium, and yttrium. Significant negative Pearson and Spearson correlations ($\leq$-0.24) are indicated between the natural log of U and the natural log of calcium. Significant negative Pearson and Spearman correlation is also indicated between the natural log of U-NT and the natural logs of the U:U-NT ratio and calcium.

Thorium

The areal distribution plot for thorium in stream sediments (Plate 6 and Figure B-4b) indicates that thorium concentrations $\geq$8.0 ppm generally occur in the same area as the Shely and Woods Ranch uranium anomalies, but they do not generally occur in the Red Hill prospect area or the Cienega Mountain area.

The percentile plot for thorium in Figure B-4a indicates that the highest thorium concentrations are located in sediment derived from the Shely intra-caldera units (TECI).

The correlation matrix (Table B-2) indicates a significant positive Pearson and Spearman correlation (≧0.24) between the natural log of thorium and the natural logs of U, U-NT, the thorium:U-NT ratio, beryllium and niobium. Significant negative Pearson and Spearman correlations (≦-0.24) are indicated between the natural log of thorium and the natural log of calcium.

Figure B-5b, an areal distribution plot of the thorium:U-NT ratio, can be used to delineate those areas which have been depleted or enriched in uranium with respect to thorium. The thorium:uranium ratio generally remains about 3.5 throughout differentiation of igneous rocks, however, hydrothermal veins tend to have lower thorium:uranium ratios suggesting that thorium is less efficiently separated into late stage fluids (Levinson, 1980). Assuming normal thorium:uranium ratio values of between 3 and 7, a low value (≦2.10) may indicate uranium enrichment with respect to thorium. The sites of low thorium:uranium ratios are the Woods Ranch and the Red Hill prospect areas. Samples representing the Shely prospect and Cienega Mountain areas exhibit normal values for the thorium:U-NT ratio (2.5 to 4.7).

Related Variables

In addition to U, U-NT, the U:U-NT ratio, thorium and the thorium:U-NT ratio, other variables which may be useful in identifying areas of potential uranium mineralization include arsenic, boron, barium, beryllium, cerium, cobalt, chromium, iron, potassium, lithium, manganese, molybdenum, sodium, niobium, nickel, phosphorus, scandium, selenium, strontium, titanium, vanadium, yttrium, and zirconium. The association of these variables with uranium is based on areal distribution plots, percentile plots, and the correlation matrix presented in Appendix B. A discussion of these related variables for each of the four designated anomalous areas within the Chinati Mountains project area follows.

Shely prospect area (lat. 30°00' N. and long. 104°29' W.). Samples which exhibit high values for uranium and were collected from catchments draining the Tertiary Allen Intrusive Complex in the Shely prospect area also exhibit relatively high values for the elements boron (Figure B-7b), beryllium (Figure B-9b), cerium (Figure B-10b), lithium (Figure B-15b), manganese (Figure B-16b), niobium (Figure B-19b), nickel (Figure B-20b), and yttrium (Figure B-27b). Samples collected from catchments draining the Paleozoic marine sediments (CPUD) in the Shely prospect area which exhibit high uranium values also exhibit high concentrations of the elements boron (Figure B-7b), barium (Figure B-8b), beryllium (Figure B-9b), cerium (Figure B-10b), chromium (Figure B-12b), iron (Figure B-13b), nickel (Figure B-20b), phosphorus (Figure B-21b), scandium (Figure B-22b), selenium (Figure B-23b), titanium (Figure B-25b), vanadium (Figure B-26b), yttrium (Figure B-27b), and zirconium (Figure B-28b).

The U:U-NT ratios for samples from both the Tertiary intrusives and the Paleozoic marine sediments are high (≧0.86), while the thorium:U-NT ratios decrease westward from the Tertiary intrusives to Paleozoic marine sediments (4.0 to 1.1). The area of anomalous uranium concentrations (lat. 30°01' N. and long. 104°30' W.) (southwestern section of the Organ Pipe Hills) represents the contact between Tertiary intrusives and Paleozoic marine sediments. The elements beryllium, lithium, iron, manganese, vanadium and sodium are noted constituents of oxides and clays (Levinson, 1980). According to Cofer (1980) and Henry (1980), the known uranium mineralization present is derived from the Tertiary intrusives. The rhyolite porphyries have been weathered to oxides and clays with which the uranium has been adsorbed. The formation of the Shely prospect is a result of supergene weathering and precipitation of uranium in a fracture zone within the Tertiary intrusive. It is possible, therefore, that groundwater could also have transported uranium (derived from TI) to the older, fractured, marly marine sediments (CPUD) where the presence of carbonates and phosphates would have allowed precipitation of uranium. Therefore, the contact between the source rock (TI) and the Paleozoic marine sediments (CPUD) may be a favorable site for uranium mineralization as urano-phosphates or uraniferous Fe-Mn oxyhydroxides.

Woods Ranch area (lat. 29°56' N. and long. 104°27' W.). Samples which exhibit high values of uranium in the Woods Ranch area also exhibit high values for the variables barium (Figure B-8b), beryllium (Figure B-9b), cerium (Figure B-10b), iron (Figure B-13b), potassium (Figure B-14b), manganese (Figure B-16b), sodium (Figure B-18b), niobium (Figure B-19b), phosphorus (Figure B-21b), scandium (Figure B-22b), strontium (Figure B-24b), titanium (Figure B-25b), yttrium (Figure B-27b), and zirconium (Figure B-28b). High values for the U:U-NT ratio (≧0.71) indicate that the samples representing basins draining the higher areas of the Chinati Mountains have a high percentage of soluble uranium. Low thorium:U-NT ratios in this same area signify uranium enrichment with respect to thorium. This enrichment may be associated in part with the presence of manganese and phosphorus, perhaps as Fe-Mn oxyhydroxides and/or urano-phosphates. However, high concentrations of elements such as zirconium, yttrium, and cerium also indicate an association of uranium with resistate minerals such as zircon, allanite, pyrochlore, monazite and xenotime. The correlation matrix (Table B-2) also suggests an association between uranium and elements commonly found in resistate minerals.

Red Hill prospect area (lat. 29°45' N. and long. 104°28' W.). Samples which exhibit high values of uranium in the Red Hill prospect area also exhibit relatively high values for the variables arsenic (Figure B-6b), barium (Figure B-8b), beryllium (Figure B-9b), cobalt (Figure B-11b), iron (Figure B-13b), lithium (Figure B-15b), manganese (Figure B-16b), molybdenum (Figure B-17b), niobium (Figure B-19b), sodium (Figure B-18b), nickel (Figure B-20b), phosphorus (Figure B-21b), scandium (Figure B-22b), strontium (Figure B-24b), titanium (Figure B-25b),

yttrium (Figure B-27b), and zirconium (Figure B-28b). The high concentrations of elements such as zirconium, yttrium, niobium, and titanium indicate an association of uranium with resistate minerals. The correlation matrix (Table B-2) also suggests an association between uranium and elements commonly found in resistate minerals. The portion of uranium that is soluble (mobile) may be associated with clays and oxides (supported by high values for iron, manganese, beryllium, and lithium) or with phosphates as urano-phosphate complexes in the marly interbeds within the Cretaceous and Permian carbonate units.

The source rock for the soluble uranium is unknown. However, mineralization within the Red Hill and Shafter mining districts is attributed to hydrothermal fluid migration from the South Chinati Laccolith intrusive into brecciated, faulted, and fractured zones of the Cretaceous and Permian limestones.

Cienega Mountain area (lat. 29°46' N. and long. 104°12' W.). Samples which exhibit high values of uranium in the Cienega Mountain area also exhibit relatively high values for the variables barium (Figure B-8b), beryllium (Figure B-9b), cerium (Figure B-10b), chromium (Figure B-12b), iron (Figure B-13b), lithium (Figure B-15b), manganese (Figure B-16b), sodium (Figure B-18b), niobium (Figure B-19b), phosphorus (Figure B-21b), strontium (Figure B-24b), titanium (Figure B-25b), vanadium (Figure B-26b), yttrium (Figure B-27b), and zirconium (Figure B-28b).

Once again, the high concentrations for elements such as zirconium, yttrium, niobium, titanium, and cerium indicate an association of uranium with resistate minerals. The soluble (mobile) uranium present may be associated with oxides and clays since high values for the elements iron, manganese, beryllium, and lithium (common lithophile elements) are also exhibited.

Summary of Stream Sediment Data

Anomalous values for U, U-NT, and thorium are concentrated in four areas designated as: the Shely prospect, the Woods Ranch, the Red Hill prospect, and Cienega Mountain. In the project area, values for the U:U-NT ratio indicate the existence of soluble uranium in the Sheley prospect, Red Hill prospect, and Cienega Mountain areas, whereas insoluble uranium is apparently present in the Woods Ranch area.

In each area, insoluble uranium is interpreted to be associated with the elements zirconium, yttrium, niobium, titanium, and cerium. Soluble uranium is interpreted to be associated with the elements iron, manganese, beryllium, lithium, phosphorus, and vanadium.

Within the Shely prospect area, the soluble uranium probably originated from the Allen Intrusive Complex. However, sources for the soluble uranium in the other areas are unknown.

BIBLIOGRAPHY

1. Amsbury, D. L., *Geologic Map of the Pinto Canyon Area, Presidio County, Texas,* University of Texas, Austin, Bureau of Economic Geology, No. 22 (1958).

2. Arendt, J. W., Butz, T. R., Cagle, G. W., Kane, V. E., and Nichols, C. E., *Hydrogeochemical and Stream Sediment Reconnaissance Procedures of the Uranium Resource Evaluation Project,* Union Carbide Corporation, Nuclear Division, Oak Ridge Gaseous Diffusion Plant, Oak Ridge, Tennessee, K/UR-100 (December 1979).

3. Baker, C. L., *Note on the Permian Chinati Series of West Texas,* University of Texas, Austin, Bureau of Economic Geology, Bulletin 2901 (1929).

4. Barnes, V. E., *Geologic Atlas of Texas, Emory Peak-Presidio Sheet,* University of Texas, Austin, Bureau of Economic Geology (Preliminary Sheet) (1977).

5. Barnes, V. E., *Geologic Atlas of Texas, Marfa Sheet,* University of Texas, Austin, Bureau of Economic Geology (Preliminary Sheet) (1978).

6. Butz, T. R., Payne, A. G., Grimes, J. G., Helgerson, R. N., and Bard, C. S., *Hydrogeochemical Stream Sediment Detailed Geochemical Survey for Trans-Pecos Texas,* Union Carbide Corporation, Nuclear Division, Oak Ridge Gaseous Diffusion Plant, Oak Ridge, Tennessee, K/UR-29, Parts 1-4 (November 1979). United States Department of Energy, Grand Junction, Colorado [GJBX-29(80)].

7. Cagle, G. W., "The Oak Ridge Analytical Program," *Symposium on Hydrogeochemical and Stream Sediment Reconnaissance for Uranium in the United States, March 16 and 17, 1977.* United States Energy Research and Development Administration, Grand Junction, Colorado, pp 133-156 [GJBX-77(77)] (October 1977).

8. Cebull, S. E., Shurbet, D. H., Keller, G. R., and Russell, L. R., "Possible Role of Transform Faults in the Development of Apparent Offsets in the Ouachita-Southern Appalachian Tectonic Belt," *Journal of Geology,* Vol. 84, pp 107-114 (1976).

9. Cepeda, J. C., "The Chinati Mountains Caldera, Presidio County, Texas," *Cenozoic Geology of the Trans-Pecos Volcanic Field of Texas, Proceedings and Field Guide,* pp 64-84 (1978).

10. Cofer, L., "Geology of the Shely Cauldron, Pinto Canyon Area Presido County, Texas," *Energy Exploration in the 80's,* Southwestern Section of AAPG, Annual Meeting, February 25-27, 1980, El Paso, Texas, p 20 (1980).

11. D'Silva, A. P., Grabau, F., and Haas, W. J., Jr., *Multilaboratory Analytical Quality Control Program for the Hydrogeochemical and Stream Sediment Reconnaissance*, Ames Laboratory, Iowa State University, Ames, Iowa, IS-4736 (April 1980) (Available from National Technical Information Service, U. S. Department of Commerce, 5285 Port Royal Road, Springfield, Virginia 22161).

12. Files, F. G., *Uranium in Volcanic Environments in the Great Basin*, United States Department of Energy, Grand Junction, Colorado [GJBX-98(78)].

13. Greenwood, E., "Oil and Gas Possibilities in the Chihuahua Area," in *The Geologic Framework of the Chihuahua Tectonic Belt Symposium, November 4-6, 1970*, West Texas Geological Society, Midland, Texas (1970).

14. Hem, J. D., *Study of Interpretation of the Chemical Characteristics of Natural Water*, U.S. Geological Survey, Water Supply Paper 1473, p. 155 (1970).

15. Henry, C. D., Deux, T. W., and Wilbert, W., *Uranium Resource Evaluation-Marfa 1° x 2° NTMS Quadrangle, Texas*, U.S. Department of Energy, PGJ-001 (1980).

16. Henry, C. D. and Tyner, G. N., "Alteration and Uranium Release From Rhyolitic Igneous Rocks: Examples from Mitchell Mesa, Santana Tuff, Chinati Mountains Group and Allen Complex, Trans-Pecos, Texas," in *Formation of Uranium Ore by Diagenesis of Volcanic Sediments*, United States Department of Energy, Grand Junction, Colorado, pp. VII-17 to VII-109 [GJBX-22(78)].

17. Jordan, J. M., "Perdiz Conglomerate," in *Formation of Uranium Ore by Diagenesis of Volcanic Sediments*, United States Department of Energy, Grand Junction, Colorado, pp. IV-3 to IV-26 [GJBX-22(78)].

18. Kane, V. E., Baer, T., and Begovich, C. L., *Principal Component Testing for Outliers*, Union Carbide Corporation, Nuclear Division, Oak Ridge Gaseous Diffusion Plant, Oak Ridge, Tennessee, K/UR-7 (July 1977). United States Department of Energy, Grand Junction, Colorado [GJBX-71(77)].

19. King, P. B., Beikman, H. M., and Edmonston, G. J., *Geologic Map of the United States*, U.S. Geological Survey (1974).

20. Levinson, A. A., *Introduction of Exploration Geochemistry*, The 1980 Supplement, Allied Publishing Ltd., Alberta, Canada (1980).

21. Matthews, G. W., "Classification of Uranium Occurrences in and Related to Plutonic Igneous Rocks," in *A Preliminary Classification of Uranium Deposits*, U.S. Department of Energy, Grand Junction, Colorado [GJBX-63(78)].

22. Maxwell, R. A. and Dietrich, J. W., *Correlation of Tertiary Rock Units, West Texas,* University of Texas, Austin, Bureau of Economic Geology, Report of Investigation No. 70 (1970).

23. McAnulty, N., "Resurgent Cauldrons and Associated Mineralization, Trans-Pecos, Texas," *Tectonics and Mineral Resources of Southwestern North America,* New Mexico Geological Society, Special Publication No. 6, pp 180-186 (1976).

24. McAnulty, W. N., Sr., *Mineral Deposits of the West Chinati Stock, Chinati Mountains, Presidio County, Texas,* University of Texas, Austin, Bureau of Economic Geology, Geological Circular No. 72-1 (1975).

25. Muehlberger, W. R. and Wiley, M. A., "The Texas Lineament," in *The Geologic Framework of the Chihuahua Tectonic Belt,* West Texas Geological Society and University of Texas at Austin, pp 15-24 (1970).

26. National Oceanic and Atmospheric Administration, *Climates of the States, Vol. II-Western States Including Alaska and Hawaii,* Department of Commerce, Water Information Center, Port Washington, New York, pp. 877-920 (1974).

27. Reeves, C. C., Kenney, P., and Wright, E., "Known Radioactive Anomalies and Uranium Potential of Cenozoic Sediments, Trans-Pecos, Texas," *Cenozoic Geology of the Trans-Pecos Volcanic Field of Texas,* pp 86-99 (1978).

28. Rix, C. C., *Geology of Chinati Peak Quadrangle, Presidio County, Trans-Pecos Texas,* University of Texas, Austin, Ph.D. Dissertation (1953).

29. Smith, C. I., "Lower Cretaceous Sedimentation and Tectonics of the Coahuila and West Texas Platforms," in *The Geologic Framework of the Chihuahua Tectonic Belt,* West Texas Geological Society and University of Texas at Austin, pp 75-82 (1970).

30. Smith, R. L. and Bailey, R. A., "Resurgent Cauldrons," in Coats, R. R., Hay, R., and Anderson, C. (Editors), *Studies in Volcanology,* Geological Society of America, Memoir No. 116, pp 613-662 (1968).

31. Southern Interstate Nuclear Board, *Uranium in the Southern United States,* Division of Raw Materials, United States Atomic Energy Commission, TID UC-51, pp 97-146 (1969).

32. Strain, W. S., "Late Cenozoic Bolson Integration in the Chihuahua Tectonic Belt," in *The Geologic Framework of the Chihuahua Tectonic Belt,* West Texas Geological Society and University of Texas at Austin, pp 167-174 (1970).

33. Twiss, P. C., "Cenozoic History of Rim Rock Country, Trans-Pecos Texas," *The Geologic Framework of the Chihuahua Tectonic Belt*, West Texas Geological Society and University of Texas at Austin, pp 139-155 (1970).

34. Uranium Resource Evaluation Project, *Hydrogeochemical and Stream Sediment Reconnaissance Basic Data For Presidio NTMS Quadrangle, Texas*, Union Carbide Corporation, Nuclear Division, Oak Ridge Gaseous Diffusion Plant, Oak Ridge, Tennessee, K/UR-113 (December 1978). United States Department of Energy, Grand Junction, Colorado [GJBX-12(79)].

35. Uranium Resource Evaluation Project, *Procedures Manual for Groundwater Reconnaissance Sampling*, Union Carbide Corporation, Nuclear Division, Oak Ridge Gaseous Diffusion Plant, Oak Ridge, Tennessee, K/UR-12 (March 1978). United States Department of Energy, Grand Junction, Colorado [GJBX-62(78)].

36. Uranium Resource Evaluation Project, *Procedures Manual for Stream Sediment Reconnaissance Sampling*, Union Carbide Corporation, Nuclear Division, Oak Ridge Gaseous Diffusion Plant, Oak Ridge, Tennessee, K/UR-13 (May 1978). United States Department of Energy, Grand Junction, Colorado [GJBX-84(78)].

APPENDIX A

GROUNDWATER

*Where probability and frequency plots are not present, they are unavailable because of the small number of samples.

APPENDIX A

GROUNDWATER

LIST OF TABLES

LIST OF FIGURES

LIST OF FIGURES, Continued

LIST OF FIGURES, Continued

LIST OF FIGURES, Continued

LIST OF FIGURES, Continued

LIST OF FIGURES, Continued

LIST OF FIGURES, Continued

Table A-1

STATISTICAL SUMMARY FOR GROUNDWATER OF THE CHINATI MOUNTAINS PROJECT AREA,
TRANS-PECOS DETAILED GEOCHEMICAL SURVEY, TEXAS

ELEMENT	NO. SAMPLES ANALYZED: MEASURABLE VALUES	BELOW DETECTION LIMIT	DETECTION LIMIT	MINIMUM VALUE	MAXIMUM VALUE	MEAN	MEDIAN	MODE	STANDARD DEVIATION	COEFFICIENT OF VARIATION	LN TRANSFORMATION: MEAN	LN TRANSFORMATION: S. D.	ROBUST: MEAN	ROBUST: S. D.
U	23	1	<0.20	<0.20	18.34	4.00	1.89	4.08	4.184	1.047	0.94	0.97	0.85	1.04
SP	24			358	2123	900	818	483	399.7	0.4	6.71	0.43	6.71	0.41
U/SP	24			0.11	17.27	4.22	3.17	1.51	4.010	0.951	1.00	1.09	1.06	1.12
U/B	23			0.37	431.76	62.64	41.02	41.91	87.047	1.390	3.43	1.49	3.51	1.47
U/SD	24			1.08	826.00	165.16	91.69	119.94	197.724	1.197	4.32	1.56	4.40	1.61
AG	13	10	<2	<2	16	8	3	<2	4.2	0.5	2.01	0.57		
AL	10	13	<10	<10	92	32	<10	<10	26.3	0.8	3.25	0.69		
AS	16	8	<0.5	<0.5	11.3	2.4	0.7	<0.5	2.69	1.13	0.48	0.85	-0.18	1.30
B	23			13	758	128	60	47	161.8	1.3	4.33	1.03	4.30	1.06
BA	22	1	<2	<2	216	30	14	13	44.1	1.5	2.89	0.98	2.82	0.99
BE	0	23	<1	<1	<1		<1	<1						
CA	23			21.8	199.9	63.9	55.3	63.5	37.20	0.58	4.04	0.48	4.02	0.46
CD	5	18	<2	<2	4	2	<2	<2	0.9	0.3	0.91	0.32		
CR	0	23	<4	<4	<4		<4	<4						
CU	5	18	<2	<2	3	2	<2	<2	0.5	0.2	0.94	0.22		
FE	16	7	<10	<10	111	19	12	15	24.6	1.3	2.69	0.56	2.48	0.27
K	23			0.7	14.2	4.8	2.8	2.9	4.50	0.94	1.16	0.91	1.17	1.11
LI	23			2	225	44	13	7	60.3	1.4	2.96	1.31	2.95	1.34
MG	23			1.8	59.6	14.4	8.3	8.5	14.30	0.99	2.32	0.82	2.31	0.82
MN	15	8	<2	<2	92	14	<2	<2	24.9	1.7	1.84	1.18		
MO	17	6	<4	<4	112	21	5	<4	32.6	1.6	2.39	1.03	1.75	1.76
NA	23			4.5	332.2	48.0	28.3	29.6	66.69	1.39	3.38	0.98	3.35	0.93
NI	10	13	<4	<4	28	8	<4	<4	7.1	0.8	1.97	0.57		
P	1	22	<40	<40	49	49	<40	<40	0.0	0.0	3.89	0.0		
SC	0	23	<1	<1	<1		<1	<1						
SE	13	11	<0.2	<0.2	0.8	0.4	0.2	<0.2	0.19	0.43	-0.91	0.45		
SI	23			4.5	27.7	16.8	15.2	15.2	6.61	0.39	2.73	0.46	2.77	0.46
SR	23			91	1095	489	474	567	244.9	0.5	6.03	0.65	6.06	0.74
TI	1	22	<2	<2	2	2	<2	<2	0.0	0.0	0.69	0.0		
V	7	16	<4	<4	8	6	<4	<4	1.6	0.3	1.76	0.29		
Y	6	17	<1	<1	1	1	<1	<1	0.0	0.0	0.0	0.0		
ZN	22	1	<4	<4	376	66	30	30	86.5	1.3	3.56	1.16	3.45	1.43
ZR	10	13	<2	<2	5	3	<2	<2	1.1	0.4	1.05	0.34		
T-AK	24			124	540	244	224	321	89.3	0.4	5.45	0.33	5.44	0.34
M-AK	24			126	528	243	216	215	88.4	0.4	5.44	0.33	5.43	0.34
P-AK	24			0	0	0	0	0	0.0	0.0				
CL	15	9	<10	<10	248	44	12	<10	59.3	1.3	3.34	0.87	2.56	1.14
NA/C	23			0.32	5.82	2.23	2.02	2.45	1.301	0.584	0.64	0.61	0.67	0.57
PH	24			5.0	8.0	6.8	7.1	7.2	0.91	0.13				
SO4	23	1	<5	<5	412	72	40	<5	92.3	1.3	3.50	1.38	3.42	1.59

NOTE: Refer to Table 1, Page 26 and Table C-1, Page C-4 for concentration units and symbol defintions.

Table A-2

CORRELATION MATRIX FOR GROUNDWATER OF THE CHINATI MOUNTAINS PROJECT AREA, TRANS-PECOS DETAILED GEOCHEMICAL SURVEY, TEXAS

	L-U	LUSP	L-AG	L-SE	PH	L-MO	L-SR	LTAK	L-SP	LSO4	L-B	L-LI	L-MN
L-U	1.00 (23)												
LUSP	0.89*** 0.86*** (23)	1.00 (24)											
L-AG	-0.22@ -0.19@ (13)	-0.45@ -0.35@ (13)	1.00 (13)										
L-SE	0.10@ 0.15@ (12)	0.33@ 0.14@ (13)	0.34@ 0.15@ (7)	1.00 (13)									
PH	0.28 0.19 (23)	0.35* 0.41** (24)	-0.33@ -0.34@ (13)	-0.38@ -0.38@ (13)	1.00 (24)								
L-MO	0.02 -0.05 (17)	0.28 0.16 (17)	0.02@ 0.24@ (9)	-0.24@ -0.29@ (11)	0.33 0.33 (17)	1.00 (17)							
L-SR	0.47** 0.43** (22)	0.11 0.17 (23)	-0.31@ -0.12@ (13)	0.21@ 0.16@ (13)	-0.08 -0.19 (23)	-0.25 -0.43* (17)	1.00 (23)						
LTAK	0.65*** 0.65*** (23)	0.33 0.51** (24)	-0.14@ -0.07@ (13)	-0.03@ -0.06@ (13)	0.06 0.05 (24)	0.04 -0.09 (17)	0.60*** 0.63*** (23)	1.00 (24)					
L-SP	0.44** 0.43** (23)	-0.05 0.01 (24)	0.31@ 0.30@ (13)	0.35@ 0.52@ (13)	-0.23 -0.30 (24)	-0.62*** -0.52** (17)	0.50** 0.73*** (23)	0.59*** 0.56*** (24)	1.00 (24)				
LSO4	0.47** 0.39* (22)	0.00 0.10 (23)	0.46@ 0.55@ (12)	0.36@ 0.40@ (13)	-0.18 -0.25 (23)	-0.07 -0.05 (16)	0.68*** 0.74*** (22)	0.47** 0.45** (23)	0.74*** 0.80*** (23)	1.00 (23)			
L-B	0.30 0.32 (22)	-0.19 -0.04 (23)	-0.28@ -0.32@ (13)	-0.03@ -0.03@ (13)	-0.24 -0.31 (23)	-0.42* -0.46* (17)	0.76*** 0.84*** (23)	0.69*** 0.52** (23)	0.69*** 0.72*** (23)	0.63*** 0.70*** (22)	1.00 (23)		
L-LI	0.10 0.13 (22)	-0.35* -0.12 (23)	-0.08@ -0.06@ (13)	-0.10@ -0.10@ (13)	-0.29 -0.29 (23)	-0.24 -0.29 (17)	0.59*** 0.73*** (23)	0.56*** 0.52** (23)	0.60*** 0.61*** (23)	0.61*** 0.61*** (22)	0.89*** 0.84*** (23)	1.00 (23)	
L-MN	-0.22@ -0.06@ (14)	-0.44 -0.30 (15)	0.10@ 0.19@ (9)	-0.26@ -0.21@ (9)	-0.35 -0.48* (15)	-0.29@ -0.40@ (12)	0.40 0.42 (15)	0.09 0.01 (15)	0.40 0.34 (15)	0.36 0.33 (15)	0.77*** 0.80*** (15)	0.77*** 0.80*** (15)	1.00 (15)
L-NA	0.30 0.23 (22)	-0.11 0.00 (23)	-0.24@ -0.18@ (13)	0.11@ -0.00@ (13)	-0.06 -0.15 (23)	0.02 -0.16 (17)	0.52** 0.65*** (23)	0.45** 0.45** (23)	0.56*** 0.60*** (23)	0.77*** 0.81*** (22)	0.76*** 0.76*** (23)	0.75*** 0.78*** (23)	0.57** 0.70*** (15)
L-CL	-0.23@ -0.32@ (14)	-0.48* -0.60** (15)	-0.10@ -0.18@ (9)	-0.01@ -0.05@ (11)	-0.27 -0.32 (15)	-0.32@ -0.27@ (12)	0.28 0.25 (15)	0.24 -0.35 (15)	0.54** 0.38 (15)	0.39 0.50* (15)	0.83*** 0.79*** (15)	0.77*** 0.77*** (15)	0.71@ 0.69@ (12)
LUSO	0.19 0.07 (23)	0.65*** 0.28 (24)	-0.28@ -0.18@ (13)	0.06@ -0.28@ (13)	0.28 0.21 (24)	0.18 0.11 (17)	-0.46** -0.59*** (23)	-0.07 -0.14 (24)	-0.40* -0.53*** (24)	-0.68*** -0.83*** (23)	-0.55*** -0.60*** (23)	-0.62*** -0.50** (23)	-0.50* -0.43 (15)
L-K	-0.22 -0.09 (22)	-0.50** -0.29 (23)	-0.14@ -0.22@ (13)	-0.23@ -0.20@ (13)	-0.31 -0.38* (23)	-0.38 -0.42* (17)	0.47** 0.47** (23)	-0.11 -0.08 (23)	0.28 0.32 (23)	0.37* 0.42* (22)	0.57*** 0.63*** (23)	0.51** 0.63*** (23)	0.66*** 0.67*** (15)
LU/B	0.56*** 0.49** (22)	0.65*** 0.60*** (23)	0.10@ 0.13@ (13)	0.36@ 0.18@ (13)	0.36* 0.35 (23)	0.33 0.16 (17)	-0.30 -0.22 (23)	-0.01 0.09 (23)	-0.25 -0.06 (23)	-0.23 -0.12 (22)	-0.63*** -0.54*** (23)	-0.70*** -0.58*** (23)	-0.60** -0.57** (15)
L-AS	-0.29 -0.23 (15)	-0.57** -0.24 (16)	-0.56@ -0.65@ (8)	-0.28@ -0.03@ (12)	-0.51** -0.61** (16)	0.13@ -0.01@ (13)	0.21 0.06 (16)	0.12 0.08 (16)	-0.14 -0.13 (16)	0.03 0.01 (15)	0.40 0.33 (16)	0.52** 0.39 (16)	0.52@ 0.50@ (11)
L-AL	-0.03@ -0.15@ (10)	-0.40@ -0.55@ (10)	0.33@ 0.71@ (6)	-0.29@ -0.21@ (5)	0.22@ 0.02@ (10)	-0.29@ -0.07@ (7)	-0.34@ -0.45@ (10)	0.03@ -0.26@ (10)	0.37@ 0.23@ (10)	0.16@ 0.03@ (9)	0.08@ -0.29@ (10)	-0.00@ -0.24@ (10)	-0.59@ -0.56@ (5)
L-CA	0.40* 0.47** (22)	0.39@ 0.42** (23)	0.27@ 0.15@ (13)	0.67@ 0.72@ (13)	-0.23 -0.27 (23)	-0.12 -0.17 (17)	0.30 0.31 (23)	0.09 0.21 (23)	0.15 0.26 (23)	0.31 0.25 (22)	-0.14 -0.03 (23)	-0.14 -0.10 (23)	-0.17 -0.12 (15)
L-MG	0.34 0.36 (22)	0.38@ 0.47** (23)	0.33@ 0.32@ (13)	0.07@ 0.20@ (13)	0.24 0.32 (23)	0.05 0.12 (17)	0.39* 0.50** (23)	0.28 0.49** (23)	0.12 0.28 (23)	0.24 0.31 (22)	-0.08 0.10 (23)	-0.07 0.07 (23)	-0.12 -0.16 (15)
L-BA	0.38@ 0.42@ (21)	0.04 0.16 (22)	-0.14@ -0.12@ (12)	-0.43@ -0.38@ (13)	0.38@ 0.28 (22)	-0.17 0.01 (16)	0.30 0.29 (22)	0.40@ 0.39@ (22)	0.37@ 0.37@ (22)	0.20 0.31 (22)	0.23 0.28 (22)	0.08 0.08 (22)	-0.09 -0.03 (15)
LV/C	-0.03 -0.12 (22)	0.21 0.22 (23)	-0.39@ -0.17@ (13)	0.30@ 0.11@ (13)	-0.13 -0.12 (23)	0.42@ 0.36 (17)	-0.23 -0.29 (23)	-0.23 -0.09 (23)	-0.41@@ -0.44@@ (23)	-0.04 -0.22 (22)	-0.30 -0.37@ (23)	-0.18 -0.16 (23)	-0.18 -0.24 (15)
L-SI	0.06 -0.12 (22)	0.20 0.11 (23)	-0.07@ -0.06@ (13)	0.38@ 0.42@ (13)	0.03 0.01 (23)	0.28 0.17 (17)	-0.21 -0.26 (23)	0.02 -0.14 (23)	-0.37@ -0.39@ (23)	-0.27 -0.37@ (22)	-0.31 -0.44@@ (23)	-0.12 -0.13 (23)	-0.21 -0.14 (15)
L-NI	0.25@ 0.25@ (10)	0.09@ 0.15@ (10)	0.71@ 0.66@ (6)	0.70@ 0.62@ (6)	0.00@ -0.04@ (10)	-0.59@ -0.64@ (6)	0.29@ 0.21@ (10)	-0.01@ -0.10@ (10)	0.38@ 0.32@ (10)	0.58@ 0.64@ (10)	0.45@ 0.30@ (10)	0.40@ 0.29@ (10)	0.41@ 0.01@ (7)
L-ZR	-0.45@ -0.49@ (9)	-0.43@ -0.51@ (10)	0.49@ 0.39@ (6)	-0.18@ -0.15@ (7)	-0.37@ -0.47@ (10)	0.59@ 0.60@ (7)	-0.27@ -0.33@ (10)	-0.41@ -0.43@ (10)	-0.58@ -0.53@ (10)	-0.36@ -0.40@ (9)	-0.23@ -0.12@ (10)	-0.25@ -0.23@ (10)	0.16@ 0.12@ (7)

NOTE: (1) Pearson correlation/Spearman correlation/(sample size). If either element has a concentration below the laboratory detection limits, it is omitted from the pairwise computations.
(2) Significance levels: *-10%, **-5%, ***-1%.
(3) No correlation computed because of insufficient number of pairs: ******.

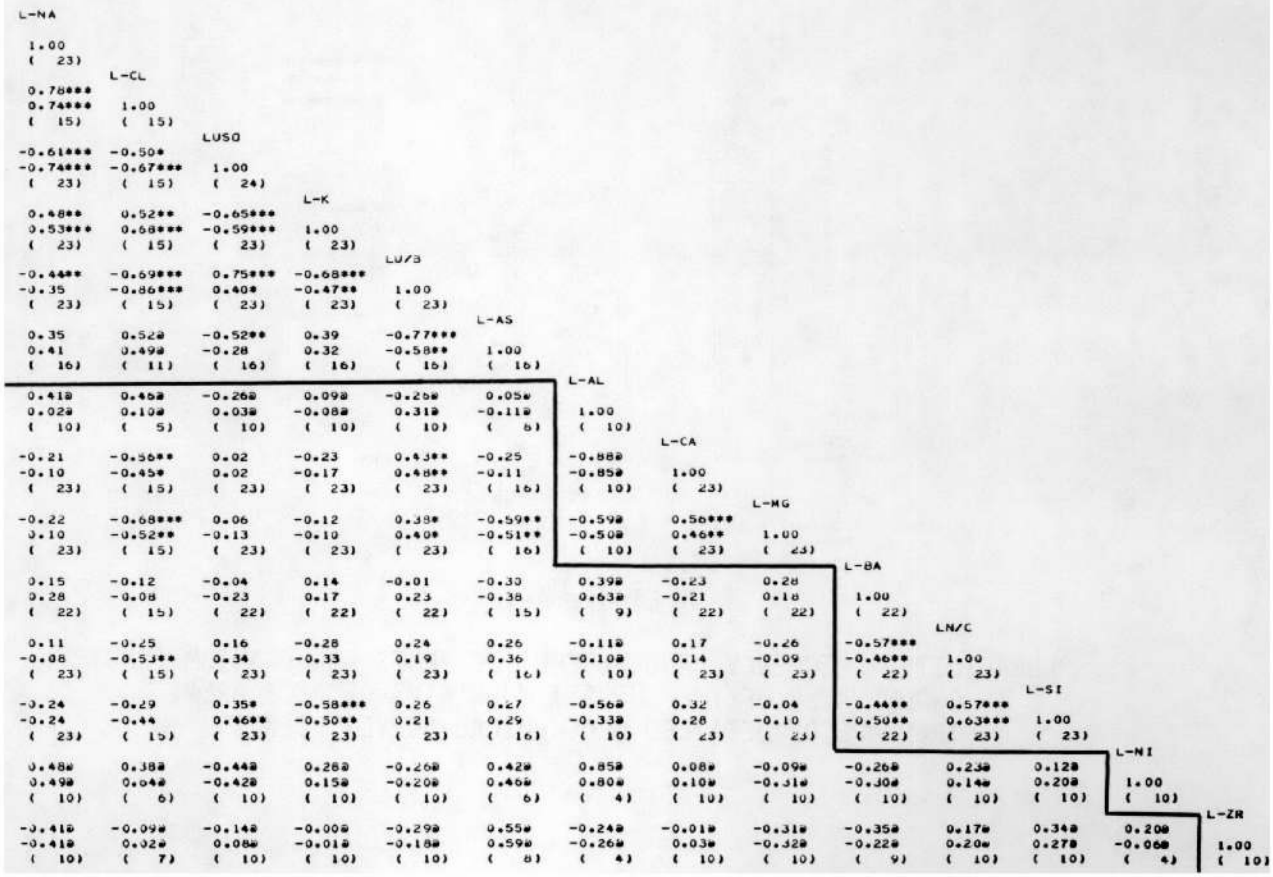

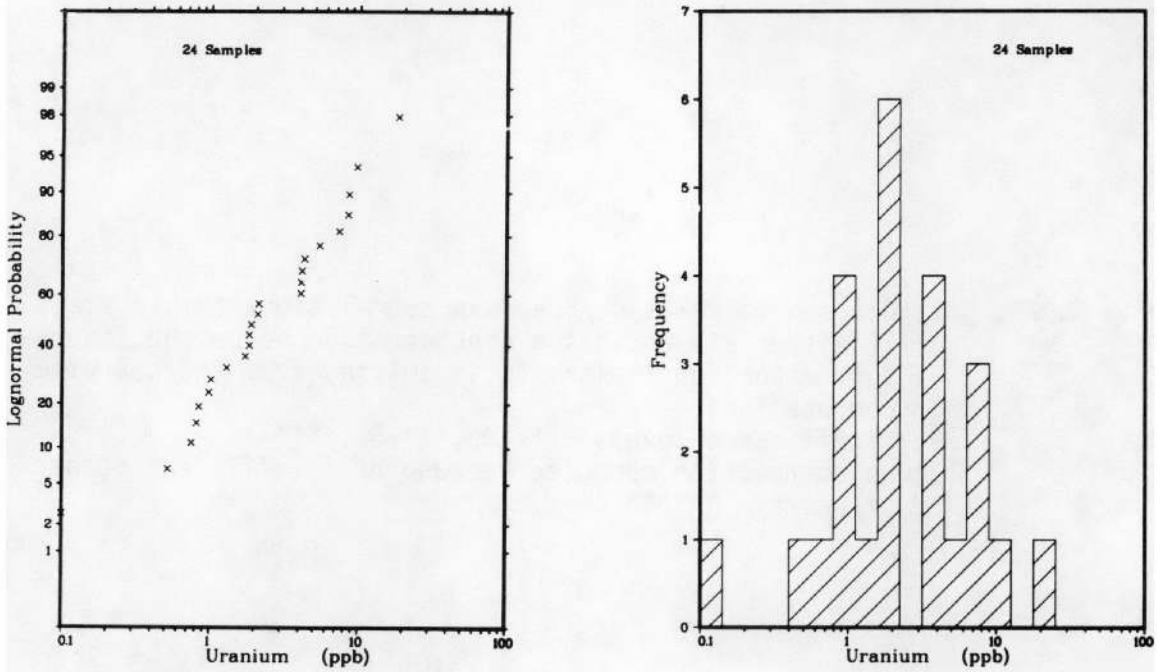

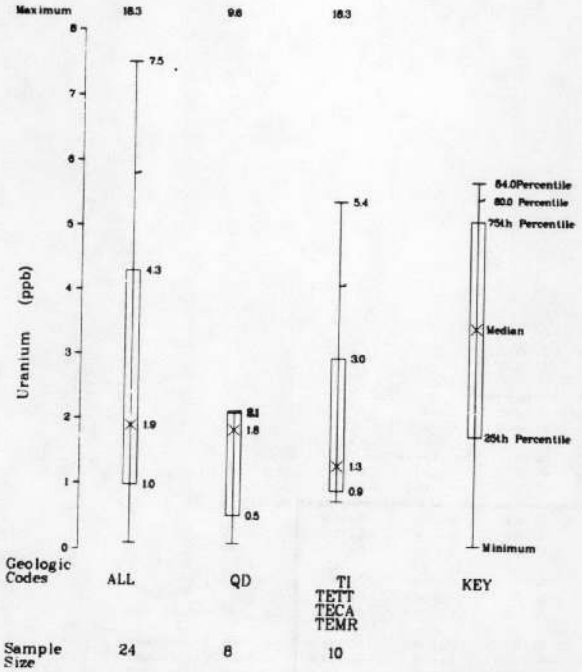

Figure A-1a

PROBABILITY, FREQUENCY, AND PERCENTILE PLOTS FOR URANIUM (PPB) IN GROUNDWATER OF THE CHINATI MOUNTAINS PROJECT AREA, TRANS-PECOS DETAILED GEOCHEMICAL SURVEY, TEXAS

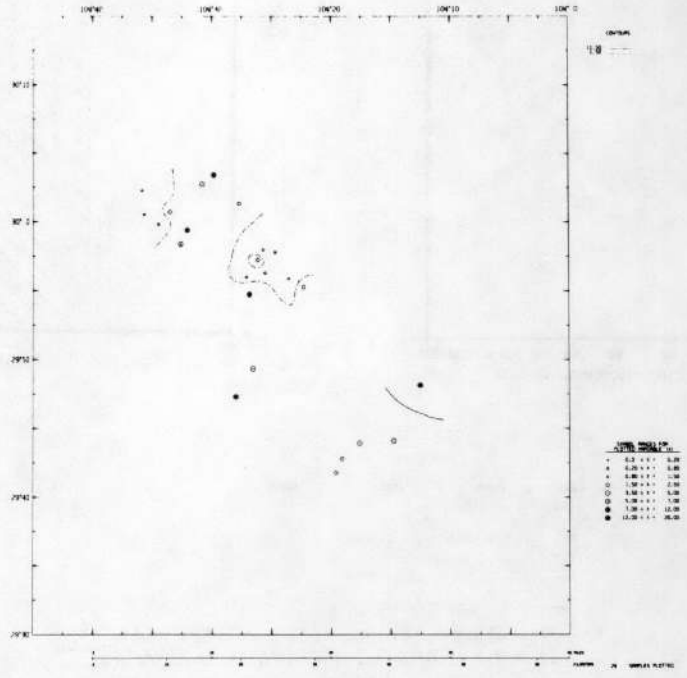

Figure A-1b

GEOCHEMICAL DISTRIBUTION OF URANIUM (PPB)
IN GROUNDWATER OF THE CHINATI MOUNTAINS PROJECT AREA,
TRANS-PECOS DETAILED GEOCHEMICAL SURVEY, TEXAS

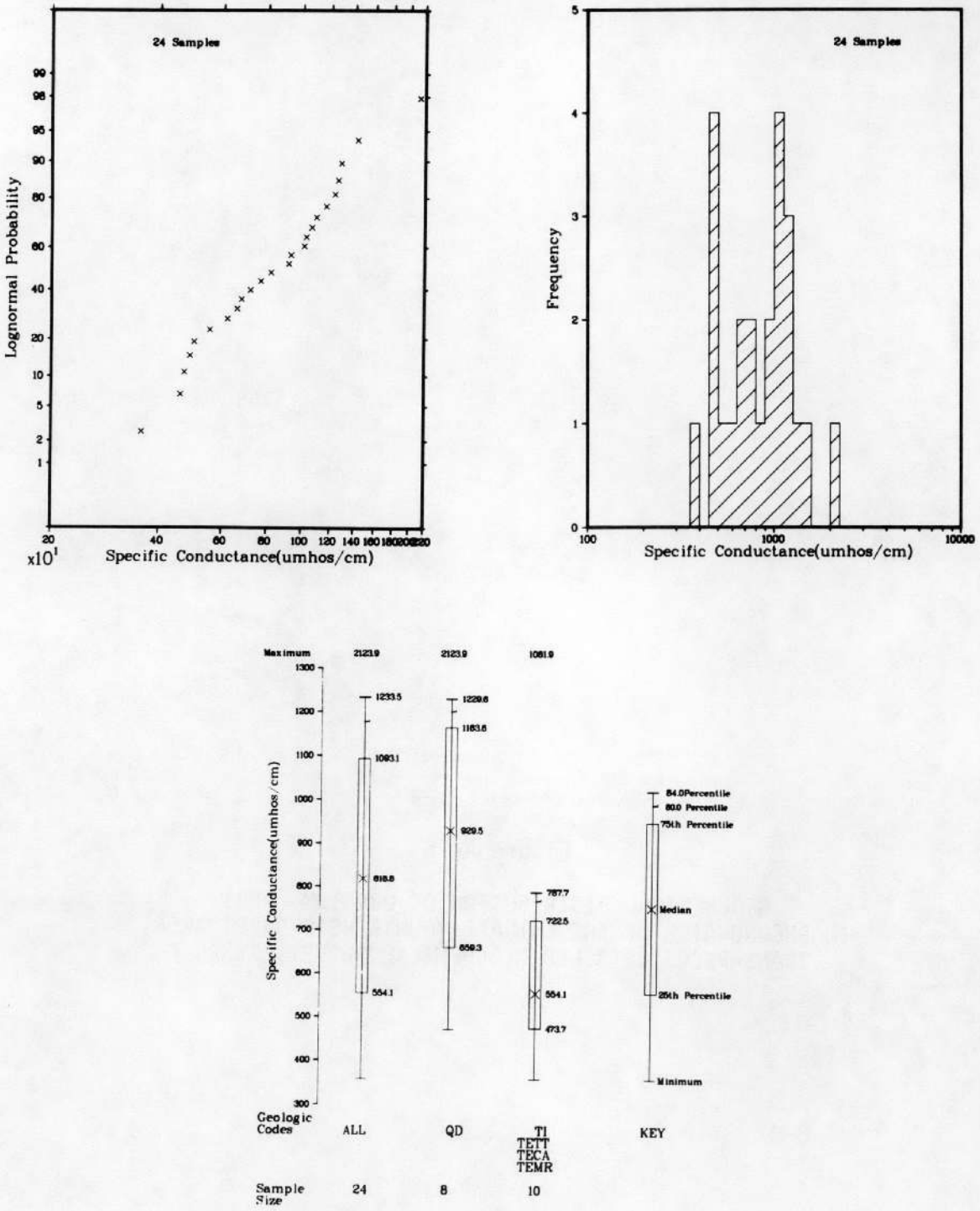

Figure A-2a

PROBABILITY, FREQUENCY, AND PERCENTILE PLOTS FOR SPECIFIC CONDUCTANCE (μMHOS/CM) IN GROUNDWATER OF THE CHINATI MOUNTAINS PROJECT AREA, TRANS-PECOS DETAILED GEOCHEMICAL SURVEY, TEXAS

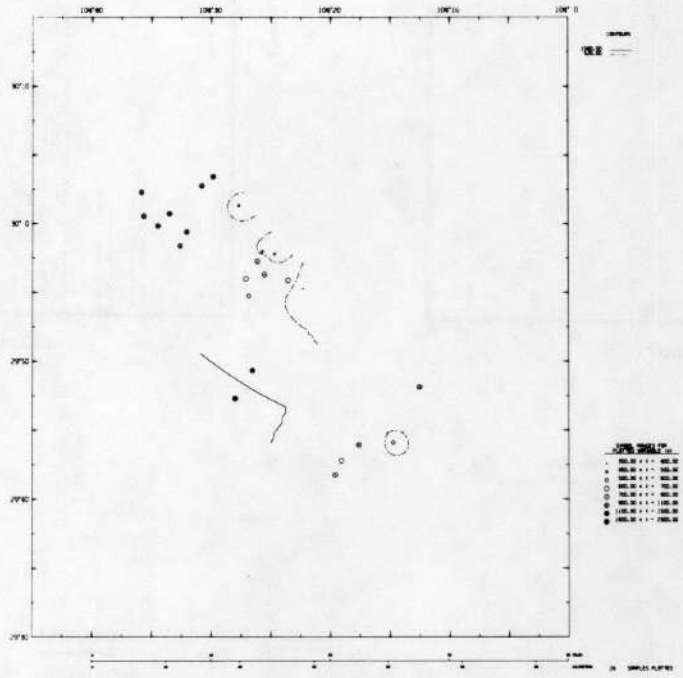

Figure A-2b

GEOCHEMICAL DISTRIBUTION OF SPECIFIC CONDUCTANCE (μMHOS/CM) IN GROUNDWATER OF THE CHINATI MOUNTAINS PROJECT AREA, TRANS-PECOS DETAILED GEOCHEMICAL SURVEY, TEXAS

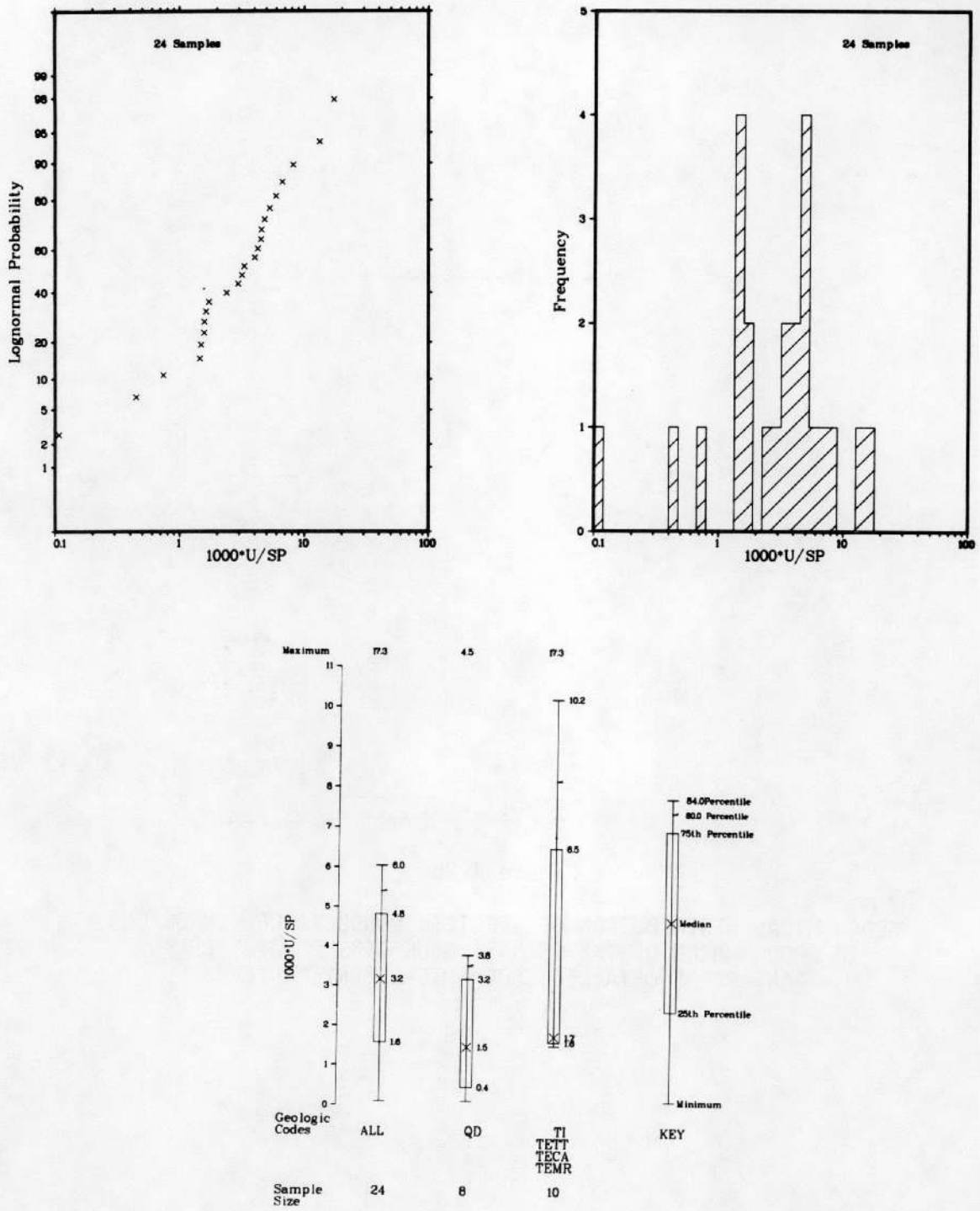

Figure A-3a

PROBABILITY, FREQUENCY, AND PERCENTILE PLOTS FOR 1,000·URANIUM/ SPECIFIC CONDUCTANCE IN GROUNDWATER OF THE CHINATI MOUNTAINS PROJECT AREA, TRANS-PECOS DETAILED GEOCHEMICAL SURVEY, TEXAS

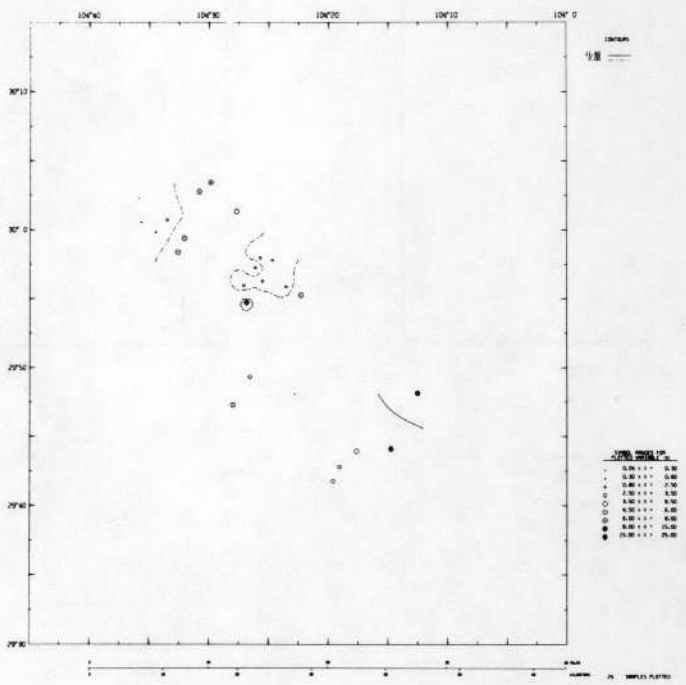

Figure A-3b

GEOCHEMICAL DISTRIBUTION OF 1,000·URANIUM/SPECIFIC CONDUCTANCE IN GROUNDWATER OF THE CHINATI MOUNTAINS PROJECT AREA, TRANS-PECOS DETAILED GEOCHEMICAL SURVEY, TEXAS

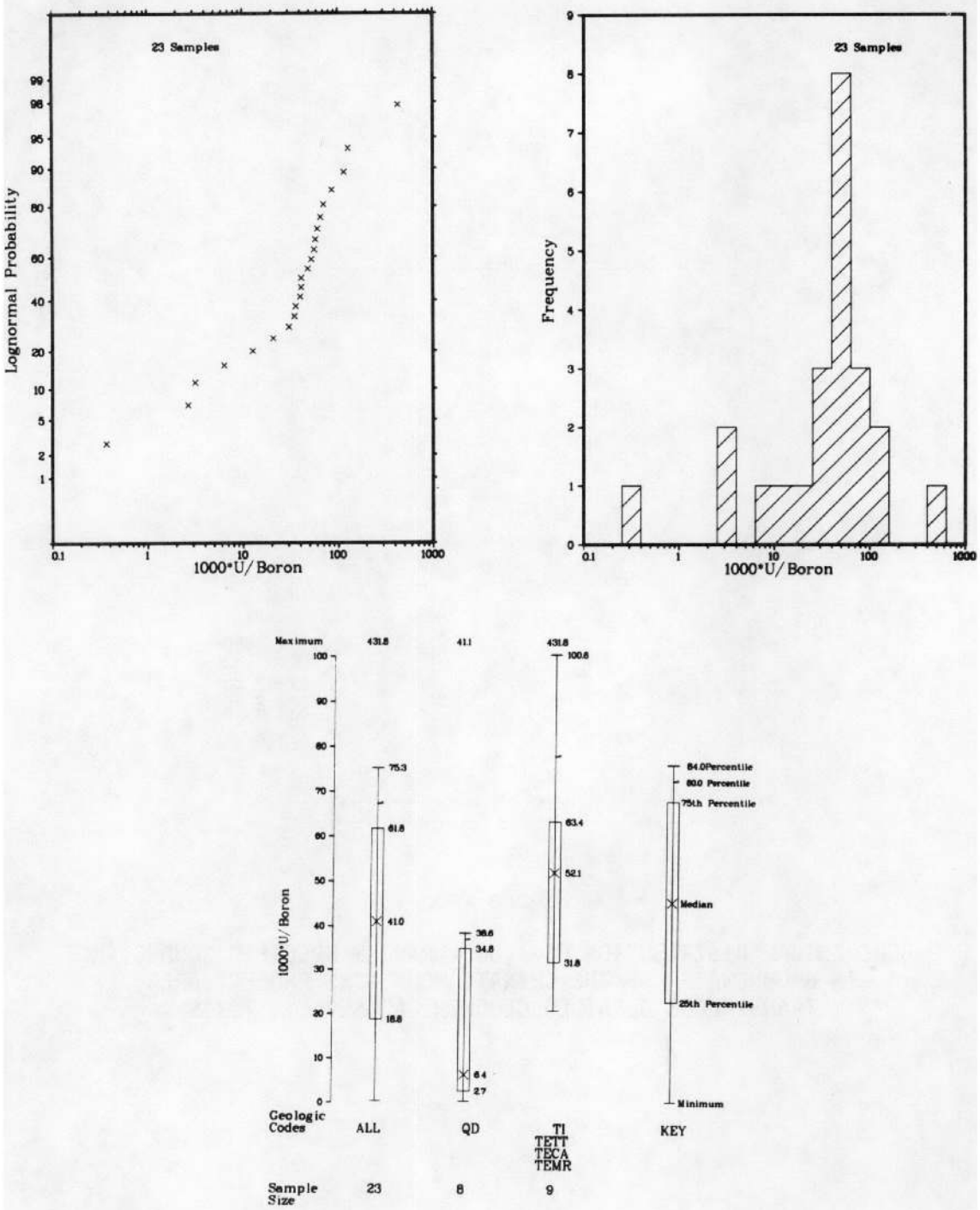

Figure A-4a

PROBABILITY, FREQUENCY, AND PERCENTILE PLOTS FOR 1,000·URANIUM/BORON IN GROUNDWATER OF THE CHINATI MOUNTAINS PROJECT AREA, TRANS-PECOS DETAILED GEOCHEMICAL SURVEY, TEXAS

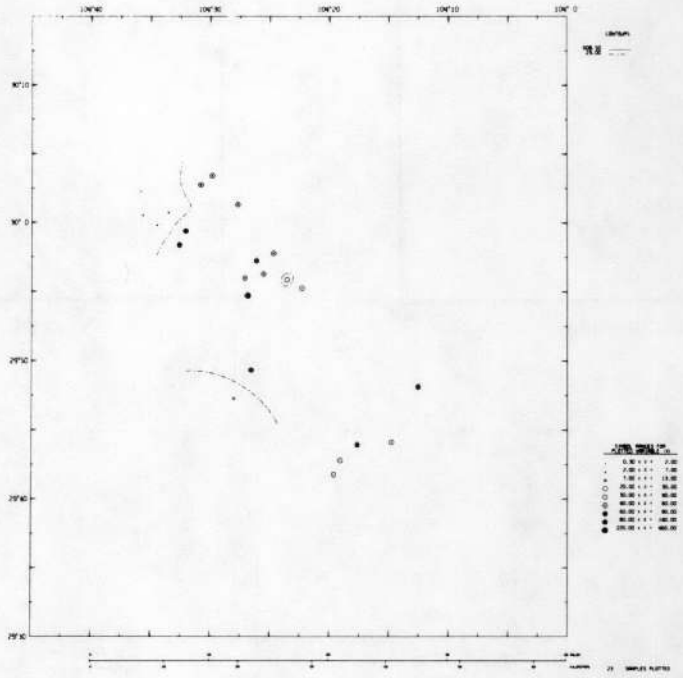

Figure A-4b

GEOCHEMICAL DISTRIBUTION OF 1,000·URANIUM/BORON IN GROUNDWATER OF THE CHINATI MOUNTAINS PROJECT AREA, TRANS-PECOS DETAILED GEOCHEMICAL SURVEY, TEXAS

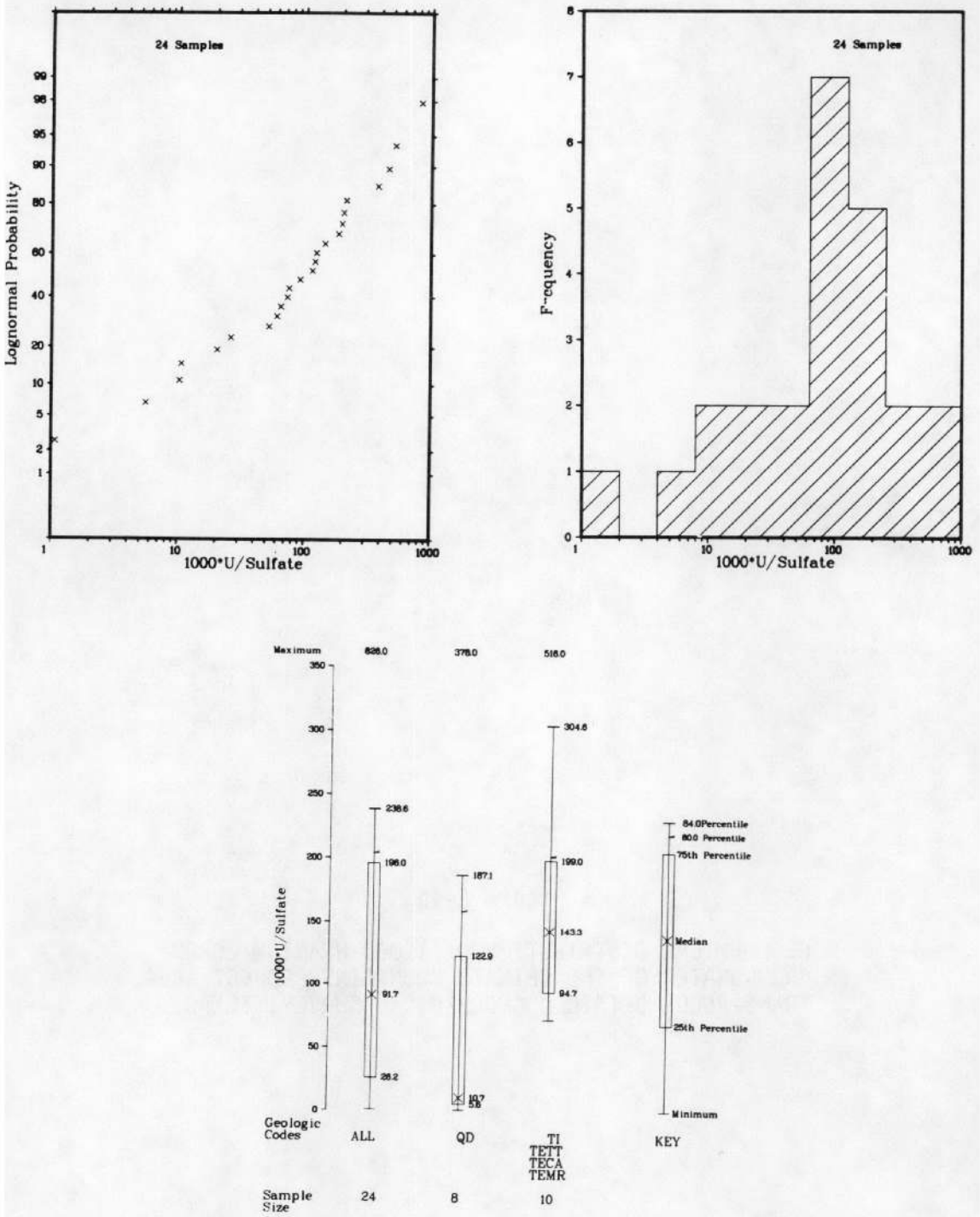

Figure A-5a

PROBABILITY, FREQUENCY, AND PERCENTILE PLOTS FOR 1,000·URANIUM/SULFATE IN GROUNDWATER OF THE CHINATI MOUNTAINS PROJECT AREA, TRANS-PECOS DETAILED GEOCHEMICAL SURVEY, TEXAS

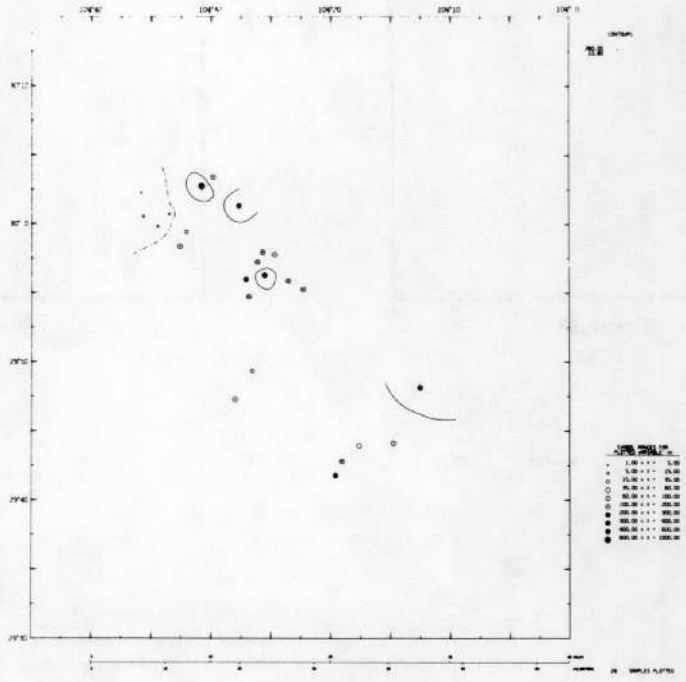

Figure A-5b

GEOCHEMICAL DISTRIBUTION OF 1,000·URANIUM/SULFATE IN GROUNDWATER OF THE CHINATI MOUNTAINS PROJECT AREA, TRANS-PECOS DETAILED GEOCHEMICAL SURVEY, TEXAS

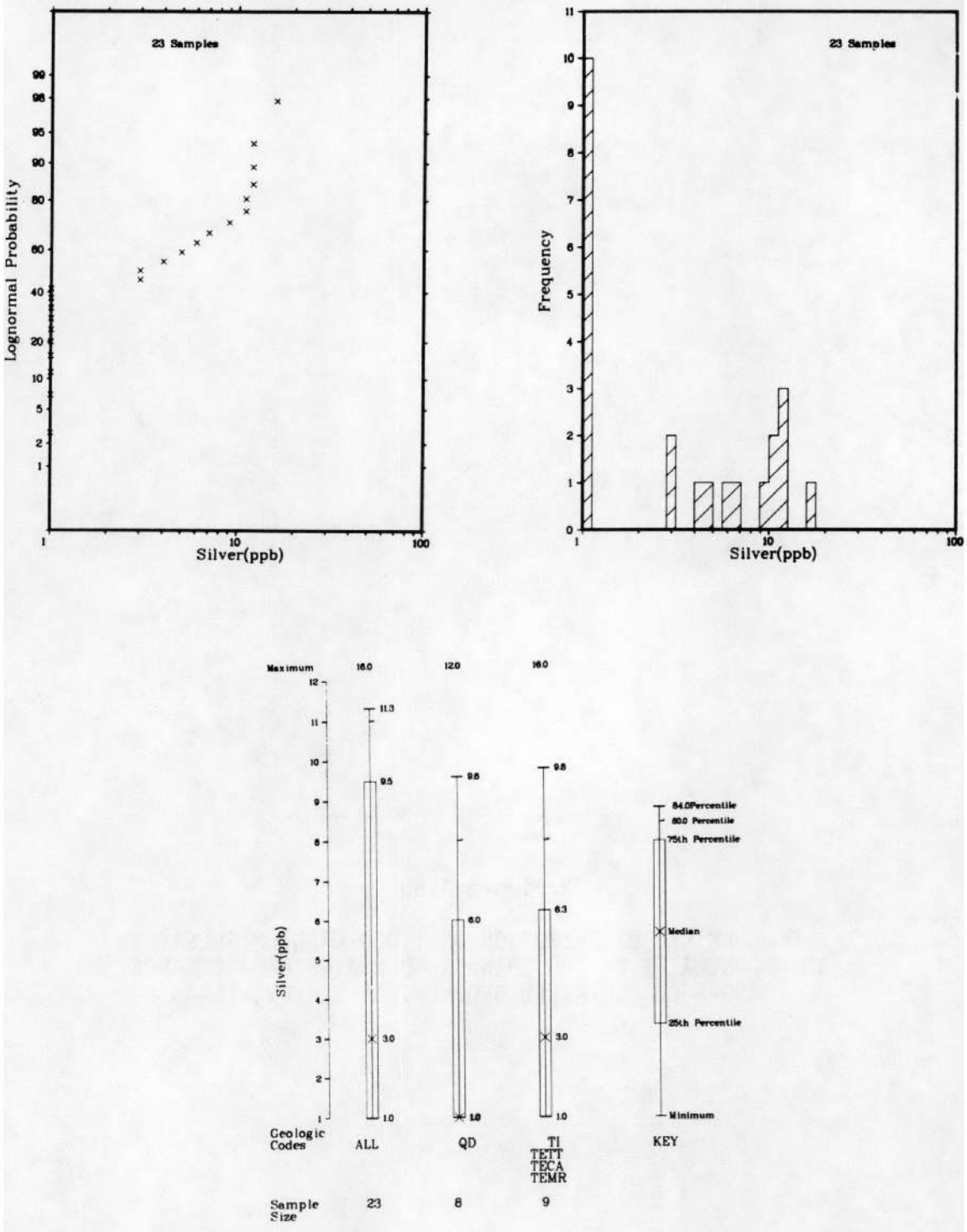

Figure A-6a

PROBABILITY, FREQUENCY, AND PERCENTILE PLOTS FOR SILVER (PPB) IN GROUNDWATER OF THE CHINATI MOUNTAINS PROJECT AREA, TRANS-PECOS DETAILED GEOCHEMICAL SURVEY, TEXAS

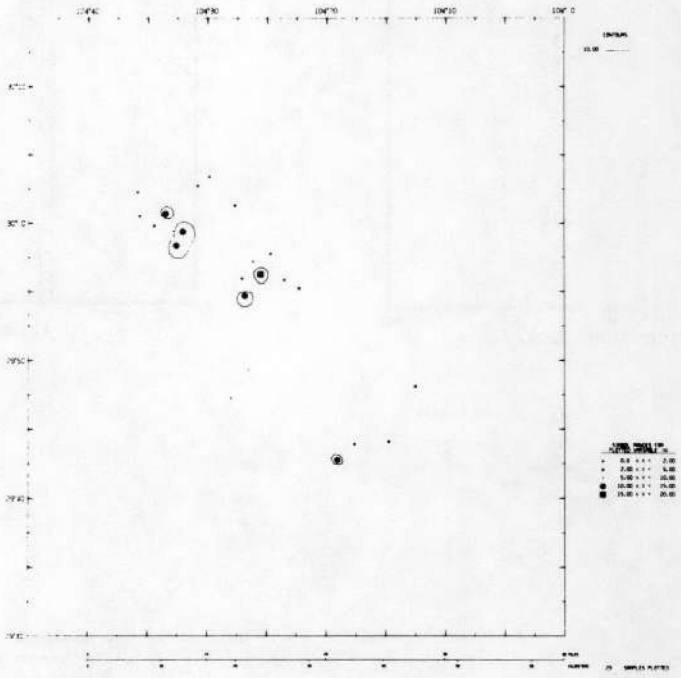

Figure A-6b

GEOCHEMICAL DISTRIBUTION OF SILVER (PPB)
IN GROUNDWATER OF THE CHINATI MOUNTAINS PROJECT AREA,
TRANS-PECOS DETAILED GEOCHEMICAL SURVEY, TEXAS

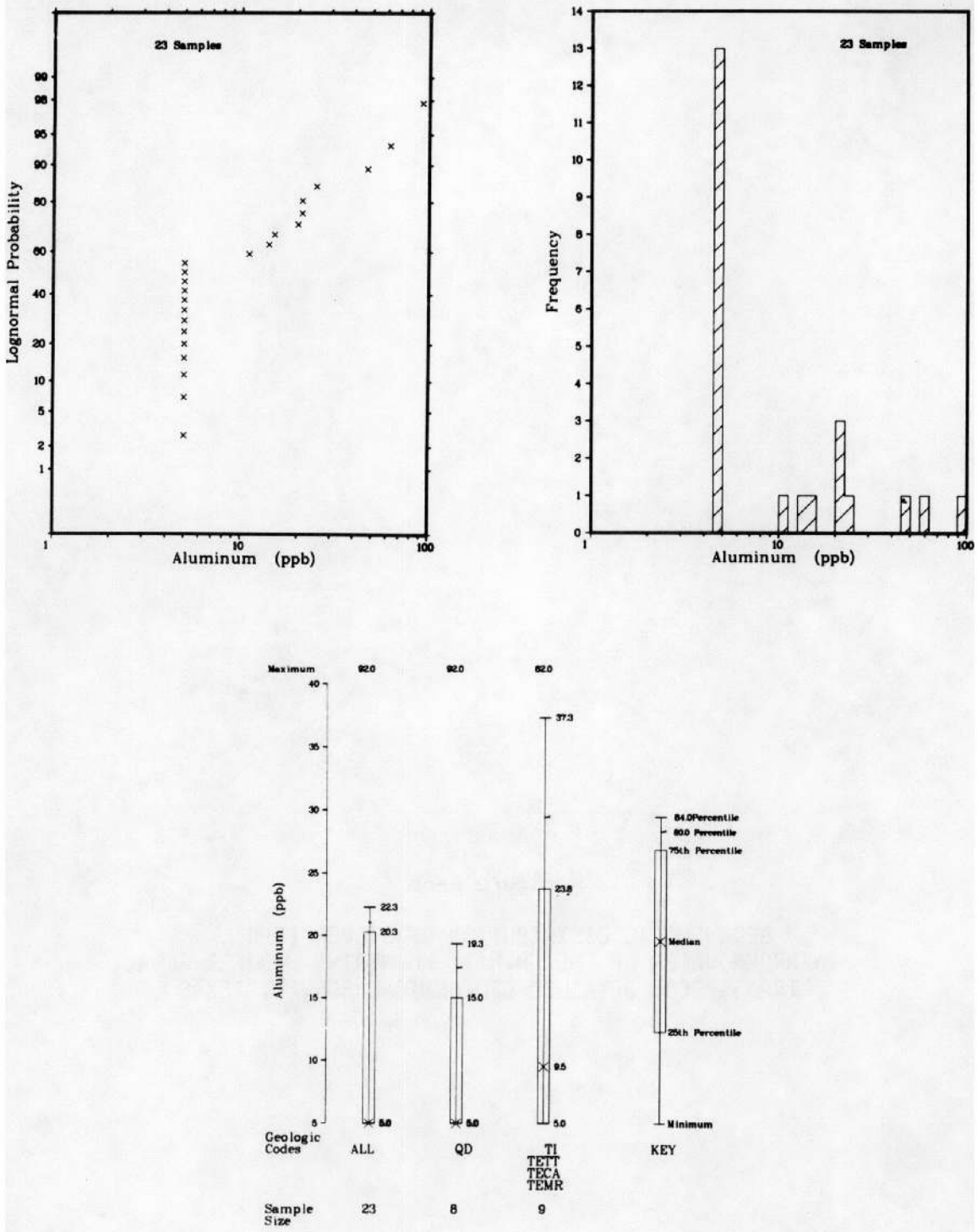

Figure A-7a

PROBABILITY, FREQUENCY, AND PERCENTILE PLOTS FOR ALUMINUM (PPB) IN GROUNDWATER OF THE CHINATI MOUNTAINS PROJECT AREA, TRANS-PECOS DETAILED GEOCHEMICAL SURVEY, TEXAS

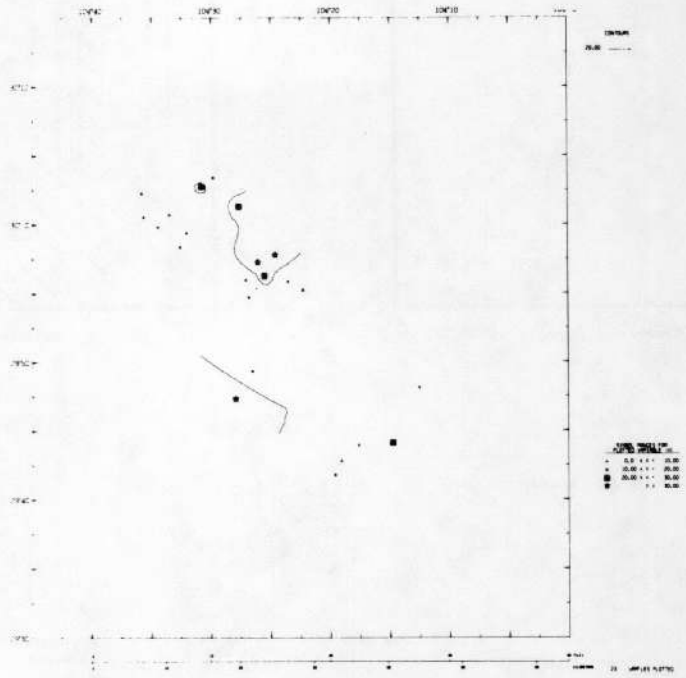

Figure A-7b

GEOCHEMICAL DISTRIBUTION OF ALUMINUM (PPB)
IN GROUNDWATER OF THE CHINATI MOUNTAINS PROJECT AREA,
TRANS-PECOS DETAILED GEOCHEMICAL SURVEY, TEXAS

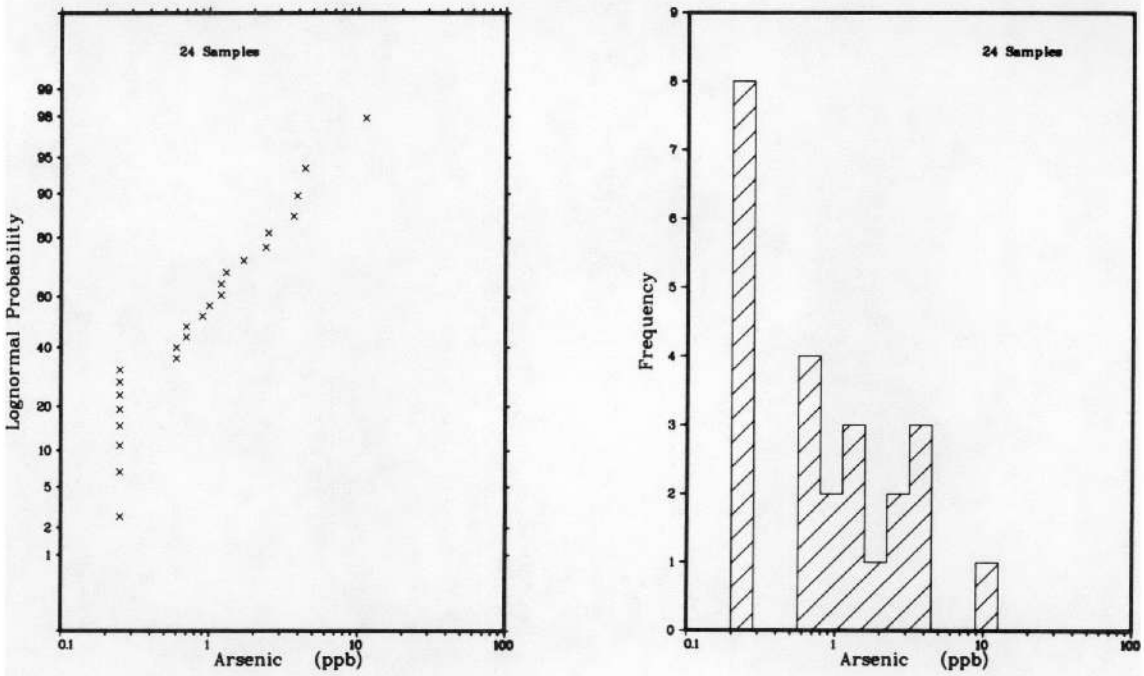

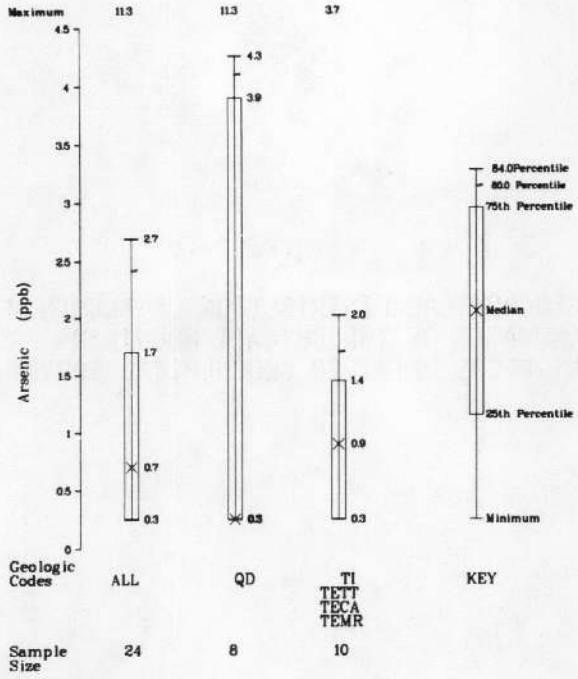

Figure A-8a

PROBABILITY, FREQUENCY, AND PERCENTILE PLOTS FOR ARSENIC (PPB) IN GROUNDWATER OF THE CHINATI MOUNTAINS PROJECT AREA, TRANS-PECOS DETAILED GEOCHEMICAL SURVEY, TEXAS

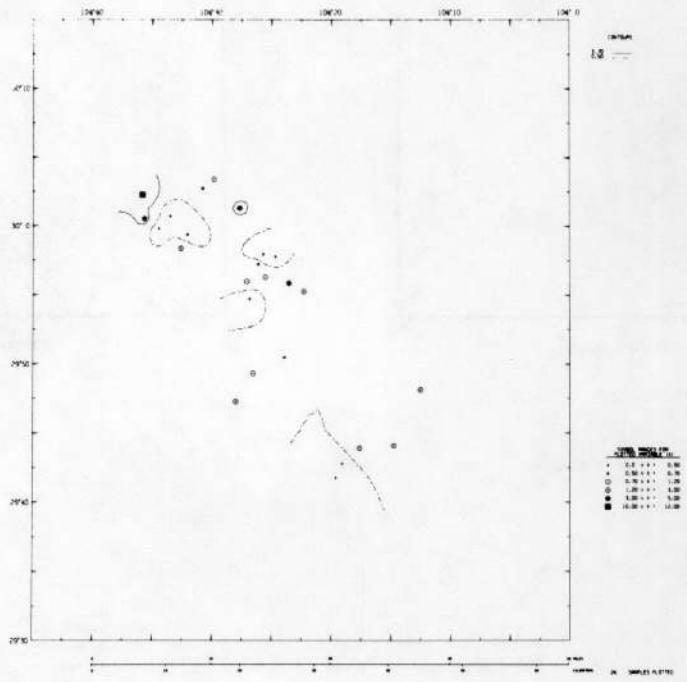

Figure A-8b

GEOCHEMICAL DISTRIBUTION OF ARSENIC (PPB)
IN GROUNDWATER OF THE CHINATI MOUNTAINS PROJECT AREA,
TRANS-PECOS DETAILED GEOCHEMICAL SURVEY, TEXAS

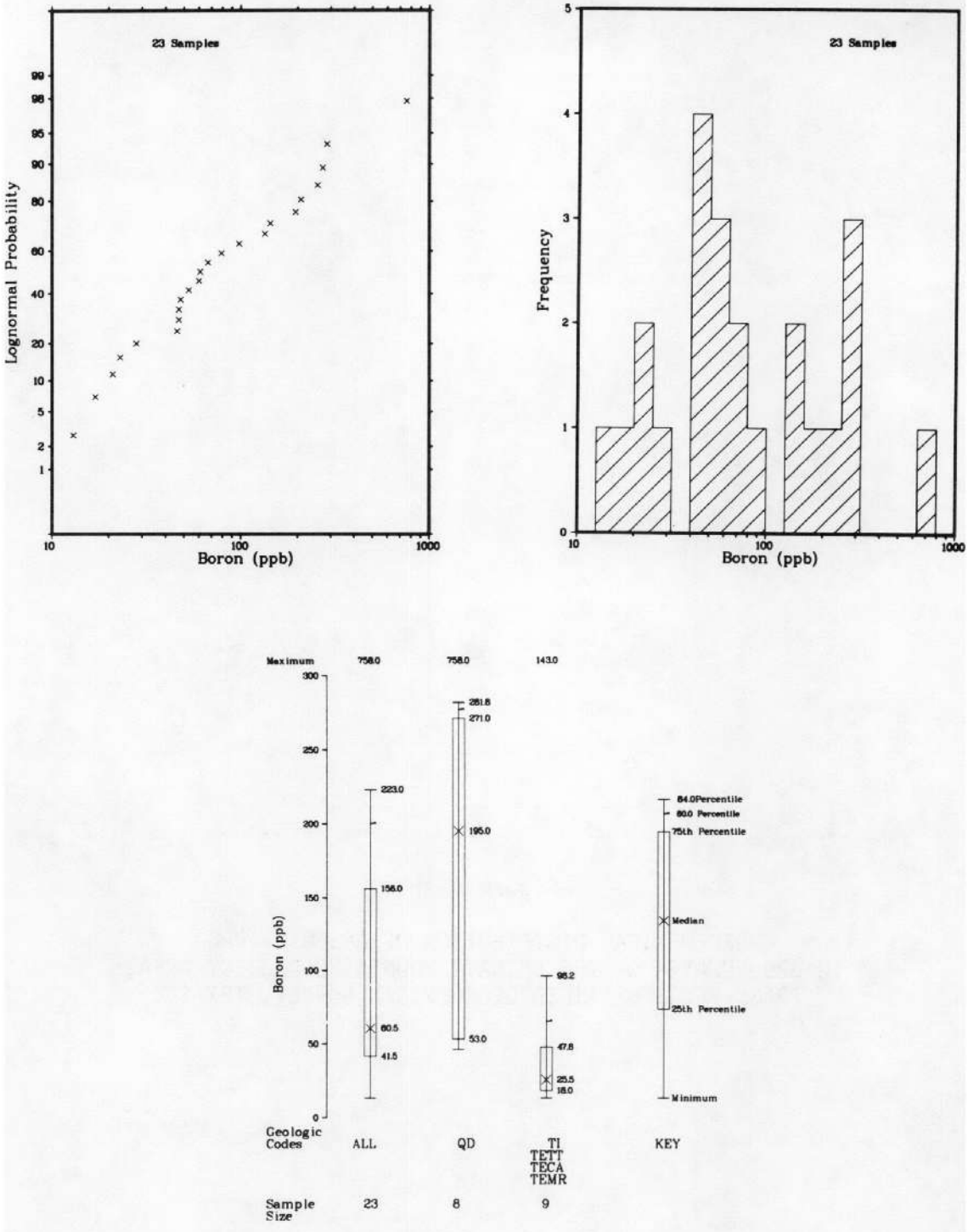

Figure A-9a

PROBABILITY, FREQUENCY, AND PERCENTILE PLOTS FOR BORON (PPB) IN GROUNDWATER OF THE CHINATI MOUNTAINS PROJECT AREA, TRANS-PECOS DETAILED GEOCHEMICAL SURVEY, TEXAS

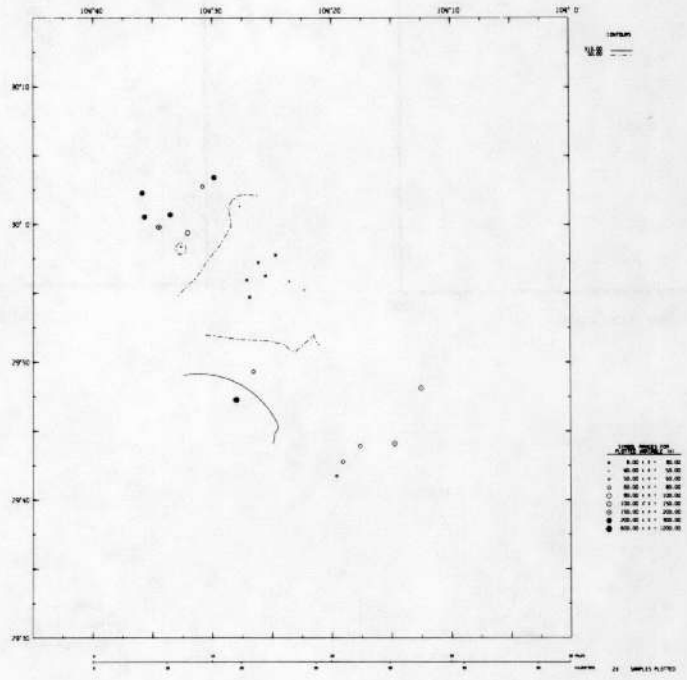

Figure A-9b

GEOCHEMICAL DISTRIBUTION OF BORON (PPB)
IN GROUNDWATER OF THE CHINATI MOUNTAINS PROJECT AREA,
TRANS-PECOS DETAILED GEOCHEMICAL SURVEY, TEXAS

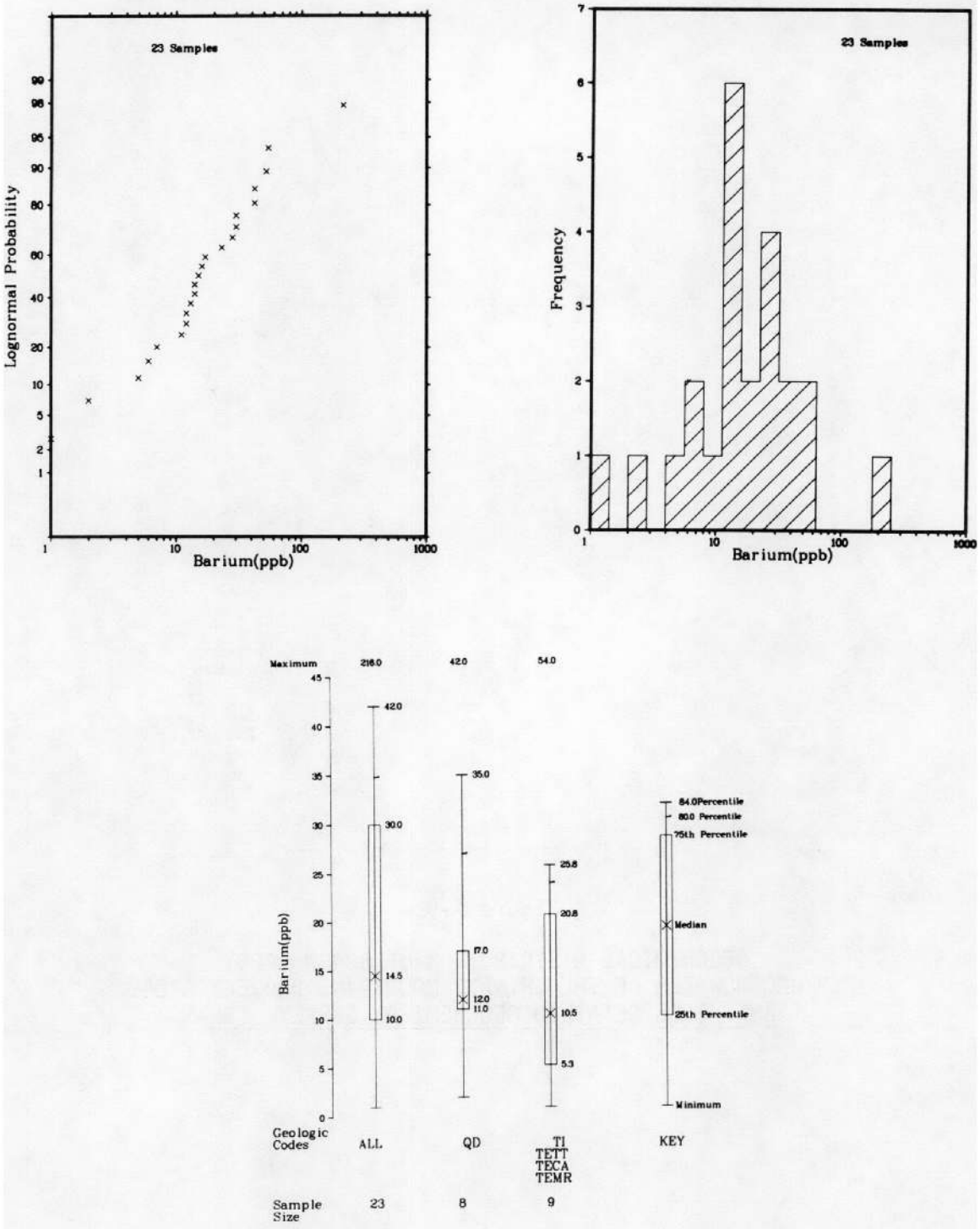

Figure A-10a

PROBABILITY, FREQUENCY, AND PERCENTILE PLOTS FOR BARIUM (PPB) IN GROUNDWATER OF THE CHINATI MOUNTAINS PROJECT AREA, TRANS-PECOS DETAILED GEOCHEMICAL SURVEY, TEXAS

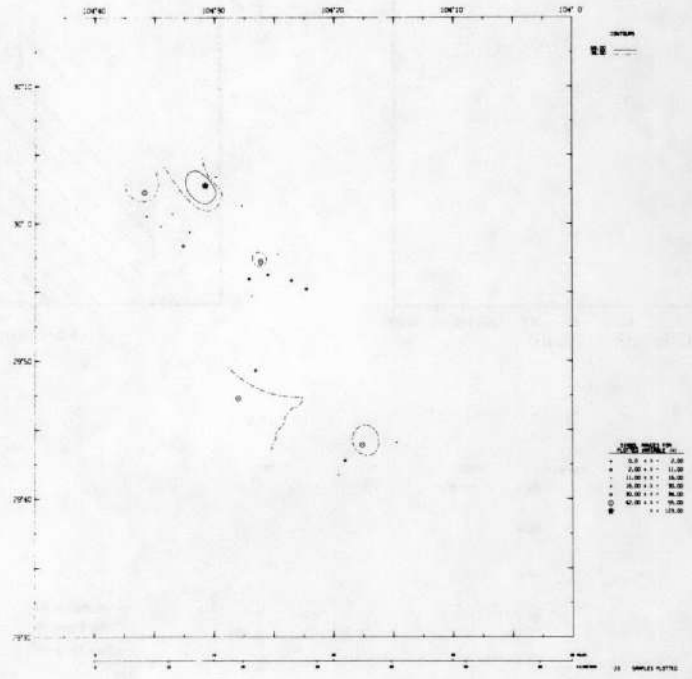

Figure A-10b

GEOCHEMICAL DISTRIBUTION OF BARIUM (PPB)
IN GROUNDWATER OF THE CHINATI MOUNTAINS PROJECT AREA,
TRANS-PECOS DETAILED GEOCHEMICAL SURVEY, TEXAS

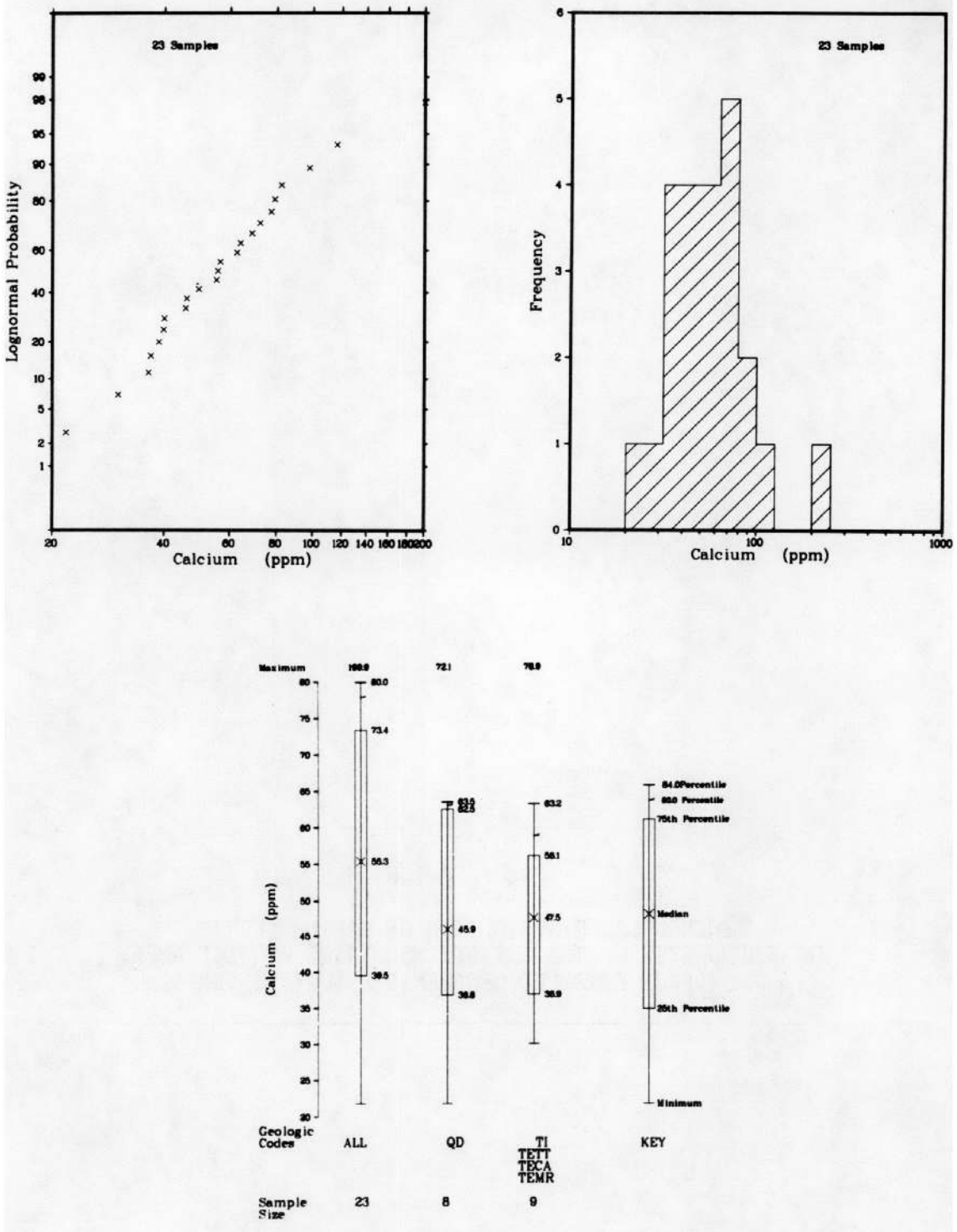

Figure A-11a

PROBABILITY, FREQUENCY, AND PERCENTILE PLOTS FOR CALCIUM (PPM) IN GROUNDWATER OF THE CHINATI MOUNTAINS PROJECT AREA, TRANS-PECOS DETAILED GEOCHEMICAL SURVEY, TEXAS

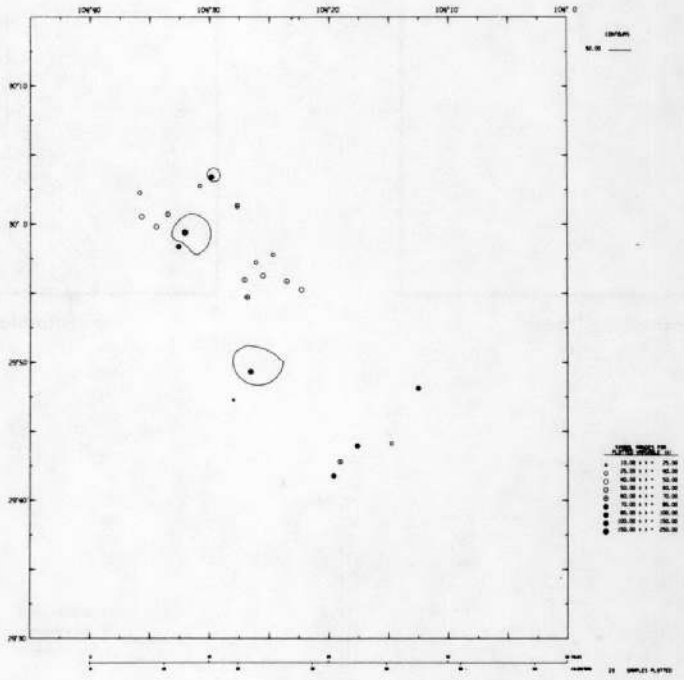

Figure A-11b

GEOCHEMICAL DISTRIBUTION OF CALCIUM (PPM)
IN GROUNDWATER OF THE CHINATI MOUNTAINS PROJECT AREA,
TRANS-PECOS DETAILED GEOCHEMICAL SURVEY, TEXAS

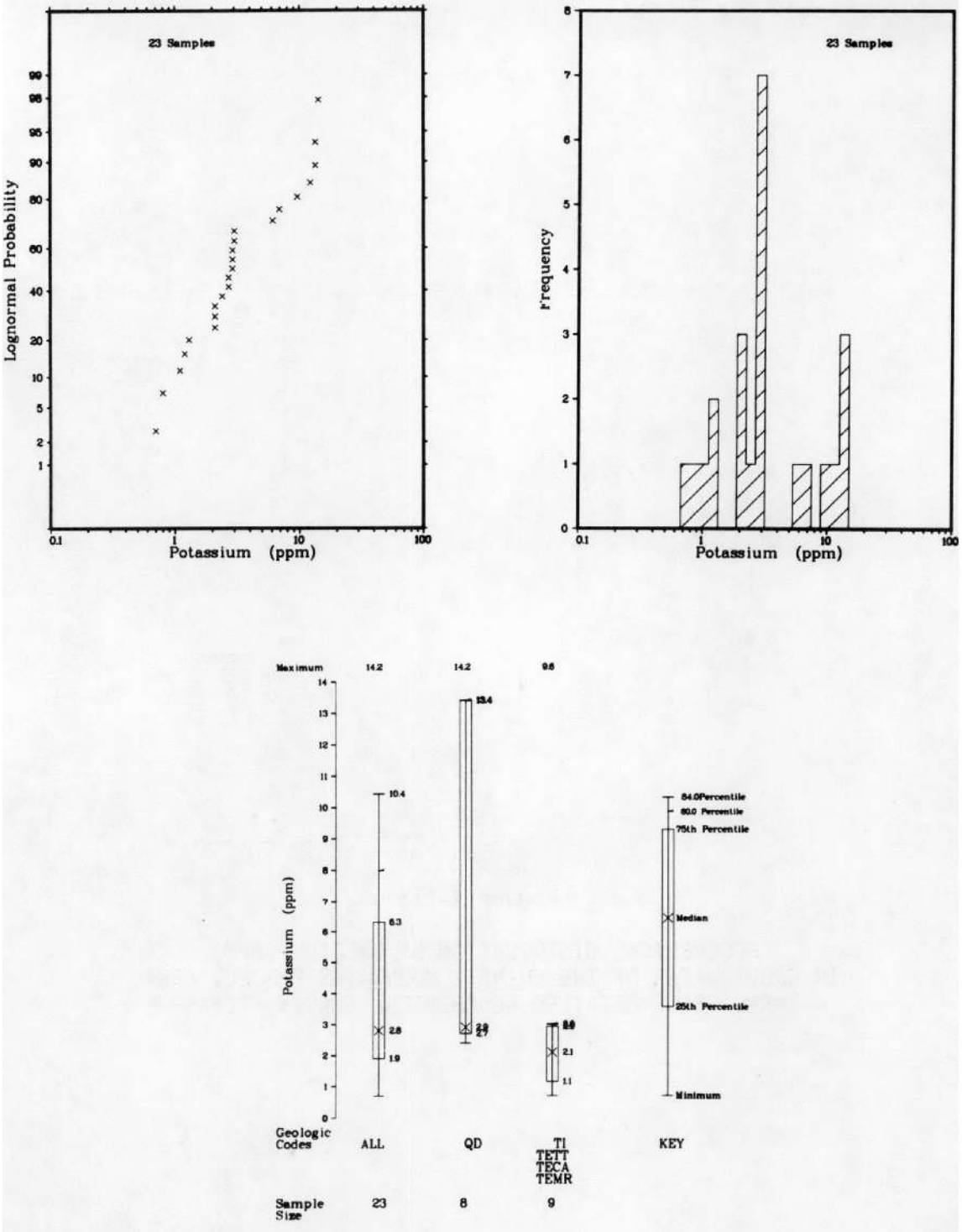

Figure A-12a

PROBABILITY, FREQUENCY, AND PERCENTILE PLOTS FOR POTASSIUM (PPM) IN GROUNDWATER OF THE CHINATI MOUNTAINS PROJECT AREA, TRANS-PECOS DETAILED GEOCHEMICAL SURVEY, TEXAS

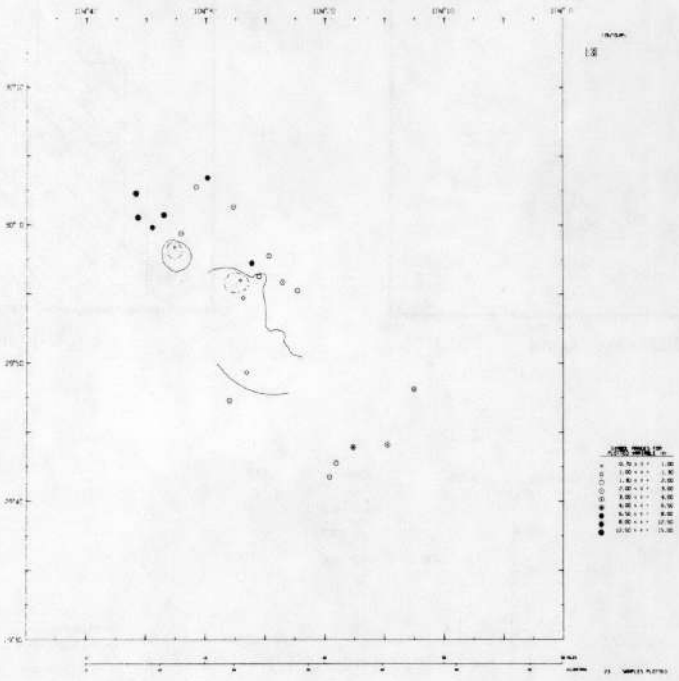

Figure A-12b

GEOCHEMICAL DISTRIBUTION OF POTASSIUM (PPM)
IN GROUNDWATER OF THE CHINATI MOUNTAINS PROJECT AREA,
TRANS-PECOS DETAILED GEOCHEMICAL SURVEY, TEXAS

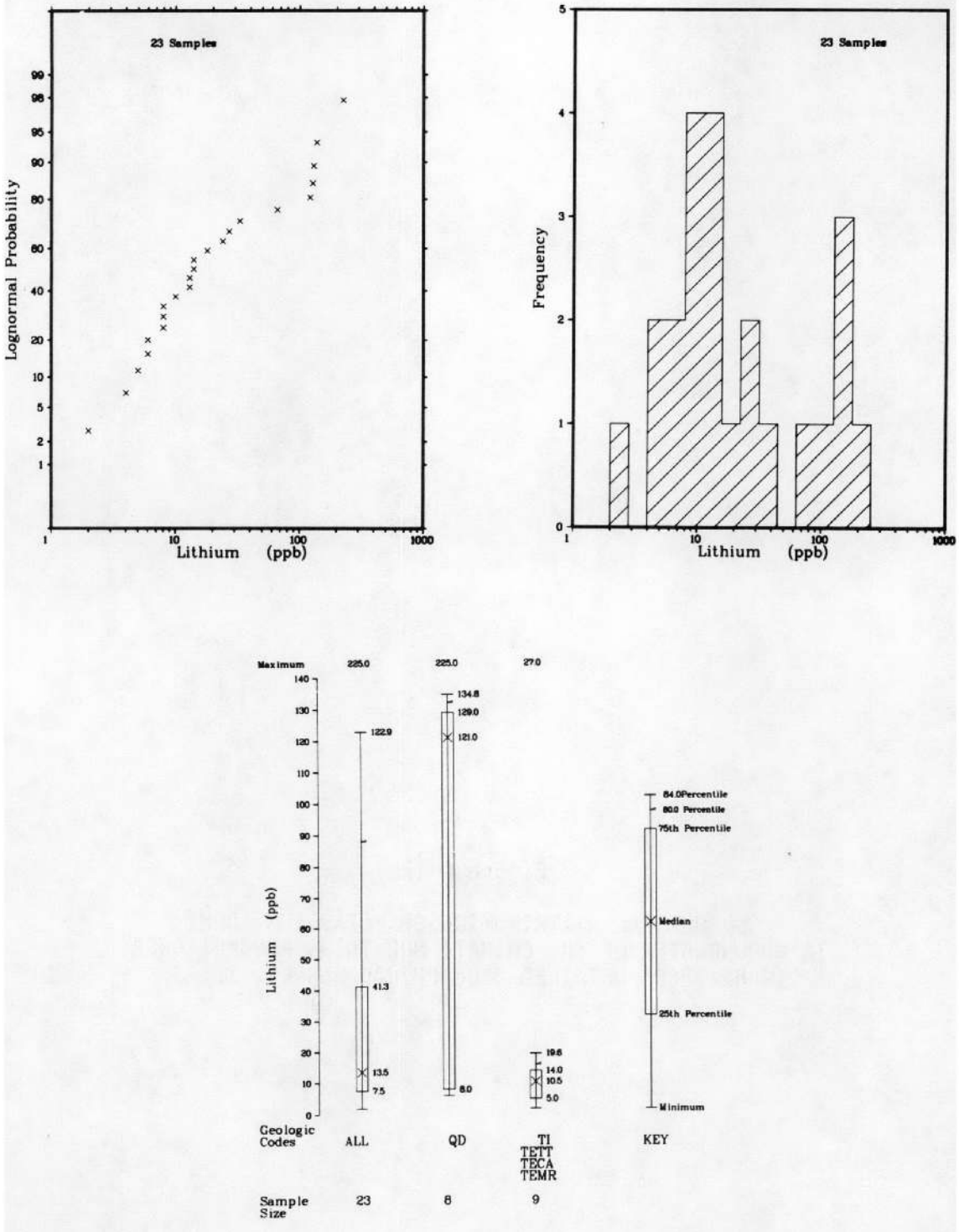

Figure A-13a

PROBABILITY, FREQUENCY, AND PERCENTILE PLOTS FOR LITHIUM (PPB) IN GROUNDWATER OF THE CHINATI MOUNTAINS PROJECT AREA, TRANS-PECOS DETAILED GEOCHEMICAL SURVEY, TEXAS

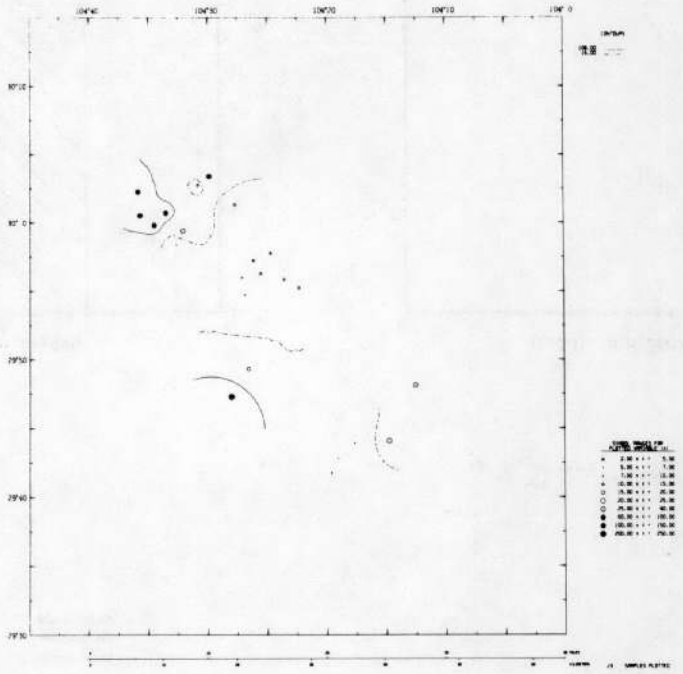

Figure A-13b

GEOCHEMICAL DISTRIBUTION OF LITHIUM (PPB)
IN GROUNDWATER OF THE CHINATI MOUNTAINS PROJECT AREA,
TRANS-PECOS DETAILED GEOCHEMICAL SURVEY, TEXAS

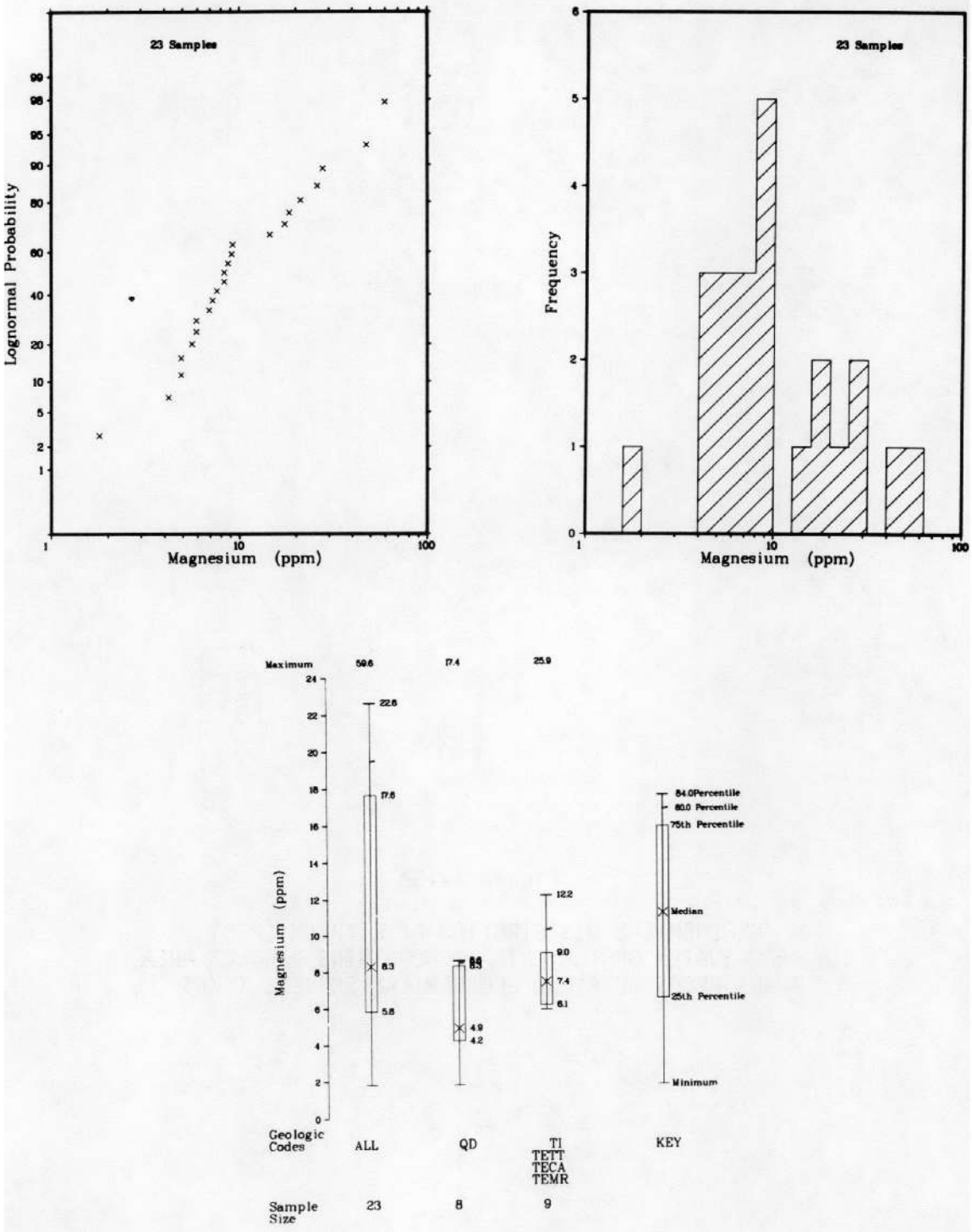

Figure A-14a

PROBABILITY, FREQUENCY, AND PERCENTILE PLOTS FOR MAGNESIUM (PPM) IN GROUNDWATER OF THE CHINATI MOUNTAINS PROJECT AREA, TRANS-PECOS DETAILED GEOCHEMICAL SURVEY, TEXAS

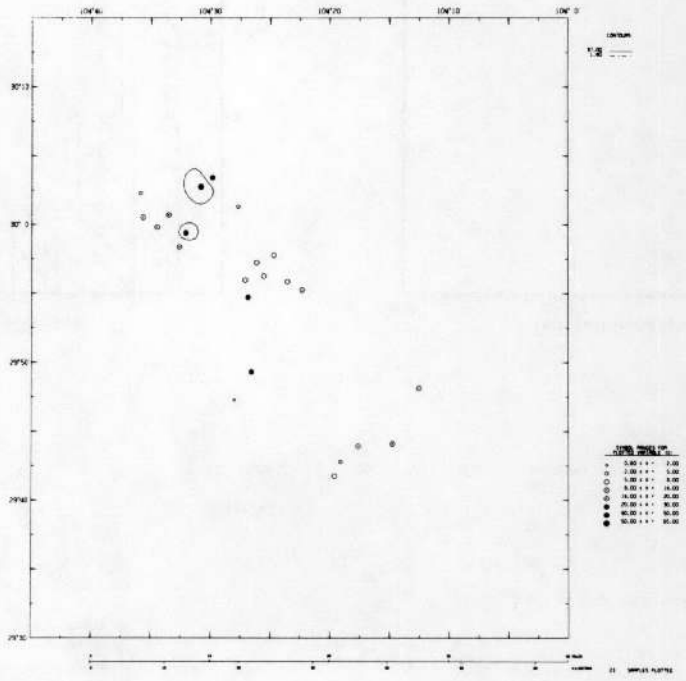

Figure A-14b

GEOCHEMICAL DISTRIBUTION OF MAGNESIUM (PPM)
IN GROUNDWATER OF THE CHINATI MOUNTAINS PROJECT AREA,
TRANS-PECOS DETAILED GEOCHEMICAL SURVEY, TEXAS

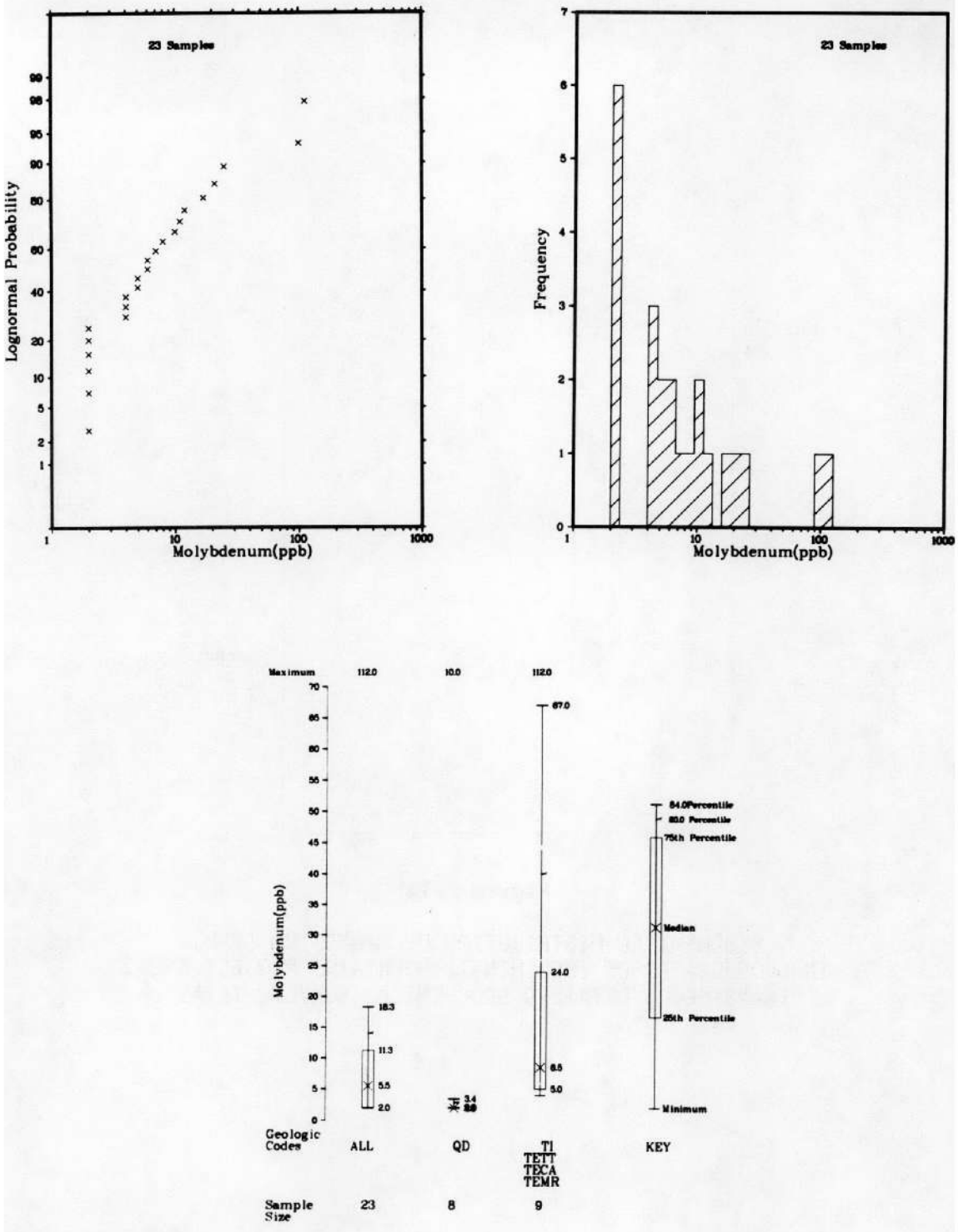

Figure A-15a

PROBABILITY, FREQUENCY, AND PERCENTILE PLOTS FOR MOLYBDENUM (PPB) IN GROUNDWATER OF THE CHINATI MOUNTAINS PROJECT AREA, TRANS-PECOS DETAILED GEOCHEMICAL SURVEY, TEXAS

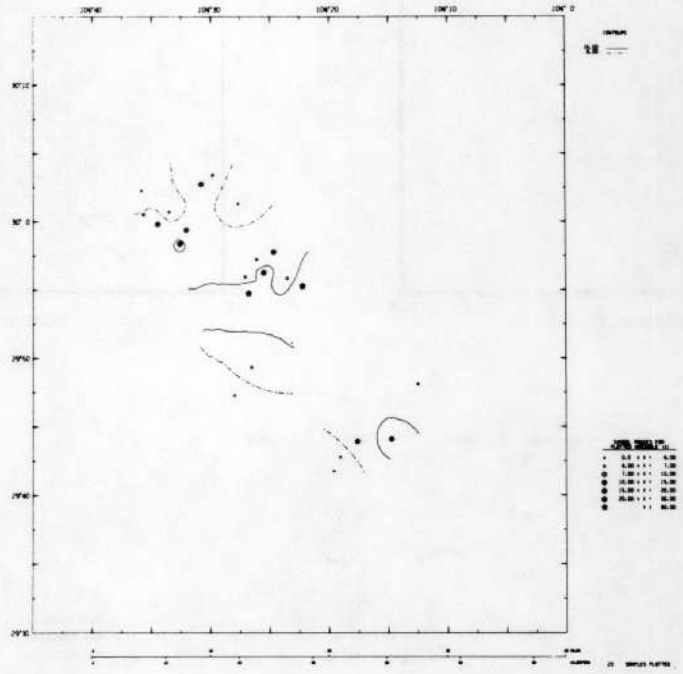

Figure A-15b

GEOCHEMICAL DISTRIBUTION OF MOLYBDENUM (PPB)
IN GROUNDWATER OF THE CHINATI MOUNTAINS PROJECT AREA,
TRANS-PECOS DETAILED GEOCHEMICAL SURVEY, TEXAS

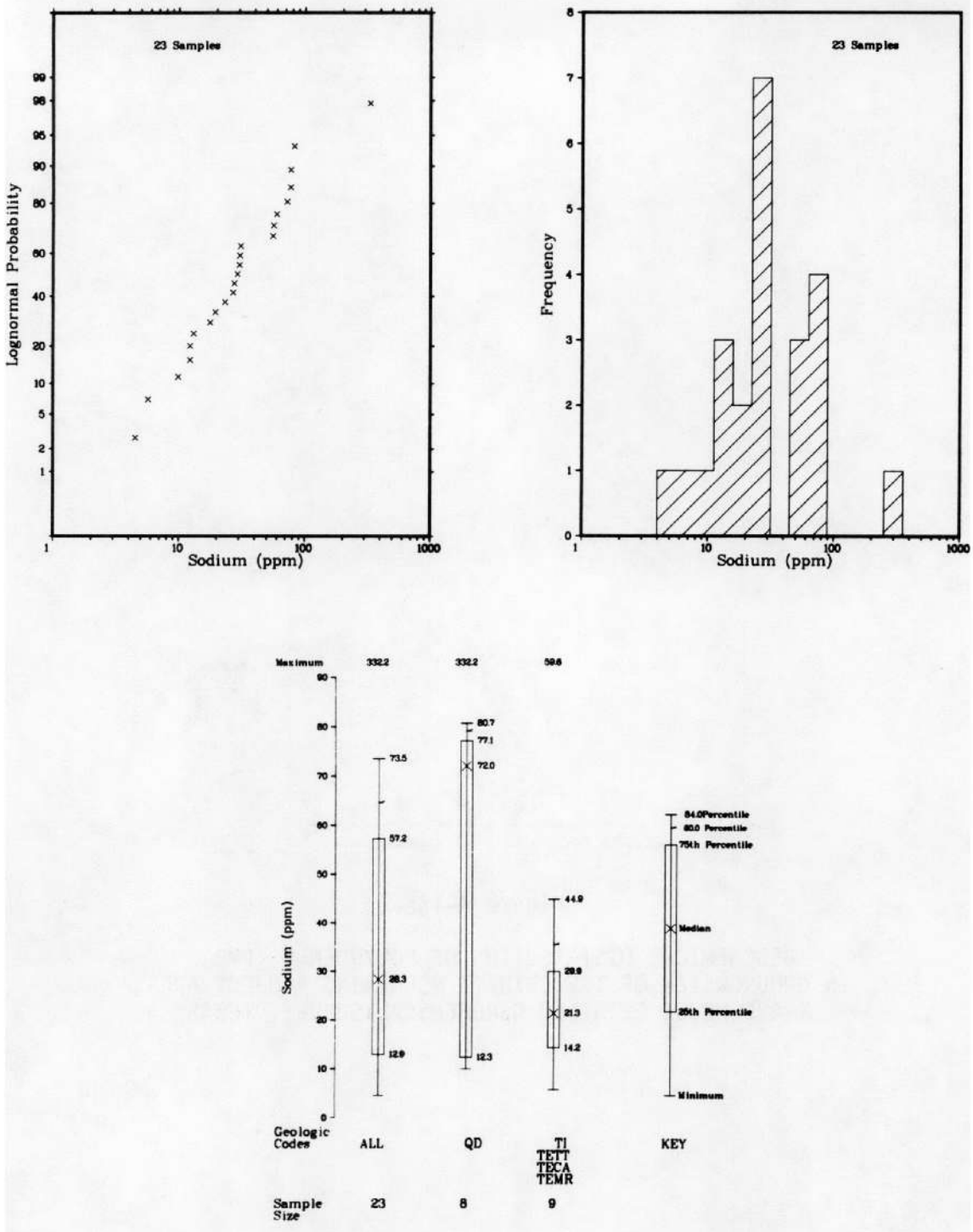

Figure A-16a

PROBABILITY, FREQUENCY, AND PERCENTILE PLOTS FOR SODIUM (PPM) IN GROUNDWATER OF THE CHINATI MOUNTAINS PROJECT AREA, TRANS-PECOS DETAILED GEOCHEMICAL SURVEY, TEXAS

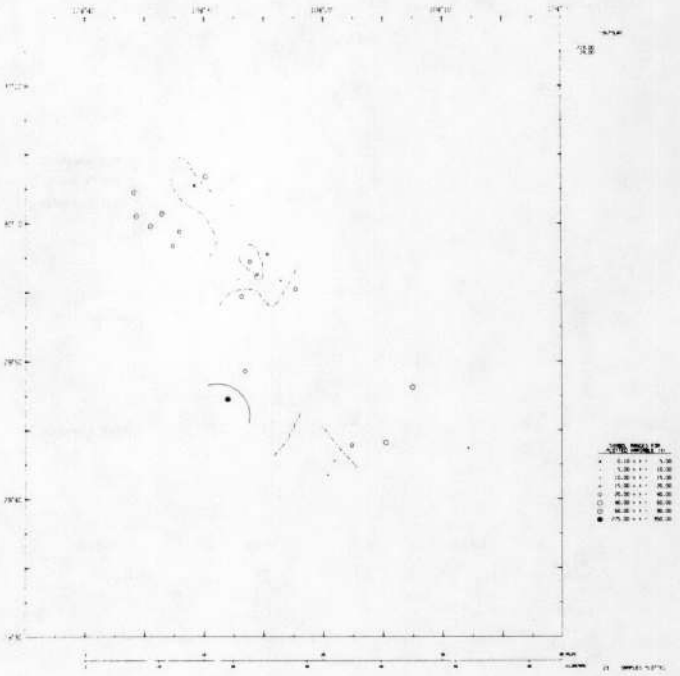

Figure A-16b

GEOCHEMICAL DISTRIBUTION OF SODIUM (PPM)
IN GROUNDWATER OF THE CHINATI MOUNTAINS PROJECT AREA,
TRANS-PECOS DETAILED GEOCHEMICAL SURVEY, TEXAS

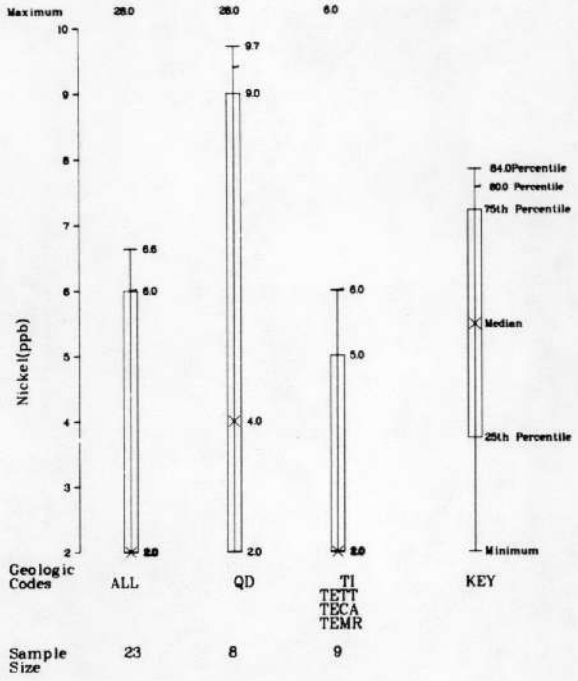

Figure A-17a

PERCENTILE PLOT FOR NICKEL (PPB)
IN GROUNDWATER OF THE CHINATI MOUNTAINS PROJECT AREA,
TRANS-PECOS DETAILED GEOCHEMICAL SURVEY, TEXAS

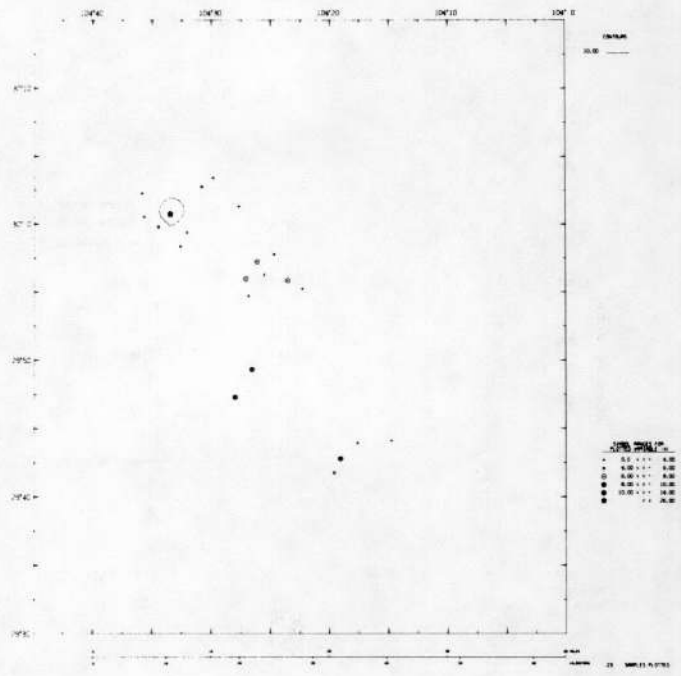

Figure A-17b

GEOCHEMICAL DISTRIBUTION OF NICKEL (PPB)
IN GROUNDWATER OF THE CHINATI MOUNTAINS PROJECT AREA,
TRANS-PECOS DETAILED GEOCHEMICAL SURVEY, TEXAS

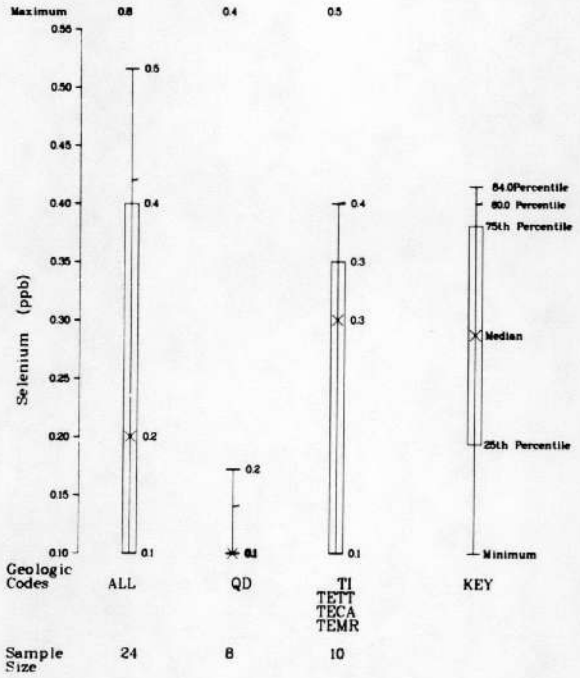

Figure A-18a

PERCENTILE PLOT FOR SELENIUM (PPB)
IN GROUNDWATER OF THE CHINATI MOUNTAINS PROJECT AREA,
TRANS-PECOS DETAILED GEOCHEMICAL SURVEY, TEXAS

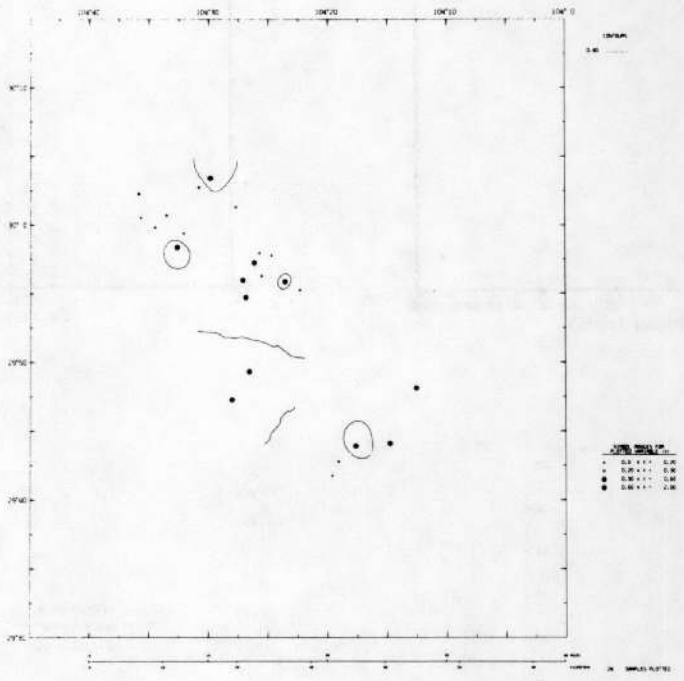

Figure A-18b

GEOCHEMICAL DISTRIBUTION OF SELENIUM (PPB)
IN GROUNDWATER OF THE CHINATI MOUNTAINS PROJECT AREA,
TRANS-PECOS DETAILED GEOCHEMICAL SURVEY, TEXAS

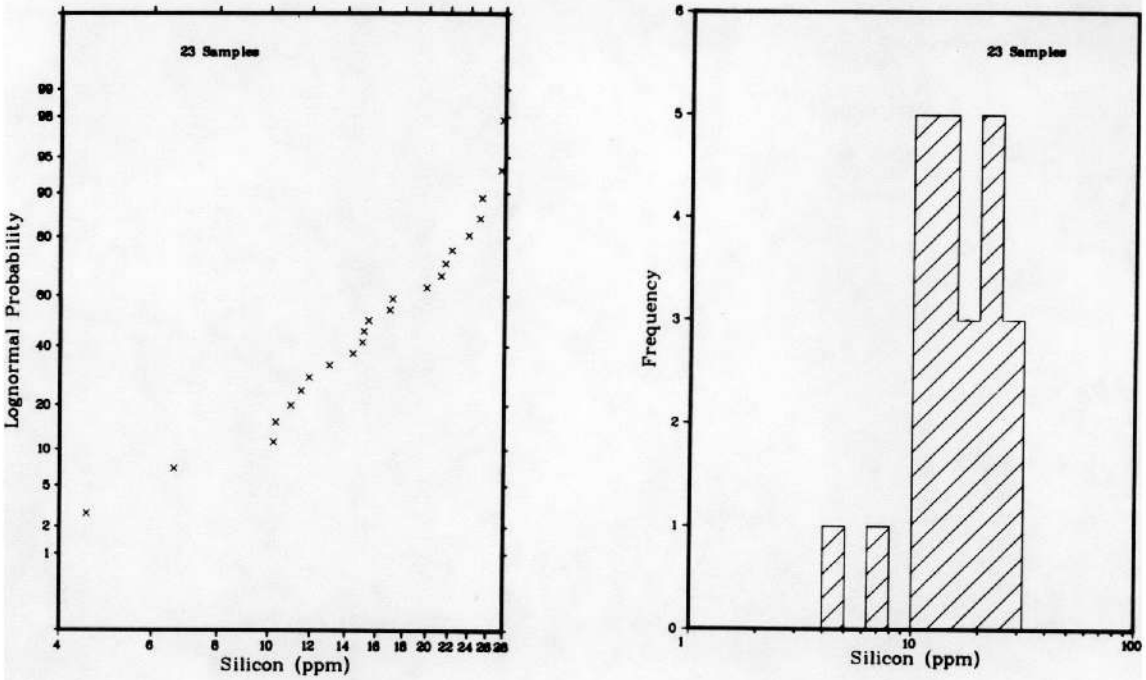

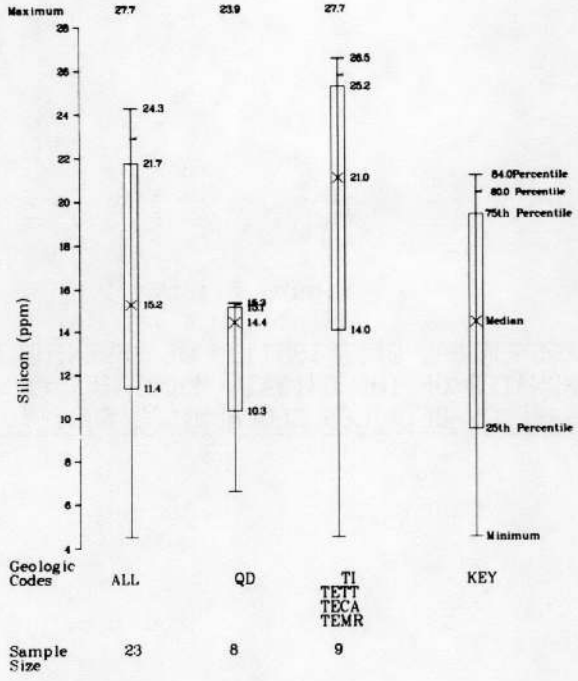

Figure A-19a

PROBABILITY, FREQUENCY, AND PERCENTILE PLOTS FOR SILICON (PPM) IN GROUNDWATER OF THE CHINATI MOUNTAINS PROJECT AREA, TRANS-PECOS DETAILED GEOCHEMICAL SURVEY, TEXAS

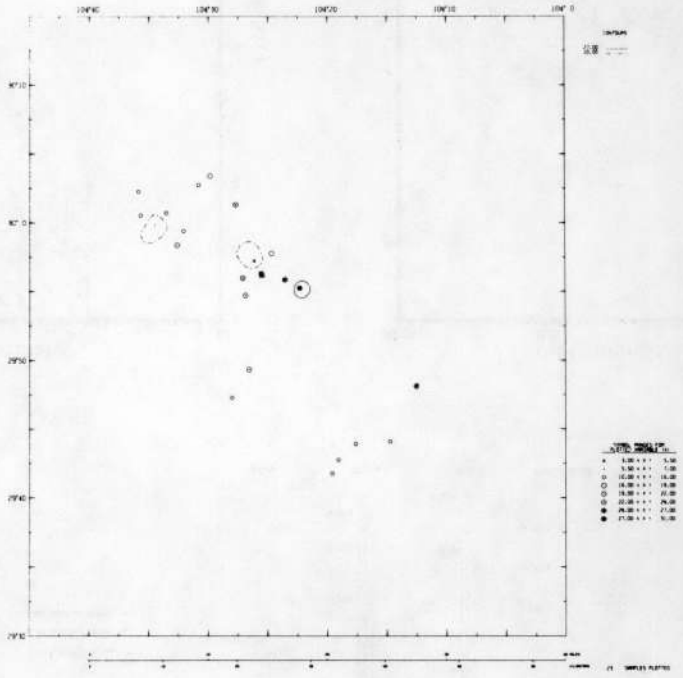

Figure A-19b

GEOCHEMICAL DISTRIBUTION OF SILICON (PPM)
IN GROUNDWATER OF THE CHINATI MOUNTAINS PROJECT AREA,
TRANS-PECOS DETAILED GEOCHEMICAL SURVEY, TEXAS

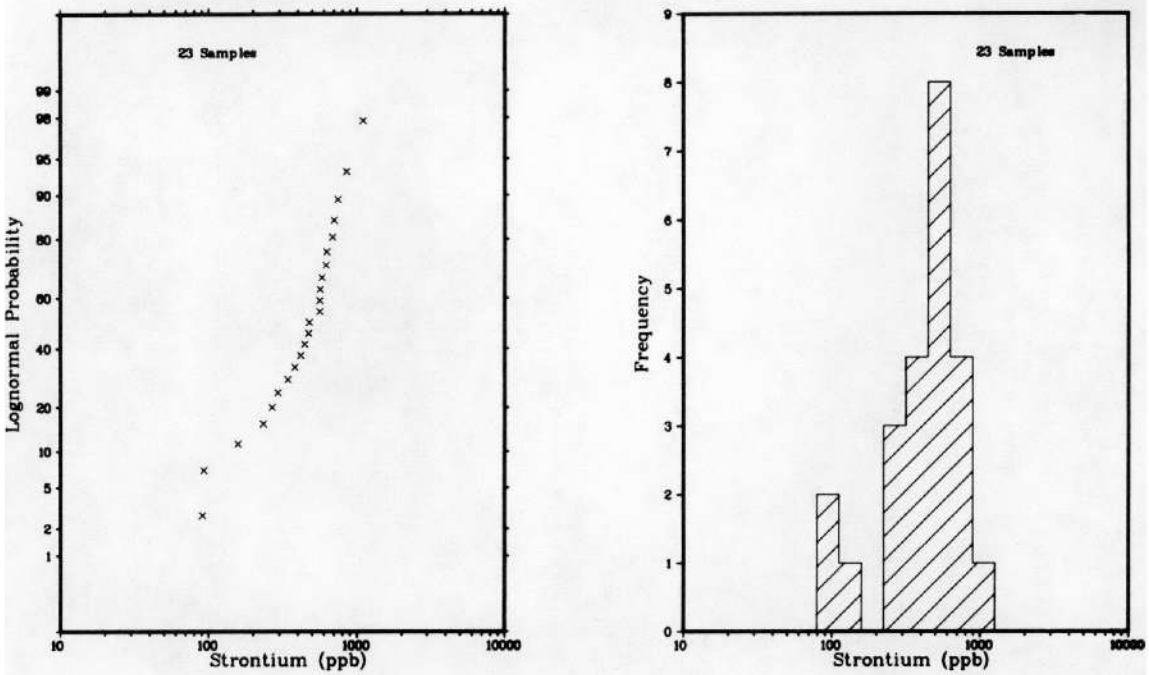

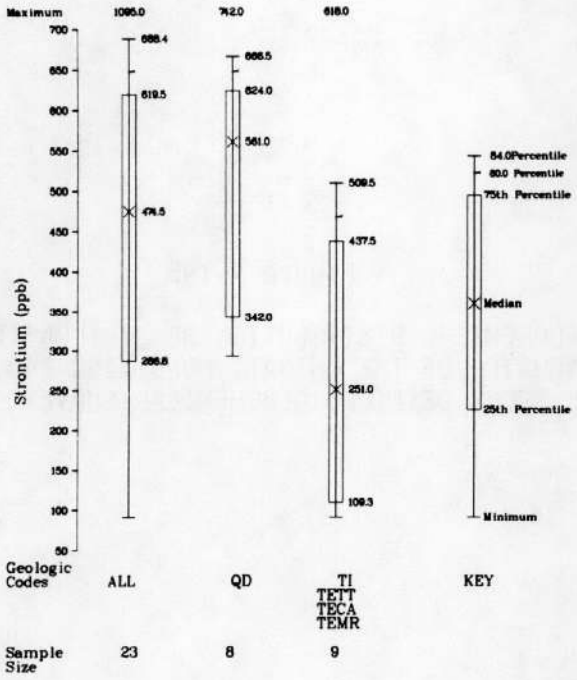

Figure A-20a

PROBABILITY, FREQUENCY, AND PERCENTILE PLOTS FOR STRONTIUM (PPB) IN GROUNDWATER OF THE CHINATI MOUNTAINS PROJECT AREA, TRANS-PECOS DETAILED GEOCHEMICAL SURVEY, TEXAS

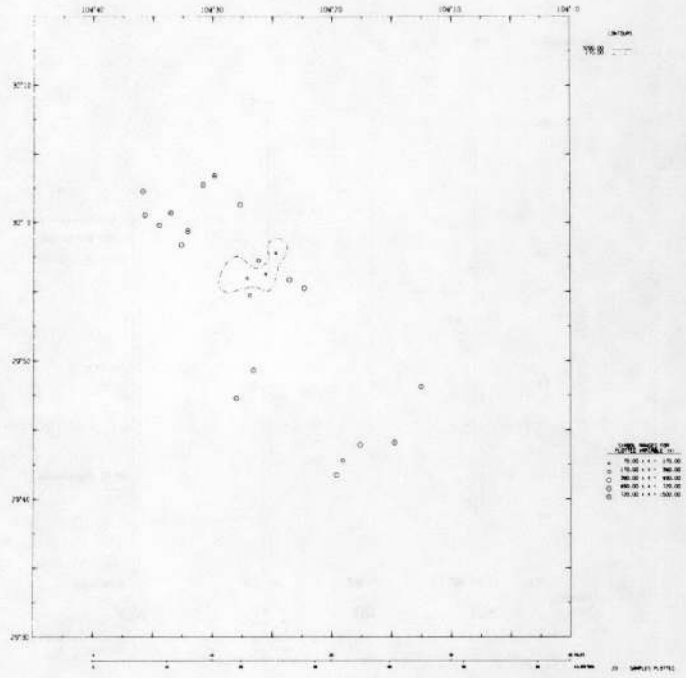

Figure A-20b

GEOCHEMICAL DISTRIBUTION OF STRONTIUM (PPB)
IN GROUNDWATER OF THE CHINATI MOUNTAINS PROJECT AREA,
TRANS-PECOS DETAILED GEOCHEMICAL SURVEY, TEXAS

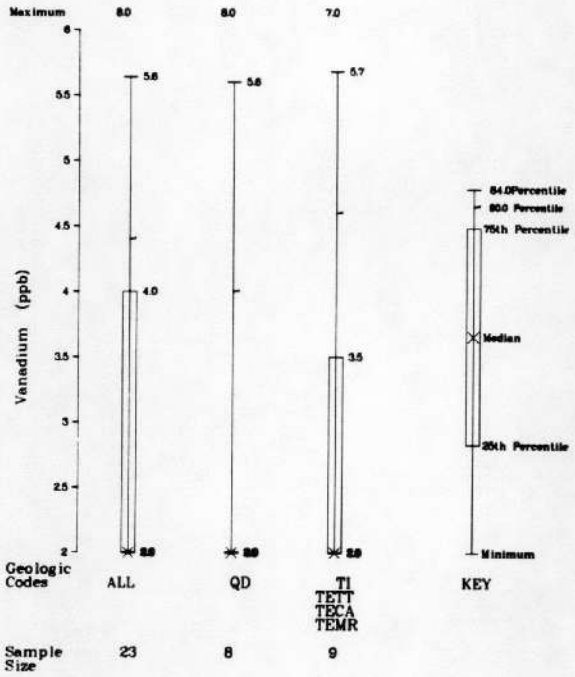

Figure A-21a

PERCENTILE PLOT FOR VANADIUM (PPB)
IN GROUNDWATER OF THE CHINTATI MOUNTAINS PROJECT AREA,
TRANS-PECOS DETAILED GEOCHEMICAL SURVEY, TEXAS

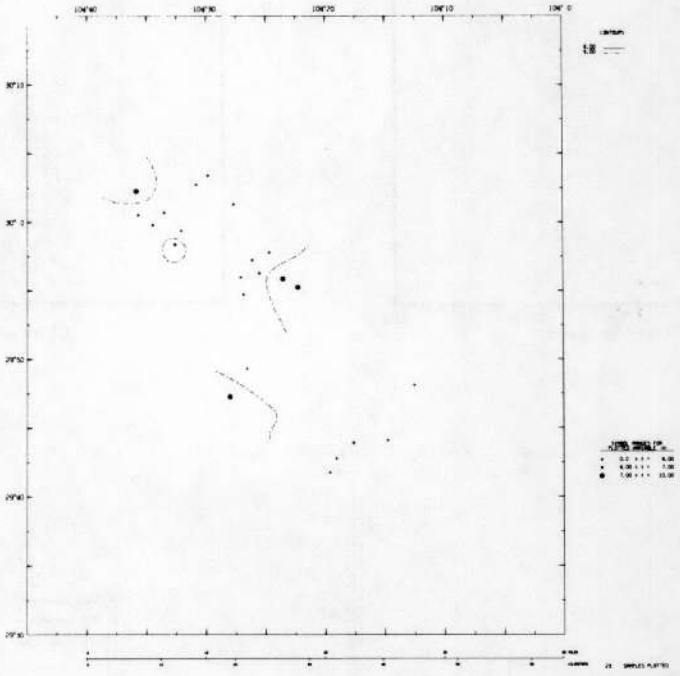

Figure A-21b

GEOCHEMICAL DISTRIBUTION OF VANADIUM (PPB)
IN GROUNDWATER OF THE CHINATI MOUNTAINS PROJECT AREA,
TRANS-PECOS DETAILED GEOCHEMICAL SURVEY, TEXAS

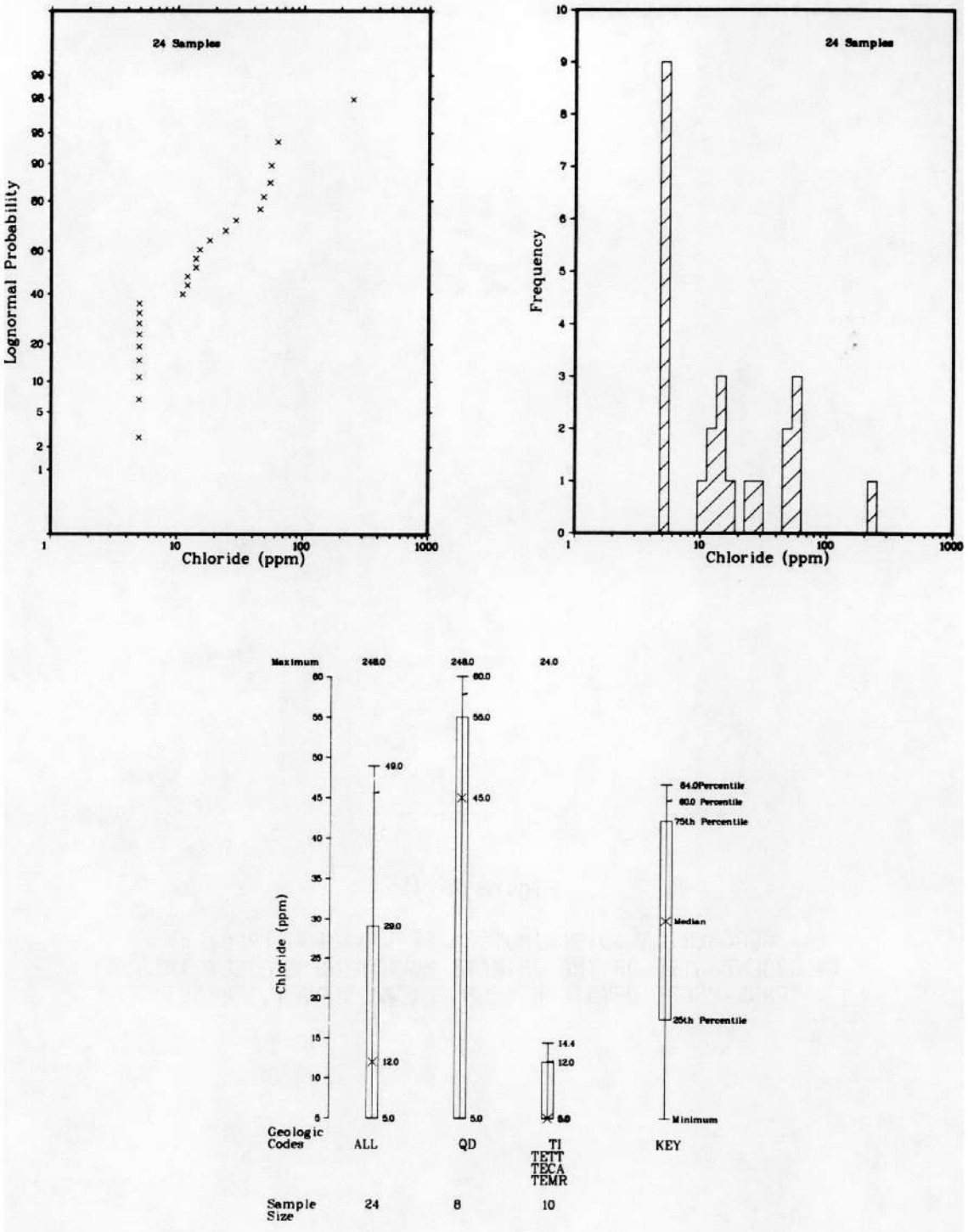

Figure A-22a

PROBABILITY, FREQUENCY, AND PERCENTILE PLOTS FOR CHLORIDE (PPM) IN GROUNDWATER OF THE CHINATI MOUNTAINS PROJECT AREA, TRANS-PECOS DETAILED GEOCHEMICAL SURVEY, TEXAS

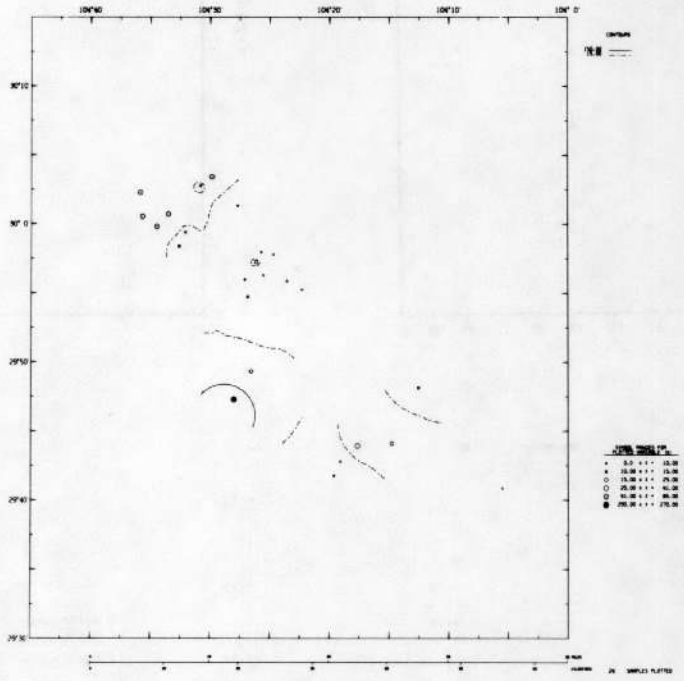

Figure A-22b

GEOCHEMICAL DISTRIBUTION OF CHLORIDE (PPM)
IN GROUNDWATER OF THE CHINATI MOUNTAINS PROJECT AREA,
TRANS-PECOS DETAILED GEOCHEMICAL SURVEY, TEXAS

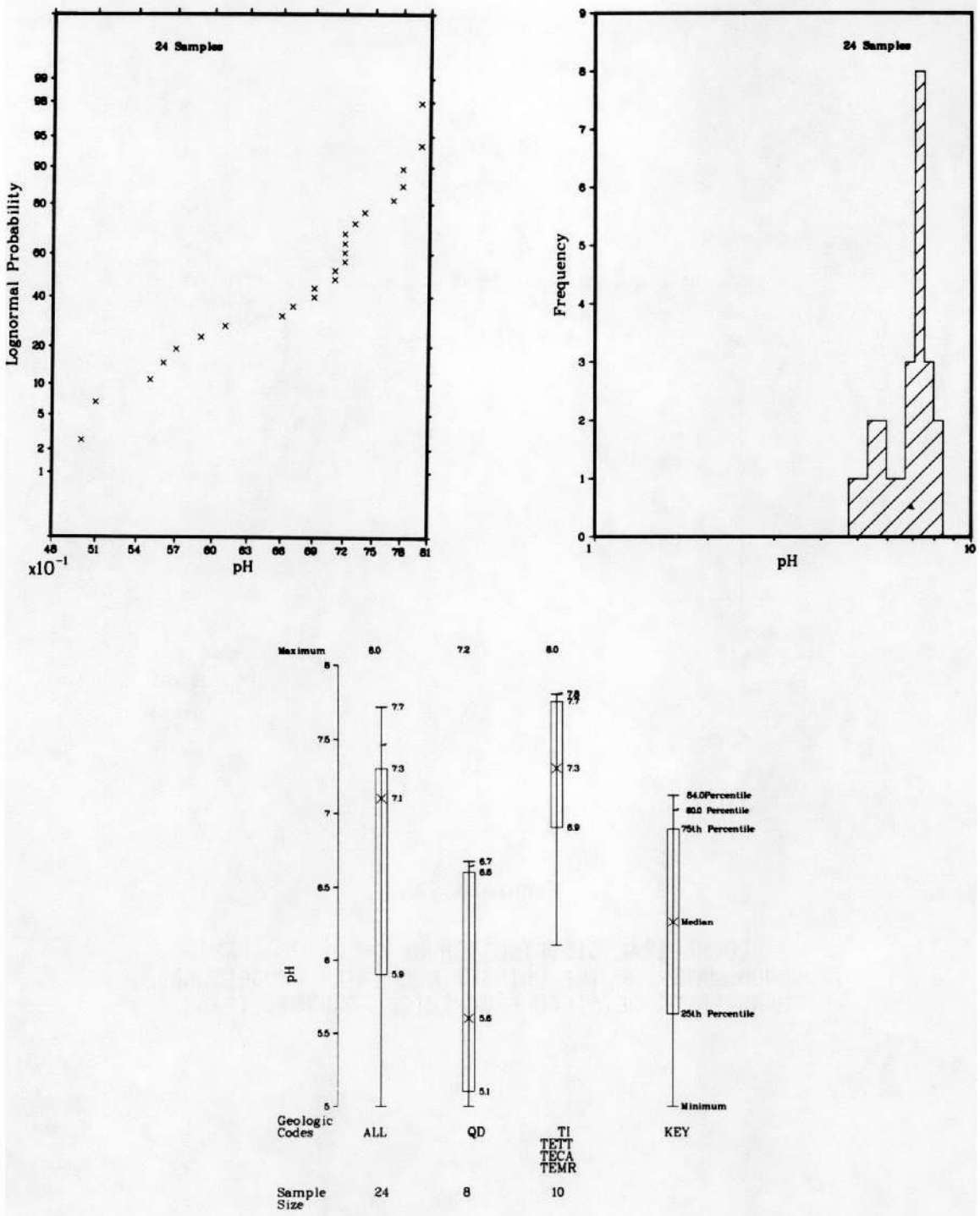

Figure A-23a

PROBABILITY, FREQUENCY, AND PERCENTILE PLOTS FOR pH IN GROUNDWATER OF THE CHINATI MOUNTAINS PROJECT AREA, TRANS-PECOS DETAILED GEOCHEMICAL SURVEY, TEXAS

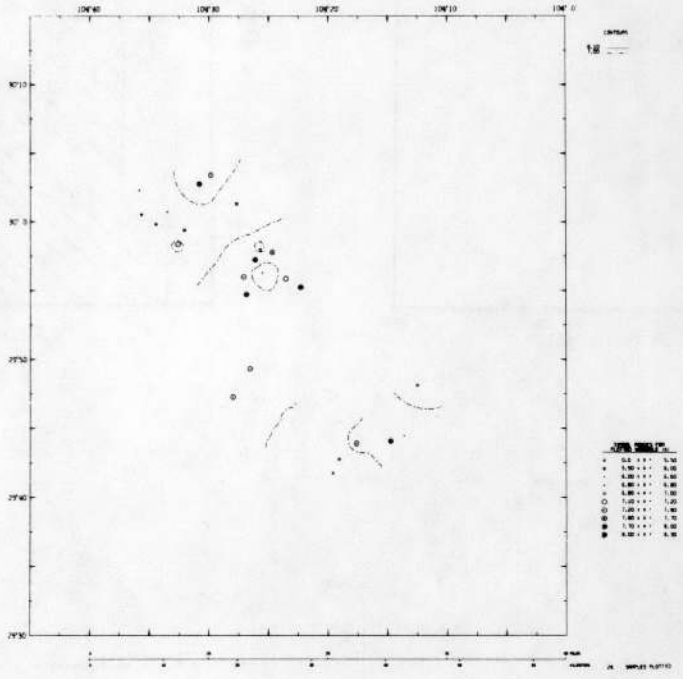

Figure A-23b

GEOCHEMICAL DISTRIBUTION OF pH
IN GROUNDWATER OF THE CHINATI MOUNTAINS PROJECT AREA,
TRANS-PECOS DETAILED GEOCHEMICAL SURVEY, TEXAS

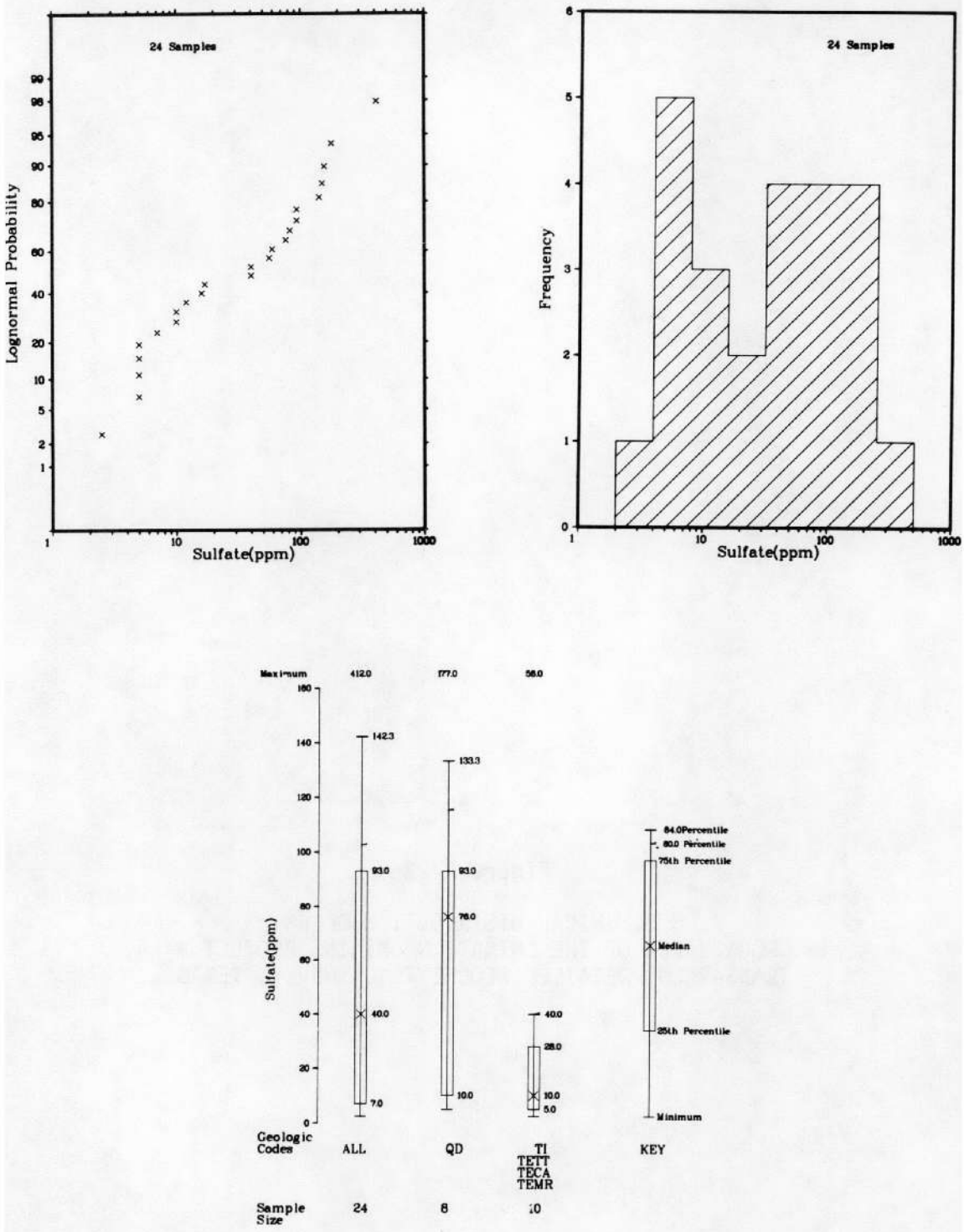

Figure A-24a

PROBABILITY, FREQUENCY, AND PERCENTILE PLOTS FOR SULFATE (PPM) IN GROUNDWATER OF THE CHINATI MOUNTAINS PROJECT AREA, TRANS-PECOS DETAILED GEOCHEMICAL SURVEY, TEXAS

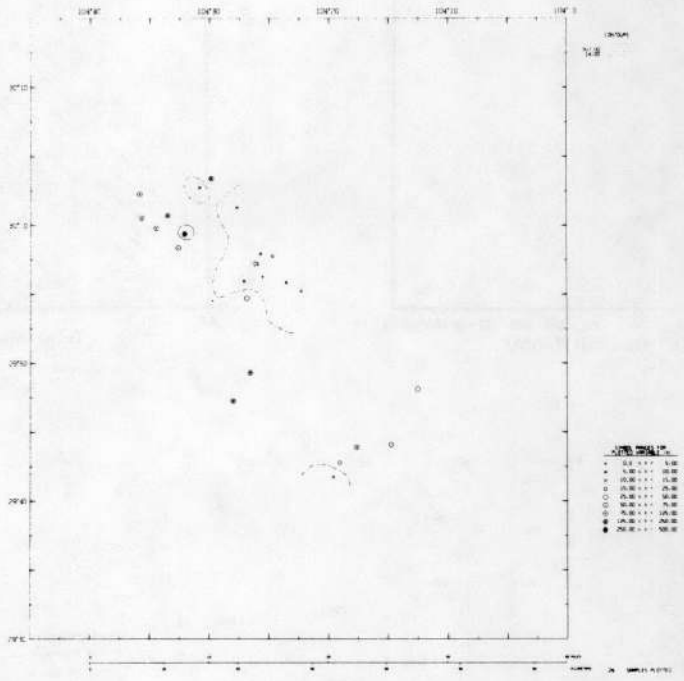

Figure A-24b

GEOCHEMICAL DISTRIBUTION OF SULFATE (PPM)
IN GROUNDWATER OF THE CHINATI MOUNTAINS PROJECT AREA,
TRANS-PECOS DETAILED GEOCHEMICAL SURVEY, TEXAS

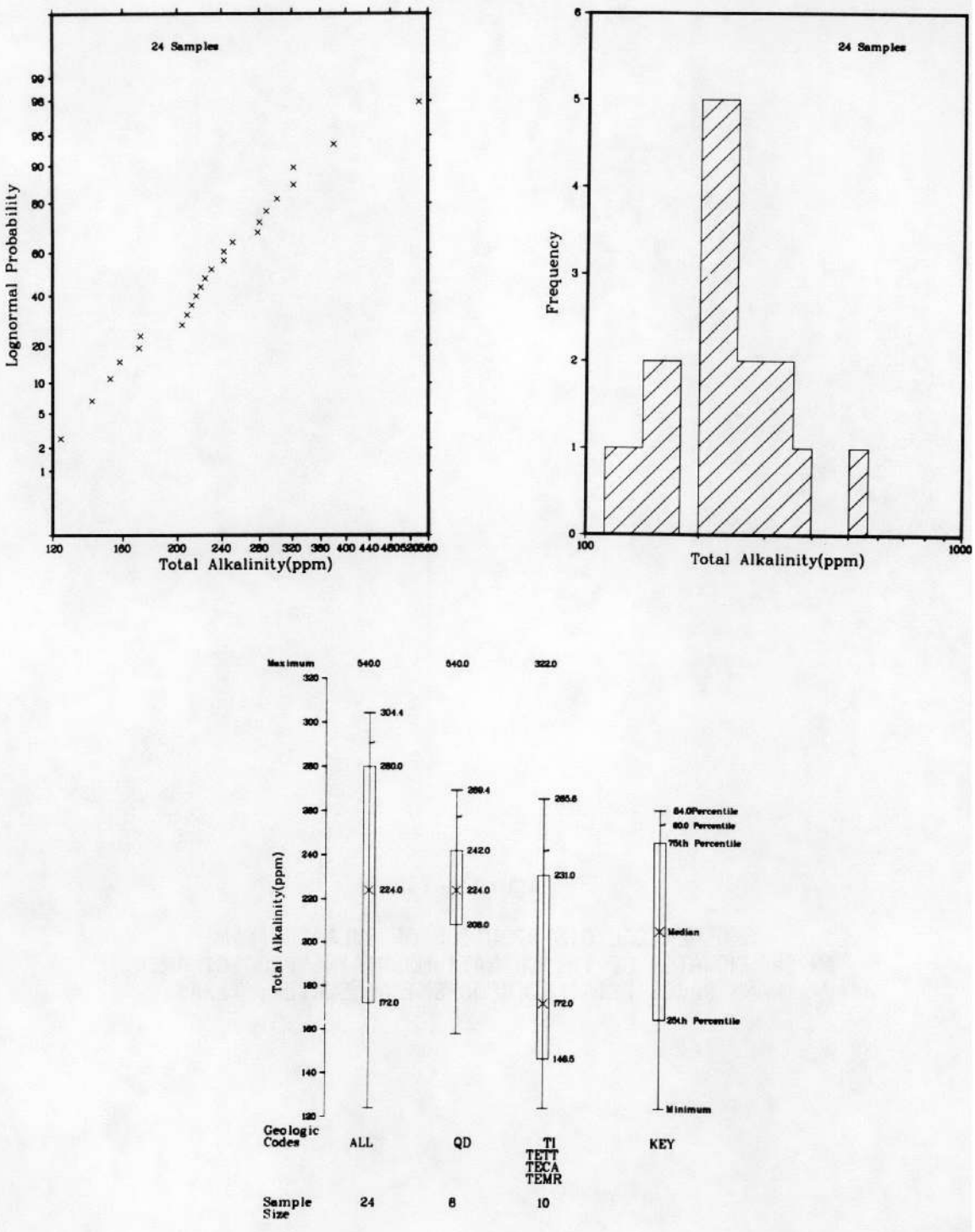

Figure A-25a

PROBABILITY, FREQUENCY, AND PERCENTILE PLOTS FOR TOTAL ALKALINITY (PPM) IN GROUNDWATER OF THE CHINATI MOUNTAINS PROJECT AREA, TRANS-PECOS DETAILED GEOCHEMICAL SURVEY, TEXAS

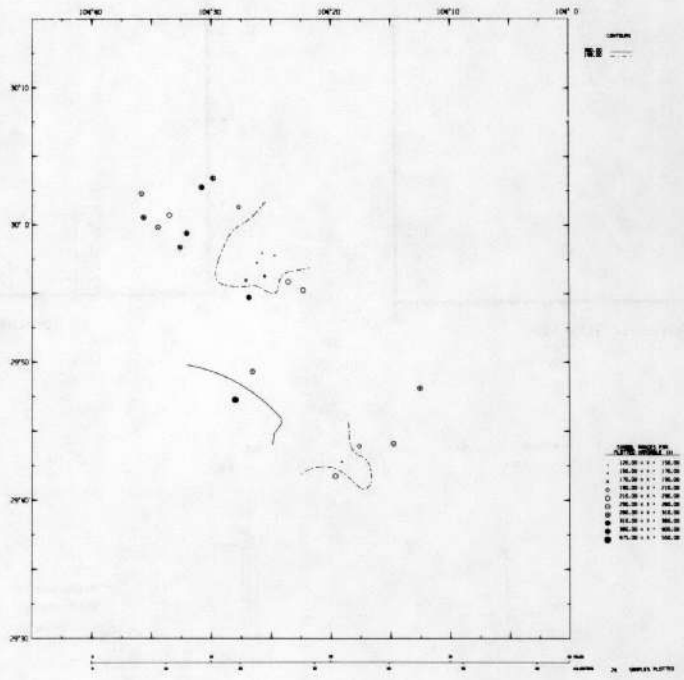

Figure A-25b

GEOCHEMICAL DISTRIBUTION OF TOTAL ALKALINITY (PPM) IN GROUNDWATER OF THE CHINATI MOUNTAINS PROJECT AREA, TRANS-PECOS DETAILED GEOCHEMICAL SURVEY, TEXAS

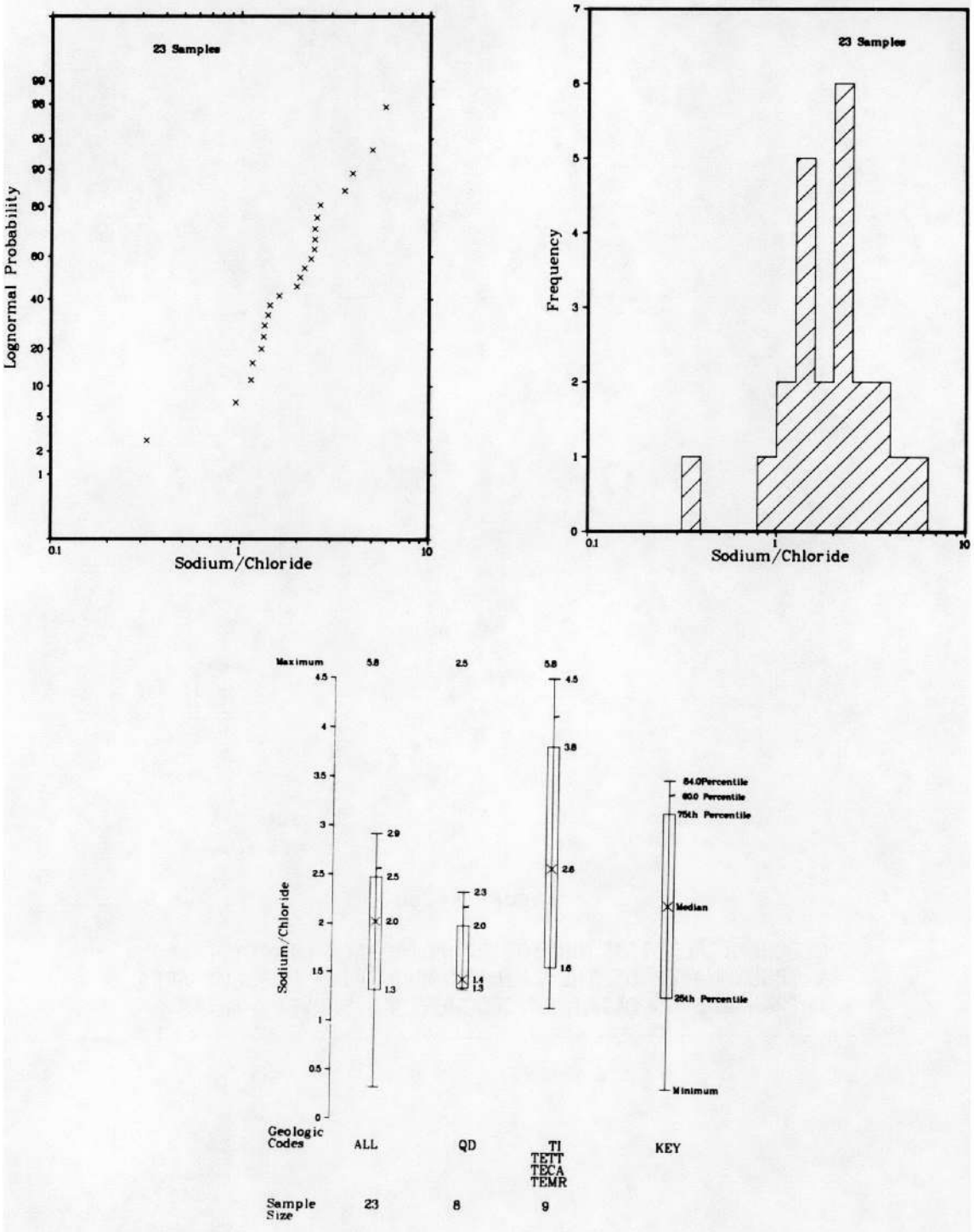

Figure A-26a

PROBABILITY, FREQUENCY, AND PERCENTILE PLOTS FOR SODIUM/CHLORIDE IN GROUNDWATER OF THE CHINATI MOUNTAINS PROJECT AREA, TRANS-PECOS DETAILED GEOCHEMICAL SURVEY, TEXAS

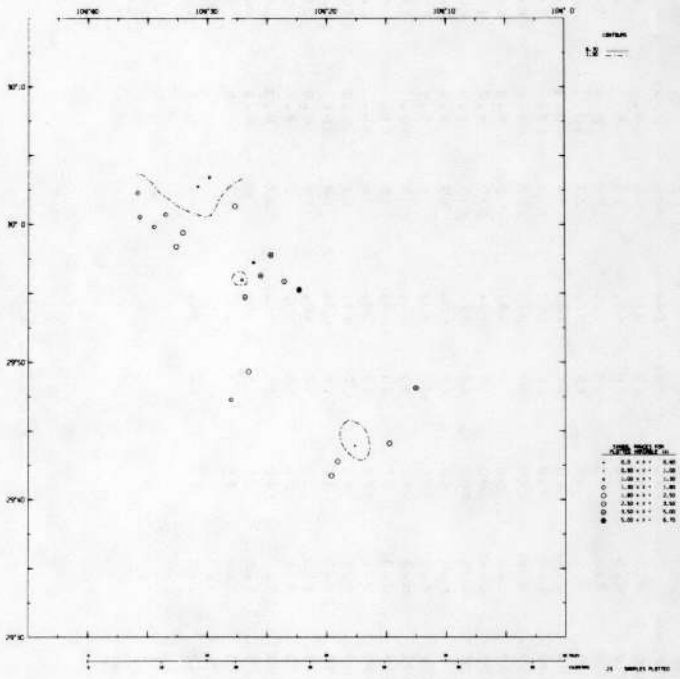

Figure A-26b

GEOCHEMICAL DISTRIBUTION OF SODIUM/CHLORIDE
IN GROUNDWATER OF THE CHINATI MOUNTAINS PROJECT AREA,
TRANS-PECOS DETAILED GEOCHEMICAL SURVEY, TEXAS

Table A-3

PARTIAL DATA LISTING FOR GROUNDWATER OF THE CHINATI MOUNTAINS PROJECT AREA, TRANS-PECOS DETAILED GEOCHEMICAL SURVEY, TEXAS

OR SAMPLE NUMBER	D. O. E. SAMPLE NUMBER ST	LAT	LONG	L TY REP	U (PPB)	SP UMHOS/CM	U/SP	B (PPB)	BA (PPB)	CA (PPM)	LI (PPB)	MG (PPM)	MO (PPB)	SR (PPB)	SO4 (PPM)
27279	48	30.057	-104.498	-3-03-	8.5	1300	6.7	210	13	98.	66	28.	4	1100	140
27280	48	30.046	-104.514	-3-03-	4.1	920	4.5	79	220	40.	13	60.	7	580	5
27289	48	29.696	-104.327	-3-03-	2.1	720	3.0	53	12	72.	8	5.6	<4	340	10
27303	48	29.990	-104.535	-3-03-	8.4	1400	5.9	98	16	200.	33	48.	8	850	410
27307	48	30.009	-104.595	-3-03-	0.81	1100	0.74	260	17	46.	120	8.3	4	680	76
27313	48	30.012	-104.555	-3-03-	1.8	1300	1.5	290	11	56.	130	17.	<4	740	180
27319	48	30.038	-104.598	-3-01-	<0.20	930	0.11	270	42	37.	140	4.2	<4	620	93
27323	48	29.713	-104.318	-3-03-	2.1	660	3.2	60	2	64.	6	4.9	<4	290	17
27325	48	29.997	-104.575	-3-03-	0.52	1200	0.45	200	15	40.	130	E.7	10	560	93
27331	48	29.788	-104.467	-3-01-	9.6	2100	4.5	760	42	22.	230	1.8	<4	560	150
27413	48	30.022	-104.462	-3-03-	1.9	470	4.0	46	12	63.	10	4.9	<4	380	5
27428	48	29.732	-104.294	-3-01-	4.3	1000	4.2	61	52	82.	6	9.1	12	470	82
27432	48	29.973	-104.544	-3-01-	5.4	1000	5.3	47	30	77.	5	18.	17	480	59
27440	48	29.822	-104.443	-3-01-	4.1	1200	3.3	67	30	120.	18	21.	6	700	160
29154	48	29.735	-104.246	-3-03-	4.1	500	8.1	130	28	39.	24	15.	21	560	56
29186	48	29.921	-104.372	-3-01-	1.7	360	4.8	48	7	49.	14	9.2	110	440	12
29189	48	29.912	-104.448	-3-01-	7.3	550	13.	17	14	69.	8	26.	100	270	40
29190	48	29.938	-104.426	-3-01-	1.3	820	1.6	23	<2	46.	14	6.9	25	93	<5
29191	48	29.954	-104.436	-3-01-	1.8	770	2.4	28	54	30.	2	7.2	5	230	16
29241	48	29.802	-104.205	-3-03-	18.	1100	17.	140	23	79.	27	8.3	4	620	40
29246	48	29.933	-104.452	-3-01-	1.0	680	1.5	21	6	55.	8	5.9	6	91	5
29257	48	29.931	-104.393	-3-03-	0.98	620	1.6	47	5	56.	13	7.6	5	420	5
29275	48	29.966	-104.425	-3-01-	0.84	490	1.7								7
29283	48	29.963	-104.412	-3-01-	0.75	460	1.6	13	14	36.	4	5.9	11	160	10

APPENDIX B

STREAM SEDIMENT

*Where probability and frequency plots are not present, they are unavailable because of the small number of samples.

APPENDIX B

STREAM SEDIMENT

LIST OF TABLES

LIST OF FIGURES

LIST OF FIGURES, Continued

LIST OF FIGURES, Continued

LIST OF FIGURES, Continued

LIST OF FIGURES, Continued

LIST OF FIGURES, Continued

LIST OF FIGURES, Continued

Table B-1

STATISTICAL SUMMARY FOR STREAM SEDIMENT OF THE CHINATI MOUNTAINS PROJECT AREA, TRANS-PECOS DETAILED GEOCHEMICAL SURVEY, TEXAS

ELEMENT	NO. SAMPLES ANALYZED: MEASURABLE VALUES	BELOW DETECTION LIMIT	DETECTION LIMIT	MINIMUM VALUE	MAXIMUM VALUE	MEAN	MEDIAN	MODE	STANDARD DEVIATION	COEFFICIENT OF VARIATION	LN TRANSFORMATION: MEAN	LN TRANSFORMATION: S. D.	ROBUST: MEAN	ROBUST: S. D.
U-FL	121			1.13	12.11	2.46	2.26	2.47	1.284	0.523	0.82	0.35	0.80	0.30
U-NT	121			1.30	11.10	3.15	2.99	1.89	1.527	0.485	1.07	0.37	1.05	0.37
TH	117	4	<2	<2	21	6	5	3	3.5	0.6	1.67	0.56	1.65	0.60
U/TU	121			0.21	1.24	0.80	0.79	0.75	0.175	0.218	-0.24	0.25	-0.23	0.21
TH/U	121			0.33	7.65	2.02	1.82	1.56	1.126	0.558	0.55	0.59	0.56	0.61
AG	2	119	<2	<2	3	2	<2	<2	0.7	0.3	0.90	0.29		
AL	121			1.40	7.71	4.92	5.47	5.64	1.484	0.301	1.53	0.38	1.57	0.36
AS	120	1	<0.1	<0.1	9.8	2.4	2.0	1.7	1.44	0.60	0.74	0.55	0.73	0.61
B	17	104	<10	<10	40	15	<10	<10	7.4	0.5	2.65	0.38		
BA	121			118	1326	688	720	793	271.0	0.4	6.44	0.48	6.46	0.46
BE	119	2	<1	<1	6	2	2	1	1.2	0.5	0.79	0.51	0.86	0.43
CA	121			0.98	22.54	6.65	5.49	4.10	4.254	0.640	1.68	0.69	1.70	0.71
CE	121			12	208	67	61	55	35.9	0.5	4.07	0.54	4.08	0.56
CO	77	44	<4	<4	19	5	<4	<4	2.7	0.5	1.69	0.34		
CR	121			6	118	27	23	15	17.7	0.6	3.18	0.52	3.17	0.53
CU	120	1	<2	<2	40	9	9	9	5.0	0.5	2.20	0.42	2.19	0.40
FE	121			0.74	17.18	3.69	3.36	2.76	2.419	0.656	1.13	0.59	1.13	0.61
K	121			0.28	2.99	1.44	1.44	1.29	0.506	0.352	0.28	0.42	0.32	0.43
LI	121			11	43	23	22	19	6.2	0.3	3.13	0.25	3.13	0.25
MG	121			0.31	2.61	0.72	0.60	0.52	0.383	0.534	-0.44	0.43	-0.46	0.47
MN	121			198	2901	854	750	538	481.8	0.6	6.62	0.52	6.61	0.55
MO	15	106	<4	<4	5	4	<4	<4	0.5	0.1	1.49	0.12		
NA	121			0.06	2.69	1.30	1.42	1.80	0.606	0.468	0.06	0.77	0.15	0.73
NB	121			5	134	21	18	17	15.3	0.7	2.91	0.54	2.90	0.58
NI	121			3	101	26	12	10	26.3	1.0	2.87	0.89	2.85	0.80
P	121			99	4358	1104	866	756	839.1	0.8	6.71	0.81	6.73	0.86
SC	121			2	14	6	5	5	2.7	0.5	1.70	0.44	1.70	0.48
SE	45	76	<0.1	<0.1	4.1	0.5	<0.1	<0.1	0.80	1.58	-1.16	0.83		
SR	121			50	804	292	262	222	139.2	0.5	5.57	0.49	5.57	0.49
TI	121			843	37636	7367	5975	1713	6476.1	0.9	8.60	0.80	8.60	0.82
V	121			19	520	102	82	83	85.3	0.8	4.39	0.67	4.37	0.69
Y	121			7	86	25	24	20	10.7	0.4	3.14	0.42	3.14	0.43
ZN	121			21	397	116	106	117	63.4	0.5	4.64	0.49	4.64	0.54
ZR	121			30	485	159	156	162	81.6	0.5	4.93	0.58	4.95	0.58

NOTE: Refer to Table 1, Page 26 and Table C-1, Page C-4 for concentration units and symbol definitions.

Table B-2

CORRELATION MATRIX FOR STREAM SEDIMENT OF THE CHINATI MOUNTAINS PROJECT AREA, TRANS-PECOS DETAILED GEOCHEMICAL SURVEY, TEXAS

	L-U	LUNT	L-LI	L-CD	L-CR	L-MG	L-BA	L-ZR	L-SR	L-CU	L-NI	L-SE	L-AS	L-TH	LTUN
L-U	1.00 (121)	0.77*** 0.76*** (121)	0.33*** 0.34*** (121)	-0.17 -0.03 (77)	-0.12 -0.19** (121)	-0.15* -0.15 (121)	-0.08 -0.00 (121)	0.17* 0.26*** (121)	-0.25*** -0.21** (121)	0.07 0.07 (120)	0.24*** 0.13 (121)	0.02 0.07 (45)	0.20** 0.14 (120)	0.41*** 0.32*** (117)	-0.83 -0.05 (121)
LUNT		1.00 (121)	0.28*** 0.34*** (121)	-0.25** -0.03 (77)	-0.07 -0.14 (121)	-0.22** -0.24*** (121)	0.11 0.15* (121)	0.31*** 0.41*** (121)	-0.21** -0.14 (121)	-0.14 -0.09 (120)	-0.02 0.04 (121)	-0.06 0.01 (45)	0.14 0.12 (120)	0.36*** 0.33*** (117)	-0.22** -0.17*
L-LI			1.00 (121)	-0.10 0.22* (77)	0.08 0.06 (121)	0.08 0.10 (121)	-0.08 0.02 (121)	0.21** 0.26*** (121)	-0.04 0.04 (121)	0.12 0.23** (120)	0.09 0.17* (121)	0.19 0.25** (45)	0.12 0.28*** (120)	0.20*** 0.19*** (117)	0.02 0.00
L-CD				1.00 (77)	0.49*** 0.39*** (77)	0.24** 0.28** (77)	0.47*** 0.63*** (77)	0.39*** 0.44*** (77)	0.53*** 0.53*** (77)	0.57*** 0.38*** (76)	0.24*** 0.33*** (77)	0.36*** 0.41*** (77)	0.17 0.29 (26)	0.14 0.33*** (76)	0.09 0.15
L-CR					1.00 (121)	0.33*** 0.39*** (121)	0.16* 0.13 (121)	0.18* 0.14 (121)	0.42*** 0.45*** (121)	0.34*** 0.32*** (120)	0.26*** 0.21** (120)	0.21** 0.29*** (121)	0.27* 0.29 (45)	0.35*** 0.33*** (120)	0.02 0.02
L-MG						1.00 (121)	-0.16* 0.08 (121)	-0.18** -0.00 (121)	-0.10 0.01 (121)	0.22** 0.21** (120)	-0.12 -0.09 (121)	-0.12 -0.09 (121)	0.26* 0.32** (45)	0.32*** 0.27*** (120)	0.02 0.04
L-BA							1.00 (121)	0.30*** 0.73*** (121)	0.71*** 0.57*** (121)	-0.38 -0.37 (120)	-0.12 -0.39 (121)	-0.04 -0.01 (121)	0.31 0.19 (45)	0.22** 0.06 (117)	-0.12 -0.06
L-ZR								1.00 (121)	0.54*** 0.49*** (121)	-0.02 -0.03 (120)	-0.04 -0.01 (121)	0.03 0.19 (45)	0.11 0.00 (120)	0.06 0.19** (117)	0.11 0.00
L-SR									1.00 (121)	0.12 0.10 (120)	-0.07 0.00 (121)	-0.11 0.02 (45)	-0.09 0.15* (117)	-0.09 -0.06 (117)	0.07 0.07
L-CU										1.00 (120)	0.74*** 0.82*** (120)	0.40*** 0.31** (44)	0.27*** 0.20** (119)	0.23** 0.22** (116)	0.32*** 0.27***
L-NI											1.00 (121)	0.60*** 0.45*** (45)	0.18* 0.16*	0.26*** 0.23** (117)	0.27*** 0.27***
L-SE												1.00 (45)	0.19 0.17 (45)	-0.08 -0.18 (45)	-0.06 -0.15
L-AS													1.00 (120)	0.14 0.03 (116)	0.09 0.00
L-TH														1.00 (117)	0.77*** 0.80*** (117)
LTUN															1.00 (121)
L-FE	0.09 0.12 (121)	0.32*** 0.28*** (121)	-0.09 -0.08 (121)	0.43*** 0.44*** (77)	0.47*** 0.45*** (121)	0.04 0.16* (121)	0.36*** 0.51*** (121)	0.65*** 0.61*** (121)	0.45*** 0.40*** (121)	-0.03 -0.07 (120)	0.04 0.06 (121)	0.03 0.17 (45)	0.29*** 0.23** (120)	0.00 -0.08 (117)	-0.15 -0.17*
L-TI	0.08 0.15 (121)	0.33*** 0.38*** (121)	-0.12 -0.12 (121)	0.32*** 0.36*** (77)	0.41*** 0.38*** (121)	-0.00 0.12 (121)	0.66*** 0.56*** (121)	0.65*** 0.58*** (121)	0.40*** 0.32*** (121)	-0.13 -0.15* (120)	-0.03 -0.01 (121)	0.05 0.18 (45)	0.22** 0.19** (120)	-0.03 -0.10 (117)	-0.18* -0.19**
L-V	0.03 0.04 (121)	0.23** 0.17* (121)	-0.11 -0.12 (121)	0.36*** 0.37*** (77)	0.56*** 0.53*** (121)	0.13 0.19** (121)	0.53*** 0.48*** (121)	0.50*** 0.44*** (121)	0.39*** 0.36*** (121)	-0.00 -0.03 (120)	0.06 0.09 (121)	0.07 0.21 (45)	0.32*** 0.29*** (120)	-0.06 -0.15	-0.16* -0.18**
L-ZN	0.24*** 0.27*** (121)	0.43*** 0.42*** (121)	0.04 -0.02 (121)	0.15 0.18 (77)	0.42*** 0.32*** (121)	-0.00 0.02 (121)	0.45*** 0.37*** (121)	0.57*** 0.53*** (121)	0.22** 0.16* (121)	-0.01 -0.08 (120)	0.07 0.02 (121)	0.09 0.13 (45)	0.34*** 0.28*** (120)	0.03 -0.03 (117)	-0.18** -0.19**
L-MN	0.37*** 0.39*** (121)	0.56*** 0.53*** (121)	0.02 0.05 (121)	0.27** 0.32*** (77)	0.27*** 0.18** (121)	0.00 0.12 (121)	0.54*** 0.49*** (121)	0.63*** 0.60*** (121)	0.16* 0.10 (121)	-0.07 -0.08 (120)	0.09 0.07 (121)	0.02 0.19 (45)	0.23** 0.18* (120)	0.13 0.03 (117)	-0.17* -0.19**
L-P	0.16* 0.23*** (121)	0.36*** 0.36*** (121)	-0.02 0.05 (121)	0.39*** 0.49*** (77)	0.22** 0.18** (121)	0.12 0.25*** (121)	0.79*** 0.77*** (121)	0.73*** 0.71*** (121)	0.46*** 0.40*** (121)	-0.12 -0.12 (120)	-0.04 -0.03 (121)	0.13 0.28* (45)	0.19** 0.17* (120)	-0.11 -0.17* (117)	-0.25*** -0.28***
L-SC	0.10 0.12 (121)	0.26*** 0.22** (121)	-0.04 0.02 (121)	0.50*** 0.50*** (77)	0.46*** 0.40*** (121)	0.28*** 0.36*** (121)	0.61*** 0.53*** (121)	0.60*** 0.61*** (121)	0.38*** 0.37*** (121)	0.11 0.08 (120)	0.14 0.16* (121)	0.21 0.39*** (45)	0.26*** 0.23*** (120)	-0.00 -0.08 (117)	-0.11 -0.12
LUTU	0.26*** 0.28*** (121)	-0.42*** -0.34*** (121)	0.04 0.02 (121)	0.12 -0.03 (77)	-0.06 -0.06 (121)	0.11 0.11 (121)	-0.27*** -0.27*** (121)	-0.23** -0.23** (121)	-0.05 -0.11 (121)	0.32*** 0.28*** (120)	0.32*** 0.30*** (121)	0.13 0.12 (45)	0.08 0.01 (120)	0.04 0.02 (117)	0.28*** 0.19**
L-BE	0.58*** 0.53*** (119)	0.70*** 0.73*** (119)	0.37*** 0.39*** (119)	0.16 0.18 (75)	-0.03 -0.09 (119)	-0.25*** -0.15 (119)	0.40*** 0.37*** (119)	0.64*** 0.63*** (119)	0.12 0.10 (119)	0.15 0.17* (118)	0.23** 0.16* (119)	-0.07 0.02 (44)	0.08 0.01 (118)	0.42*** 0.43*** (115)	0.03 0.05 (119)
L-MB	0.49*** 0.45*** (121)	0.73*** 0.71*** (121)	0.18** 0.25*** (121)	0.01 0.11 (77)	0.05 0.02 (121)	-0.35*** -0.31*** (121)	0.42*** 0.35*** (121)	0.54*** 0.54*** (121)	0.19** 0.19** (121)	-0.14 -0.16* (120)	-0.06 -0.12 (121)	-0.10 -0.01 (45)	0.17* 0.11 (120)	0.39*** 0.35*** (117)	-0.02 -0.00
L-AL	0.30*** 0.23** (121)	0.43*** 0.39*** (121)	0.24*** 0.26*** (121)	0.46*** 0.56*** (77)	0.12 -0.01 (121)	-0.24*** -0.02 (121)	0.75*** 0.73*** (121)	0.84*** 0.79*** (121)	0.52*** 0.49*** (121)	0.15 0.12 (120)	0.06 0.04 (121)	-0.00 0.12 (45)	0.18** 0.07 (120)	0.25*** 0.16* (117)	0.02 0.01
L-NA	0.25*** 0.20** (121)	0.40*** 0.38*** (121)	0.16* 0.25*** (121)	0.40*** 0.47*** (77)	0.14 0.08 (121)	-0.32*** -0.15 (121)	0.82*** 0.73*** (121)	0.84*** 0.73*** (121)	0.56*** 0.59*** (121)	0.00 -0.07 (120)	-0.01 -0.09 (121)	-0.00 0.12 (45)	0.19** 0.16* (120)	0.19** 0.09 (117)	-0.02 -0.07
L-K	0.42*** 0.48*** (121)	0.56*** 0.66*** (121)	0.33*** 0.46*** (121)	0.23** 0.31*** (77)	-0.05 -0.22** (121)	-0.33*** -0.18* (121)	0.56*** 0.56*** (121)	0.75*** 0.60*** (121)	0.30*** 0.17* (121)	-0.02 -0.00 (120)	0.01 -0.06 (121)	0.08 0.15 (45)	0.16* 0.12 (120)	0.26*** 0.22** (117)	-0.01 -0.08
L-CE	0.34*** 0.42*** (121)	0.57*** 0.62*** (121)	0.11 0.19** (121)	0.25** 0.32*** (77)	-0.05 -0.12 (121)	-0.19** -0.07 (121)	0.74*** 0.59*** (121)	0.75*** 0.74*** (121)	0.26*** 0.20** (121)	-0.16* -0.14 (120)	-0.04 -0.08 (121)	0.07 0.25* (45)	0.15* 0.12 (120)	0.19** 0.14 (117)	-0.11 -0.12
L-Y	0.49*** 0.48*** (121)	0.69*** 0.69*** (121)	0.22** 0.30*** (121)	0.20* 0.24** (77)	0.06 -0.05 (121)	-0.10 -0.00 (121)	0.53*** 0.39*** (121)	0.76*** 0.78*** (121)	0.21** 0.17* (121)	-0.08 -0.10 (120)	0.04 -0.03 (121)	0.09 0.28* (45)	0.17* 0.08 (120)	0.27*** 0.18** (117)	-0.12 -0.14
L-CA	-0.42*** -0.47*** (121)	-0.62*** -0.71*** (121)	-0.17* -0.19** (121)	-0.13 -0.18 (77)	0.22** 0.20** (121)	0.27*** 0.24*** (121)	-0.37*** -0.42*** (121)	-0.56*** -0.59*** (121)	0.11 0.02 (121)	-0.00 -0.02 (120)	-0.01 0.02 (121)	0.04 -0.04 (45)	0.03 -0.01 (120)	-0.31*** -0.30*** (117)	0.06 0.06 (121)

NOTE: (1) Pearson correlation/Spearman correlation/(sample size). If either element has a concentration below the laboratory detection limits, it is omitted from the pairwise computations.
(2) Significance levels: *-10%, **-5%, ***-1%.
(3) No correlation computed because of insufficient number of pairs: ******.

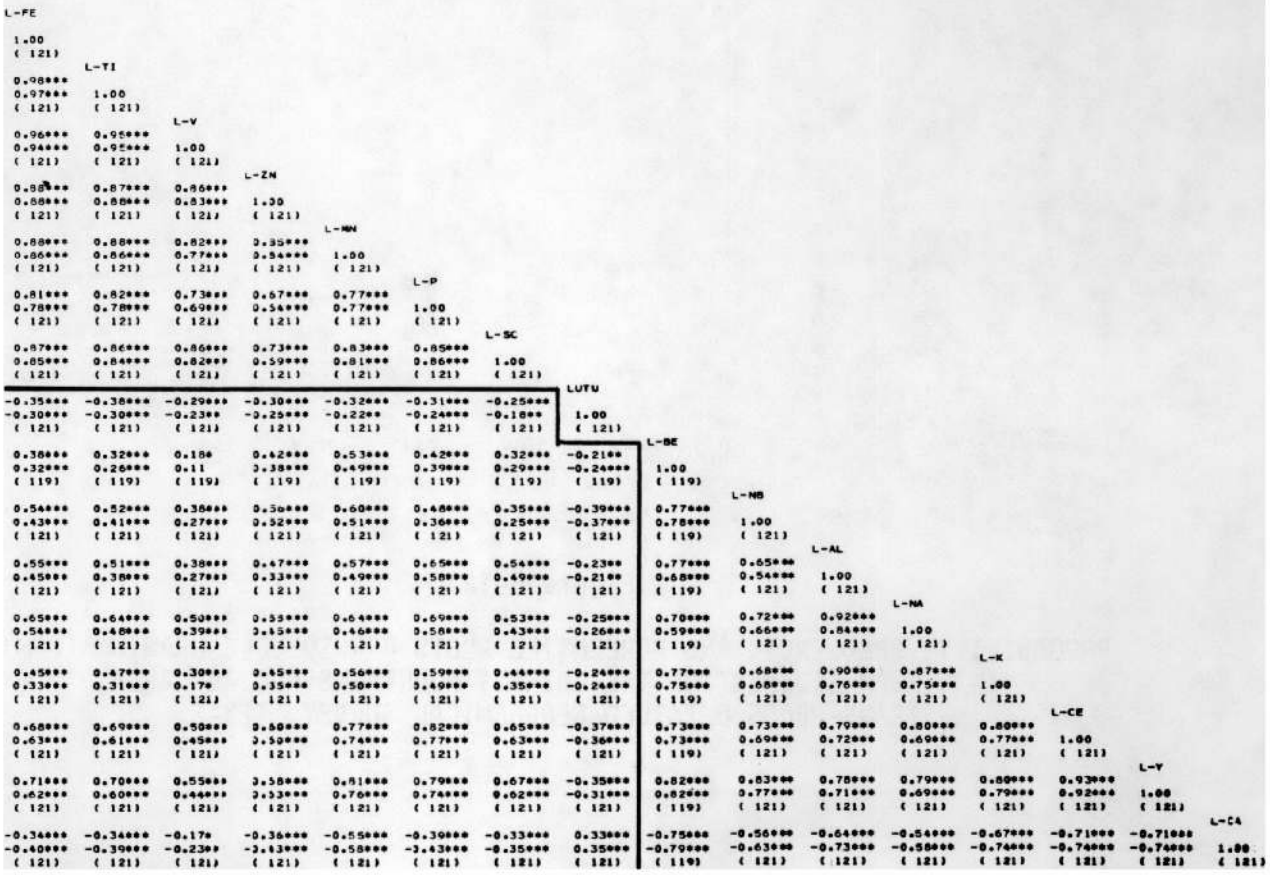

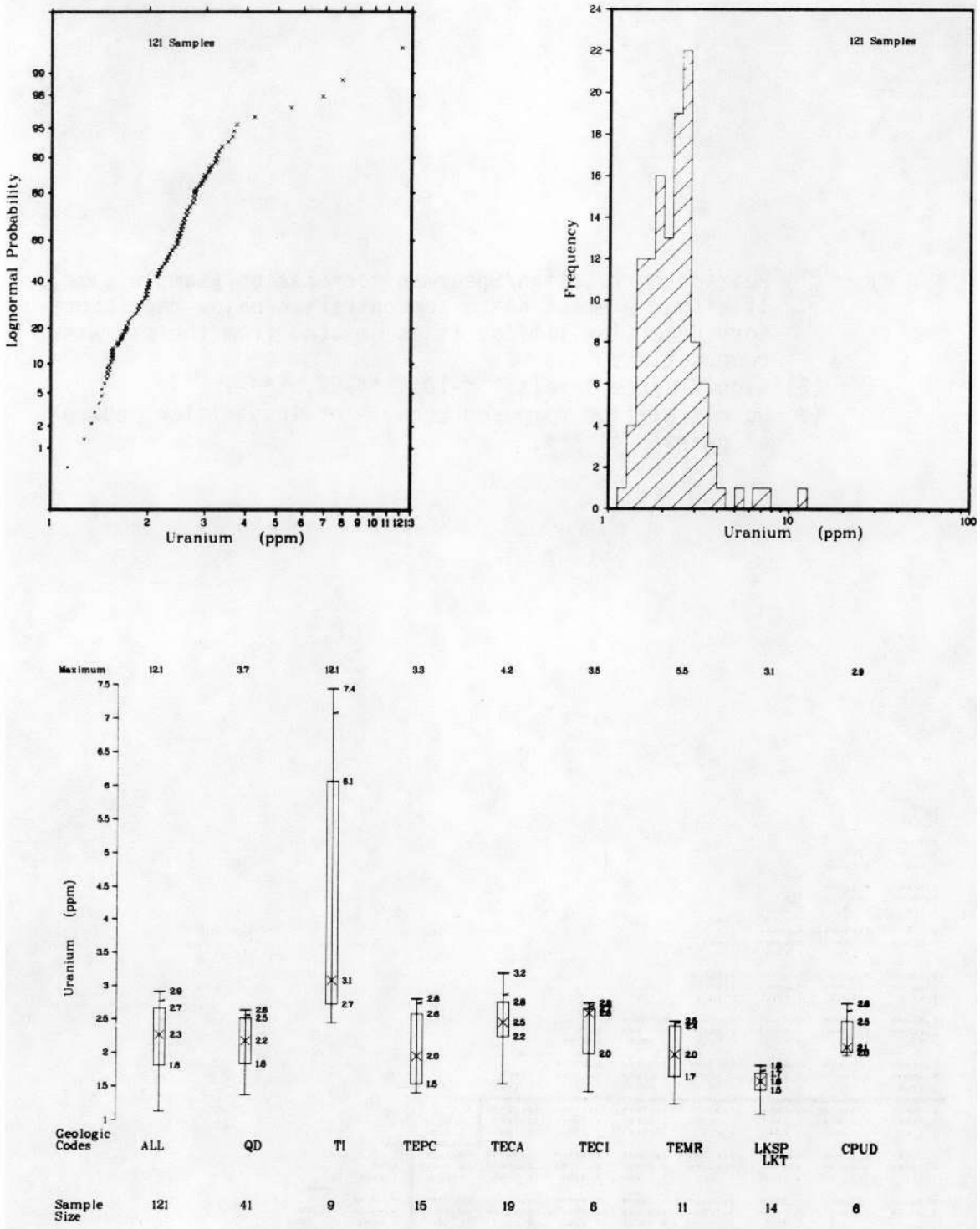

Figure B-1a

PROBABILITY, FREQUENCY, AND PERCENTILE PLOTS FOR SOLUBLE URANIUM (PPM) IN STREAM SEDIMENT OF THE CHINATI MOUNTAINS PROJECT AREA, TRANS-PECOS DETAILED GEOCHEMICAL SURVEY, TEXAS

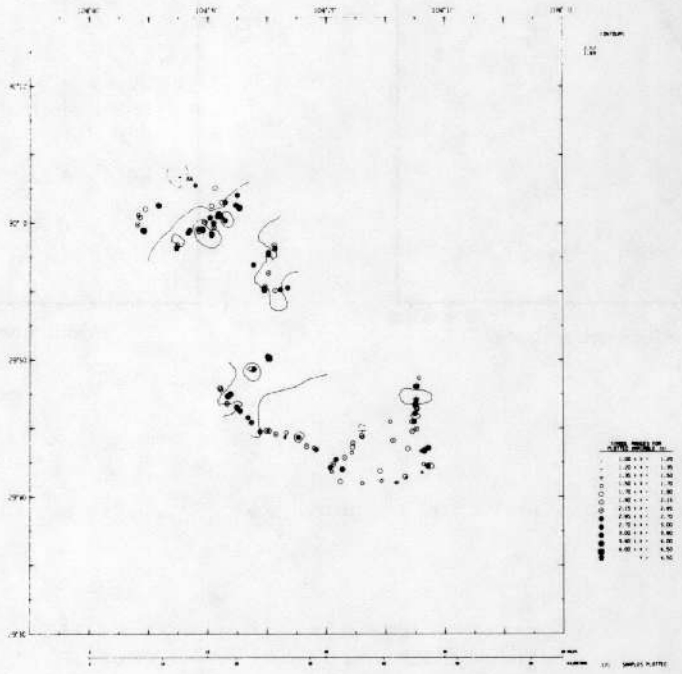

Figure B-1b

GEOCHEMICAL DISTRIBUTION OF SOLUBLE URANIUM (PPM)
IN STREAM SEDIMENT OF THE CHINATI MOUNTAINS PROJECT AREA,
TRANS-PECOS DETAILED GEOCHEMICAL SURVEY, TEXAS

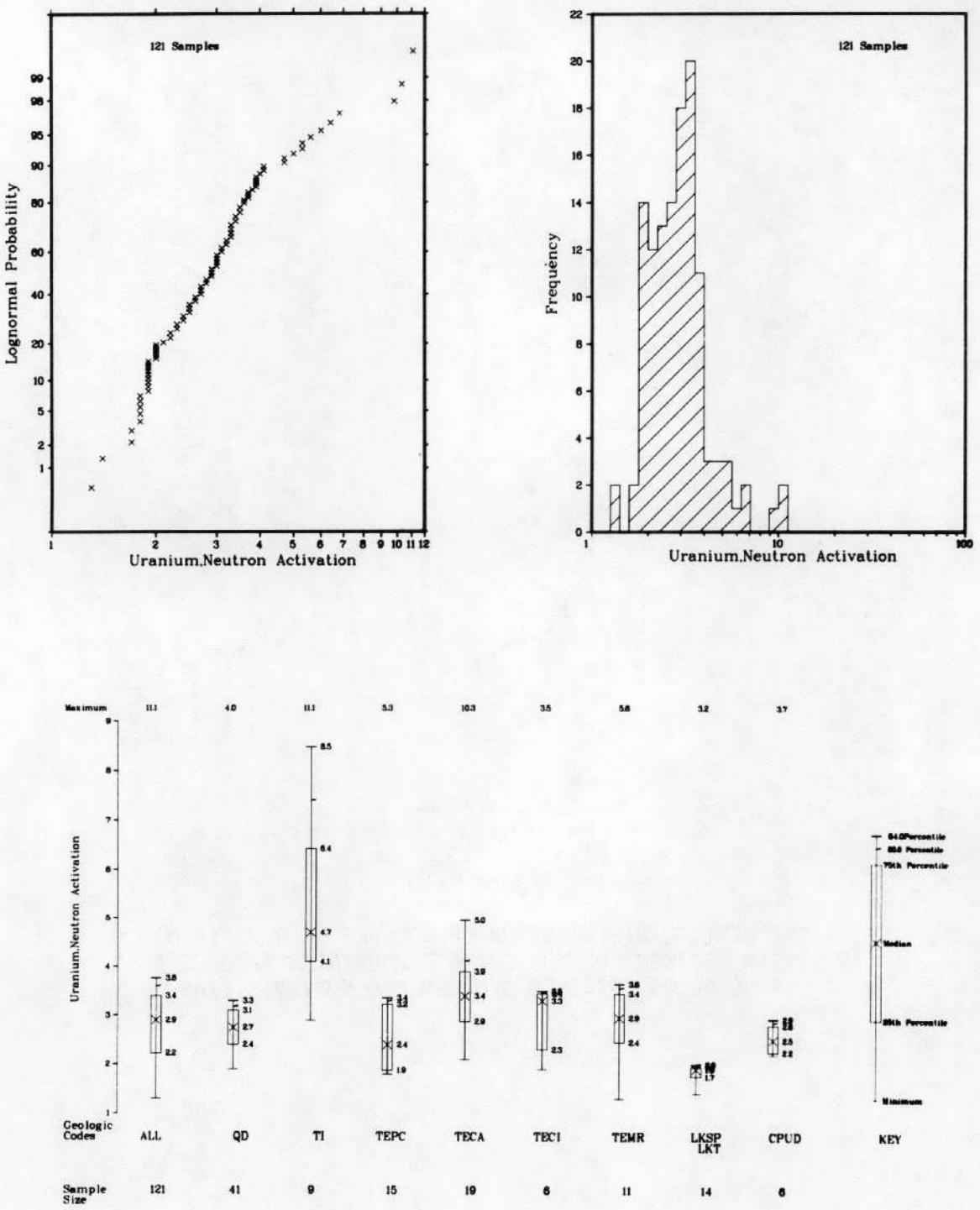

Figure B-2a

PROBABILITY, FREQUENCY, AND PERCENTILE PLOTS FOR URANIUM BY NEUTRON ACTIVATION IN STREAM SEDIMENT OF THE CHINATI MOUNTAINS PROJECT AREA, TRANS-PECOS DETAILED GEOCHEMICAL SURVEY, TEXAS

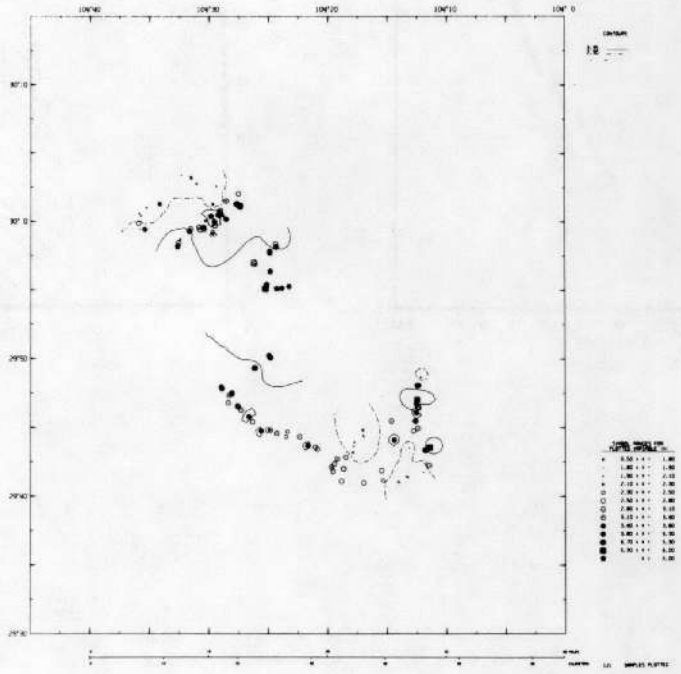

Figure B-2b

GEOCHEMICAL DISTRIBUTION OF URANIUM BY NEUTRON ACTIVATION IN STREAM SEDIMENT OF THE CHINATI MOUNTAINS PROJECT AREA, TRANS-PECOS DETAILED GEOCHEMICAL SURVEY, TEXAS

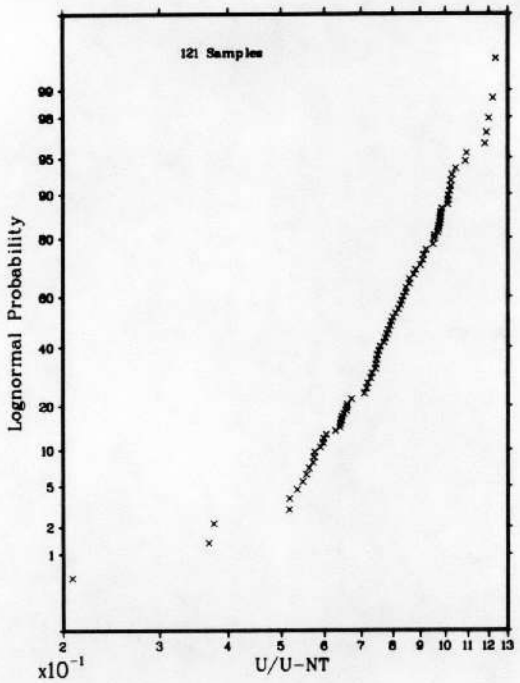

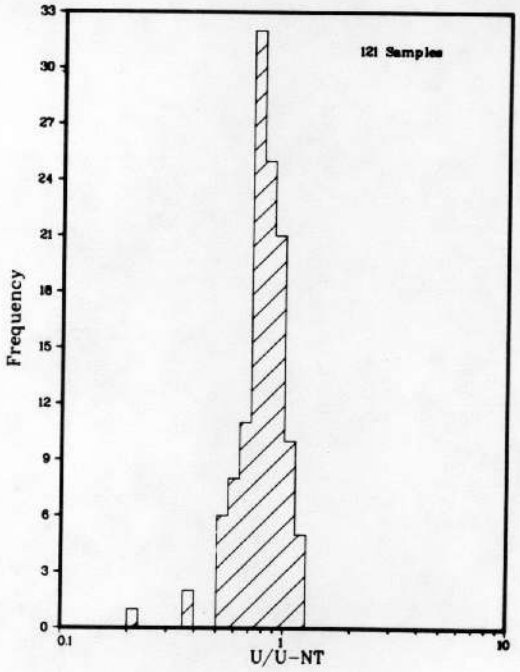

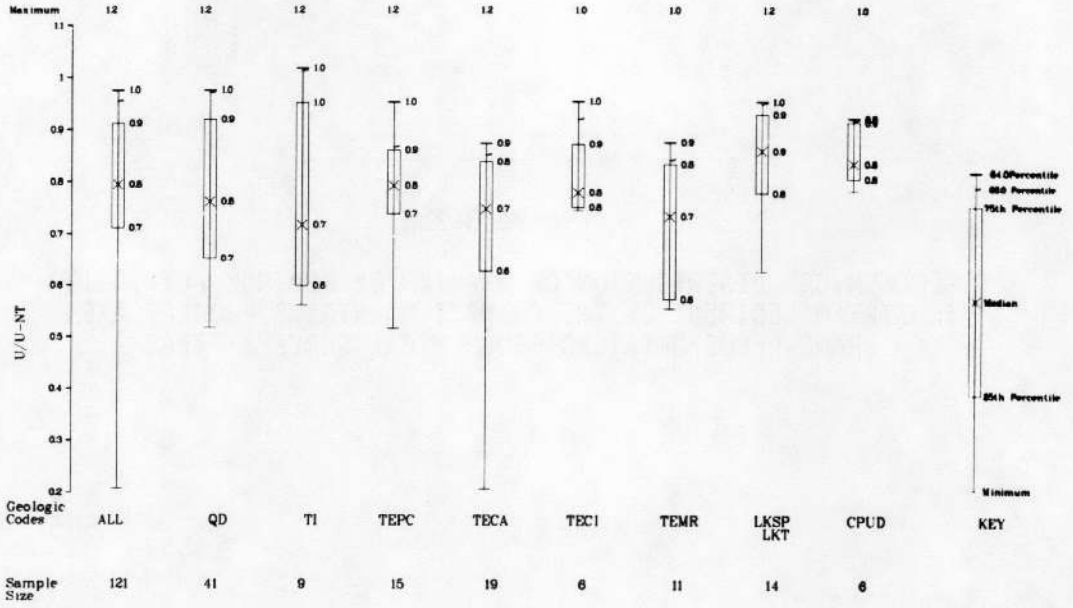

Figure B-3a

PROBABILITY, FREQUENCY, AND PERCENTILE PLOTS FOR URANIUM FLUOROMETRIC/ URANIUM NEUTRON ACTIVATION IN STREAM SEDIMENT OF THE CHINATI MOUNTAINS PROJECT AREA, TRANS-PECOS DETAILED GEOCHEMICAL SURVEY, TEXAS

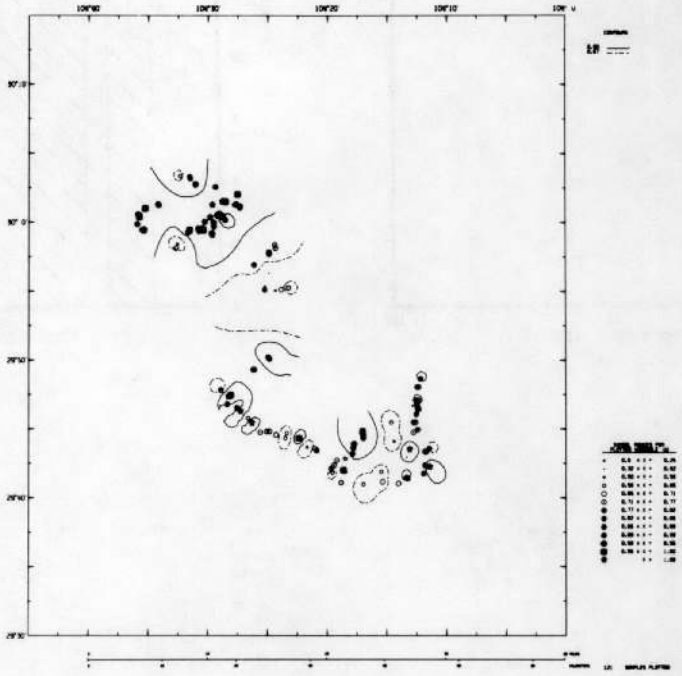

Figure B-3b

GEOCHEMICAL DISTRIBUTION OF URANIUM FLUOROMETRIC/URANIUM NEUTRON ACTIVATION IN STREAM SEDIMENT OF THE CHINATI MOUNTAINS PROJECT AREA, TRANS-PECOS DETAILED GEOCHEMICAL SURVEY, TEXAS

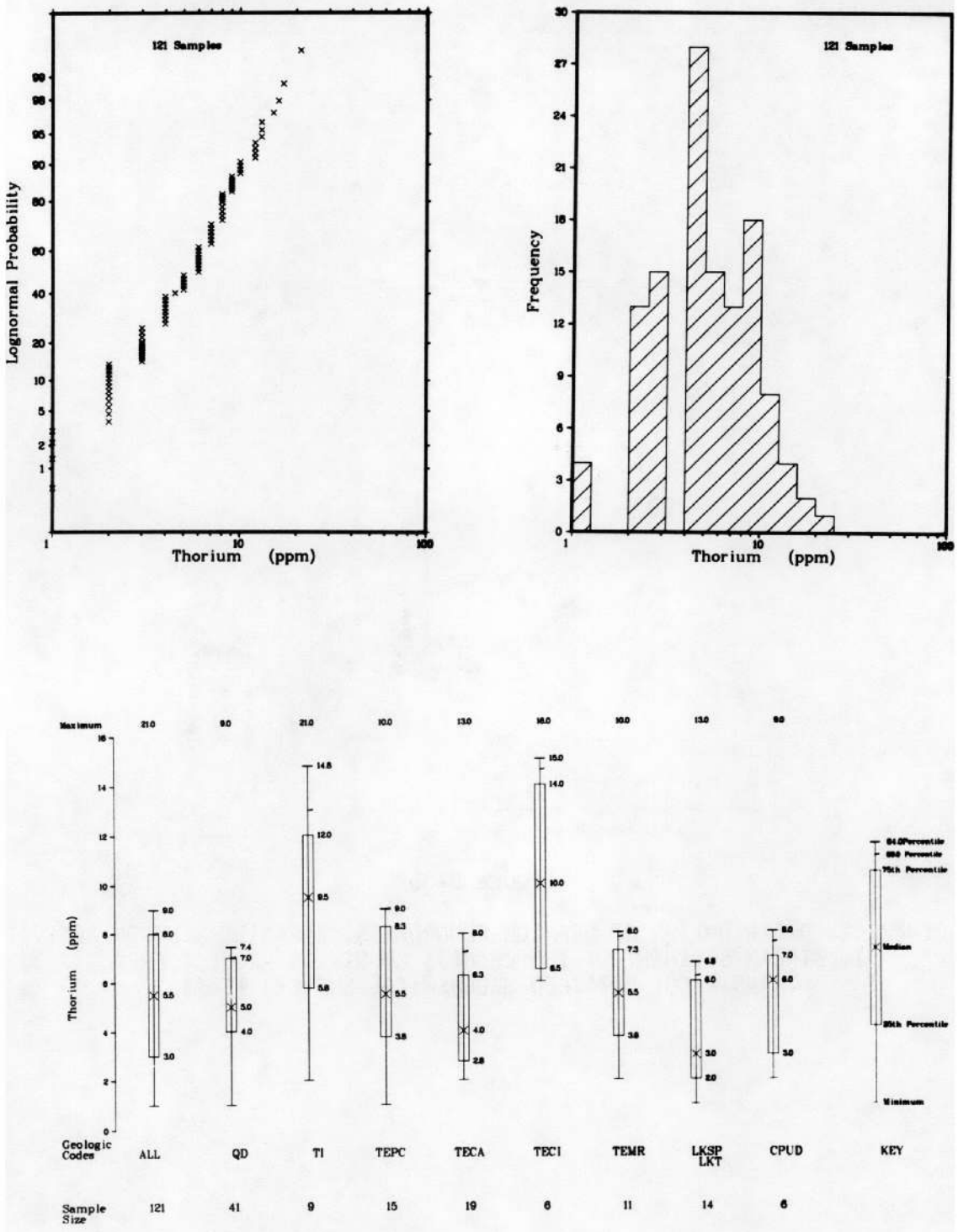

Figure B-4a

PROBABILITY, FREQUENCY, AND PERCENTILE PLOTS FOR THORIUM (PPM) IN STREAM SEDIMENT OF THE CHINATI MOUNTAINS PROJECT AREA, TRANS-PECOS DETAILED GEOCHEMICAL SURVEY, TEXAS

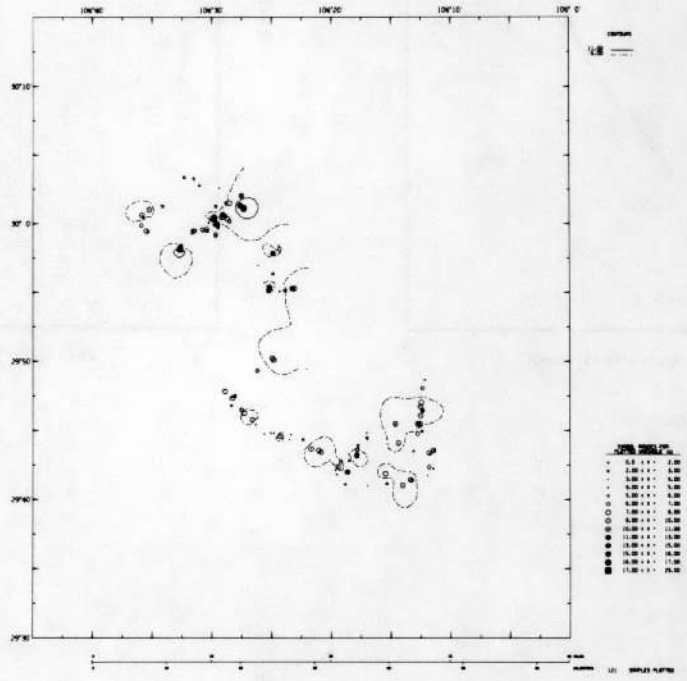

Figure B-4b

GEOCHEMICAL DISTRIBUTION OF THORIUM (PPM)
IN STREAM SEDIMENT OF THE CHINATI MOUNTAINS PROJECT AREA,
TRANS-PECOS DETAILED GEOCHEMICAL SURVEY, TEXAS

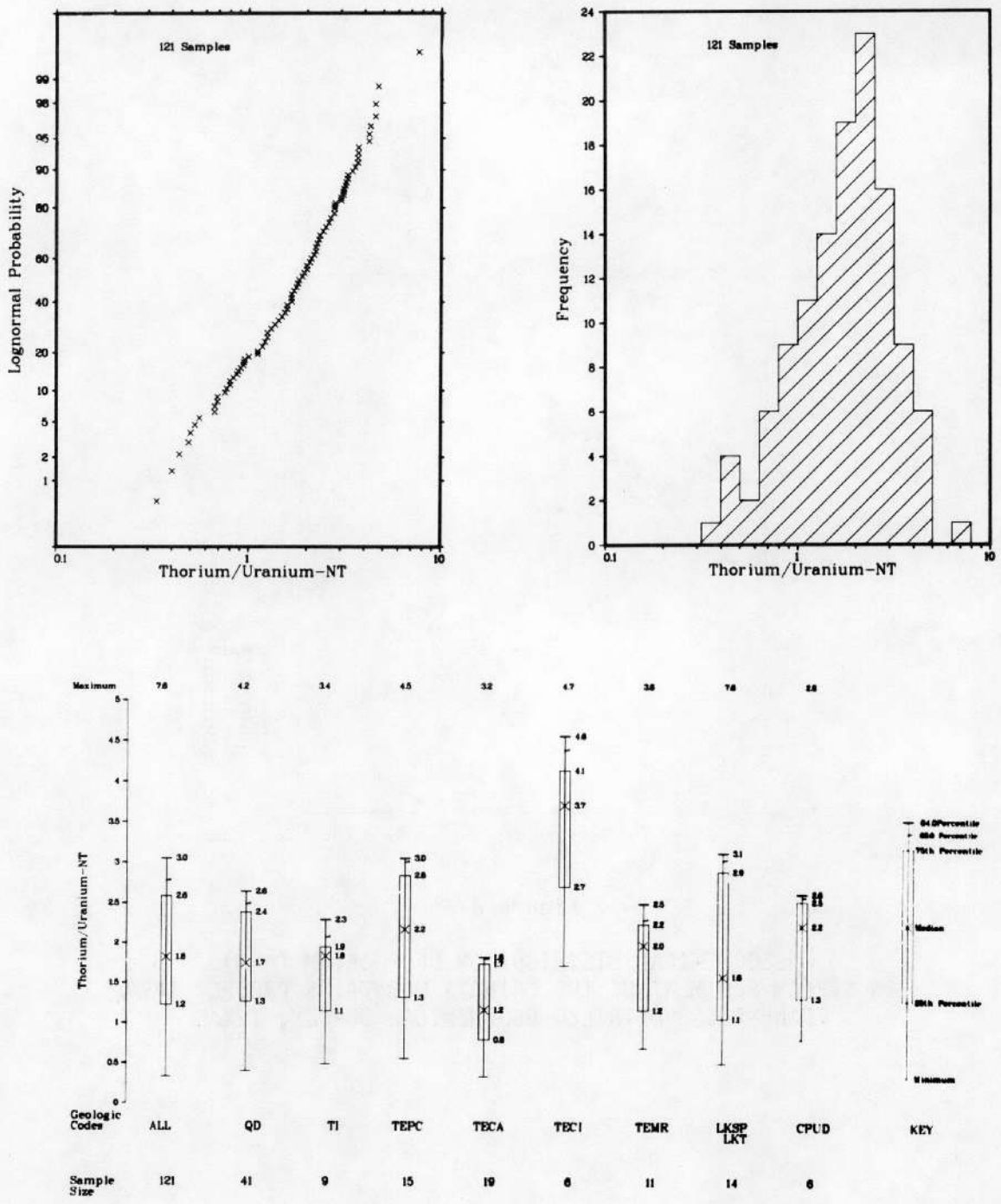

Figure B-5a

PROBABILITY, FREQUENCY, AND PERCENTILE PLOTS FOR THORIUM/URANIUM NEUTRON ACTIVATION IN STREAM SEDIMENT OF THE CHINATI MOUNTAINS PROJECT AREA, TRANS-PECOS DETAILED GEOCHEMICAL SURVEY, TEXAS

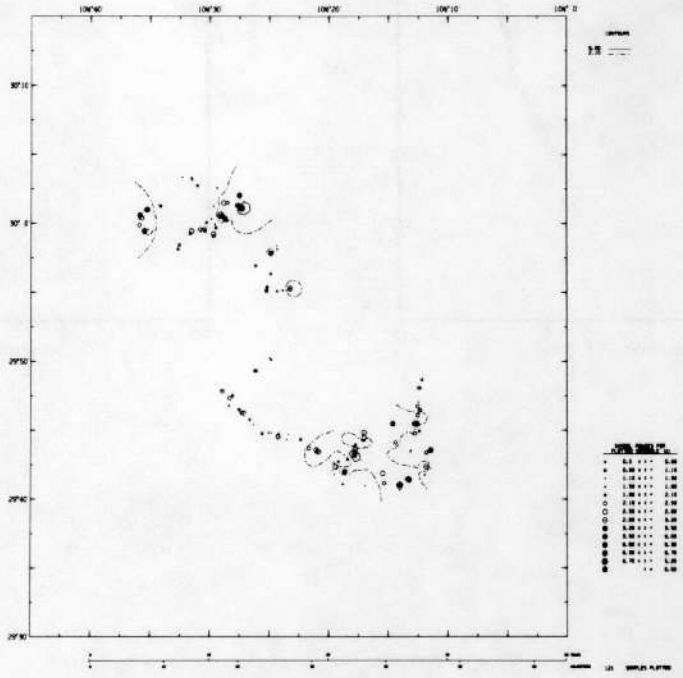

Figure B-5b

GEOCHEMICAL DISTRIBUTION OF THORIUM/URANIUM NEUTRON ACTIVATION IN STREAM SEDIMENT OF THE CHINATI MOUNTAINS PROJECT AREA, TRANS-PECOS DETAILED GEOCHEMICAL SURVEY, TEXAS

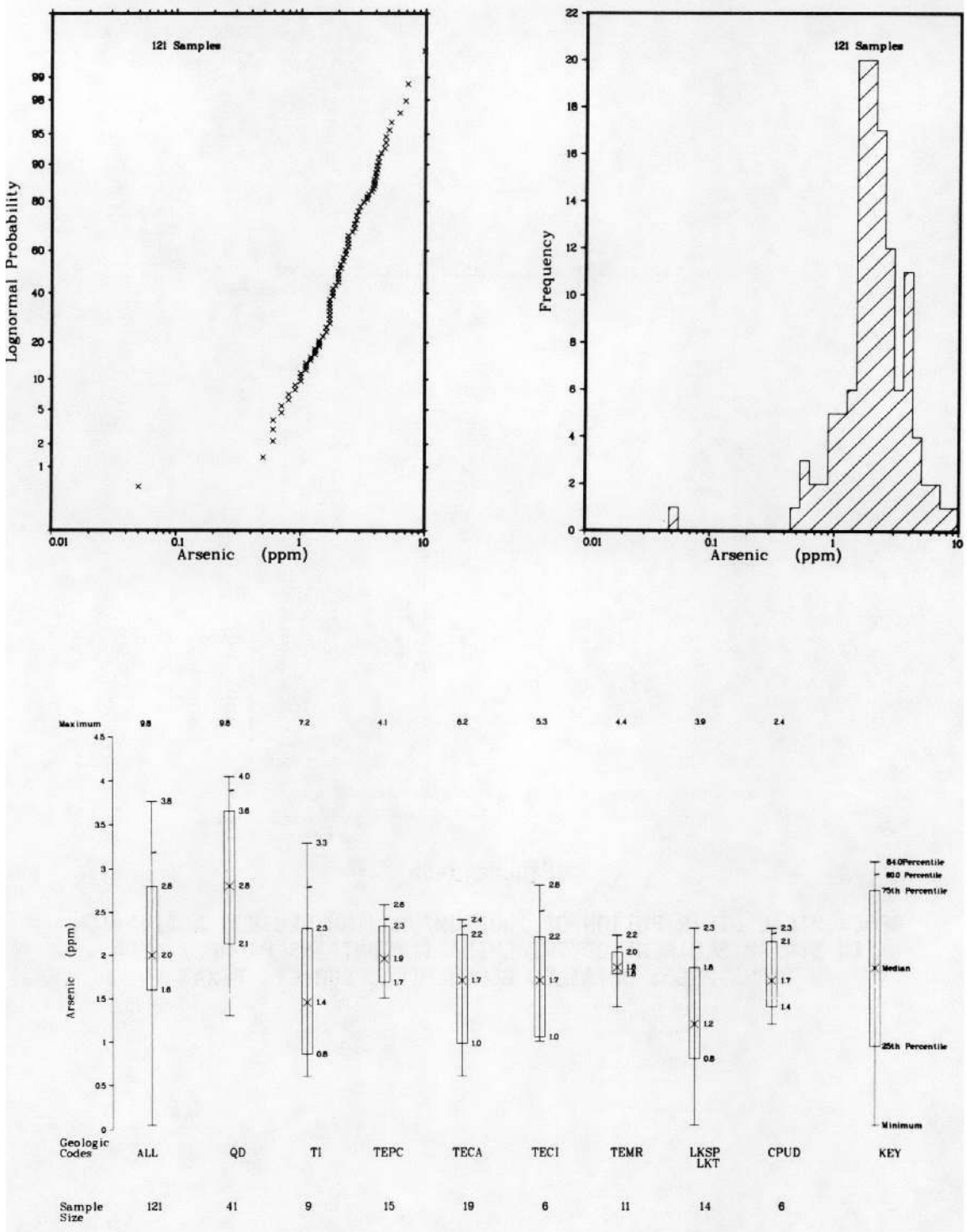

Figure B-6a

PROBABILITY, FREQUENCY, AND PERCENTILE PLOTS FOR ARSENIC (PPM) IN STREAM SEDIMENT OF THE CHINATI MOUNTAINS PROJECT AREA, TRANS-PECOS DETAILED GEOCHEMICAL SURVEY, TEXAS

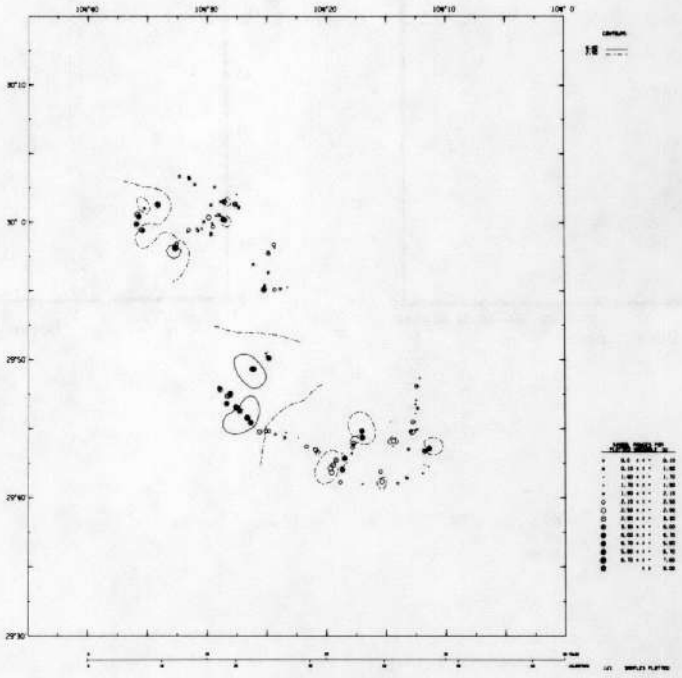

Figure B-6b

GEOCHEMICAL DISTRIBUTION OF ARSENIC (PPM)
IN STREAM SEDIMENT OF THE CHINATI MOUNTAINS PROJECT AREA,
TRANS-PECOS DETAILED GEOCHEMICAL SURVEY, TEXAS

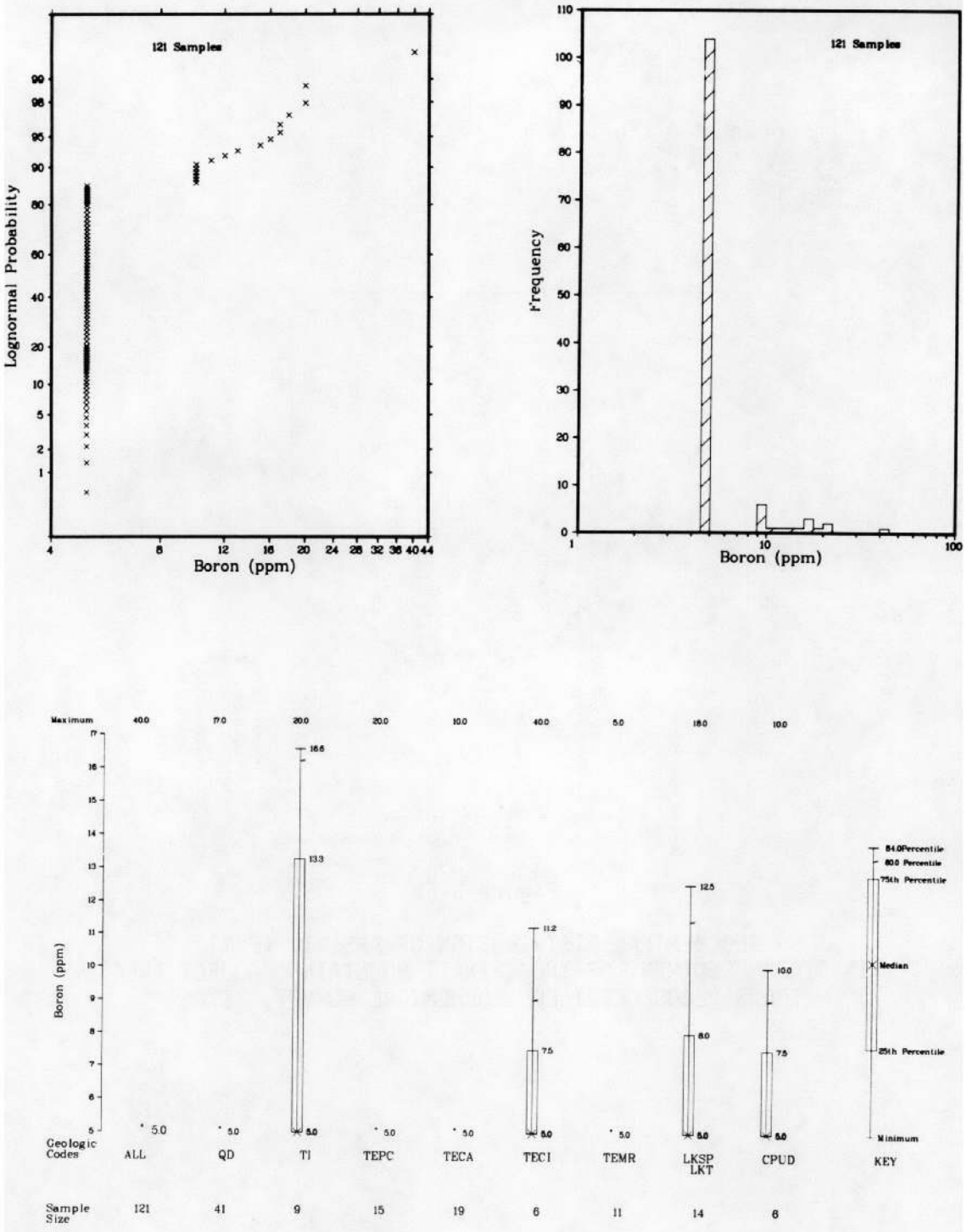

Figure B-7a

PROBABILITY, FREQUENCY, AND PERCENTILE PLOTS FOR BORON (PPM) IN STREAM SEDIMENT OF THE CHINATI MOUNTAINS PROJECT AREA, TRANS-PECOS DETAILED GEOCHEMICAL SURVEY, TEXAS

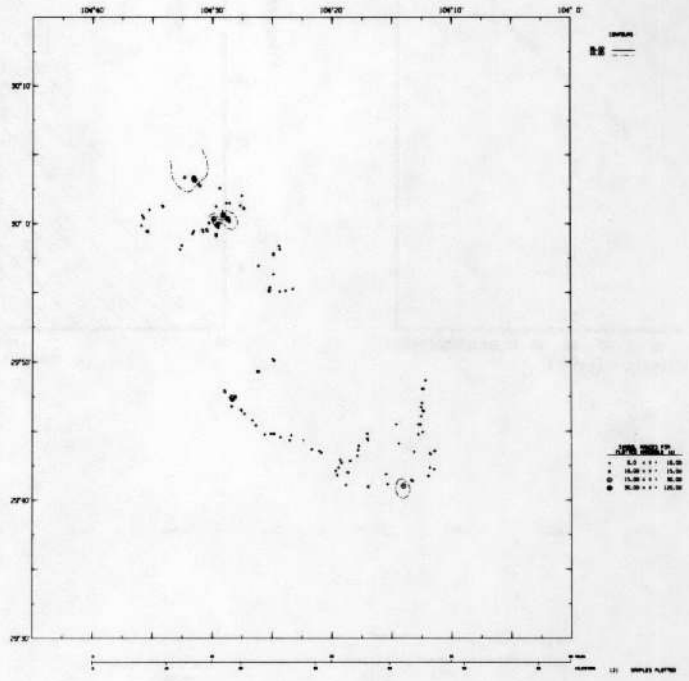

Figure B-7b

GEOCHEMICAL DISTRIBUTION OF BORON (PPM)
IN STREAM SEDIMENT OF THE CHINATI MOUNTAINS PROJECT AREA,
TRANS-PECOS DETAILED GEOCHEMICAL SURVEY, TEXAS

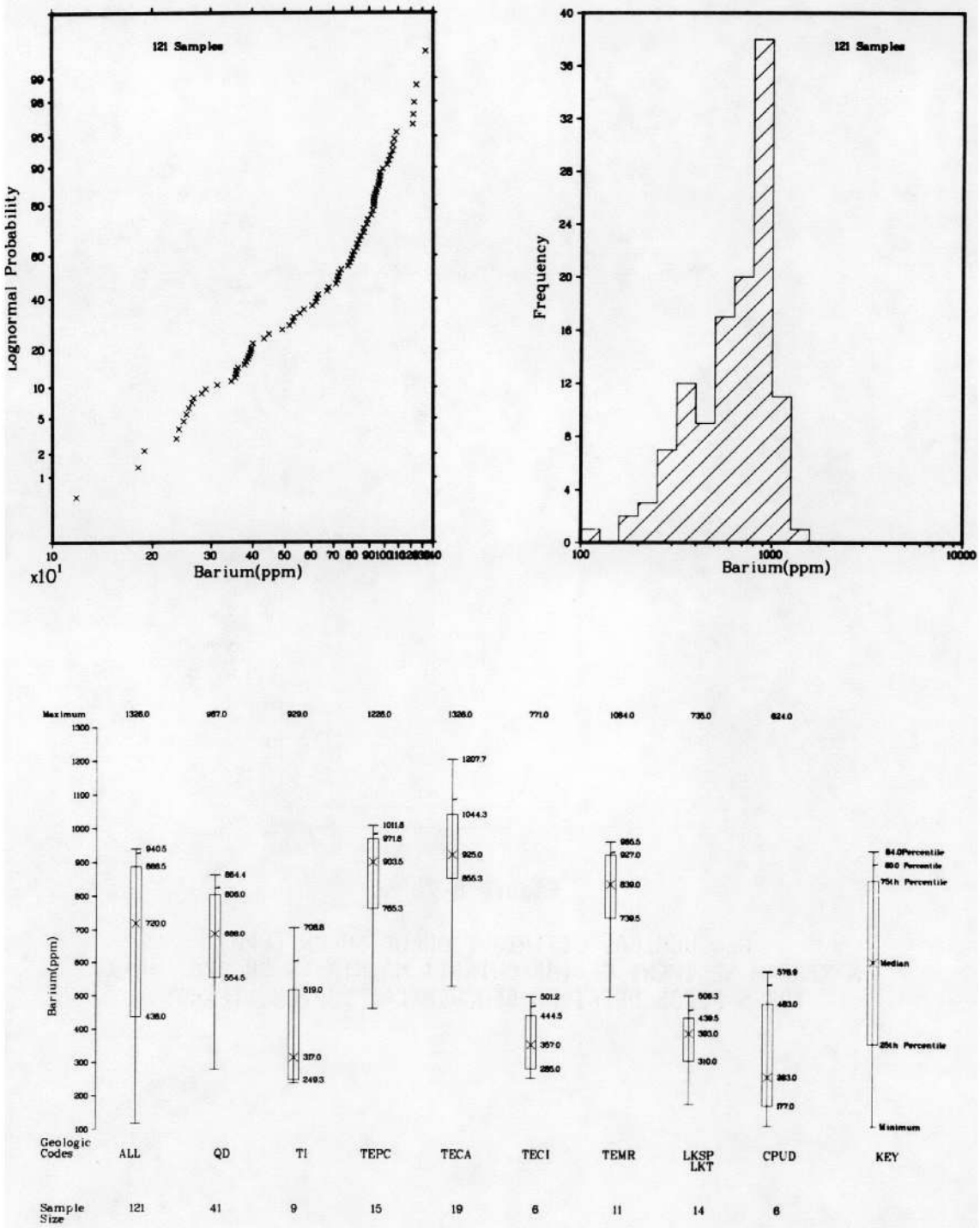

Figure B-8a

PROBABILITY, FREQUENCY, AND PERCENTILE PLOTS FOR BARIUM (PPM) IN STREAM SEDIMENT OF THE CHINATI MOUNTAINS PROJECT AREA, TRANS-PECOS DETAILED GEOCHEMICAL SURVEY, TEXAS

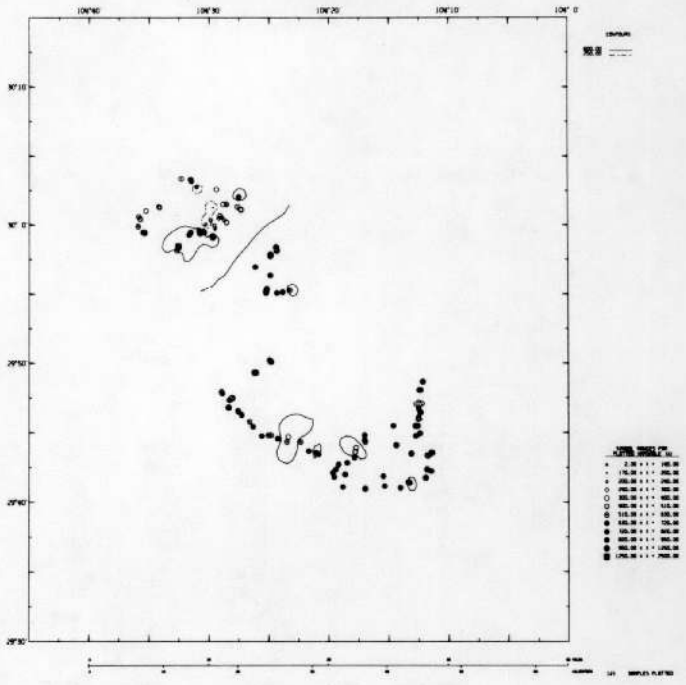

Figure B-8b

GEOCHEMICAL DISTRIBUTION OF BARIUM (PPM)
IN STREAM SEDIMENT OF THE CHINATI MOUNTAINS PROJECT AREA,
TRANS-PECOS DETAILED GEOCHEMICAL SURVEY, TEXAS

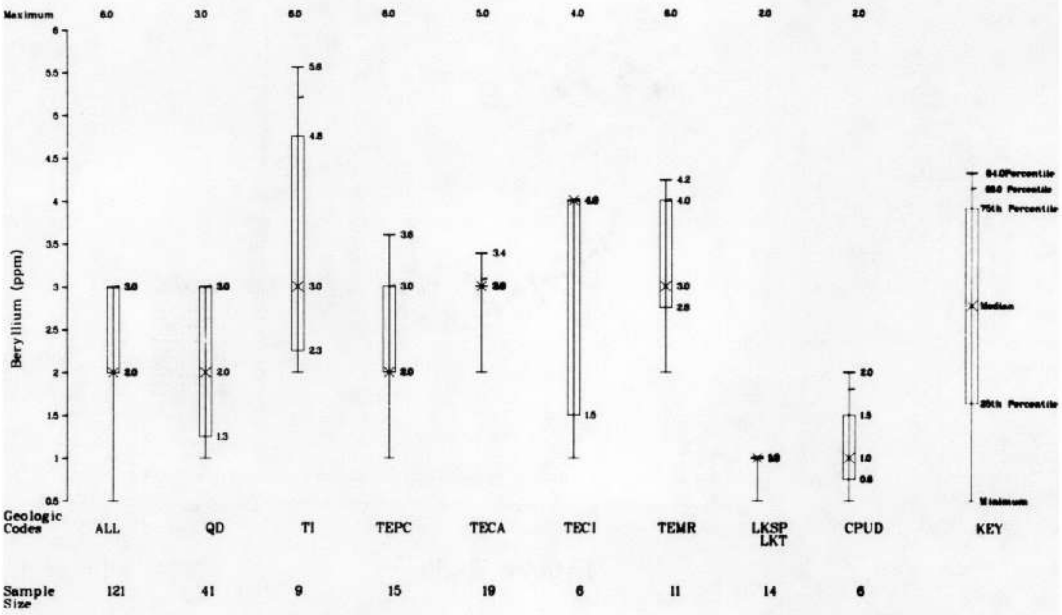

Figure B-9a

PERCENTILE PLOT FOR BERYLLIUM (PPM)
IN STREAM SEDIMENT OF THE CHINATI MOUNTAINS PROJECT AREA,
TRANS-PECOS DETAILED GEOCHEMICAL SURVEY, TEXAS

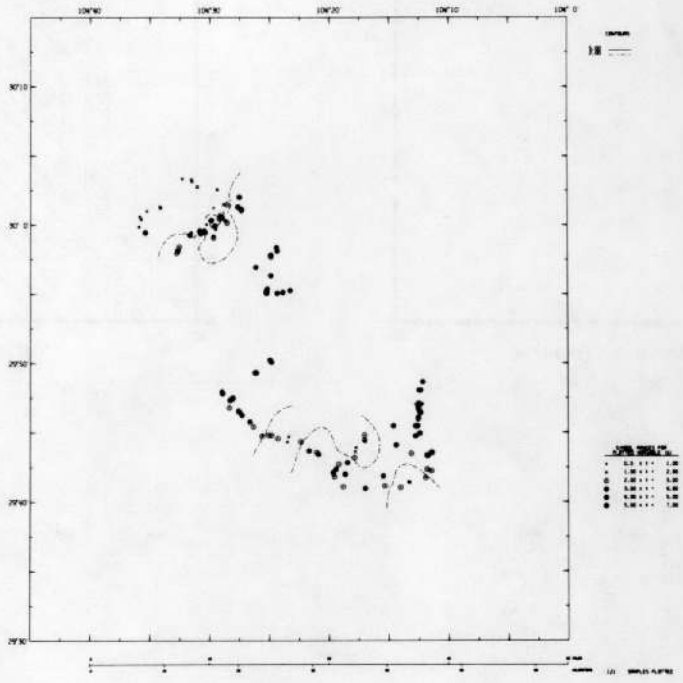

Figure B-9b

GEOCHEMICAL DISTRIBUTION OF BERYLLIUM (PPM)
IN STREAM SEDIMENT OF THE CHINATI MOUNTAINS PROJECT AREA,
TRANS-PECOS DETAILED GEOCHEMICAL SURVEY, TEXAS

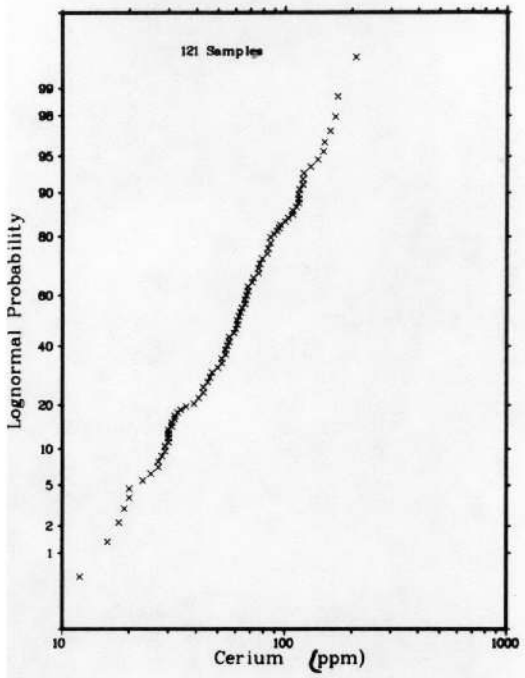

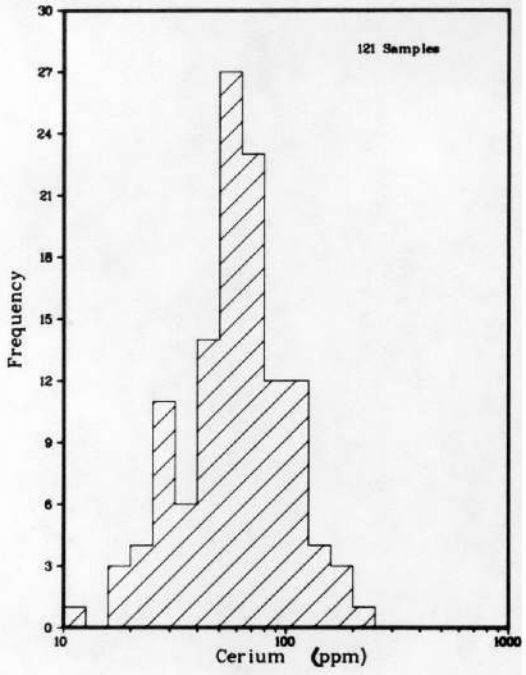

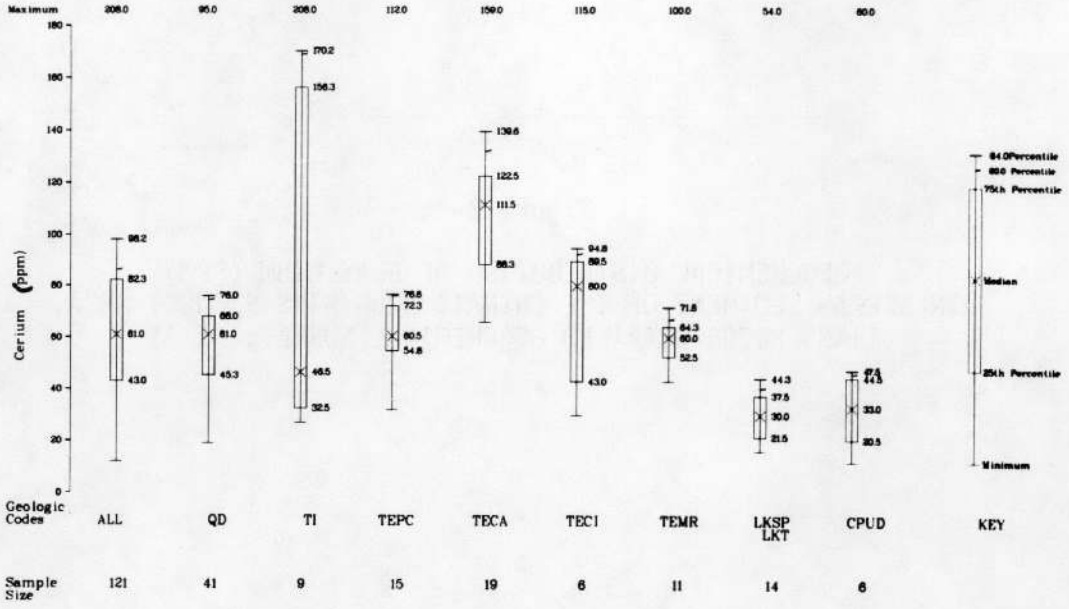

Figure B-10a

PROBABILITY, FREQUENCY, AND PERCENTILE PLOTS FOR CERIUM (PPM) IN STREAM SEDIMENT OF THE CHINATI MOUNTAINS PROJECT AREA, TRANS-PECOS DETAILED GEOCHEMICAL SURVEY, TEXAS

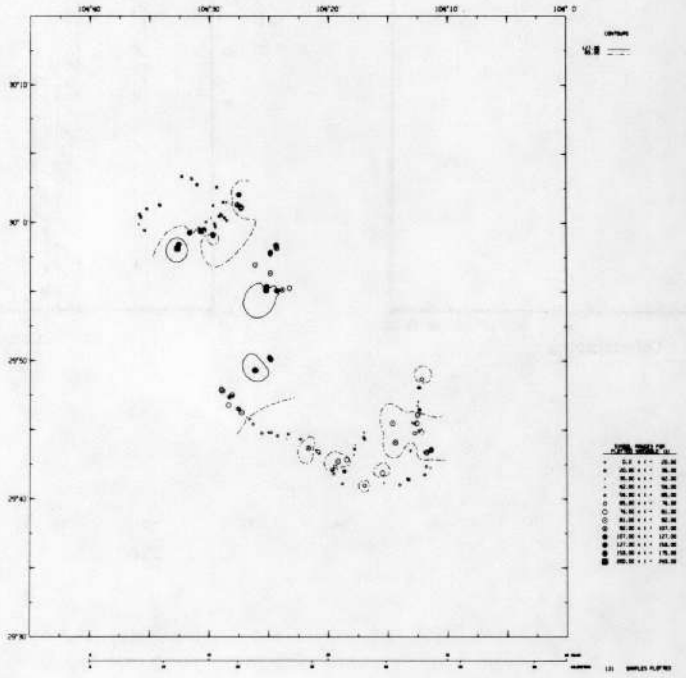

Figure B-10b

GEOCHEMICAL DISTRIBUTION OF CERIUM (PPM)
IN STREAM SEDIMENT OF THE CHINATI MOUNTAINS PROJECT AREA,
TRANS-PECOS DETAILED GEOCHEMICAL SURVEY, TEXAS

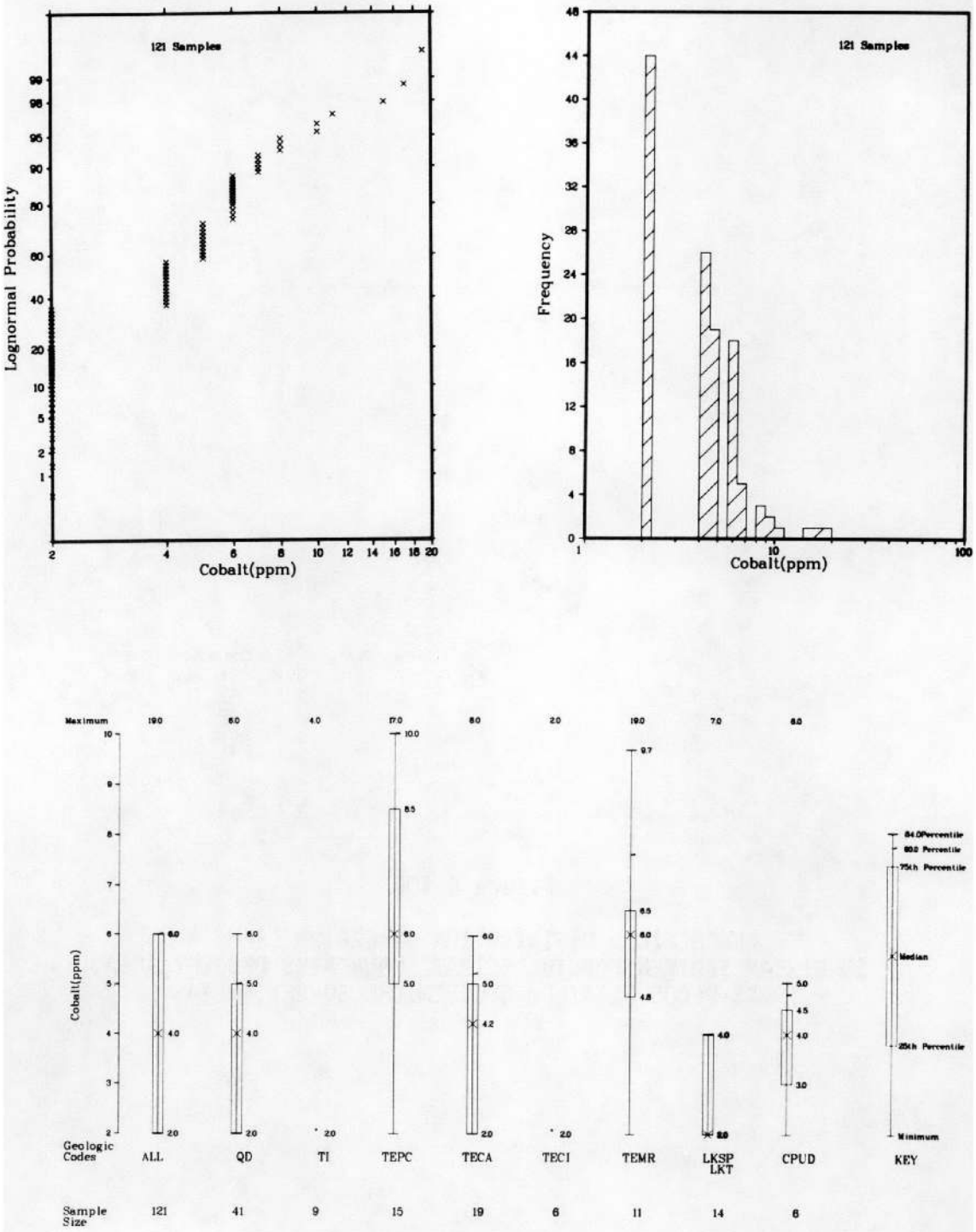

Figure B-11a

PROBABILITY, FREQUENCY, AND PERCENTILE PLOTS FOR COBALT (PPM) IN STREAM SEDIMENT OF THE CHINATI MOUNTAINS PROJECT AREA, TRANS-PECOS DETAILED GEOCHEMICAL SURVEY, TEXAS

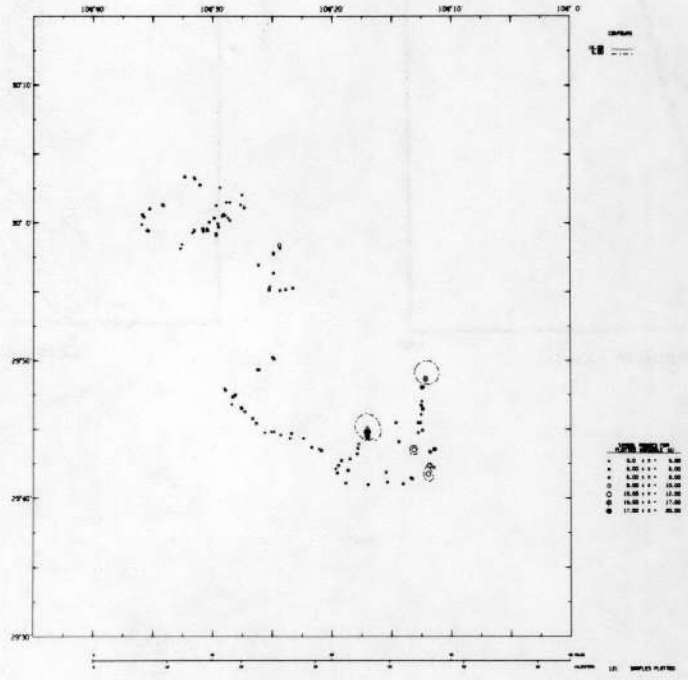

Figure B-11b

GEOCHEMICAL DISTRIBUTION OF COBALT (PPM)
IN STREAM SEDIMENT OF THE CHINATI MOUNTAINS PROJECT AREA,
TRANS-PECOS DETAILED GEOCHEMICAL SURVEY, TEXAS

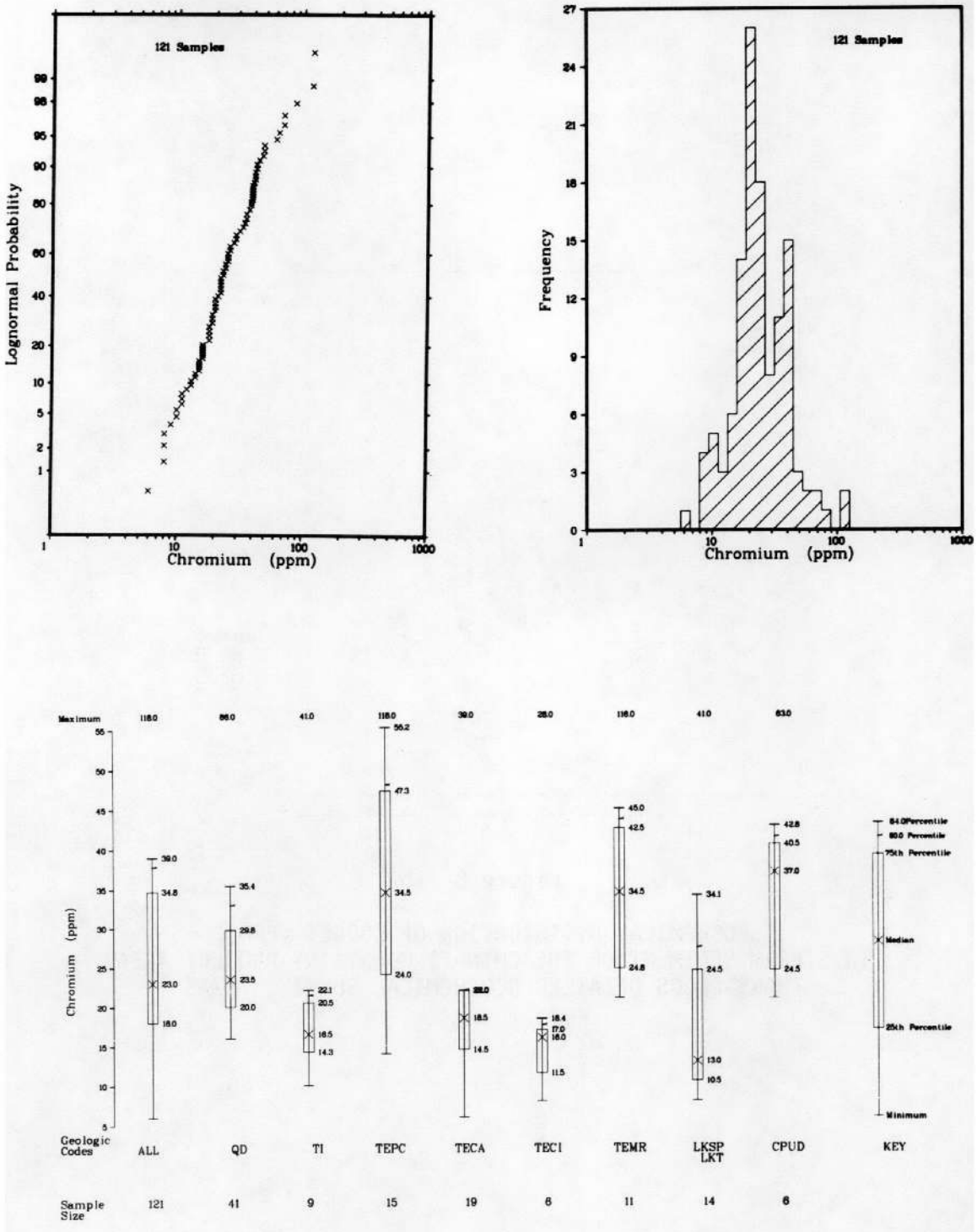

Figure B-12a

PROBABILITY, FREQUENCY, AND PERCENTILE PLOTS FOR CHROMIUM (PPM) IN STREAM SEDIMENT OF THE CHINATI MOUNTAINS PROJECT AREA, TRANS-PECOS DETAILED GEOCHEMICAL SURVEY, TEXAS

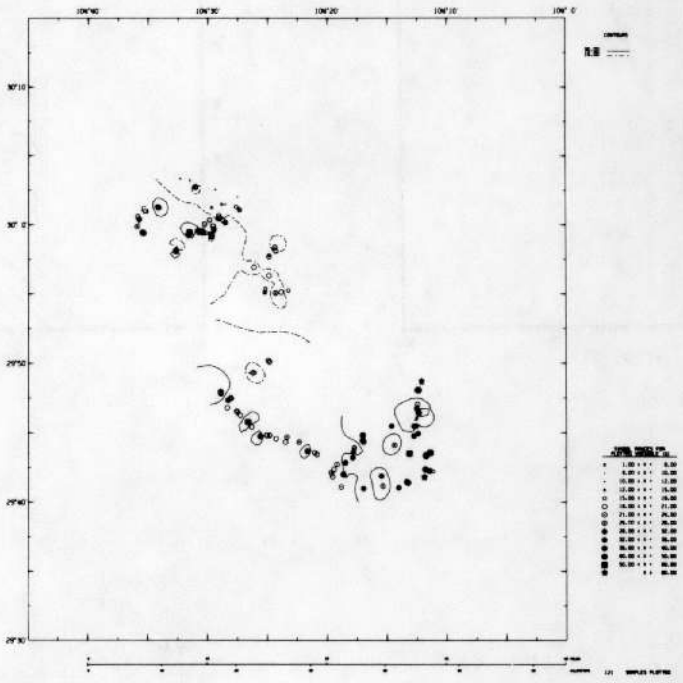

Figure B-12b

GEOCHEMICAL DISTRIBUTION OF CHROMIUM (PPM)
IN STREAM SEDIMENT OF THE CHINATI MOUNTAINS PROJECT AREA,
TRANS-PECOS DETAILED GEOCHEMICAL SURVEY, TEXAS

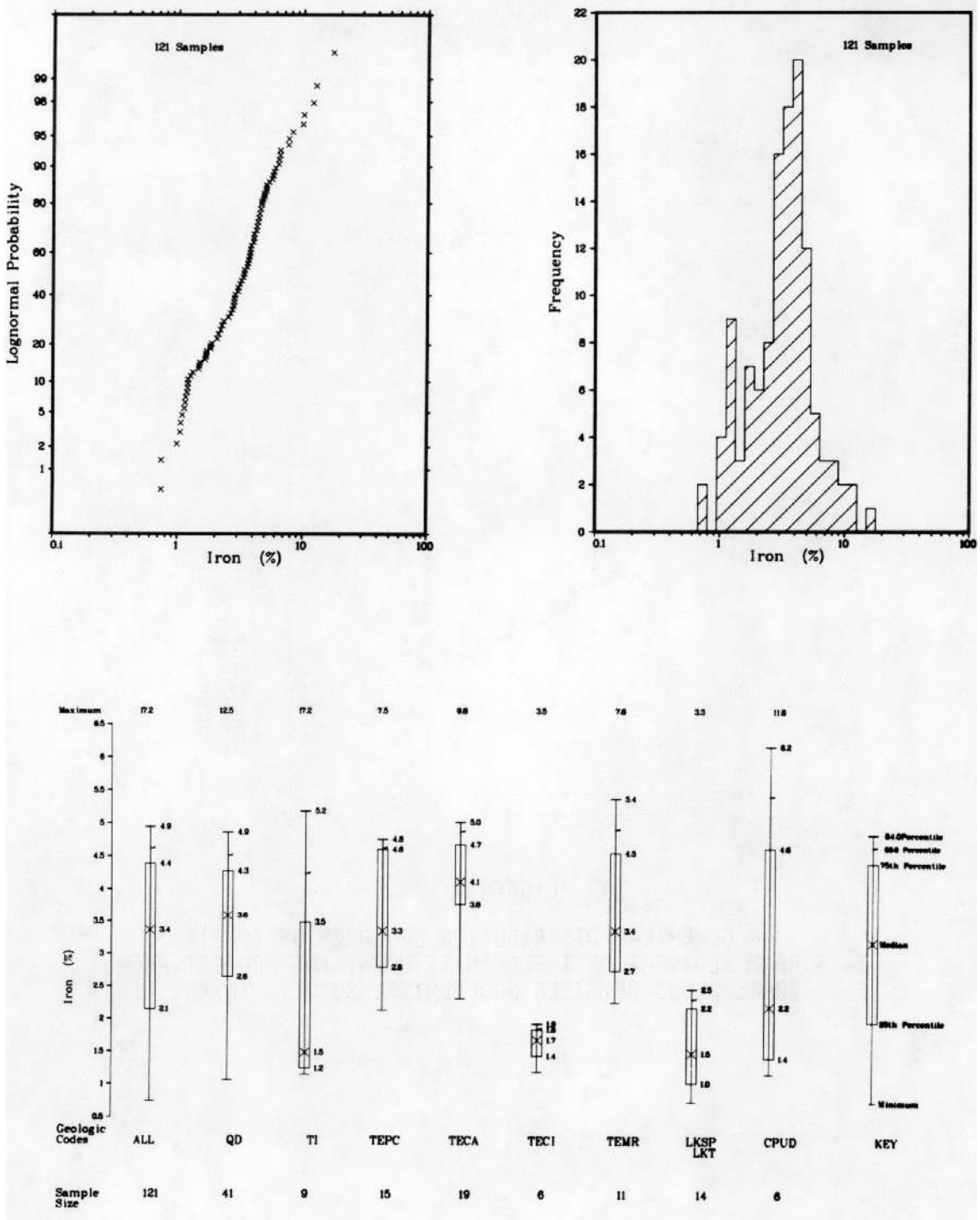

Figure B-13a

PROBABILITY, FREQUENCY, AND PERCENTILE PLOTS FOR IRON (%) IN STREAM SEDIMENT OF THE CHINATI MOUNTAINS PROJECT AREA, TRANS-PECOS DETAILED GEOCHEMICAL SURVEY, TEXAS

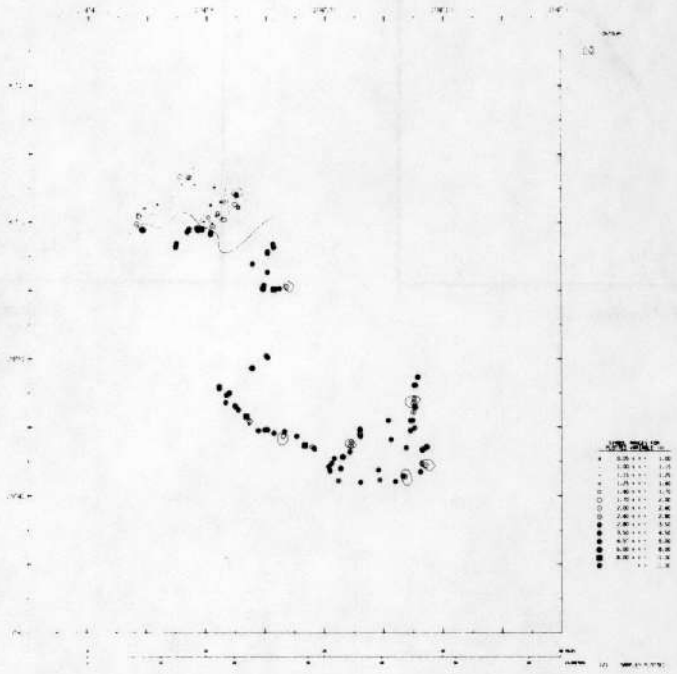

Figure B-13b

GEOCHEMICAL DISTRIBUTION OF IRON (%)
IN STREAM SEDIMENT OF THE CHINATI MOUNTAINS PROJECT AREA,
TRANS-PECOS DETAILED GEOCHEMICAL SURVEY, TEXAS

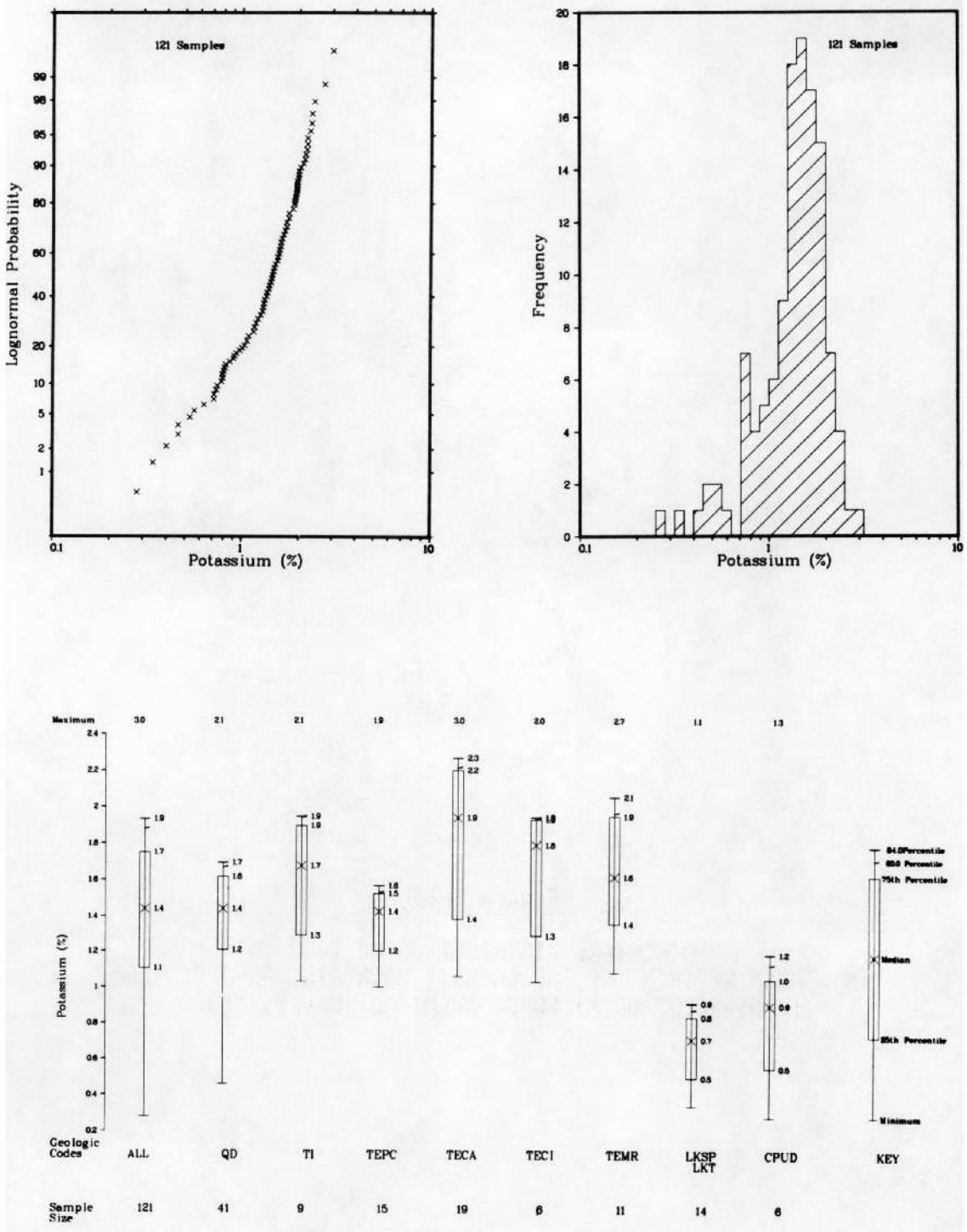

Figure B-14a

PROBABILITY, FREQUENCY, AND PERCENTILE PLOTS FOR POTASSIUM (%) IN STREAM SEDIMENT OF THE CHINATI MOUNTAINS PROJECT AREA, TRANS-PECOS DETAILED GEOCHEMICAL SURVEY, TEXAS

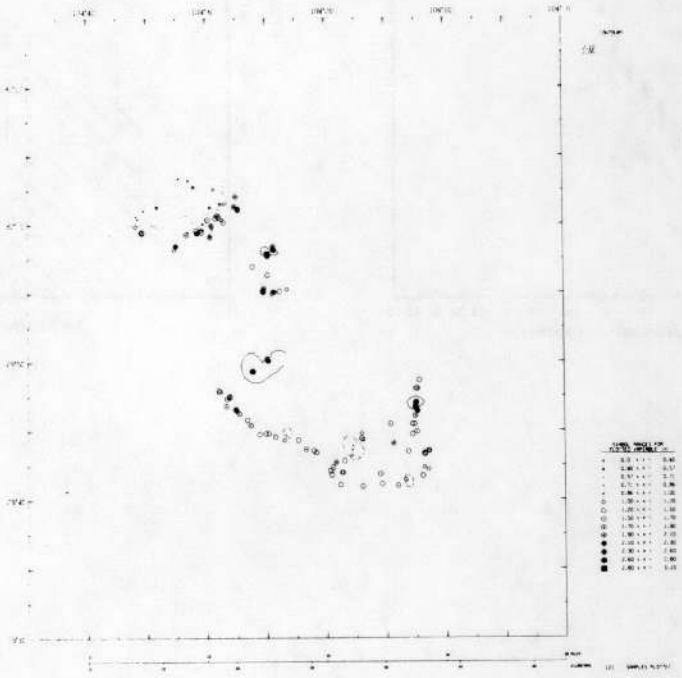

Figure B-14b

GEOCHEMICAL DISTRIBUTION OF POTASSIUM (%)
IN STREAM SEDIMENT OF THE CHINATI MOUNTAINS PROJECT AREA,
TRANS-PECOS DETAILED GEOCHEMICAL SURVEY, TEXAS

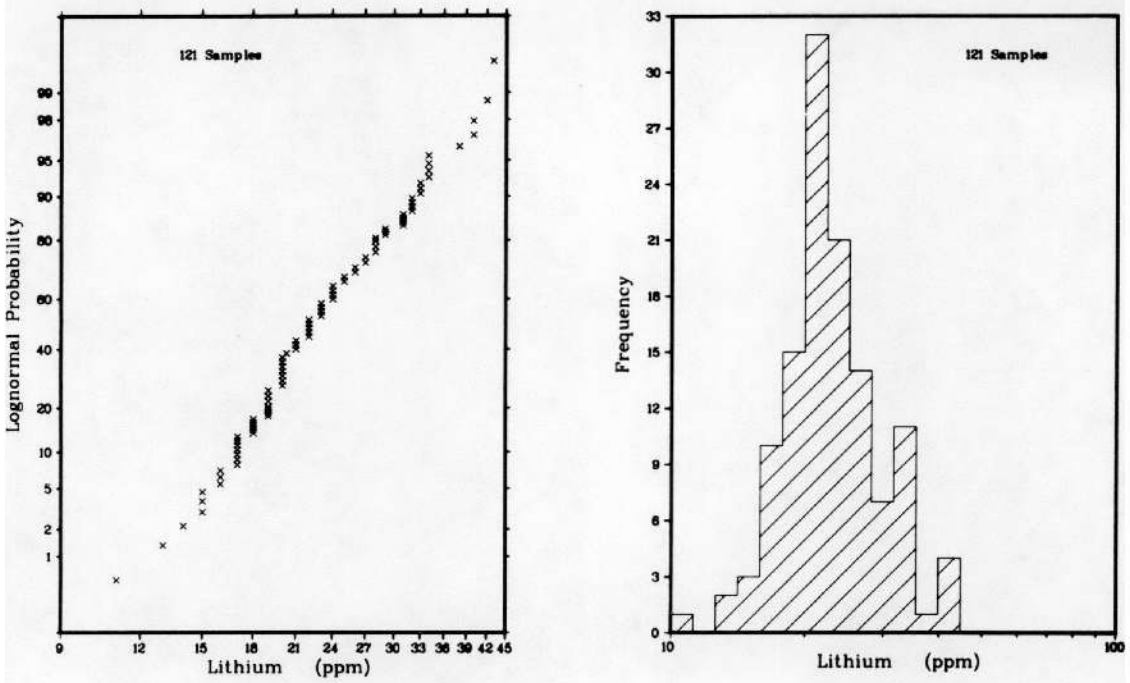

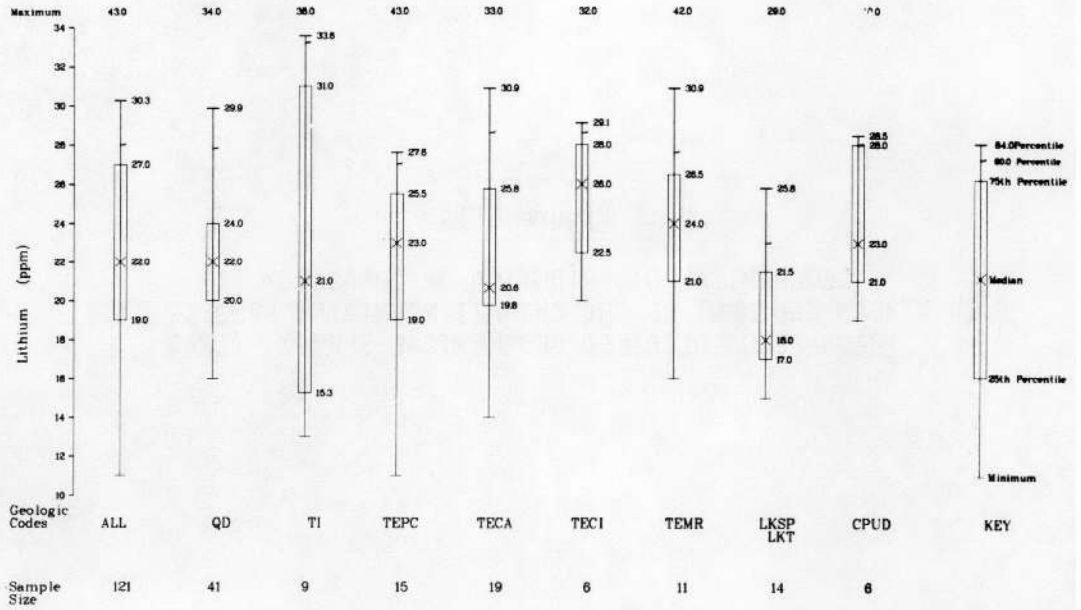

Figure B-15a

PROBABILITY, FREQUENCY, AND PERCENTILE PLOTS FOR LITHIUM (PPM) IN STREAM SEDIMENT OF THE CHINATI MOUNTAINS PROJECT AREA, TRANS-PECOS DETAILED GEOCHEMICAL SURVEY, TEXAS

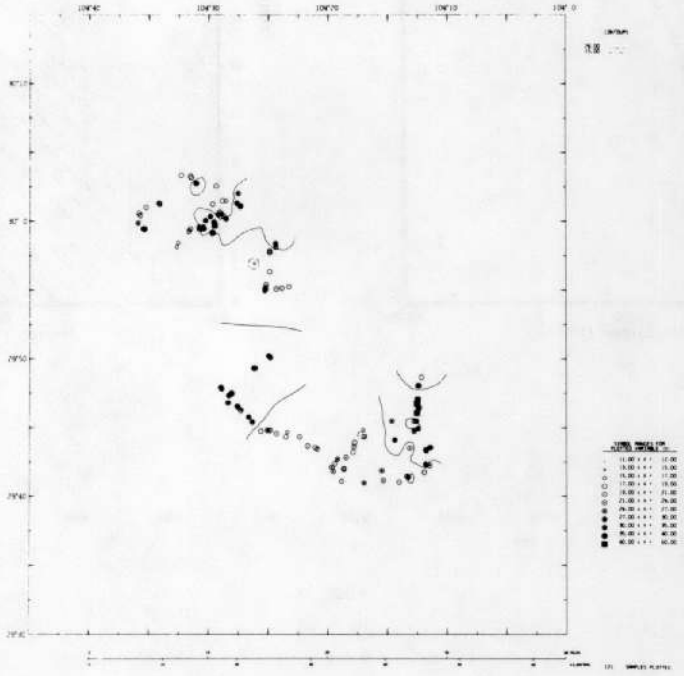

Figure B-15b

GEOCHEMICAL DISTRIBUTION OF LITHIUM (PPM)
IN STREAM SEDIMENT OF THE CHINATI MOUNTAINS PROJECT AREA,
TRANS-PECOS DETAILED GEOCHEMICAL SURVEY, TEXAS

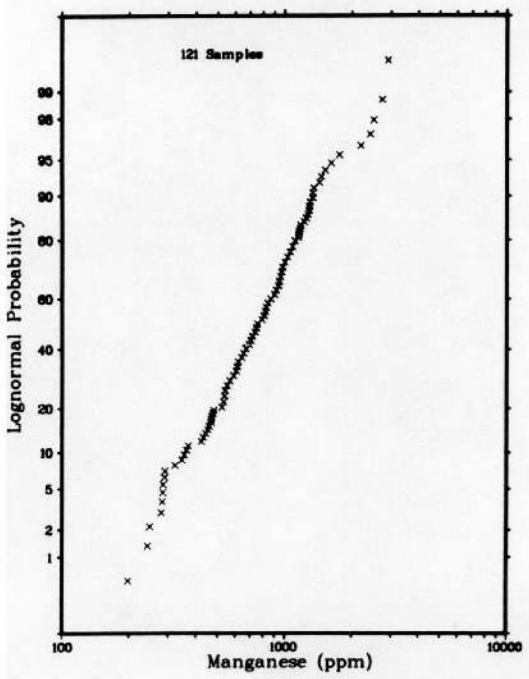

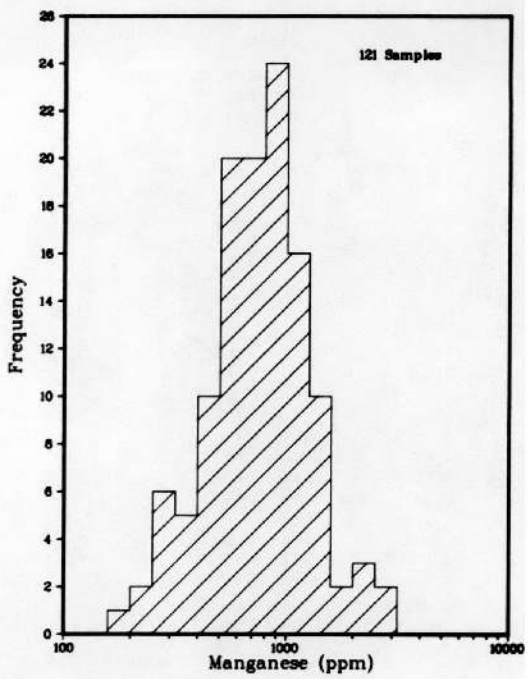

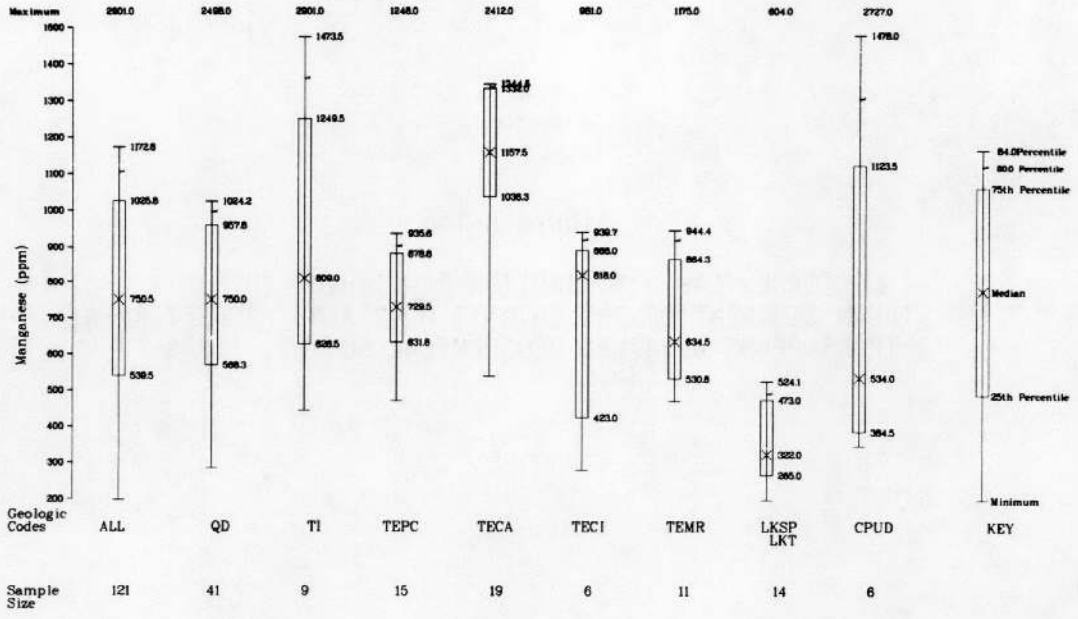

Figure B-16a

PROBABILITY, FREQUENCY, AND PERCENTILE PLOTS FOR MANGANESE (PPM) IN STREAM SEDIMENT OF THE CHINATI MOUNTAINS PROJECT AREA, TRANS-PECOS DETAILED GEOCHEMICAL SURVEY, TEXAS

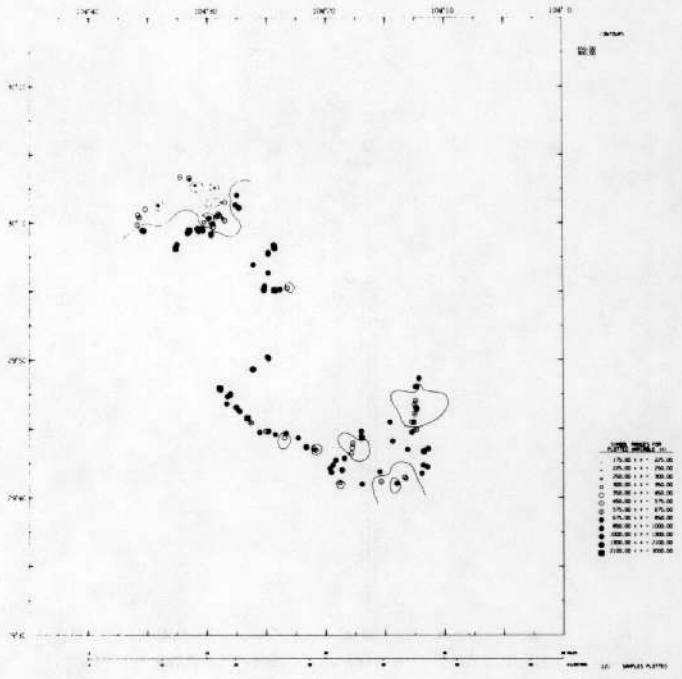

Figure B-16b

GEOCHEMICAL DISTRIBUTION OF MANGANESE (PPM)
IN STREAM SEDIMENT OF THE CHINATI MOUNTAINS PROJECT AREA,
TRANS-PECOS DETAILED GEOCHEMICAL SURVEY, TEXAS

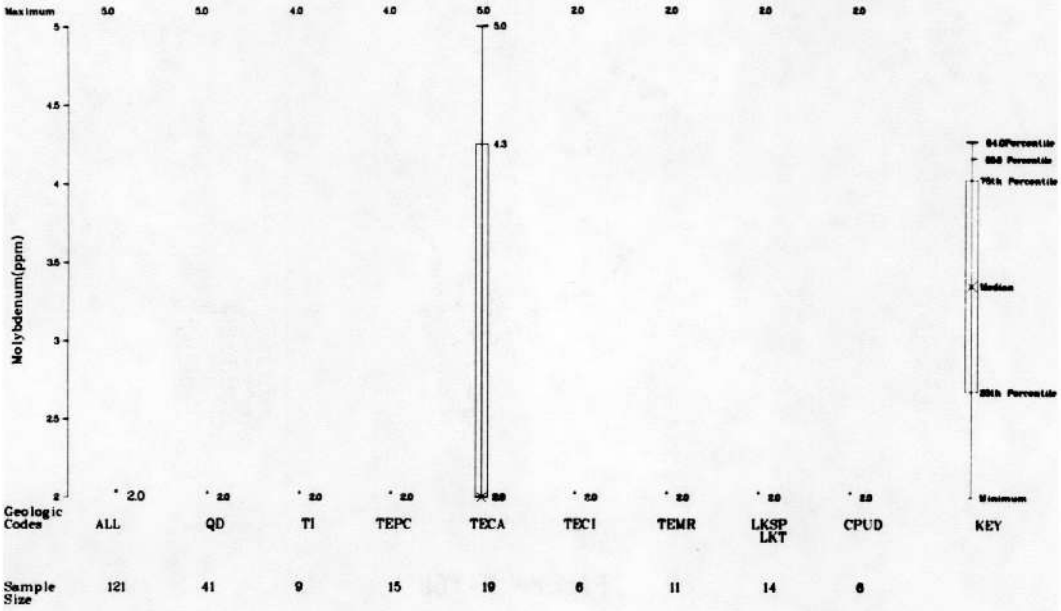

Figure B-17a

PERCENTILE PLOT FOR MOLYBDENUM (PPM)
IN STREAM SEDIMENT OF THE CHINATI MOUNTAINS PROJECT AREA,
TRANS-PECOS DETAILED GEOCHEMICAL SURVEY, TEXAS

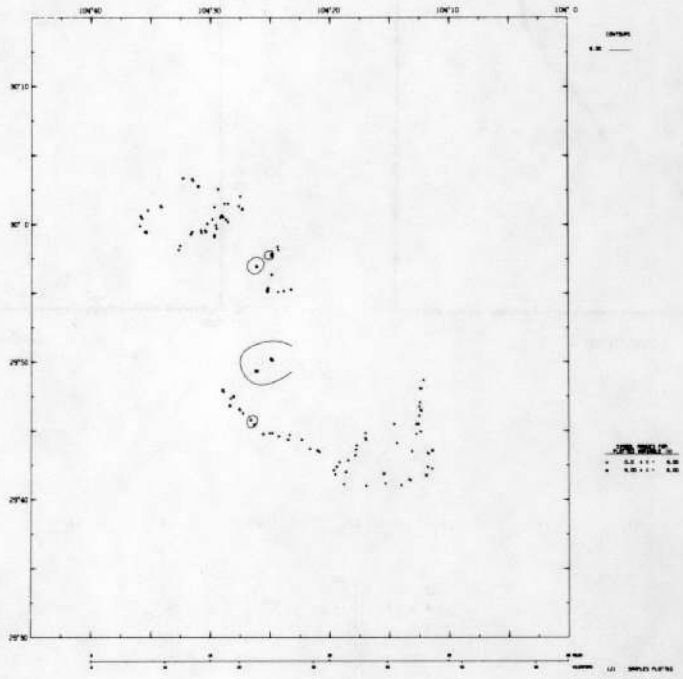

Figure B-17b

GEOCHEMICAL DISTRIBUTION OF MOLYBDENUM (PPM)
IN STREAM SEDIMENT OF THE CHINATI MOUNTAINS PROJECT AREA,
TRANS-PECOS DETAILED GEOCHEMICAL SURVEY, TEXAS

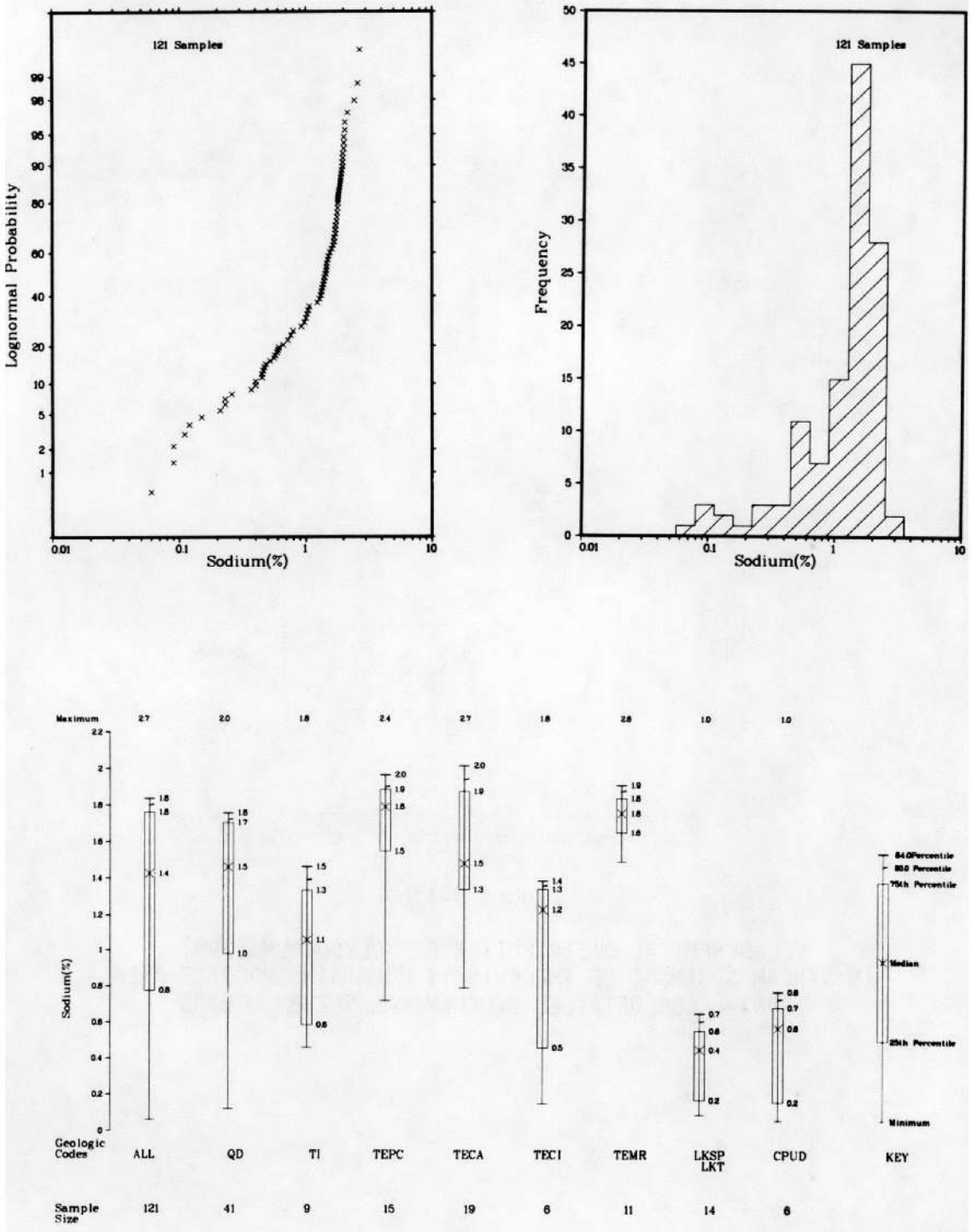

Figure B-18a

PROBABILITY, FREQUENCY, AND PERCENTILE PLOTS FOR SODIUM (%) IN STREAM SEDIMENT OF THE CHINATI MOUNTAINS PROJECT AREA, TRANS-PECOS DETAILED GEOCHEMICAL SURVEY, TEXAS

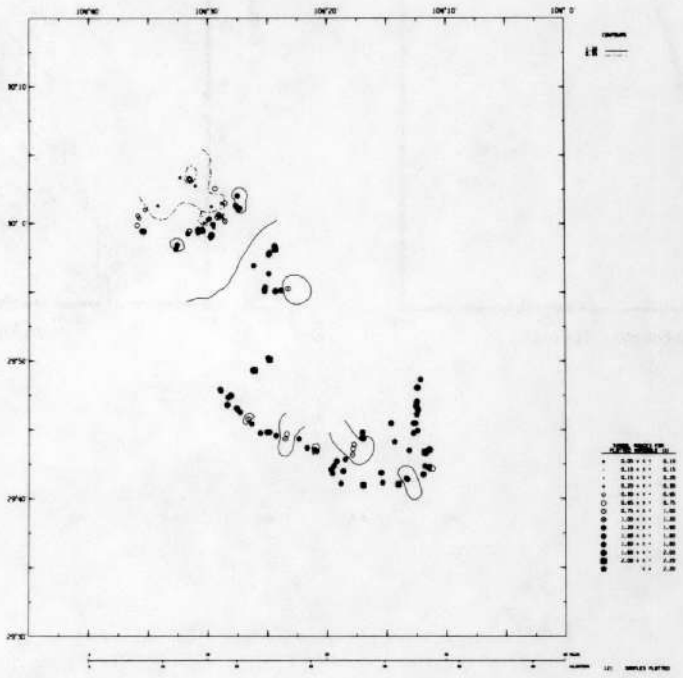

Figure B-18b

GEOCHEMICAL DISTRIBUTION OF SODIUM (%)
IN STREAM SEDIMENT OF THE CHINATI MOUNTAINS PROJECT AREA,
TRANS-PECOS DETAILED GEOCHEMICAL SURVEY, TEXAS

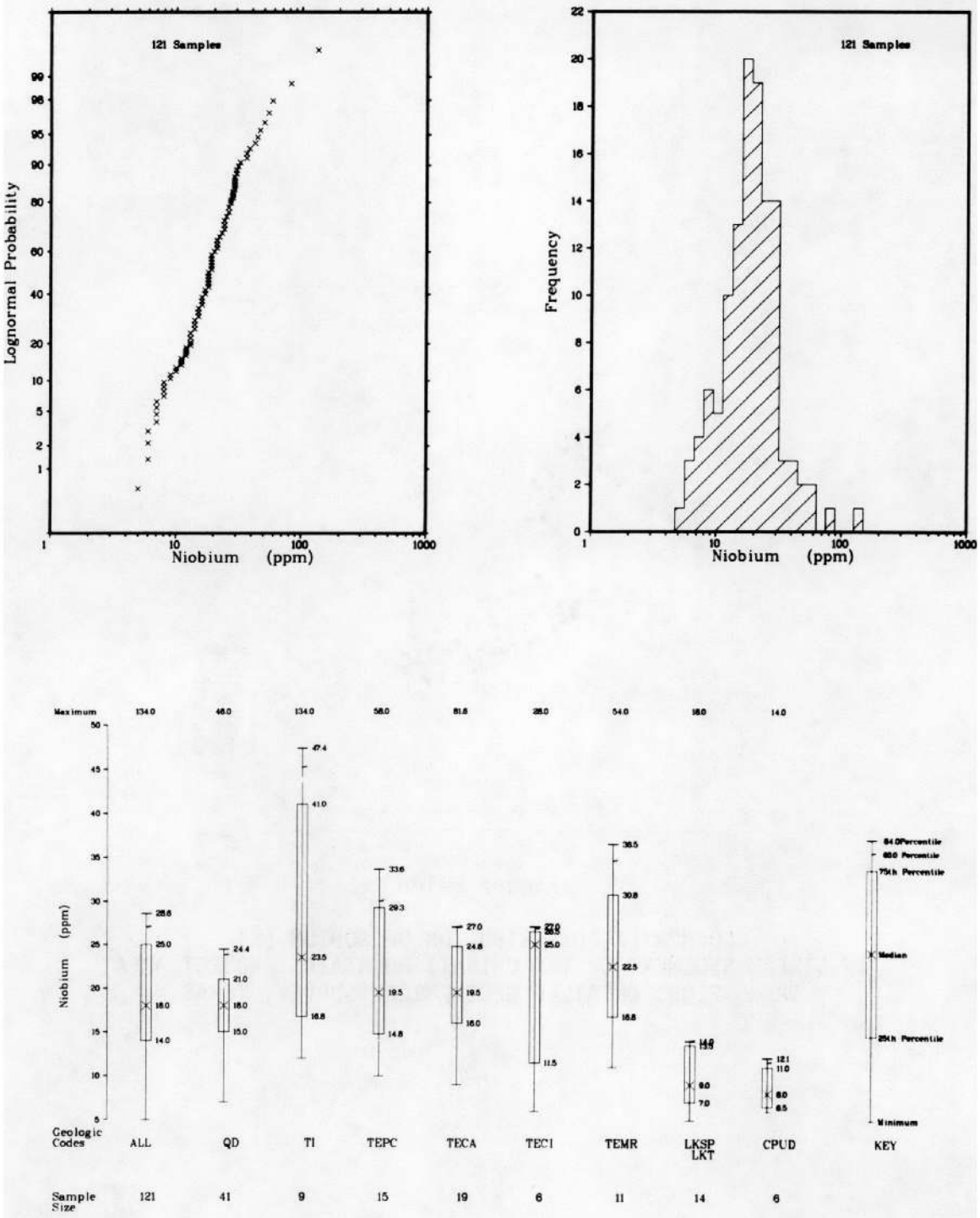

Figure B-19a

PROBABILITY, FREQUENCY, AND PERCENTILE PLOTS FOR NIOBIUM (PPM) IN STREAM SEDIMENT OF THE CHINATI MOUNTAINS PROJECT AREA, TRANS-PECOS DETAILED GEOCHEMICAL SURVEY, TEXAS

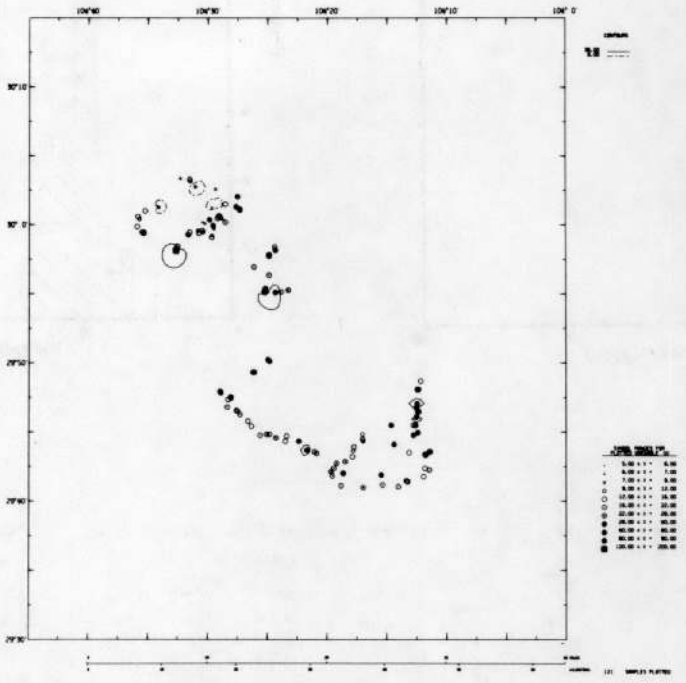

Figure B-19b

GEOCHEMICAL DISTRIBUTION OF NIOBIUM (PPM)
IN STREAM SEDIMENT OF THE CHINATI MOUNTAINS PROJECT AREA,
TRANS-PECOS DETAILED GEOCHEMICAL SURVEY, TEXAS

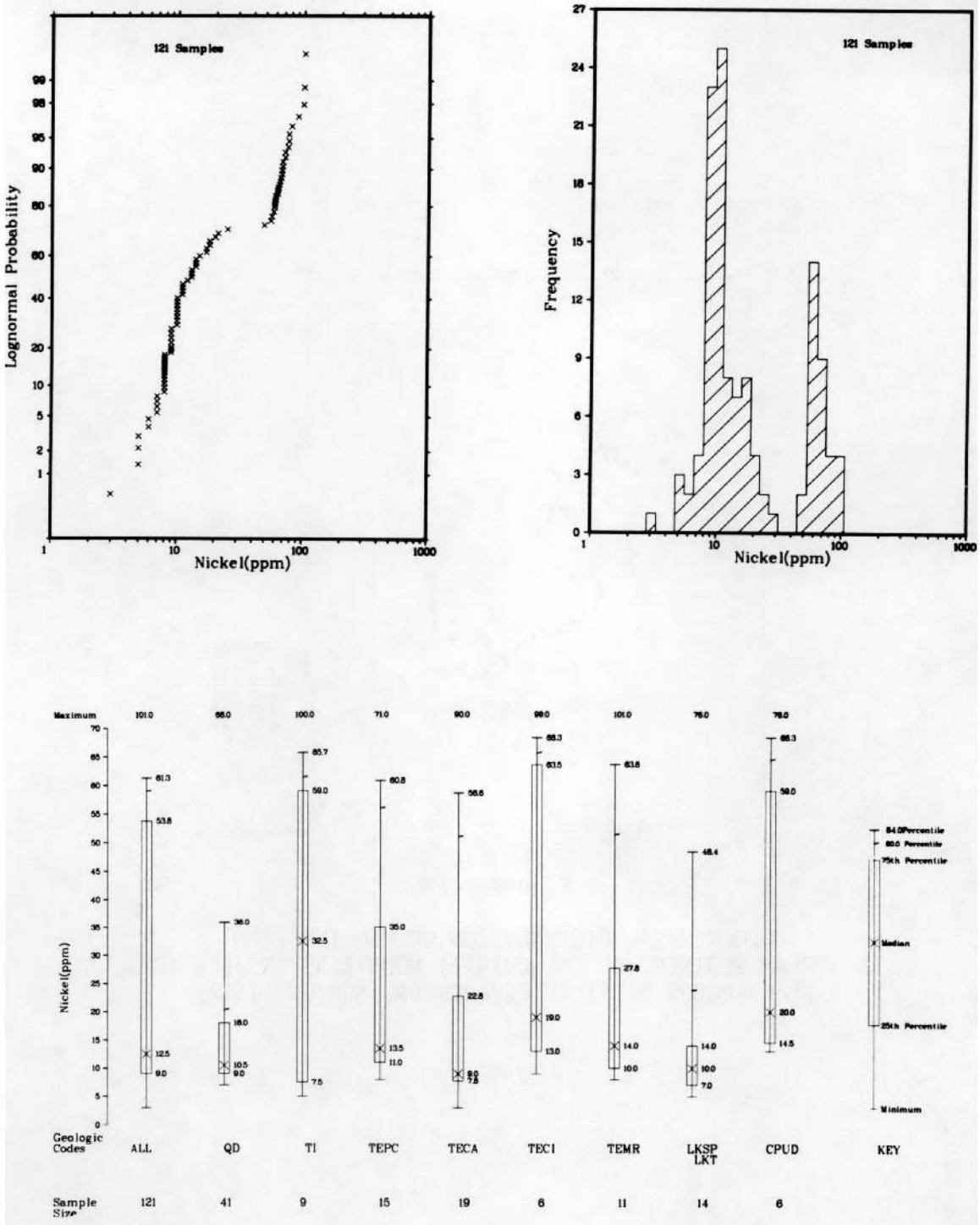

Figure B-20a

PROBABILITY, FREQUENCY, AND PERCENTILE PLOTS FOR NICKEL (PPM) IN STREAM SEDIMENT OF THE CHINATI MOUNTAINS PROJECT AREA, TRANS-PECOS DETAILED GEOCHEMICAL SURVEY, TEXAS

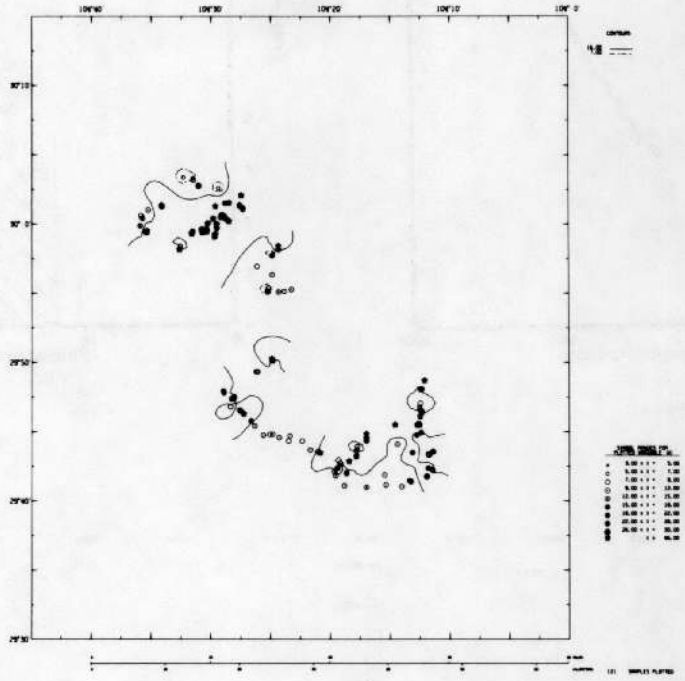

Figure B-20b

GEOCHEMICAL DISTRIBUTION OF NICKEL (PPM)
IN STREAM SEDIMENT OF THE CHINATI MOUNTAINS PROJECT AREA,
TRANS-PECOS DETAILED GEOCHEMICAL SURVEY, TEXAS

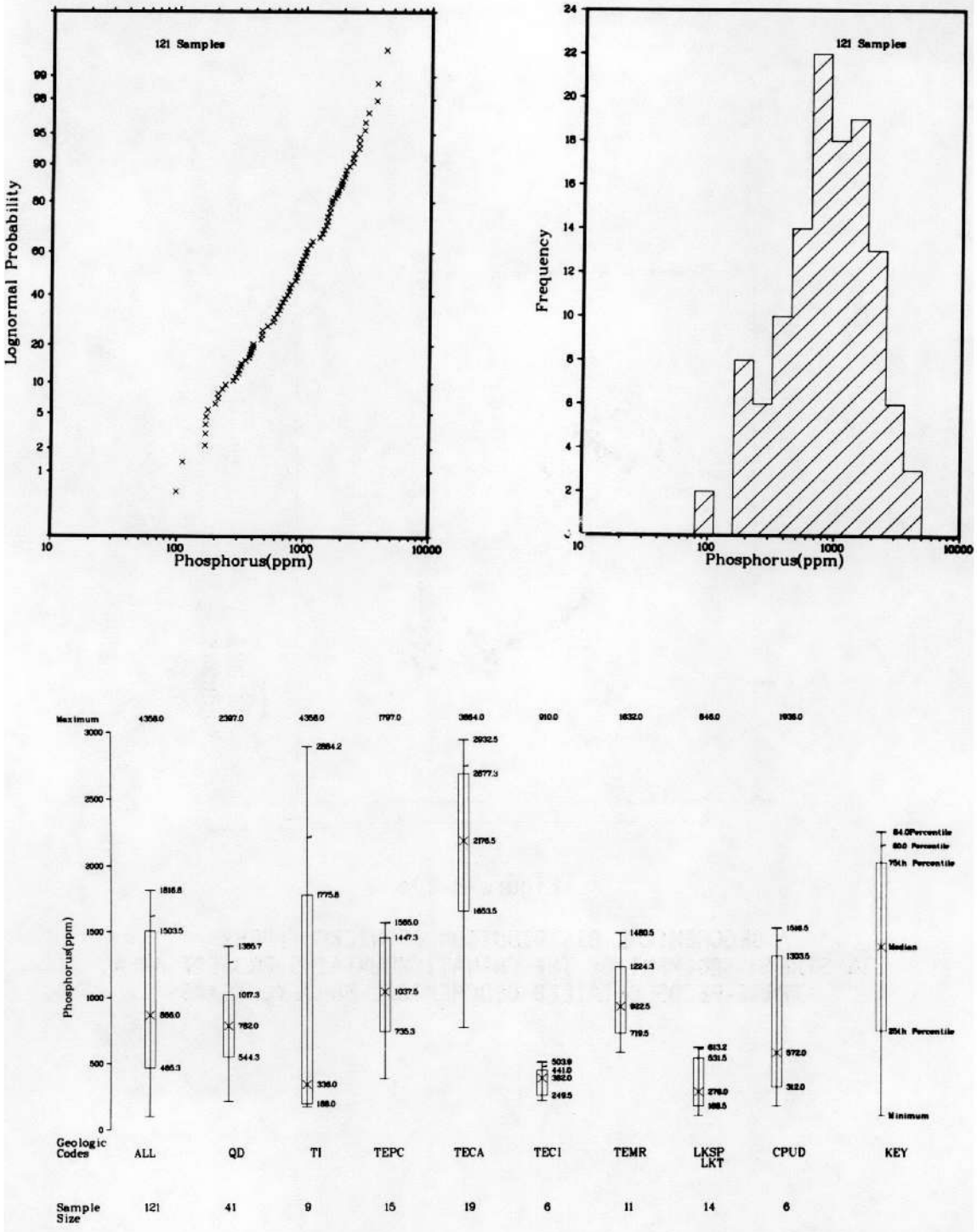

Figure B-21a

PROBABILITY, FREQUENCY, AND PERCENTILE PLOTS FOR PHOSPHORUS (PPM) IN STREAM SEDIMENT OF THE CHINATI MOUNTAINS PROJECT AREA, TRANS-PECOS DETAILED GEOCHEMICAL SURVEY, TEXAS

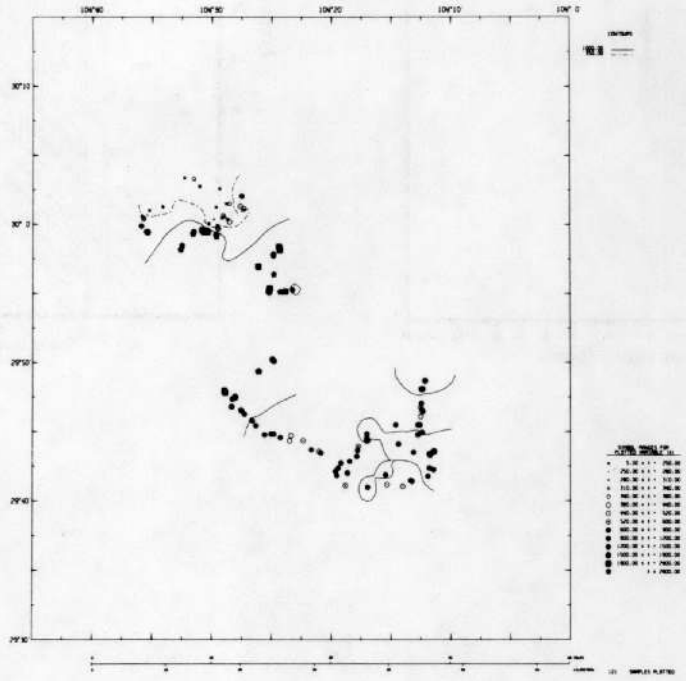

Figure B-21b

GEOCHEMICAL DISTRIBUTION OF PHOSPHORUS (PPM)
IN STREAM SEDIMENT OF THE CHINATI MOUNTAINS PROJECT AREA,
TRANS-PECOS DETAILED GEOCHEMICAL SURVEY, TEXAS

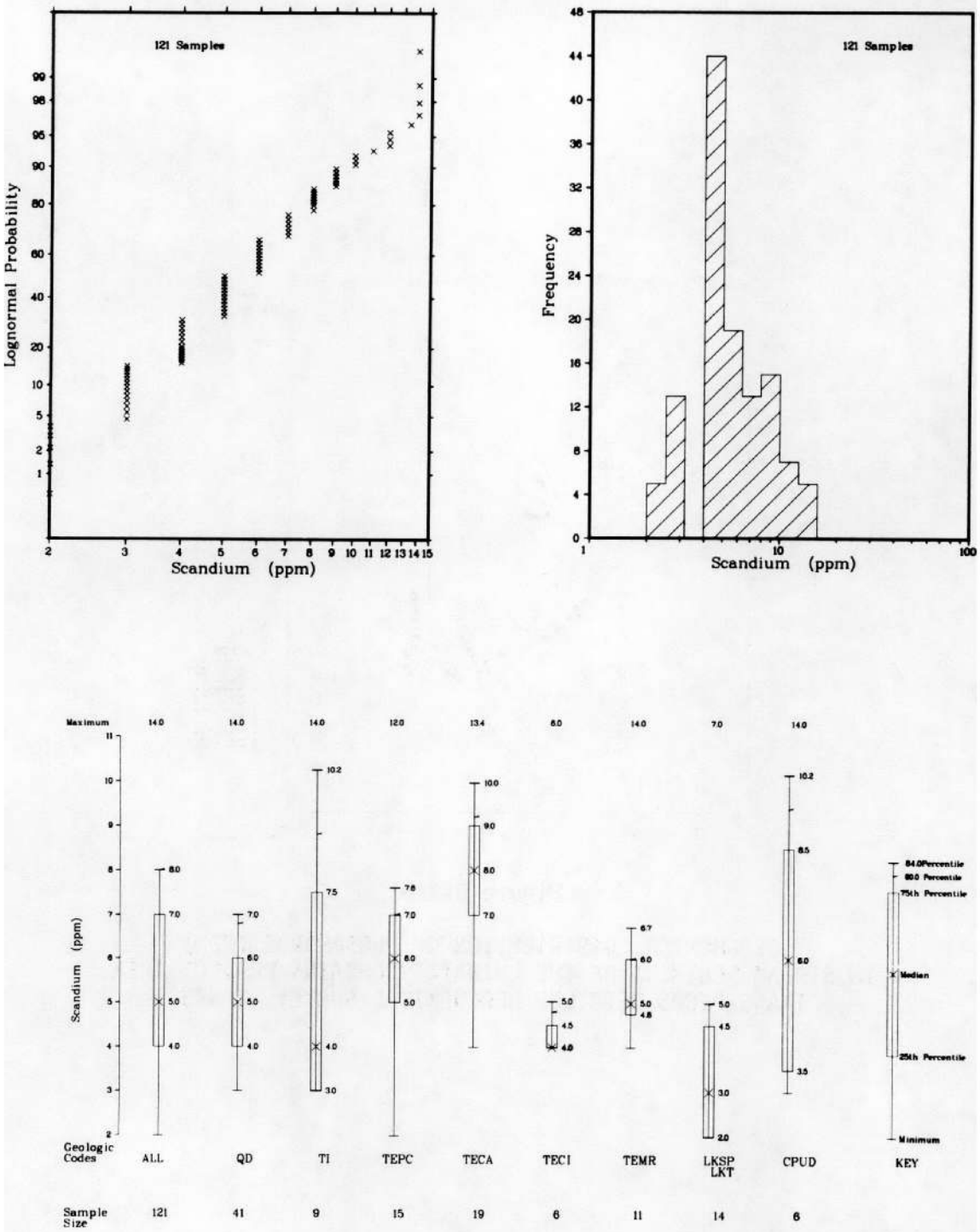

Figure B-22a

PROBABILITY, FREQUENCY, AND PERCENTILE PLOTS FOR SCANDIUM (PPM) IN STREAM SEDIMENT OF THE CHINATI MOUNTAINS PROJECT AREA, TRANS-PECOS DETAILED GEOCHEMICAL SURVEY, TEXAS

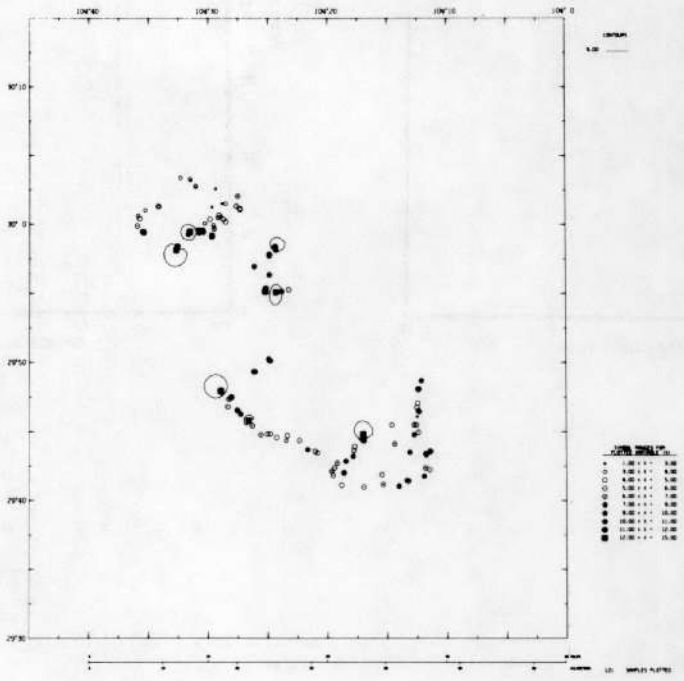

Figure B-22b

GEOCHEMICAL DISTRIBUTION OF SCANDIUM (PPM)
IN STREAM SEDIMENT OF THE CHINATI MOUNTAINS PROJECT AREA,
TRANS-PECOS DETAILED GEOCHEMICAL SURVEY, TEXAS

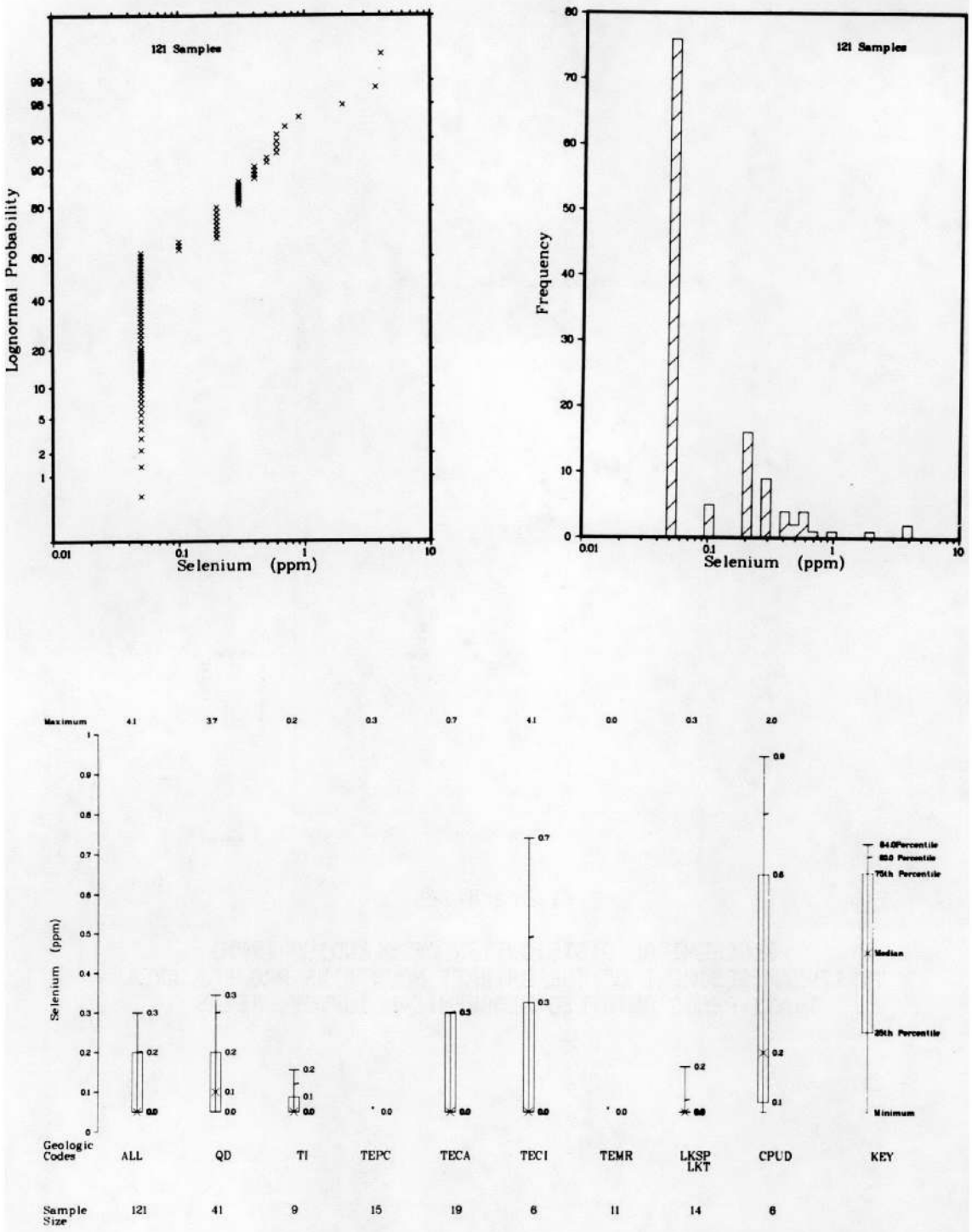

Figure B-23a

PROBABILITY, FREQUENCY, AND PERCENTILE PLOTS FOR SELENIUM (PPM) IN STREAM SEDIMENT OF THE CHINATI MOUNTAINS PROJECT AREA, TRANS-PECOS DETAILED GEOCHEMICAL SURVEY, TEXAS

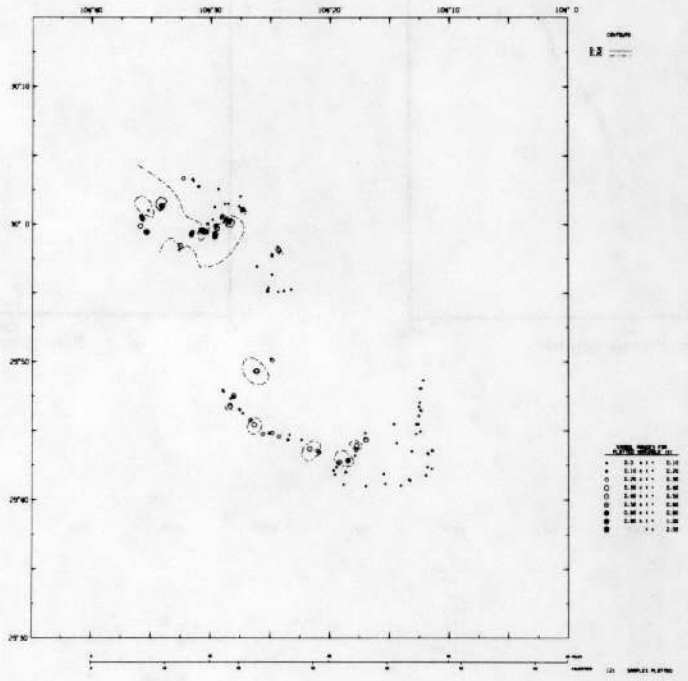

Figure B-23b

GEOCHEMICAL DISTRIBUTION OF SELENIUM (PPM)
IN STREAM SEDIMENT OF THE CHINATI MOUNTAINS PROJECT AREA,
TRANS-PECOS DETAILED GEOCHEMICAL SURVEY, TEXAS

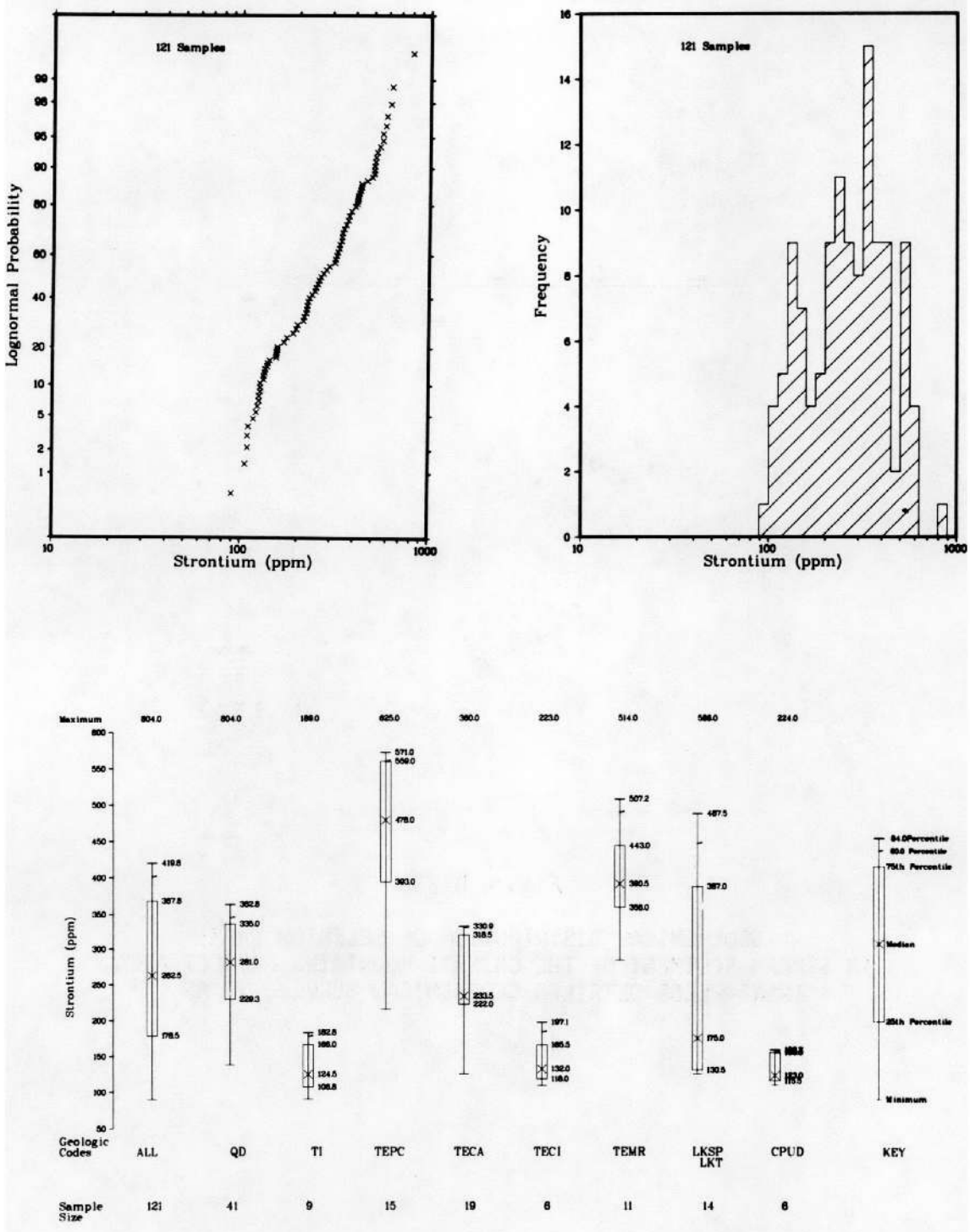

Figure B-24a

PROBABILITY, FREQUENCY, AND PERCENTILE PLOTS FOR STRONTIUM (PPM) IN STREAM SEDIMENT OF THE CHINATI MOUNTAINS PROJECT AREA, TRANS-PECOS DETAILED GEOCHEMICAL SURVEY, TEXAS

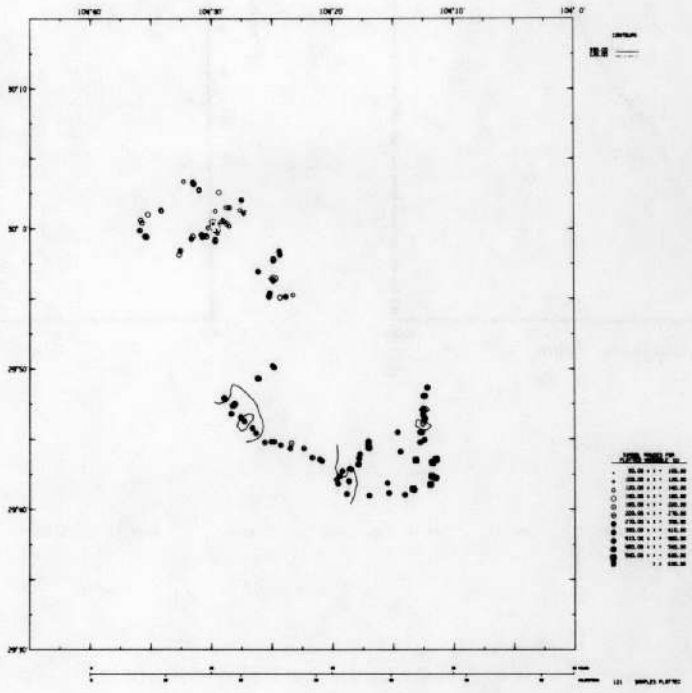

Figure B-24b

GEOCHEMICAL DISTRIBUTION OF STRONTIUM (PPM)
IN STREAM SEDIMENT OF THE CHINATI MOUNTAINS PROJECT AREA,
TRANS-PECOS DETAILED GEOCHEMICAL SURVEY, TEXAS

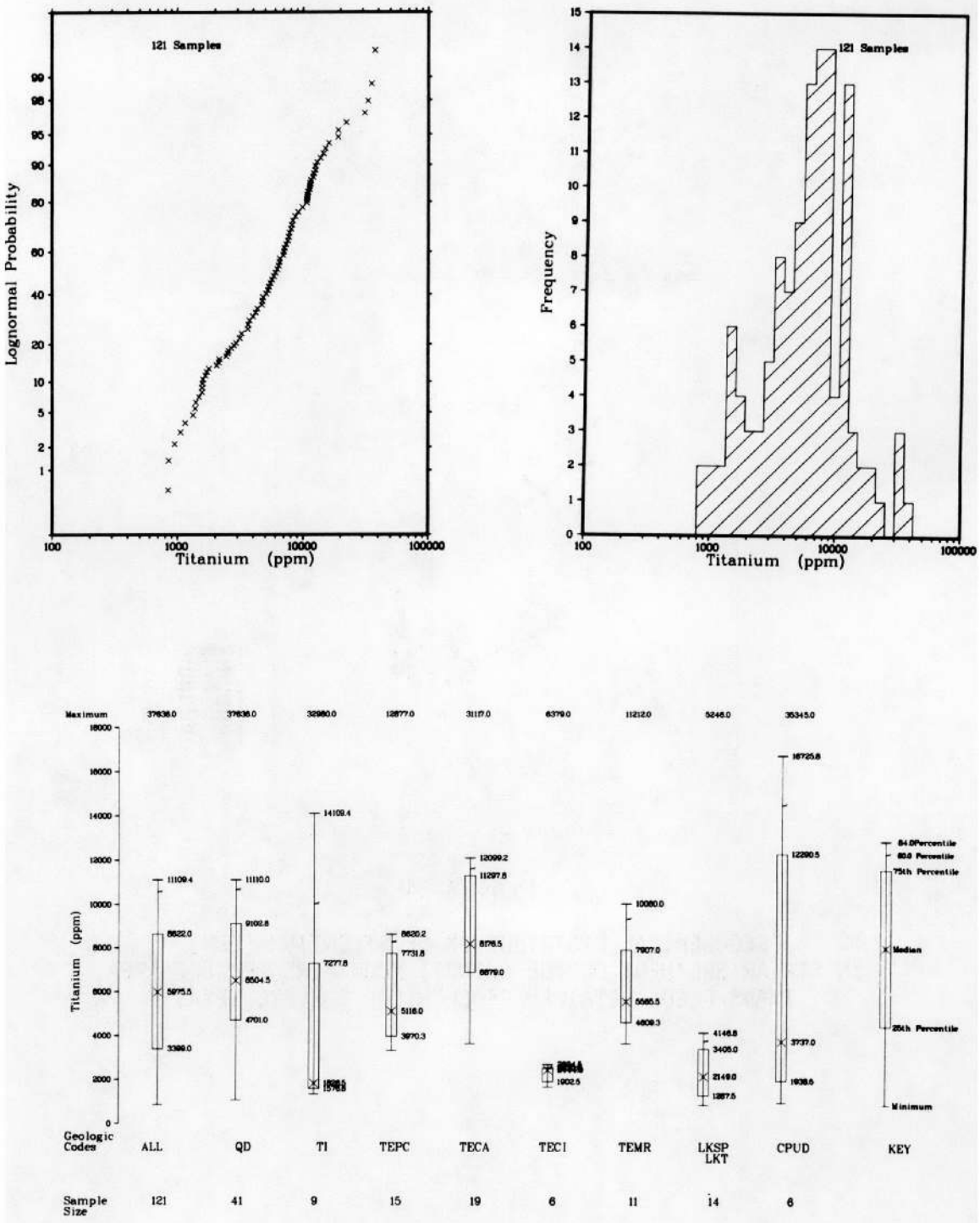

Figure B-25a

PROBABILITY, FREQUENCY, AND PERCENTILE PLOTS FOR TITANIUM (PPM) IN STREAM SEDIMENT OF THE CHINATI MOUNTAINS PROJECT AREA, TRANS-PECOS DETAILED GEOCHEMICAL SURVEY, TEXAS

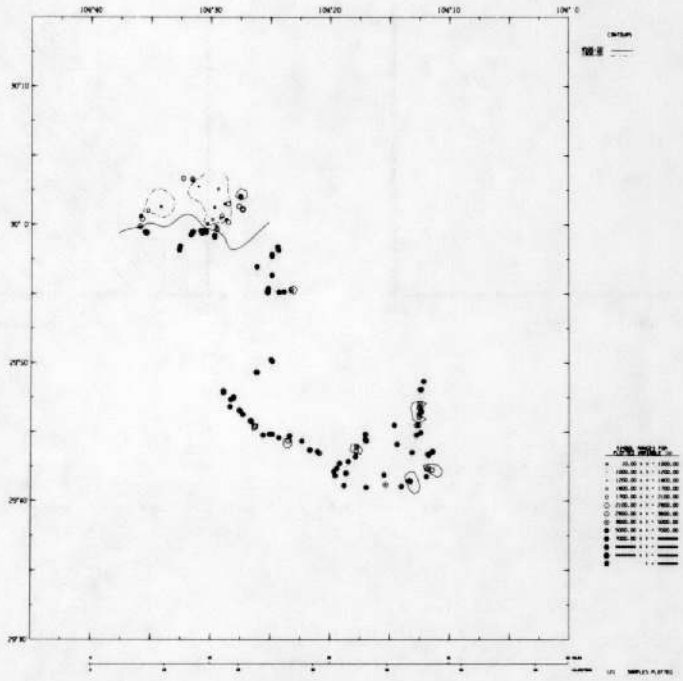

Figure B-25b

GEOCHEMICAL DISTRIBUTION OF TITANIUM (PPM)
IN STREAM SEDIMENT OF THE CHINATI MOUNTAINS PROJECT AREA,
TRANS-PECOS DETAILED GEOCHEMICAL SURVEY, TEXAS

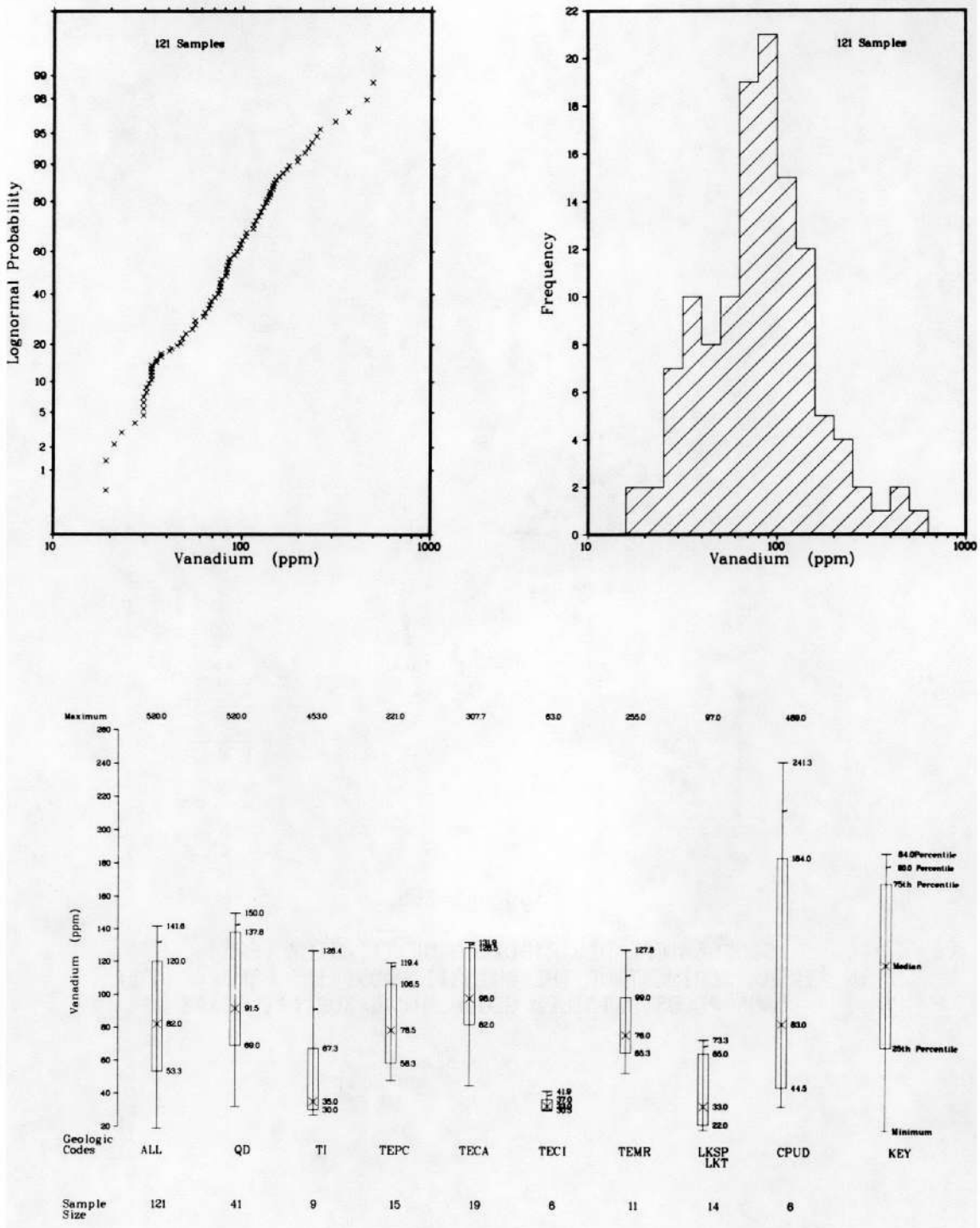

Figure B-26a

PROBABILITY, FREQUENCY, AND PERCENTILE PLOTS FOR VANADIUM (PPM) IN STREAM SEDIMENT OF THE CHINATI MOUNTAINS PROJECT AREA, TRANS-PECOS DETAILED GEOCHEMICAL SURVEY, TEXAS

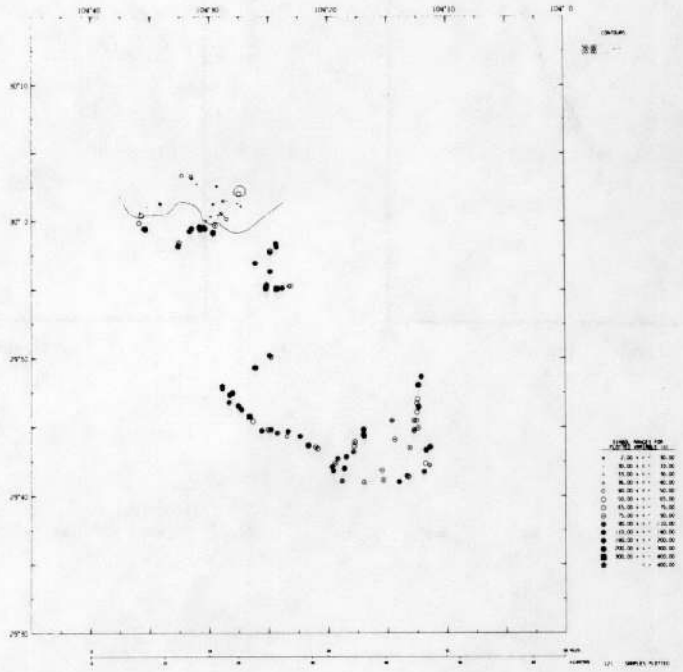

Figure B-26b

GEOCHEMICAL DISTRIBUTION OF VANADIUM (PPM)
IN STREAM SEDIMENT OF THE CHINATI MOUNTAINS PROJECT AREA,
TRANS-PECOS DETAILED GEOCHEMICAL SURVEY, TEXAS

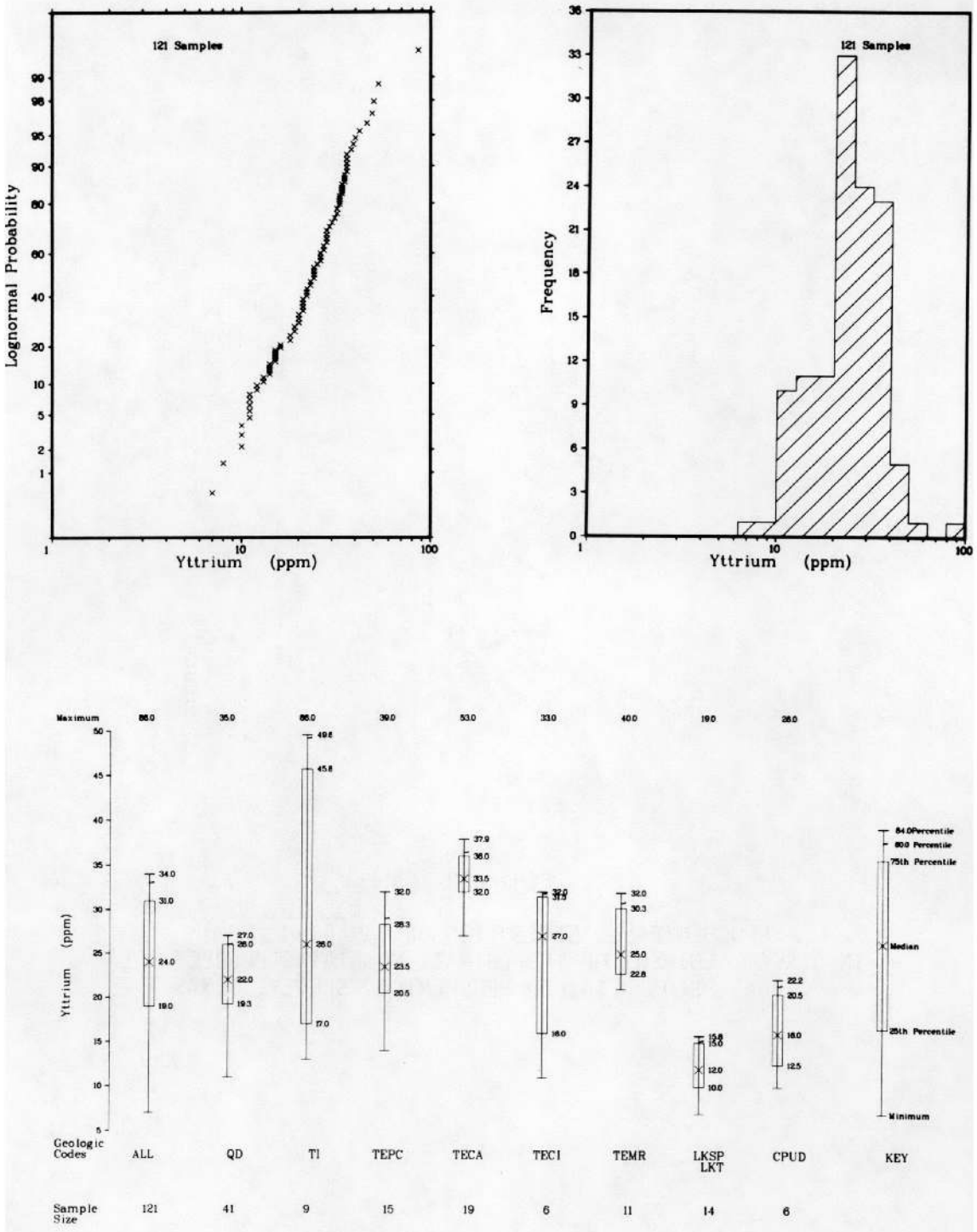

Figure B-27a

PROBABILITY, FREQUENCY, AND PERCENTILE PLOTS FOR YTTRIUM (PPM) IN STREAM SEDIMENT OF THE CHINATI MOUNTAINS PROJECT AREA, TRANS-PECOS DETAILED GEOCHEMICAL SURVEY, TEXAS

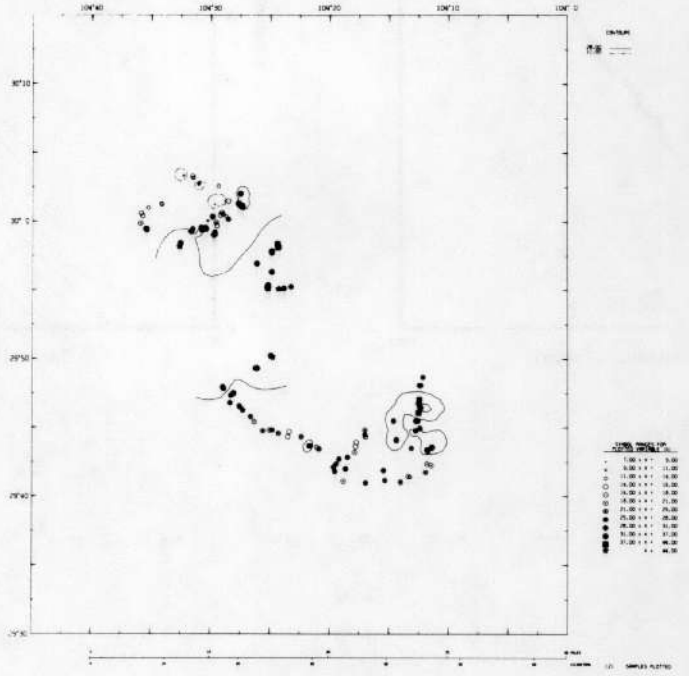

Figure B-27b

GEOCHEMICAL DISTRIBUTION OF YTTRIUM (PPM)
IN STREAM SEDIMENT OF THE CHINATI MOUNTAINS PROJECT AREA,
TRANS-PECOS DETAILED GEOCHEMICAL SURVEY, TEXAS

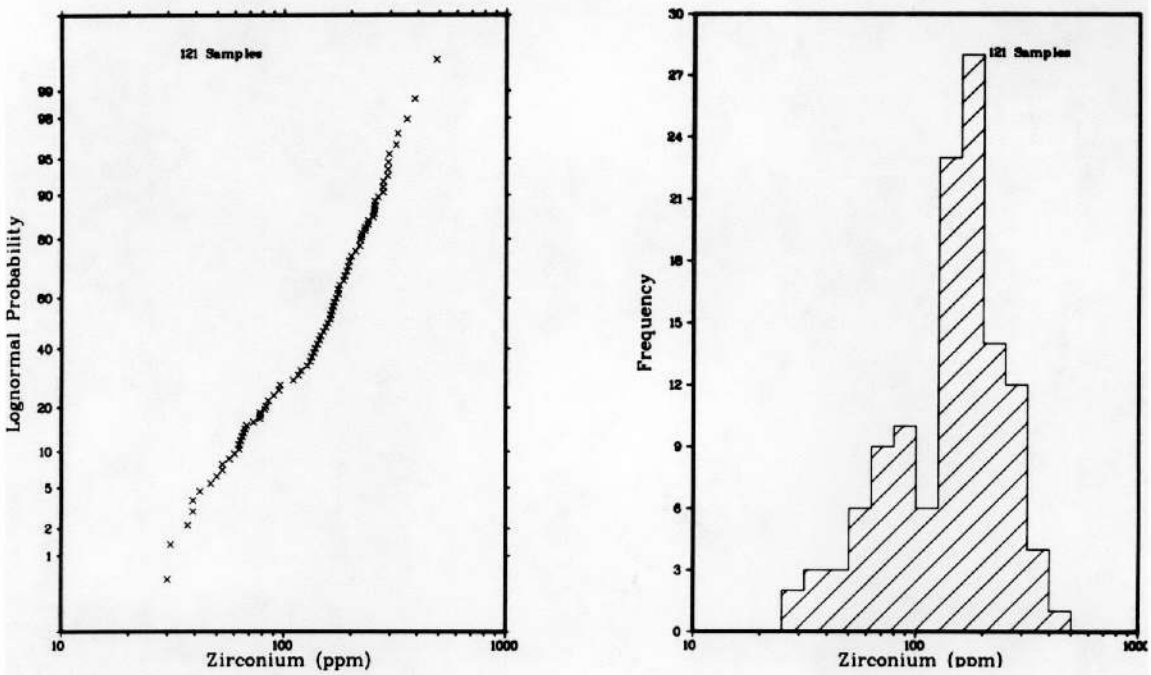

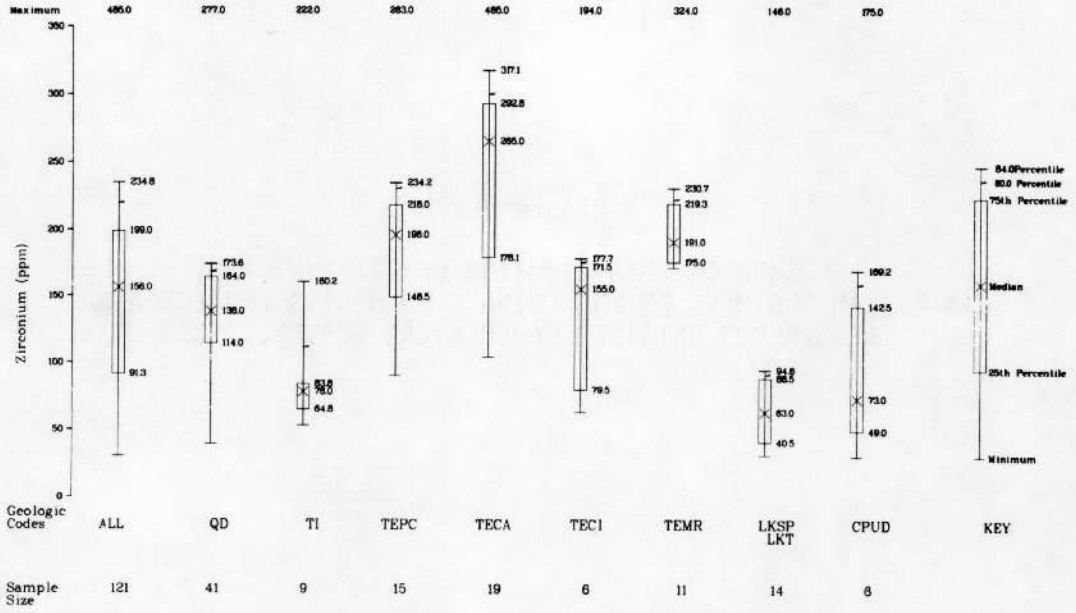

Figure B-28a

PROBABILITY, FREQUENCY, AND PERCENTILE PLOTS FOR ZIRCONIUM (PPM) IN STREAM SEDIMENT OF THE CHINATI MOUNTAINS PROJECT AREA, TRANS-PECOS DETAILED GEOCHEMICAL SURVEY, TEXAS

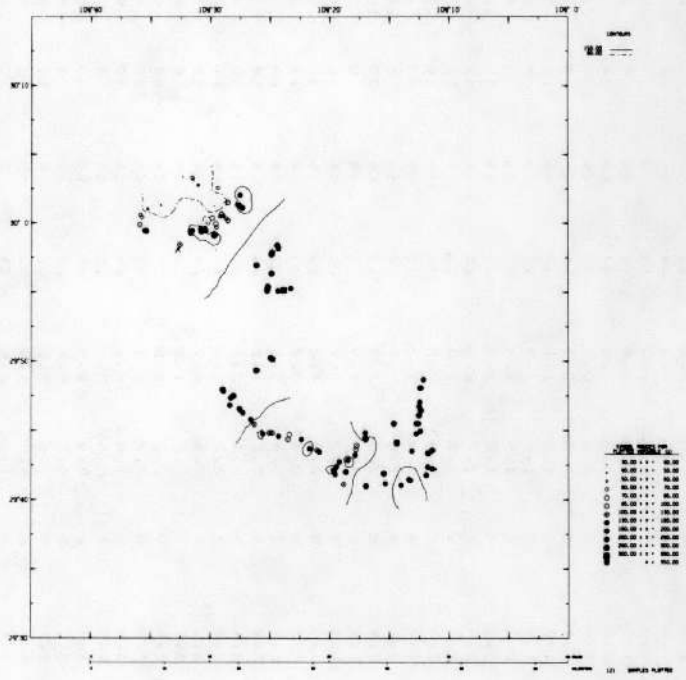

Figure B-28b

GEOCHEMICAL DISTRIBUTION OF ZIRCONIUM (PPM)
IN STREAM SEDIMENT OF THE CHINATI MOUNTAINS PROJECT AREA,
TRANS-PECOS DETAILED GEOCHEMICAL SURVEY, TEXAS

Table B-3

PARTIAL DATA LISTING FOR STREAM SEDIMENT OF THE CHINATI MOUNTAINS PROJECT AREA, TRANS-PECOS DETAILED GEOCHEMICAL SURVEY, TEXAS

OR SAMPLE NUMBER	D. O. E. SAMPLE NUMBER ST	LAT	LONG	L TY REP	U (PPM)	U-NT (PPM)	TH (PPM)	TH/U	AS (PPM)	LI (PPM)	MO (PPM)	NI (PPM)	P (PPM)	TI (PPM)	V (PPM)
27270	48	29.728	-104.362	-3-15-	2.0	3.6	8	2.2	2.4	20	<4	10	730	19000	250
27271	48	29.739	-104.373	-3-15-	2.9	3.0	2	0.67	1.6	19	<4	8	460	11000	140
27272	48	29.739	-104.392	-3-15-	1.4	2.3	3	1.3	1.3	17	<4	7	430	2900	47
27273	48	29.745	-104.390	-3-15-	1.5	2.4	3	1.3	1.7	16	<4	9	400	8000	130
27274	48	29.743	-104.405	-3-15-	2.3	3.3	8	2.4	2.0	20	<4	9	640	7700	100
27275	48	29.747	-104.414	-3-15-	2.3	3.1	4	1.3	2.4	22	<4	10	670	8000	120
27276	48	29.747	-104.418	-3-15-	2.0	2.6	4	1.5	2.4	24	<4	8	740	5300	77
27277	48	29.746	-104.427	-3-15-	2.8	3.6	3	0.83	2.9	18	4	11	960	14000	190
27278	48	30.043	-104.490	-3-15-	1.7	1.9	3	1.6	0.8	20	<4	5	200	1500	23
27281	48	30.046	-104.518	-3-15-	1.5	2.0	<2	0.50	1.6	27	<4	11	170	1200	33
27282	48	30.046	-104.517	-3-15-	1.5	1.9	3	1.6	0.9	29	<4	10	170	1400	31
27284	48	30.053	-104.525	-3-15-	1.3	1.7	3	1.8	0.5	18	<4	8	280	1600	21
27285	48	30.055	-104.526	-3-15-	1.6	1.9	<2	0.53	1.1	17	<4	6	340	3600	47
27286	48	30.056	-104.539	-3-15-	1.1	1.8	2	1.1	1.3	17	<4	6	240	3100	42
27290	48	29.697	-104.326	-3-15-	1.6	2.8	4	1.4	2.8	22	<4	9	870	6200	96
27291	48	29.702	-104.328	-3-15-	2.7	3.3	4	1.2	2.8	21	<4	10	1000	11000	140
27292	48	29.700	-104.311	-3-15-	2.5	2.6	7	2.7	2.6	21	<4	11	680	10000	150
27293	48	29.700	-104.311	-3-15-	1.9	2.5	5	2.0	2.0	19	<4	11	700	6500	100
27294	48	29.685	-104.314	-3-15-	1.8	2.5	<2	0.40	2.2	20	<4	10	570	6000	90
27300	48	30.001	-104.505	-3-15-	2.0	2.2	4	1.8	1.2	28	<4	13	170	950	33
27302	48	29.791	-104.468	-3-15-	3.1	3.2	5	1.6	3.9	29	<4	8	1600	5900	84
27304	48	29.991	-104.526	-3-12-	2.8	2.9	8	2.8	2.3	19	<4	20	1500	35000	490
27308	48	30.017	-104.588	-3-15-	1.9	1.9	8	4.2	1.9	19	<4	9	210	1800	32
27309	48	30.010	-104.598	-3-15-	1.7	1.9	8	4.2	2.7	20	<4	8	320	1700	33
27310	48	30.007	-104.596	-3-15-	2.0	2.0	5	2.5	4.2	19	<4	18	540	2800	54
27311	48	30.021	-104.569	-3-15-	2.1	2.3	2	0.87	3.2	20	<4	17	320	1100	37
27312	48	30.022	-104.570	-3-15-	2.0	2.2	3	1.4	3.8	22	<4	68	300	1400	37
27315	48	29.991	-104.590	-3-15-	2.6	2.4	4	1.7	1.8	20	<4	58	790	4800	67
27316	48	29.990	-104.590	-3-15-	2.4	2.4	5	2.1	2.2	21	<4	10	940	11000	160
27317	48	29.991	-104.592	-3-15-	2.0	2.2	7	3.2	2.8	19	<4	11	860	12000	180
27318	48	29.998	-104.595	-3-15-	2.3	2.5	6	2.4	4.0	24	<4	12	780	4200	67
27320	48	29.726	-104.351	-3-15-	1.6	2.5	7	2.8	1.7	18	<4	8	470	5300	75
27321	48	29.724	-104.348	-3-15-	2.4	2.9	9	3.1	2.8	22	<4	62	650	4400	65
27322	48	29.706	-104.324	-3-15-	2.2	2.9	8	2.8	3.0	20	<4	58	730	5500	77
27324	48	29.712	-104.320	-3-15-	2.5	3.3	6	1.8	3.5	24	<4	10	920	7700	110
27326	48	29.974	-104.543	-3-15-	1.5	2.9	2	0.69	2.3	15	<4	5	3100	7600	82
27333	48	29.792	-104.468	-3-15-	2.5	3.0	2	0.67	4.8	34	<4	10	1500	5800	85
27334	48	29.780	-104.473	-3-12-	2.4	3.0	5	1.7	4.2	27	4	8	1800	6700	93
27336	48	29.757	-104.439	-3-15-	2.8	2.7	4	1.5	5.1	31	4	11	870	3200	56
27337	48	29.763	-104.444	-3-15-	2.6	4.0	8	2.0	6.9	32	5	18	960	22000	360
27339	48	29.799	-104.483	-3-15-	1.8	3.4	4	1.2	2.4	34	5	17	2400	38000	520
27340	48	30.011	-104.485	-3-15-	3.6	4.7	12	2.6	1.5	20	<4	10	370	2100	35
27342	48	30.003	-104.476	-3-15-	2.6	3.5	6	1.7	5.3	26	<4	67	380	2500	41
27344	48	29.999	-104.493	-3-15-	6.9	6.8	12	1.8	1.7	34	<4	59	170	1600	30
27345	48	29.987	-104.495	-3-12-	2.1	2.3	6	2.6	2.0	23	<4	68	1100	8600	140
27411	48	29.988	-104.528	-3-15-	3.2	3.9	3	0.77	1.7	21	<4	59	2700	12000	150
27412	48	29.993	-104.514	-3-12-	2.2	2.7	6	2.2	1.6	23	<4	50	1900	16000	230
27414	48	30.022	-104.461	-3-15-	2.7	3.5	13	3.7	2.7	27	<4	99	490	2400	33
27415	48	30.034	-104.459	-3-15-	2.6	2.7	10	3.7	1.7	25	<4	60	910	6400	63
27418	48	30.025	-104.476	-3-15-	3.1	3.2	7	2.2	3.9	15	<4	65	370	2100	30
27419	48	30.021	-104.495	-3-15-	1.7	1.4	2	1.4	0.8	17	<4	59	99	840	19
27420	48	30.006	-104.498	-3-15-	12.	9.8	17	1.7	2.5	33	<4	100	310	1600	35
27421	48	29.993	-104.508	-3-15-	2.9	3.7	9	2.4	1.7	28	<4	76	460	2900	56
27422	48	29.991	-104.507	-3-15-	2.4	2.5	2	0.80	1.4	25	<4	80	2000	14000	210
27423	48	29.990	-104.513	-3-15-	2.2	2.7	3	1.1	1.1	23	<4	90	3000	7000	82

Table B-3, Continued

PARTIAL DATA LISTING FOR STREAM SEDIMENT OF THE CHINATI MOUNTAINS PROJECT AREA, TRANS-PECOS DETAILED GEOCHEMICAL SURVEY, TEXAS

OR SAMPLE NUMBER	D. O. E. SAMPLE NUMBER ST LAT LONG L TY REP	U (PPM)	U-NT (PPM)	TH (PPM)	TH/U	AS (PPM)	LI (PPM)	MO (PPM)	NI (PPM)	(PPM)	TI (PPM)	V (PPM)
27424	48-29.714 -104.308 -3-15-	1.9	3.0	5	1.7	4.1	22	<4	62	880	12000	200
27425	48-29.720 -104.298 -3-15-	1.5	1.7	13	7.6	<0.1	18	<4	76	850	5200	97
27426	48-29.727 -104.297 -3-15-	1.7	2.0	6	3.0	2.4	22	<4	9	620	3200	68
27427	48-29.732 -104.296 -3-15-	1.9	2.0	2	1.0	2.9	17	<4	10	600	4300	75
27429	48-29.739 -104.283 -3-15-	1.5	1.9	3	1.6	4.1	19	<4	13	650	3900	85
27430	48-29.741 -104.284 -3-15-	2.1	1.8	5	2.8	1.6	11	<4	71	1800	13000	220
27431	48-29.747 -104.284 -3-15-	1.3	1.3	4	3.1	4.4	16	<4	75	1100	11000	260
27433	48-29.969 -104.545 -3-15-	7.9	11.	21	1.9	7.2	15	<4	71	4400	33000	450
27441	48-29.822 -104.437 -3-15-	2.7	3.3	6	1.8	6.2	28	5	10	2700	8100	110
27443	48-29.822 -104.435 -3-15-	2.3	3.2	3	0.94	4.8	31	5	8	2500	6000	84
27446	48-29.835 -104.414 -3-15-	4.2	5.0	8	1.6	4.7	31	5	8	1500	6500	82
27447	48-29.837 -104.416 -3-15-	3.6	3.9	7	1.8	2.0	32	4	66	1700	7100	99
27452	48-30.009 -104.483 -3-15-	3.0	2.9	10	3.4	1.3	25	<4	59	180	1300	27
27453	48-30.008 -104.487 -3-15-	3.0	4.1	8	2.0	1.4	22	<4	55	230	1600	30
27455	48-30.006 -104.479 -3-15-	1.4	1.9	7	3.7	1.0	20	<4	9	210	1700	30
27459	48-29.995 -104.492 -3-15-	2.1	2.5	2	0.80	2.4	40	<4	16	570	3700	83
27460	48-29.985 -104.495 -3-12-	2.5	2.1	2	0.95	0.6	21	<4	8	3700	7300	82
29152	48-29.735 -104.240 -3-15-	2.0	3.6	8	2.2	2.6	28	<4	10	1500	7300	76
29153	48-29.725 -104.219 -3-15-	1.8	1.8	<2	0.56	1.9	23	<4	24	1100	5400	83
29155	48-29.746 -104.213 -3-15-	2.0	2.7	6	2.2	2.7	25	<4	13	1400	8300	100
29158	48-29.749 -104.207 -3-15-	2.4	2.9	2	0.69	1.9	24	<4	14	970	5600	76
29160	48-29.684 -104.234 -3-15-	1.4	2.1	9	4.3	2.0	20	<4	11	460	7000	120
29162	48-29.691 -104.223 -3-15-	1.7	1.9	7	3.7	1.7	21	<4	12	630	5100	90
29172	48-29.690 -104.221 -3-15-	1.5	1.9	6	3.2	2.0	27	<4	13	470	2700	62
29174	48-29.706 -104.197 -3- -	1.5	2.0	6	3.0	1.5	27	<4	25	1000	4000	61
29176	48-29.696 -104.199 -3- -	1.4	1.8	3	1.7	1.7	19	4	28	1300	7600	120
29177	48-29.704 -104.191 -3-12-	3.1	3.0	4	1.3	1.8	22	<4	14	1000	3300	49
29178	48-29.722 -104.196 -3-15-	2.5	3.2	4	1.3	2.2	23	<4	11	1600	8900	100
29179	48-29.723 -104.197 -3-15-	2.9	3.3	7	2.1	2.2	34	<4	8	1000	4100	48
29182	48-29.726 -104.190 -3-15-	2.7	5.3	4	0.75	4.0	28	<4	10	1600	12000	140
29183	48-29.726 -104.191 -3-15-	1.9	2.6	8	3.1	2.3	23	<4	11	1600	6200	74
29223	48-29.758 -104.210 -3-15-	2.5	3.4	9	2.6	1.7	25	<4	67	770	4800	72
29225	48-29.758 -104.213 -3-15-	1.8	2.2	10	4.5	2.4	19	<4	64	820	4800	66
29226	48-29.758 -104.244 -3-15-	1.6	2.8	10	3.6	1.4	25	<4	60	910	7100	93
29227	48-29.768 -104.209 -3-15-	3.3	3.9	9	2.3	1.5	43	<4	56	380	3600	50
29229	48-29.811 -104.203 -3-15-	1.7	2.0	4	2.0	1.8	18	<4	100	1500	11000	160
29230	48-29.779 -104.209 -3-15-	2.2	3.8	8	2.1	1.8	42	<4	10	580	3700	53
29231	48-29.775 -104.207 -3-15-	2.0	3.0	5	1.7	1.8	24	<4	15	930	5100	70
29232	48-29.774 -104.206 -3-15-	1.9	2.6	6	2.3	2.0	26	<4	14	760	5500	81
29234	48-29.784 -104.208 -3-15-	5.5	5.6	7	1.3	1.7	40	<4	8	610	4200	63
29238	48-29.683 -104.283 -3-15-	1.5	2.7	3	1.1	1.7	24	<4	13	1400	6900	83
29239	48-29.686 -104.256 -3-15-	1.5	2.3	5	2.2	2.7	22	<4	10	510	4700	76
29240	48-29.698 -104.258 -3-15-	1.7	2.7	7	2.6	2.1	24	4	10	1300	6500	75
29242	48-29.801 -104.208 -3-15-	2.5	3.4	3	0.88	2.1	22	<4	14	1600	9900	120
29243	48-29.801 -104.206 -3-15-	2.5	3.1	6	1.9	2.0	23	<4	17	870	4700	66
29244	48-29.919 -104.421 -3-15-	2.6	4.7	9	1.9	0.7	13	<4	9	3700	19000	170
29245	48-29.918 -104.421 -3-15-	3.2	5.3	5	0.94	3.9	38	<4	7	1600	7800	71
29247	48-29.920 -104.421 -3-15-	2.4	4.1	2	0.49	0.6	15	4	5	1800	5800	56
29248	48-29.923 -104.420 -3-15-	2.4	6.4	13	2.0	1.0	20	<4	7	1900	11000	96
29249	48-29.939 -104.415 -3-15-	2.3	6.0	2	0.33	0.6	17	<4	9	2700	11000	130
29250	48-29.918 -104.406 -3-15-	2.1	10.	4	0.44	2.1	20	<4	13	2900	31000	310
29251	48-29.919 -104.398 -3-15-	2.6	3.9	6	1.5	1.0	20	<4	9	2400	11000	130
29252	48-29.921 -104.388 -3-15-	2.8	3.7	12	3.2	1.7	20	<4	9	770	3600	45
29256	48-29.949 -104.436 -3-15-	2.8	3.3	3	0.91	0.7	14	5	7	2200	9100	110
29277	48-29.962 -104.415 -3-15-	2.3	3.3	4	1.2	2.4	19	4	14	1200	8300	97

Table B-3, Continued

PARTIAL DATA LISTING FOR STREAM SEDIMENT OF THE CHINATI MOUNTAINS PROJECT AREA, TRANS-PECOS DETAILED GEOCHEMICAL SURVEY, TEXAS

OR SAMPLE NUMBER	D. D. E. SAMPLE NUMBER ST LAT	LONG	L TY REP	U (PPM)	U-NT (PPM)	TH (PPM)	TH/U	AS (PPM)	LI (PPM)	MO (PPM)	NI (PPM)	P (PPM)	TI (PPM)	V (PPM)
29278	48-29.964	-104.415	-3-12-	3.2	3.7	12	3.2	0.9	20	5	3	1500	6400	55
29280	48-29.973	-104.407	-3-15-	2.0	2.8	4	1.4	2.2	33	<4	49	2100	11000	130
29281	48-29.969	-104.406	-3-15-	2.6	3.5	6	1.7	1.8	23	<4	9	2000	15000	130
29331	48-29.789	-104.472	-3-15-	3.7	3.1	7	2.3	3.1	33	<4	63	1000	7300	120
29332	48-29.771	-104.455	-3-15-	3.3	3.0	7	2.3	9.8	23	<4	55	1400	8100	110
29333	48-29.776	-104.460	-3-15-	2.2	3.4	4	1.2	3.4	32	<4	18	1100	4700	76
29334	48-29.775	-104.459	-3-15-	2.5	2.9	6	2.1	3.7	28	<4	21	1500	8600	120
29335	48-29.797	-104.482	-3-15-	2.3	3.1	7	2.3	3.4	31	<4	21	2100	9300	140
29350	48-30.025	-104.481	-3-15-	1.9	1.8	5	2.8	1.2	17	<4	15	110	850	19
29352	48-30.019	-104.456	-3-15-	3.5	3.4	16	4.7	1.7	29	<4	19	400	2100	31
29353	48-30.018	-104.456	-3-15-	2.6	3.3	15	4.5	1.1	32	<4	17	290	2500	33

APPENDIX C

FIELD FORM AND COMPUTER CODE LIST

APPENDIX C

FIELD FORM AND COMPUTER CODE LIST

LIST OF TABLES

Table C-1

COMPUTER CODE LIST OF GEOCHEMICAL VARIABLES

Variable[a]	Code	Variable[a]	Code
Uranium Measured by Fluorometry[b]	U-FL	Scandium	SC
		Silicon	SI
Uranium Measured by Mass Spectrometry[b]	U-MS	Strontium	SR
		Thorium	TH
Uranium Measured by Neutron Activation	U-NT	Titanium	TI
Arsenic	AS	Vanadium	V
Selenium	SE	Yttrium	Y
Silver	AG	Zinc	ZN
Aluminum	AL	Zirconium	ZR
Boron	B	Sulfate (ppm)	SO_4
Barium	BA	Chloride (ppm)	CL
Beryllium	BE	Conductivity from Lab (μmhos/cm)	CT-L
Calcium	CA	Conductivity from Field (μmhos/cm)	CT-F
Cerium	CE	Dissolved Oxygen (ppm)	DO
Cobalt	CO	Air Temperature (°C)	ATEM
Chromium	CR	Water Temperature (°C)	WTEM
Copper	CU	pH	PH
Iron	FE	pH Measured by Lo Ion Paper	PH-P
Hafnium	HF	Total Alkalinity (ppm)	T-AK
Potassium	K	M-Alkalinity (ppm)	M-AK
Lanthanum	LA	P-Alkalinity (ppm)	P-AK
Lithium	LI	Carbonate (ppm)[c]	CB
Mangesium	MG	Bicarbonate (ppm)[c]	BC
Manganese	MN	Undissociated Carbonic Acid (ppm)[c]	CAB
Molybdenum	MO	U-NT/U-FL	TU/U
Sodium	NA	U-FL/U-NT	U/TU
Niobium	NB	TH/U-NT	TH/U
Nickel	NI	1,000·U/SP	U/SP
Phosphorus	P	1,000·U/B	U/B
Lead	PB	1,000·U/SO	U/SO
Platinum	PT	Sodium/Chloride	NA/C
		Log of Sodium/Chloride	LN/C

[a] If natural logarithm of variable is used, L or L- precedes the variable code.

[b] If method is not specified for waters, U-FL is used, except where value is below laboratory detection limit in which case U-MS is substituted if it is available.

[c] These variables were approximated using cubic spline functions to fit the curves in Hem (1970), p. 155.

Table C-2

OAK RIDGE GEOCHEMICAL SAMPLING FORM
SHOWING FIELD DATA RECORDED ON MICROFICHE

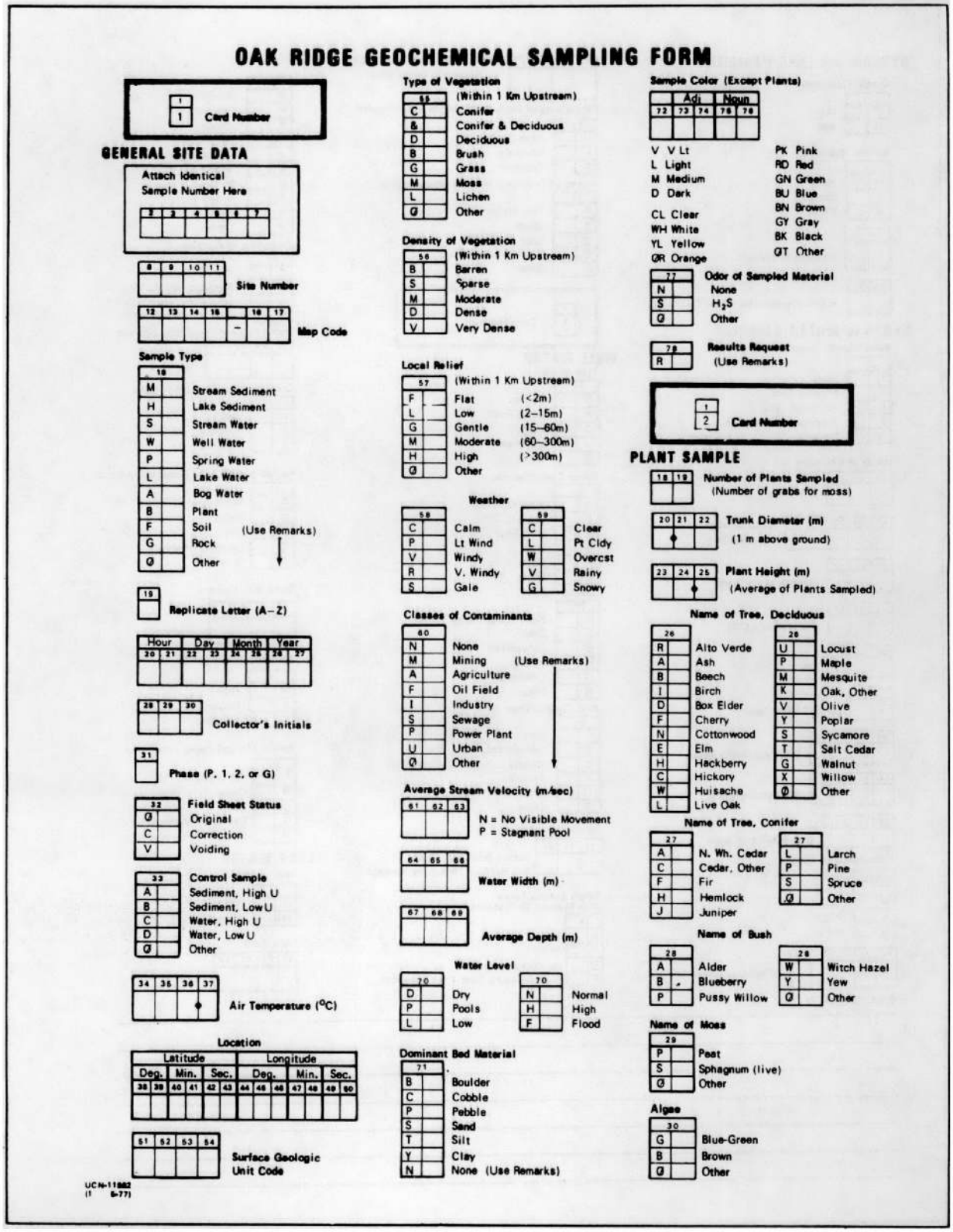

OAK RIDGE GEOCHEMICAL SAMPLING FORM

Card Number (1) = 1

GENERAL SITE DATA

Attach Identical Sample Number Here (2 3 4 5 6 7)

Site Number (8 9 10 11)

Map Code (12 13 14 15 – 16 17)

Sample Type (18)

M	Stream Sediment
H	Lake Sediment
S	Stream Water
W	Well Water
P	Spring Water
L	Lake Water
A	Bog Water
B	Plant
F	Soil
G	Rock
Ø	Other

(Use Remarks)

Replicate Letter (A–Z) (19)

Hour (20 21) Day (22 23) Month (24 25) Year (26 27)

Collector's Initials (28 29 30)

Phase (P, 1, 2, or G) (31)

Field Sheet Status (32)

Ø	Original
C	Correction
V	Voiding

Control Sample (33)

A	Sediment, High U
B	Sediment, Low U
C	Water, High U
D	Water, Low U
Ø	Other

Air Temperature (°C) (34 35 36 37)

Location

Latitude			Longitude		
Deg. (38 39)	Min. (40 41)	Sec. (42 43)	Deg. (44 45 46)	Min. (47 48)	Sec. (49 50)

Surface Geologic Unit Code (51 52 53 54)

UCN-11882 (1 6-77)

Type of Vegetation (55) (Within 1 Km Upstream)

C	Conifer
&	Conifer & Deciduous
D	Deciduous
B	Brush
G	Grass
M	Moss
L	Lichen
Ø	Other

Density of Vegetation (56) (Within 1 Km Upstream)

B	Barren
S	Sparse
M	Moderate
D	Dense
V	Very Dense

Local Relief (57) (Within 1 Km Upstream)

F	Flat (<2m)
L	Low (2–15m)
G	Gentle (15–60m)
M	Moderate (60–300m)
H	High (>300m)
Ø	Other

Weather

(58)		(59)	
C	Calm	C	Clear
P	Lt Wind	L	Pt Cldy
V	Windy	W	Overcst
R	V. Windy	V	Rainy
S	Gale	G	Snowy

Classes of Contaminants (60) (Use Remarks)

N	None
M	Mining
A	Agriculture
F	Oil Field
I	Industry
S	Sewage
P	Power Plant
U	Urban
Ø	Other

Average Stream Velocity (m/sec) (61 62 63)

N = No Visible Movement
P = Stagnant Pool

Water Width (m) (64 65 66)

Average Depth (m) (67 68 69)

Water Level (70)

D	Dry
P	Pools
L	Low
N	Normal
H	High
F	Flood

Dominant Bed Material (71)

B	Boulder
C	Cobble
P	Pebble
S	Sand
T	Silt
Y	Clay
N	None (Use Remarks)

Sample Color (Except Plants) (72 Adj 73 74 Noun 75 76)

V	V Lt	PK	Pink
L	Light	RD	Red
M	Medium	GN	Green
D	Dark	BU	Blue
CL	Clear	BN	Brown
WH	White	GY	Gray
YL	Yellow	BK	Black
ØR	Orange	ØT	Other

Odor of Sampled Material (77)

N	None
S	H_2S
Ø	Other

Results Request (78) (Use Remarks)

R

Card Number (1) = 2

PLANT SAMPLE

Number of Plants Sampled (18 19) (Number of grabs for moss)

Trunk Diameter (m) (20 21 22) (1 m above ground)

Plant Height (m) (23 24 25) (Average of Plants Sampled)

Name of Tree, Deciduous (26)

R	Alto Verde	U	Locust
A	Ash	P	Maple
B	Beech	M	Mesquite
I	Birch	K	Oak, Other
D	Box Elder	V	Olive
F	Cherry	Y	Poplar
N	Cottonwood	S	Sycamore
E	Elm	T	Salt Cedar
H	Hackberry	G	Walnut
C	Hickory	X	Willow
W	Huisache	Ø	Other
L	Live Oak		

Name of Tree, Conifer (27)

A	N. Wh. Cedar	L	Larch
C	Cedar, Other	P	Pine
F	Fir	S	Spruce
H	Hemlock	Ø	Other
J	Juniper		

Name of Bush (28)

A	Alder	W	Witch Hazel
B	Blueberry	Y	Yew
P	Pussy Willow	Ø	Other

Name of Moss (29)

P	Peat
S	Sphagnum (live)
Ø	Other

Algae (30)

G	Blue-Green
B	Brown
Ø	Other

Table C-2, Continued

OAK RIDGE GEOCHEMICAL SAMPLING FORM
SHOWING FIELD DATA RECORDED ON MICROFICHE

STREAM OR LAKE SEDIMENT

Sample Condition (31)
- D Dry
- W Wet

Sample Treatment (32)
- N None
- S Sieved
- Q Other

(33 34) Number of Grabs

(35 36) % Organic Material (Field Estimate)

GENERAL WATER SAMPLES

Water Sample Treatment (37)
- N None
- F Filtered Only
- C Acidified Only
- A Acidified and Filtered
- Q Other

Depth of Visibility (m) (38 39 40)
- C = Clear

(41 42 43 44 45) Conductivity (μmhos/cm)

(46 47 48) Dissolved O_2 (ppm)

(49 50 51) Temperature (°C)

(52 53 54) pH

(55) pH by La-Ion Paper
- P

(56 57 58 59) Total Alkalinity (ppm)

(60 61 62 63) P Alkalinity (ppm)

(64 65 66 67) M Alkalinity (ppm)

Appearance of Water (68)
- C Clear
- M Murky
- A Algal
- Q Other

(69 70 71 72 73) Discharge (liters/min)

REMARKS (Card 4)

(74 75 76 77) Identification of Producing Horizon (Geologic Unit Code)

Confidence of Producing Horizon Identification (78)
- H High Degree
- R Probable
- S Possible

Source of Producing Horizon Identification (79)
- P Publication
- W Owner
- U User
- G Geologic Inference
- Q Other

(1 3) Card Number

WELL WATER

Type of Well (18)
- D Drilled
- P Drive Point
- G Dug
- U Unknown
- Q Other

Power Classification (19)
- A Artesian Flow
- E Electric
- G Gasoline
- W Wind
- H Hand
- Q Other

Casing (20)
- N None (Below Water Table)
- S Steel
- G Galvanized
- P Plastic
- U Unknown
- Q Other

Pipe Composition (21)
- F Steel
- Z Galvanized
- C Copper
- P Plastic
- U Unknown
- Q Other

Sample Location (22 23 24)
- Meters from Well Head
- H = Holding Tank (Use Remarks)

Where Sample Taken With Respect To Pressure Tank (25)
- B Before
- A After
- N No Pressure Tank
- F From Pressure Tank (Use Remarks)

Use of Well (26)
- M Municipal
- H Household
- S Stock
- I Irrigation
- A All of above
- X H and S
- Y H and I
- Z S and I
- N None
- Q Other

Frequency of Pumping (27)
- C Constant (hourly)
- F Frequent (daily)
- I Infrequent (weekly)
- R Rare (no recent use)

Depth to top of Producing Horizon (28 29 30 31)
- (Meters)

Confidence of Producing Depth (32)
- H High
- R Probable
- S Possible

Source of Producing Depth Information (33)
- P Publication
- W Owner
- U User
- G Geologic Inference
- Q Other

Total Well Depth (34 35 36 37)
- (Meters)

Confidence of Total Depth (38)
- H High
- R Probable
- S Possible

Source of Total Depth Information (39)
- P Publications
- W Owner
- U User
- G Geologic Inference
- Q Other

LAKE WATER

Type of Lake (55)
- N Natural
- M Manmade

Lake Area (56 57 58 59)
- (sq km)

Table C-2, Continued

OAK RIDGE GEOCHEMICAL SAMPLING FORM
SHOWING FIELD DATA RECORDED ON MICROFICHE

OAK RIDGE GEOCHEMICAL SAMPLING FORM

FIELD DATA SUPPLEMENT

Attach Identical Sample Number Here

Sequence Number: 1

Procedure Number

Results for Procedure 31

Total Gamma - Scintillometer (counts/minute)

Results for Procedures 34-41

Variables and Procedures are listed below

Results for Precedure 32 Gamma Spectrometer

TOTAL COUNTS (CPM)

e POTASSIUM (%)

POTASSIUM (CPM)

e URANIUM (ppm)

URANIUM (CPM)

e THORIUM (ppm)

THORIUM (CPM)

Note To Sampler: Blocks 16-20 Not Used Should Be Marked Out.

DO NOT KEYPUNCH

Procedures 34–41

34 Uranium (ppb)
35 Fluoride (ppm)
36 Nitrate (ppm)
37 Sulphate (ppm)
38 Phosphate (ppm)
39 Ferrous Iron (ppm)
40 Total Iron (ppm)
41 Turbidity (% T)

Readings made in Counts per _____

VARIABLE	READING		BACKGROUND		RESULTS
	ACTUAL	CPM	ACTUAL	CPM	
TOTAL COUNTS					
POTASSIUM					
URANIUM					
THORIUM					

UCN-11992A
(1 3-79)

APPENDIX D

MICROFICHE OF FIELD AND LABORATORY DATA

APPENDIX D

MICROFICHE OF FIELD AND LABORATORY DATA

CONTENTS

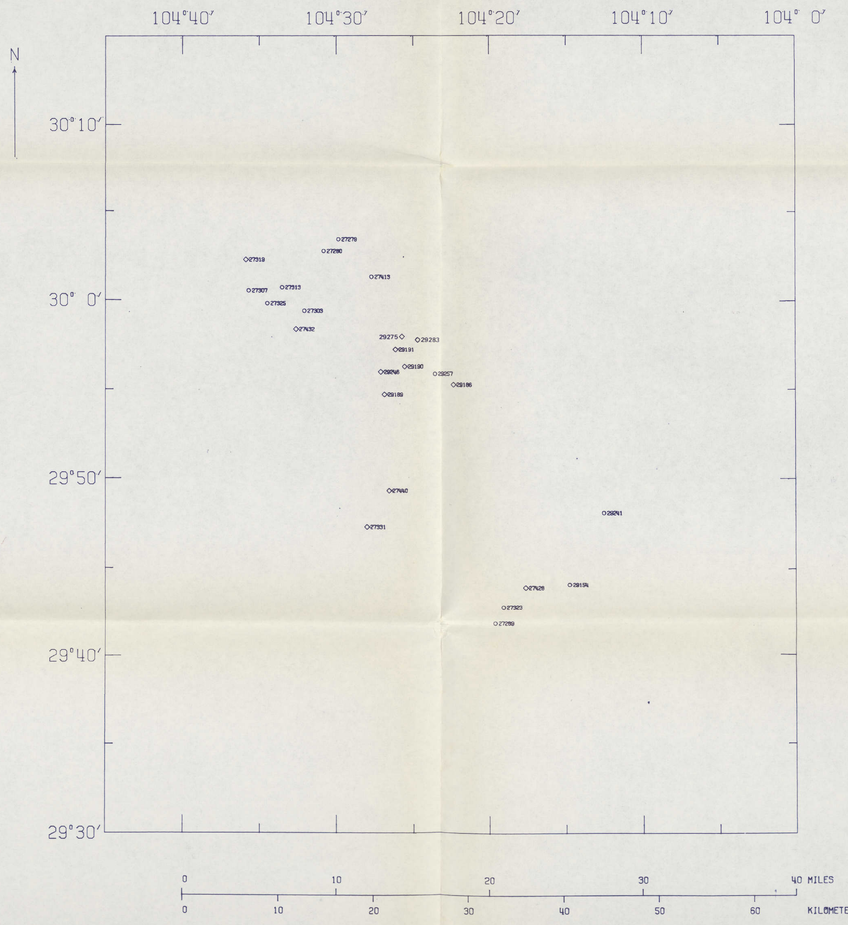

LEGEND

- ○ WELL WATER
- ◇ SPRING WATER

PLATE 1
CHINATI MOUNTAINS PROJECT AREA
TRANS-PECOS DETAILED GEOCHEMICAL SURVEY
GROUNDWATER SAMPLE LOCATION MAP

SCALE 1: 250000
24 SAMPLES PLOTTED

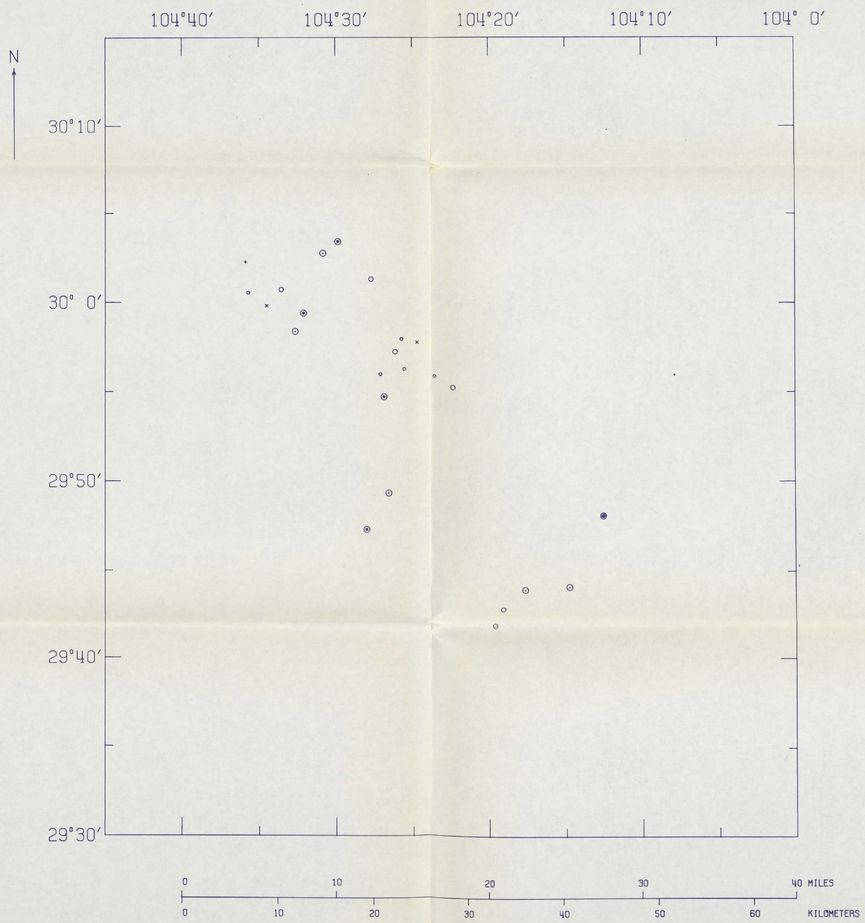

SYMBOL RANGES FOR PLOTTED VARIABLE (X)	
.	0.0 ≤ X < 0.20
x	0.20 ≤ X < 0.80
∘	0.80 ≤ X < 1.50
○	1.50 ≤ X < 2.50
⊙	3.50 ≤ X < 5.00
⊙	5.00 ≤ X < 7.00
◉	7.00 ≤ X < 12.00
●	12.00 ≤ X < 20.00

PLATE 2
CHINATI MOUNTAINS PROJECT AREA
TRANS-PECOS DETAILED GEOCHEMICAL SURVEY
SYMBOL PLOT GROUNDWATER
URANIUM (PPB)

SCALE 1: 250000

24 SAMPLES PLOTTED

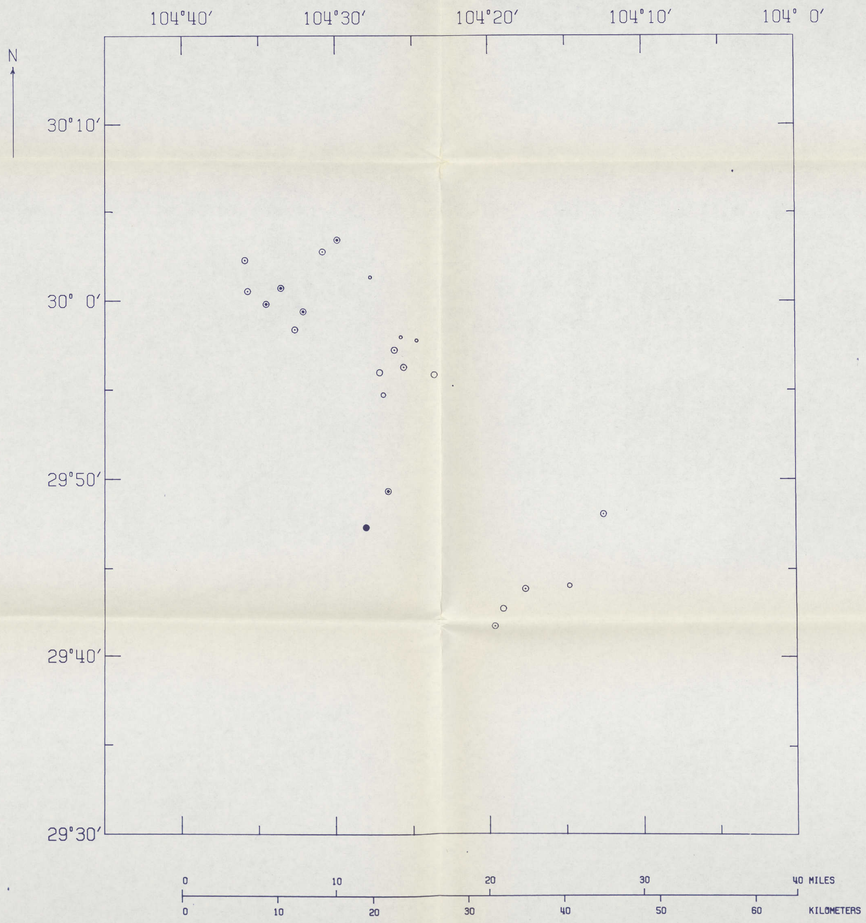

SYMBOL RANGES FOR PLOTTED VARIABLE (X)

.	350.00 ≤ X < 400.00
◦	450.00 ≤ X < 500.00
○	500.00 ≤ X < 600.00
○	600.00 ≤ X < 700.00
⊙	700.00 ≤ X < 900.00
⊙	900.00 ≤ X < 1100.00
⊛	1100.00 ≤ X < 1500.00
●	1800.00 ≤ X < 2300.00

PLATE 3
CHINATI MOUNTAINS PROJECT AREA
TRANS-PECOS DETAILED GEOCHEMICAL SURVEY
SYMBOL PLOT GROUNDWATER
SPECIFIC CONDUCTANCE (UMHOS/CM)

SCALE 1: 250000

24 SAMPLES PLOTTED

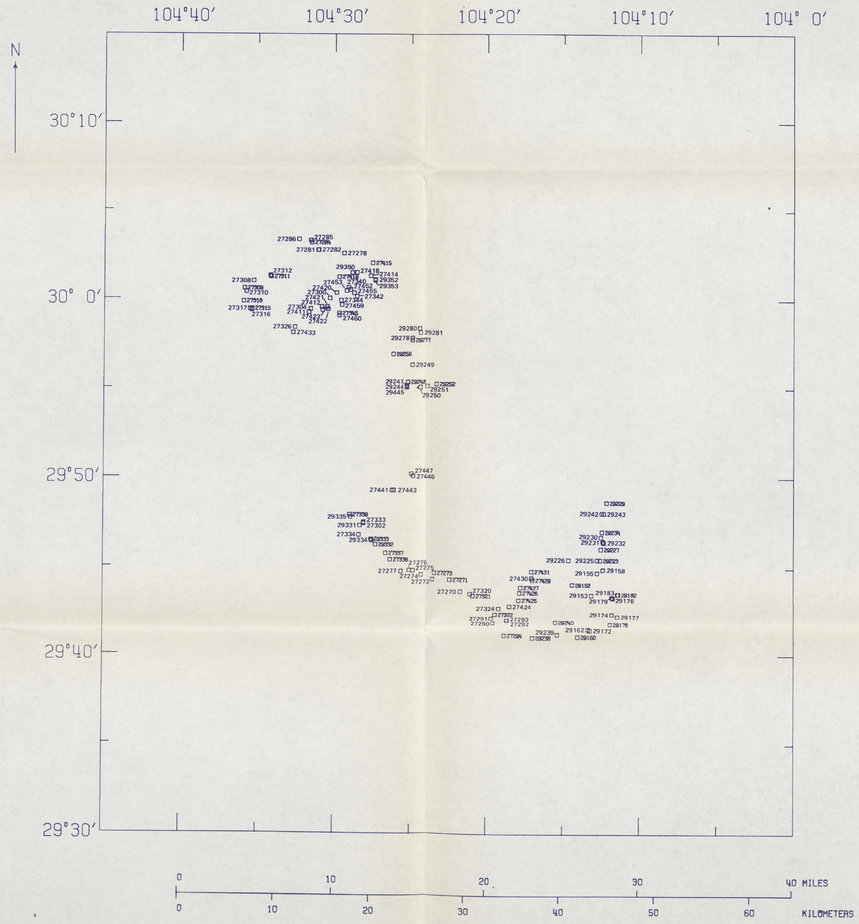

LEGEND

▫ STREAM SEDIMENT

PLATE 4
CHINATI MOUNTAINS PROJECT AREA
TRANS-PECOS DETAILED GEOCHEMICAL SURVEY
STREAM SEDIMENT SAMPLE LOCATION MAP

SCALE 1: 250000

121 SAMPLES PLOTTED

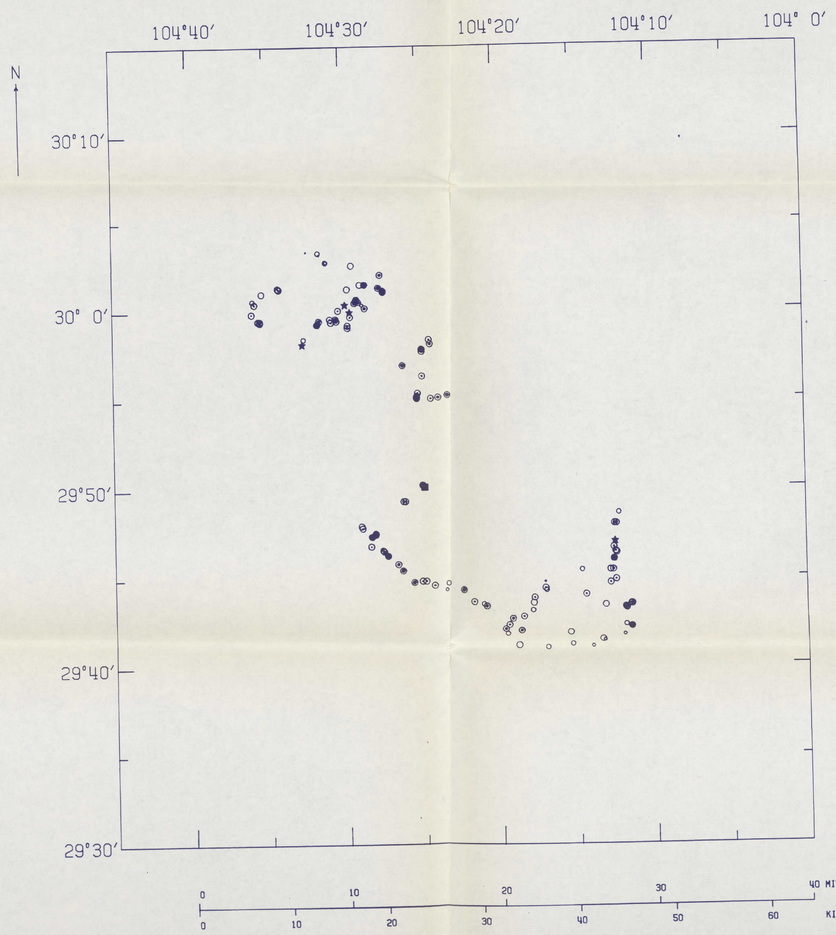

SYMBOL RANGES FOR PLOTTED VARIABLE (X)	
.	1.00 ≤ X < 1.20
.	1.20 ≤ X < 1.35
∘	1.35 ≤ X < 1.50
∘	1.50 ≤ X < 1.70
○	1.70 ≤ X < 1.90
⊙	1.90 ≤ X < 2.15
⊙	2.15 ≤ X < 2.45
⊛	2.45 ≤ X < 2.70
●	2.70 ≤ X < 3.00
●	3.00 ≤ X < 3.40
●	3.40 ≤ X < 4.00
■	4.00 ≤ X < 4.50
★	X ≥ 4.50

PLATE 5
CHINATI MOUNTAINS PROJECT AREA
TRANS-PECOS DETAILED GEOCHEMICAL SURVEY
SYMBOL PLOT STREAM SEDIMENT
URANIUM (PPM)

SCALE 1: 250000

121 SAMPLES PLOTTED

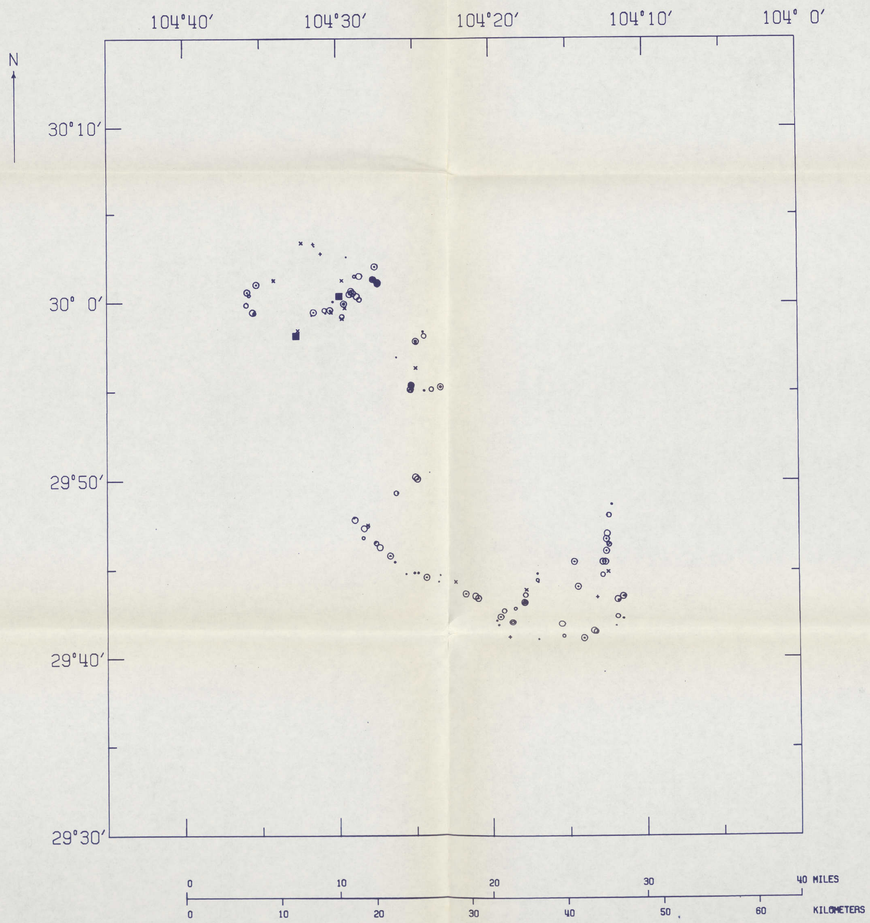

SYMBOL RANGES FOR PLOTTED VARIABLE (X)

.	0.0 ≤ X < 2.00
×	2.00 ≤ X < 3.00
.	3.00 ≤ X < 4.00
.	4.00 ≤ X < 5.00
∘	5.00 ≤ X < 6.00
∘	6.00 ≤ X < 7.00
○	7.00 ≤ X < 8.00
⊙	8.00 ≤ X < 10.00
⊙	10.00 ≤ X < 11.00
⊛	11.00 ≤ X < 13.00
●	13.00 ≤ X < 15.00
●	15.00 ≤ X < 16.00
●	16.00 ≤ X < 17.00
■	17.00 ≤ X < 23.00

PLATE 6
CHINATI MOUNTAINS PROJECT AREA
TRANS-PECOS DETAILED GEOCHEMICAL SURVEY
SYMBOL PLOT STREAM SEDIMENT
THORIUM (PPM)

SCALE 1: 250000

121 SAMPLES PLOTTED

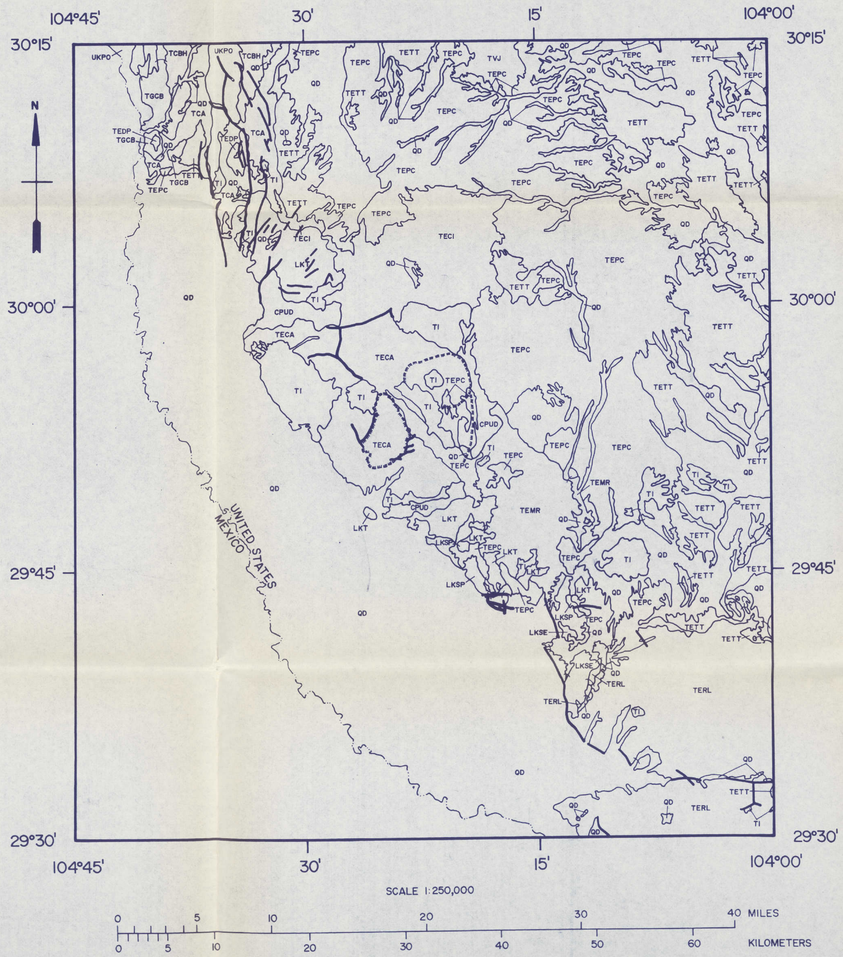

CHINATI MOUNTAINS PROJECT AREA, TRANS-PECOS DETAILED GEOCHEMICAL SURVEY

ERA	SYSTEM	SERIES	MAP CODE	GEOLOGIC UNIT
CENOZOIC	QUATERNARY	RECENT	QD	ALLUVIUM AND OTHER QUATERNARY DEPOSITS
	TERTIARY		TI	INTRUSIVE IGNEOUS ROCKS
		OLIGOCENE	TERL	RAWLS FORMATION FRESNO FORMATION
			TEPC	PERDIZ CONGLOMERATE
			TETT	PETAN BASALT TASCOTAL FORMATION MITCHELL MESA WELDED TUFF DUFF-PRUETT FORMATIONS
			TECA	CHINATI MOUNTAINS GROUP
			TECI	SHELY GROUP
			TEDP	BRITE IGNIMBRITE
			TCA	CAPOTE MOUNTAIN TUFF
			TCBH	BRACHS RHYOLITE CHAMBERS TUFF
		EOCENE	TGCB	COLMENA TUFF GILL BRECCIA BUCKSHOT IGNIMBRITE
			TVJ	VIEJA GROUP (UNDIVIDED)
			TEMR	MORITA RANCH FORMATION
MESOZOIC	CRETACEOUS	UPPER CRETACEOUS	UKPO	PICACHO FORMATION OJINAGA FORMATION SAN CARLOS FORMATION
		LOWER CRETACEOUS	LKSE	SANTA ELENA LIMESTONE
			LKSP	SUE PEAKS FORMATION DEL CARMEN LIMESTONE TELEPHONE CANYON FORMATION
			LKT	SHAFTER FORMATION PRESIDIO FORMATION
PALEOZOIC			CPUD	MINA GRANDE FORMATION ROSS MINE FORMATION PINTO CANYON FORMATION CIBOLO FORMATION ALTA FORMATION

SOURCE OF GEOLOGY:
1. BARNES, V. E.; GEOLOGIC ATLAS OF TEXAS, EMORY PEAK-PRESIDIO SHEET (PRELIMINARY SHEET, 1977).
2. BARNES, V. E.; GEOLOGIC ATLAS OF TEXAS, MARFA SHEET (PRELIMINARY SHEET, 1978).
3. CEPEDA, J.C., "THE CHINATI MOUNTAINS CALDERA, PRESIDIO COUNTY, TEXAS," IN CENOZOIC GEOLOGY OF THE TRANS-PECOS VOLCANIC FIELD OF TEXAS, pp. 65-84 (1978).

LEGEND

GEOLOGIC CONTACT

GEOLOGIC FAULT

TRACE OF TOPOGRAPHIC WALL OF CALDERA

INTERNATIONAL BOUNDARY LINE

PLATE 7

GENERALIZED GEOLOGIC MAP OF THE CHINATI MOUNTAINS PROJECT AREA, TRANS-PECOS DETAILED GEOCHEMICAL SURVEY, TEXAS

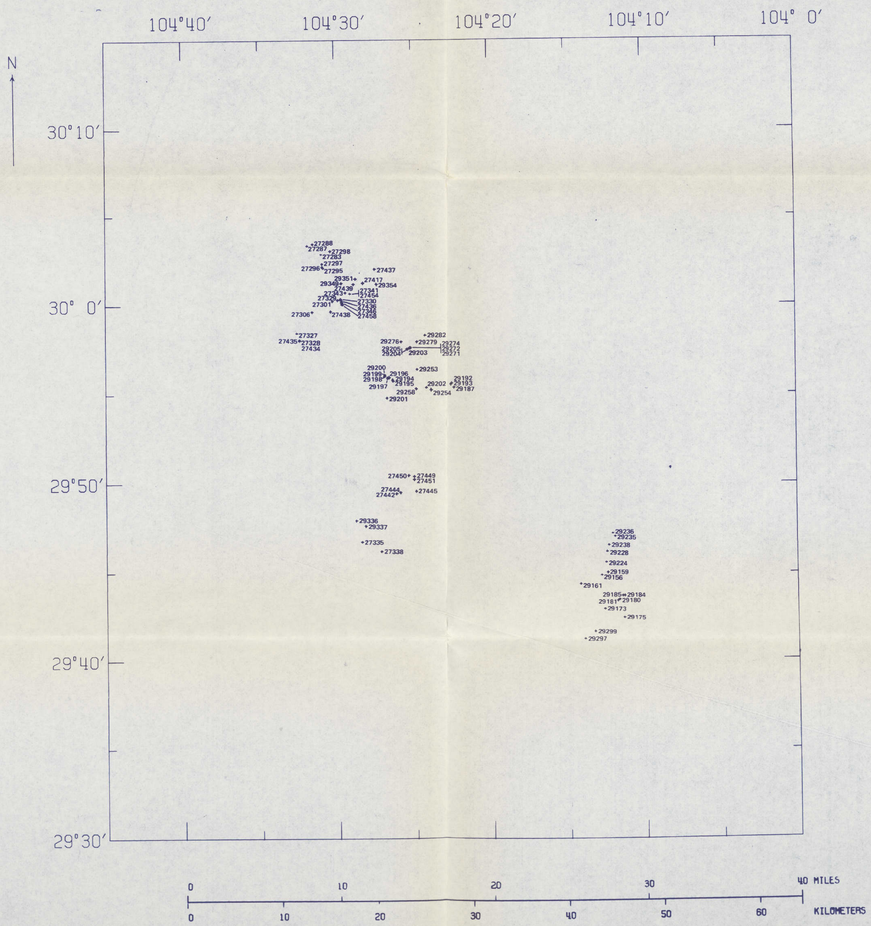

LEGEND

\+ SOIL, ROCK, AND OTHER

PLATE 8
CHINATI MOUNTAINS PROJECT AREA
TRANS-PECOS DETAILED GEOCHEMICAL SURVEY
RADIOMETRIC SAMPLE LOCATION MAP

SCALE 1: 250000

78 SAMPLES PLOTTED